Biochemical and Biophysical Characterization of Poxvirus Mediated Subversion of Apoptosis

Submitted by

Chathura Dahamjith Suraweera

Master of Chemical Sciences (MChSc), La Trobe University, Australia, 2016

Bachelor of Science (Honours), University of Peradeniya, Sri Lanka, 2013

Supervisors:

Professor Marc Kvansakul

Associate Professor Mark G Hinds

A thesis submitted in total fulfilment of the

requirements for the degree of

Doctor of Philosophy

Department of Biochemistry and Genetics

School of Molecular Sciences

College of Science, Health and Engineering

La Trobe University,

Victoria,

Australia

August 2020

Table of Contents

Statement of authorship

Except where reference is made in the text of the thesis, this thesis contains no material published elsewhere or extracted in whole or in part from a thesis submitted for the award of any other degree or diploma.

No other person's work has been used without due acknowledgment in the main text of the thesis.

This thesis has not been submitted for the award of any degree or diploma in any other tertiary institution.

Chathura Dahamjith Suraweera

August 2020

Acknowledgements

I have been very grateful to achieve my PhD study at the La Trobe University. There are plenty of people I would like to acknowledge for their part in my success. The past three and half years of my PhD journey would not have been possible without their support.

I sincerely thank my supervisors Prof. Marc Kvansakul and A/Prof Mark Hinds for their guidance, patience and ongoing support and encouragement throughout my PhD. Their expertise in apoptosis and structural biology trained me in understanding of the much of fundamental of my project. I admire Mark for his great support and selected me as his research student during my Master's degree and introduced me into Kvansakul lab group. Studying overseas is very rare chance and it is my privilege to thank both Mark and Marc for giving me the opportunity to pursue my PhD at the La Trobe University and continually support me to complete my thesis.

I am indebted to A/ Prof. Christine Hawkins, my research advisory committee chair, for her great support, guidance and insightful suggestions throughout my PhD. Over the last three and half years she demonstrated a sincere interest in my work, and I am fortunate to have such a great mentor on my committee.

I owe my sincere gratitude to Professor David Evans, my project collaborator in University of Alberta, Canada to foster my interest on poxviruses research and for his willingness to share his knowledge and experience in poxvirus research. His invaluable suggestions and comments ultimately beneficial for me to focus on my thesis about poxvirus modulated apoptosis inhibition.

I would like to acknowledge Dr Sofia Caria, who was my first mentor in Kvansakul lab and her guidance and support whilst conducting my experiments as well as in crystallography data processing did help me a lot during my PhD.

Publications

Refereed publications

Chathura D. Suraweera, Mohd Ishtiaq Anasir, Srishti Chugh, Airah J. Javorsky, Rachael E. Impey, Mohammad H. Zadeh, Tatiana P. Soares da Costa, Mark G. Hinds* and Marc Kvansakul*, Structural insight into tanapox virus mediated inhibition of apoptosis, 2020 *FEBS Journal (*10.1111/febs.15365*)*

Chathura D. Suraweera, Denis R. Burton, Mark G. Hinds* and Marc Kvansakul*, Structural basis of SPPV14 mediated inhibition of apoptosis by Sheep-pox virus, *FEBS Letters, 594 (12), 2016-2026. (2020)*

Chathura D. Suraweera, Sofia Caria, Mark G. Hinds* and Marc Kvansakul*, Monkeypox virus C7L is a Bcl-2-fold protein that binds human pro-apoptotic Bcl-2 proteins, *Viruses, Under Review (2020)*

Suresh Banjara[#], **Chathura D. Suraweera**[#], Mark G. Hinds*, and Marc Kvansakul*, The Bcl-2 Family: Ancient Origins, Conserved Structures and Divergent Mechanisms (2020). *Biomolecules*, 10(1), 128; (**[#]co-first author**)

Leah Fitzsimmons, Rachel Cartlidge, Catherine Chang, Nenad Sejic, Laura C. A. Galbraith, **Chathura D. Suraweera**, Deborah Croom-Carter, Grant Dewson, Rosemary J. Tierney, Andrew I. Bell, Clare Shannon-Lowe, Marco J. Herold, Alan B. Rickinson, Peter M. Colman, David C. S. Huang, Andreas Strasser, Marc Kvansakul, Martin Rowe, Gemma L. Kelly, EBV BCL-2 homologue BHRF1 drives chemoresistance and lymphomagenesis by inhibiting multiple cellular pro-apoptotic proteins, *Cell Death and Differentiation*, 27, 1554–1568. (2020)

Chathura D. Suraweera, Sofia Caria, Michel Järvå, Mark G. Hinds*, Marc Kvansakul*; A Structural Investigation of NRZ Mediated Apoptosis Regulation in Zebrafish. *Cell Death and Disease*. 9:1-11. (2018)

Protein Data Bank structure depositions (PDB ID)

6TPQ: Crystal structure of TANV16L in complex with Puma BH3 domain

6TQQ: Crystal structure of TANV16L in complex with Bim BH3 domain

6TRR: Crystal structure of TANV16L in complex with Bax BH3 domain

6XY4: Crystal structure of SPP14 in complex with Hrk BH3 domain

6XY6: Crystal structure of SPPC14 in complex with Bax BH3 domain

6FBX: Crystal Structure of a Zebra-fish pro-survival protein NRZ: Bad BH3 complex

6H1N: Crystal Structure of a Zebra-fish pro-survival protein NRZ *apo*

Abbreviations

%	per cent
°C	Degree Celsius
Å	Angström
A1	Bcl-2-like protein A1
ACRF	Australian Cancer Research Foundation
ANSTO	Australia's Nuclear Science and Technology Organization
APAF1	Apoptotic protease-activating factor-1
APXV	Akhmeta virus
ASFV	African swine Fever Virus
AUC	Analytical Ultra Centrifugation
Bad	Bcl-2 antagonist of cell death
Bak	Bcl-2 homologous antagonist/killer
Bax	Bcl-2 associated X protein
Bcl-2	B-cell lymphoma 2 protein
Bcl-w	Bcl-2-like protein w
Bcl-x_L	Bcl-2-like x large isoform
BH domain	Bcl-2 homology domain
BH3-only	Bcl-2 homology domain 3 only
Bid	BH3 interacting domain death agonist
Bik	Bcl-2 interacting killer
Bim	Bcl-2 interacting mediator of cell death
Bmf	Bcl-2 modifying factor
Bok	Bcl-2 ovarian killer
cBcl-2	Cellular Bcl-2

CNPV	Canarypox virus
CPXV	Cowpox virus
Crm	Cytokine response modifier
Cyt c	Cytochrome c
DDX3	Dead box RNA helicase
DNA	Deoxyribonucleic acid
cDNA	circular Deoxyribonucleic acid
DPV	Deerpox virus
DTT	Dithiothreitol
dsRNA	double-stranded Ribonucleic acid
EBV	Epstein Barr Virus
EMV	Ectromelia Virus
ER	Endoplasmic reticulum
FADD	Fas-associated death domain
FasL	Fas ligand
FasR	Fas receptor
FPV	Fowlpox virus
GAAP	Golgi Associated Anti-apoptotic Protein
GIV	Grouper Iridovirus
HEPES	4-(2-hydroxyethyl)-1-piperazineethanesulfonic acid
HEK cells	Human Embryonic Kidney cells
Hrk	Harakiri
HRV-3C	Human Rhinovirus-3C
IC_{50}	half maximum Inhibitory Concentration
IFN	Interferon

IL-1	Interleukin-1
IPTG	Isopropyl β-D-thiogalactopyranoside
IκBβ	Nuclear factor of kappa light polypeptide gene enhancer in B cells inhibitor, β
J	Joule
K	Kelvin
kDa	kilo Dalton
KsBcl-2	Kaposi-sarcoma virus associated Bcl-2 protein
Mcl-1	Myeloid cell leukaemia sequence 1
MCV	Molluscum Contagious Virus
MCMV	Murine cytomegalovirus
mg	milligram
Min	Minute
mL	Mililitre
mM	millimolar
mol	mole
MOM	Mitochondrial Outer Membrane
MOMP	Mitochondrial Outer Membrane Permeability
MPXV	Monkeypoxvirus
MX2	Micromolecular crystallography beamline2
MYXY	Myxoma virus
NA	Not Available
NB	Not Binding
NCLDV	Nucleo-cytoplasmic large DNA viruses
ND	Not detected

Nf-κB	Nuclear factor-κB
NLRP1	NACHT, LRR and PYD domains-containing protein 1
nl	nano liters
nM	nano Molar
Noxa	Phorbol-12-myristate-13-acetate-induced protein 1
N-terminus	Amino terminus
O.D.	Optical density
ORF	Open reading frame
PDB	Protein Data Bank
PEG	Polyethylene Glycol
PEG-MME	Polyethylene Glycol monomethyl ether
PKR	Protein kinase R
Puma	p53-upregulated modulator of apoptosis
RMSD	Root Mean Squire Deviation
RNA	Ribonucleic acid
Rpm	Revolution per minute
RPXV	Rabbitpox virus
SDS	Sodium dodecyl sulfate
SDS-PAGE	Sodium dodecyl sulfate polyacrylamide gel electrophoresis
SEC	Size exclusion chromatography
Serpin	Serine protease inhibitor
SFV	Shope Fibroma Virus
SOD	Superoxide dismutase
SPPV	Sheeppoxvirus
SPR	Surface Plasmon Resonance

TANV	Tanapoxvirus
tBid	truncated BH3interacting domain
TCEP	tris(2-carboxyethyl) phosphine
TIR	Toll-interleukin receptor
TLR	Toll-like Receptor
TM	Transmembrane
TNFα	Tumour necrosis factor α
TNFR	Tumour necrosis factor receptor
TRADD	Tumour necrosis factor receptor type 1-associated DEATH domain
UV	Ultra-violet
VACV	Vaccinia virus
VARV	Variola virus
VDAC2	Voltage-dependent anion-selective channel protein 2
v/v	Volume/volume
vBcl-2	Viral Bcl-2
vTNFR	viral Tumour necrosis factor receptor
w/v	Weight/volume
XDS	X-ray detector software

Abstract

Apoptosis is the highly conserved process of cellular suicide that is initiated either via extracellular (extrinsic apoptosis) or intracellular (intrinsic apoptosis) cues. This form of programmed cell death plays a crucial role in development and tissue homeostasis in multicellular organisms and its subversion is an underlying mechanism for many diseases. Intrinsic apoptosis is regulated by members of B-cell lymphoma-2 (Bcl-2) family, a family that consists of both pro and anti-apoptotic Bcl-2 genes. Bcl-2 genes are evolutionarily conserved and identified in the genomes of the earliest metazoans through to man, and pro-survival Bcl-2 genes have been assimilated by viruses. Pox viruses are one such group of viruses, that infects almost all vertebrates. Viral Bcl-2 proteins are virulence factors encoded by many pox viruses to aid the evasion of the host immune system. Viral Bcl-2 proteins mimic the activity of cellular Bcl-2 proteins and are essential for survival of virus infected cells, but often share very little sequence identity with their cellular counterparts. In this thesis I investigated the structural biology, interactions, and mechanisms of action of three novel pox virus-encoded Bcl-2 proteins, Tanapox virus TANV16L, monkeypox virus MPXV C7L and sheeppox virus SPPV14. I show that these three proteins bind BH3-motif peptides that span a subset of host pro-apoptotic Bcl-2 proteins, including Bax and Bak, with nanomolar to sub-micromolar affinities. I then determined the crystal structures of these proteins both in their *apo* and *holo* forms and compared them with known interactors of BH3 motif peptides. The structure I determined showed that all three proteins interact with BH3 motif peptides using the canonical ligand binding groove in a similar manner to other Bcl-2 proteins. Interestingly, the topology of these three proteins are different: sheeppox SPPV14 is monomer in solution, tanapox TANV16L exists in both a monomeric and dimeric forms in solution and monkeypox C7L exists as a domain swapped dimer. My results reveal the structural plasticity of poxvirus Bcl-2 proteins and how they mimic the crucial interactions found in endogenous host apoptosis pathway to enable the successful infection and proliferation of the virus inside the host cell.

Chapter 1A

Paper I: The Bcl-2 Family: Ancient Origins, Conserved Structures, and Divergent Mechanisms

1A.1   Introduction

Apoptosis is evolutionary well conserved process of cell death from early metazoans to humans (1, 2) and plays a crucial role in tissue homeostasis, development and immune responses against pathogen infected cells (3), (4). Cellular apoptosis is triggered by ether through intrinsic or extrinsic stimuli (3). Intrinsic apoptosis is initiated by cellular stress conditions such as pathogen infection whilst extrinsic apoptosis is initiated by death ligands (TNFα -Tumour Necrosis Factor or Fas ligand) that bind to cell surface death receptors (TNF receptor or Fas receptor) (5). A group of proteins called Bcl-2 family is central to the regulation of intrinsic apoptosis (3).

In this thesis, I discuss the papers resulting from my PhD studies. In Chapter 1A (Review paper) we discuss the structural, functional and evolutionary conservation of Bcl-2 family proteins and their role into cellular apoptosis regulation. Our review paper entitled "The Bcl-2 Family: Ancient Origins, Conserved Structures, and Divergent Mechanisms" was published in Biomolecules, (2020) (2). As our first review discussed more about Bcl-2 family proteins and their evolutionary conservation whilst the main thrust of this thesis focused on poxvirus Bcl-2 modulated apoptosis, in Chapter 1B, I discuss the structural and functional basis of poxvirus encoded Bcl-2 like proteins and their role into host apoptosis inhibition upon infection.

1A.2 Co-author contribution

Suresh Banjara[#]	Manuscript writing
	Structural analysis and interpretation
	Preparation of figures and tables in the manuscript
Chathura D. Suraweera[#]	Manuscript writing
	Structural analysis and interpretation
	Preparation of figures and tables in the manuscript
Mark G. Hinds	Overall scientific direction of the project
	Structural analysis and interpretation
	Drafted and revised the manuscript
Marc Kvansakul	Overall scientific direction of the project
	Structural analysis
	Drafted and revised the manuscript

 # co-first author

Review

The Bcl-2 Family: Ancient Origins, Conserved Structures, and Divergent Mechanisms

Suresh Banjara [1,†], Chathura D. Suraweera [1,†], Mark G. Hinds [2,*] and Marc Kvansakul [1,*]

[1] Department of Biochemistry & Genetics, La Trobe Institute for Molecular Science, La Trobe University, Melbourne, VIC 3086, Australia; 17843636@students.latrobe.edu.au (S.B.); C.Suraweera@latrobe.edu.au (C.D.S.)

[2] Bio21 Molecular Science and Biotechnology Institute, The University of Melbourne, Parkville, VIC 3052, Australia

[*] Correspondence: mhinds@unimelb.edu.au (M.G.H.); m.kvansakul@latrobe.edu.au (M.K.); Tel.: +61-3-9479-2263 (M.K.)

[†] These authors contributed equally to this work.

check for updates

Abstract: Intrinsic apoptosis, the response to intracellular cell death stimuli, is regulated by the interplay of the B-cell lymphoma 2 (Bcl-2) family and their membrane interactions. Bcl-2 proteins mediate a number of processes including development, homeostasis, autophagy, and innate and adaptive immune responses and their dysregulation underpins a host of diseases including cancer. The Bcl-2 family is characterized by the presence of conserved sequence motifs called Bcl-2 homology motifs, as well as a transmembrane region, which form the interaction sites and intracellular location mechanism, respectively. Bcl-2 proteins have been recognized in the earliest metazoans including Porifera (sponges), Placozoans, and Cnidarians (e.g., Hydra). A number of viruses have gained Bcl-2 homologs and subvert innate immunity and cellular apoptosis for their replication, but they frequently have very different sequences to their host Bcl-2 analogs. Though most mechanisms of apoptosis initiation converge on activation of caspases that destroy the cell from within, the numerous gene insertions, deletions, and duplications during evolution have led to a divergence in mechanisms of intrinsic apoptosis. Currently, the action of the Bcl-2 family is best understood in vertebrates and nematodes but new insights are emerging from evolutionarily earlier organisms. This review focuses on the mechanisms underpinning the activity of Bcl-2 proteins including their structures and interactions, and how they have changed over the course of evolution.

Keywords: apoptosis; Bcl-2; evolution; mechanism; structure analysis

1. Introduction

Apoptosis or programmed death of cells has played a significant role in metazoan evolution and prioritizes the organism over individual cells [1,2]. One form of apoptosis, intrinsic or mitochondrial regulated apoptosis, is initiated by a range of intra- and extracellular stimuli to regulate developmental and homeostatic processes [3]. The genes most closely associated with intrinsic apoptosis are the B-cell lymphoma 2 (Bcl-2) family and have been identified in the basal clades of metazoans, including Porifera (sponges), Cnidaria (anemones, corals, jellyfish), and Placozoa [4]. In mammals, these genes regulate the integrity of mitochondria where they either initiate the release of apoptogenic factors or prevent this process from occurring (Figure 1). The threshold for cell fate is mediated by antagonism between prosurvival and proapoptotic members of the Bcl-2 family [5] and this fundamental interaction is conserved from sponges [6] to man [7]. Evolutionary gene losses have led to simplification of this process in some organisms, such as insects and nematodes (Figure 1b). Viruses have also acquired

Bcl-2 genes to facilitate replication and counter infected cells' ability to orchestrate intrinsic apoptosis as part of antiviral defense mechanisms [8]. The molecular basis of the interaction between prosurvival and proapoptotic proteins relies on their conserved sequences and structures [7].
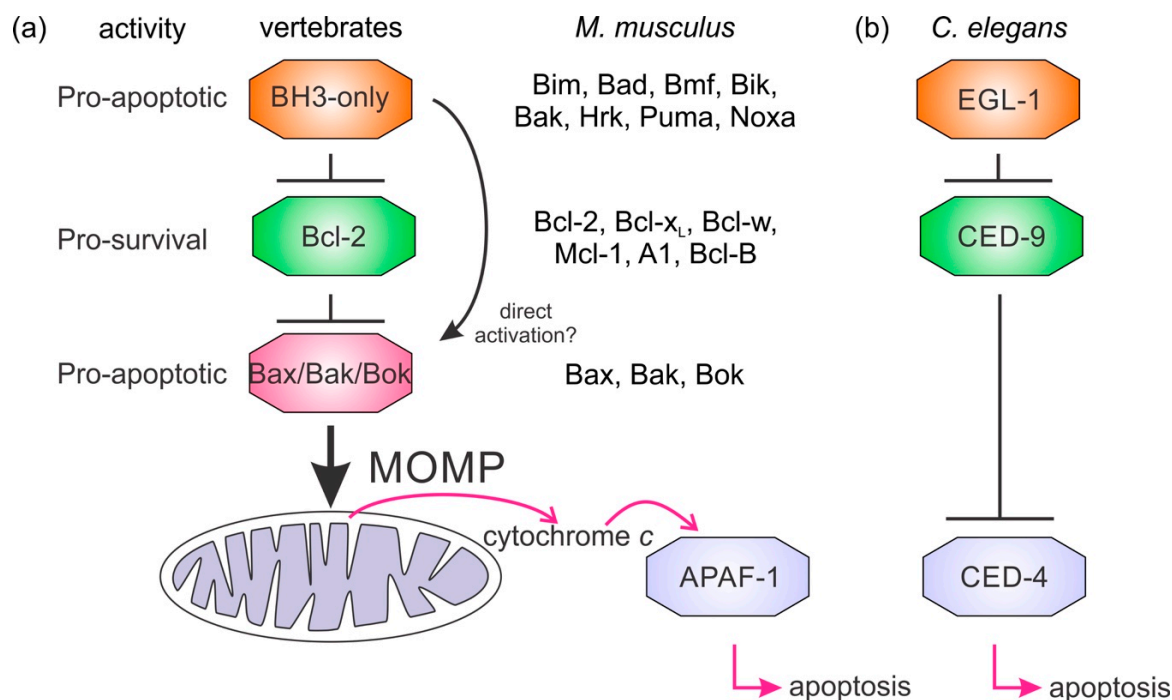
Figure 1. Mechanisms of Bcl-2 regulated apoptosis. Simplified apoptosis schemes showing the role of Bcl-2 proteins in apoptosis initiation differ between mammals (**a**) and nematodes (**b**). The Bcl-2 family members are indicated for *M. musculus.* Nematodes have a simplified activation of apoptosis where the BH3-only protein EGL–1 binds the sole prosurvival protein in the *C. elegans* genome CED-9. This event releases the caspase activating protein CED–4 to initiate the caspase cascade. In mammalian apoptosis, the BH3-only group of proteins antagonize the prosurvival Bcl-2 proteins releasing Bax, Bak, or Bok to oligomerize and form pores in mitochondria causing mitochondrial outer membrane permeabilization (MOMP). Cytochrome *c* release from the mitochondrion triggers the mammalian equivalent of CED-4, APAF-1, to oligomerize and initiate the activation of downstream caspases.

Bcl-2 proteins (Table 1) are identified by the presence of up to four conserved linear sequence motifs or domains comprising about 20 residues and known as Bcl-2 Homology (BH) motifs (Figure 2) [7,9].

Table 1. Summary of Bcl-2-related proteins and their activities.

Name(s)	Species	Functions	References
Bcl-2	*H. sapiens*	Prosurvival	[10,11]
Bcl-w	*H. sapiens*	Prosurvival	[12–14]
Bcl-x$_L$	*H. sapiens*	Prosurvival	[15,16]
Mcl-1	*H. sapiens*	Prosurvival	[17,18]
Bfl-1/A1	*H. sapiens*	Prosurvival	[19,20]
Bcl-b	*H. sapiens*	Prosurvival	[21,22]
Boo/Diva	*M. musculus*	Prosurvival	[21,23]
NRZ	*D. rerio*	Prosurvival	[24,25]
Bak	*H. sapiens*	Proapoptotic	[26,27]

Table 1. *Cont.*

Name(s)	Species	Functions	References
Bax	*H. sapiens*	Proapoptotic	[28,29]
Bok	*H. sapiens*	Proapoptotic	[30]
Bad	*H. sapiens*	Proapoptotic	[31]
Bid	*H. sapiens*	Proapoptotic	[32]
Bik	*H. sapiens*	Proapoptotic	[33]
Bim	*H. sapiens*	Proapoptotic	[34]
Bmf	*H. sapiens*	Proapoptotic	[35]
Hrk	*H. sapiens*	Proapoptotic	[36]
Noxa	*H. sapiens*	Proapoptotic	[37]
Puma	*H. sapiens*	Proapoptotic	[38]
Beclin	*H. sapiens*	Proautophagic	[39]
Bcl-wav	*D. rerio*	Proapoptotic	[40,41]
Buffy	*D. melanogaster*	Proapoptotic	[42]
DeBcl	*D. melanogaster*	Prosurvival	[43]
BHRF1	Epstein–Barr virus	Prosurvival	[44,45]
KsBcl-2	Kaposi Sarcoma herpesvirus	Prosurvival	[46]
E1B19K	Human adenovirus	Prosurvival	[47]
M11	mγ68 herpesvirus	Prosurvival	[48,49]
A179L	African swine fever virus	Prosurvival	[50,51]
F1L	Vaccina virus, variola virus	Prosurvival	[52,53]
DPV022	Deer poxvirus	Prosurvival	[54,55]
M11L	Myxomavirus	Prosurvival	[56,57]
FPV039	Fowl poxvirus	Prosurvival	[58,59]
CNP058	Canary poxvirus	Prosurvival	[60,61]
SPPV14	Sheep poxvirus	Prosurvival	[62]
ORFV125	Orf virus	Prosurvival	[63]
GIV66	Grouper iridovirus	Prosurvival	[64,65]
N1	Vaccinia virus	Prosurvival, NF-κb	[66,67]
A46	Vaccinia virus	NF-κb	[68,69]
A49	Vaccinia virus	NF-κb	[70,71]
A52	Vaccinia virus	NF-κb	[72]
B14	Vaccinia virus	NF-κb	[72,73]
K7	Vaccinia virus	NF-κb, IFN signaling	[74,75]
LB-Bcl-2	*L. baicalensis*	Prosurvival	[76]
LB-Bak-2	*L. baicalensis*	Proapoptotic	[6,76]
BHP1	*G. cydonium*	Prosurvival	[77]
BHP2	*G. cydonium*	Prosurvival	[6,77]
trBcl-2L1	*T. adherens*	Prosurvival	[78]
trBcl-2L2	*T. adherens*	Prosurvival	[78]
trBcl-2L3/trBax	*T. adherens*	Proapoptotic	[78]
trBcl-2L4/trBak	*T. adherens*	Proapoptotic	[78]
EGL-1	*C. elegans*	Proapoptotic	[79,80]
CED-9	*C. elegans*	Prosurvival	[81,82]
vMIA	Cytomegalovirus	Prosurvival	[83,84]
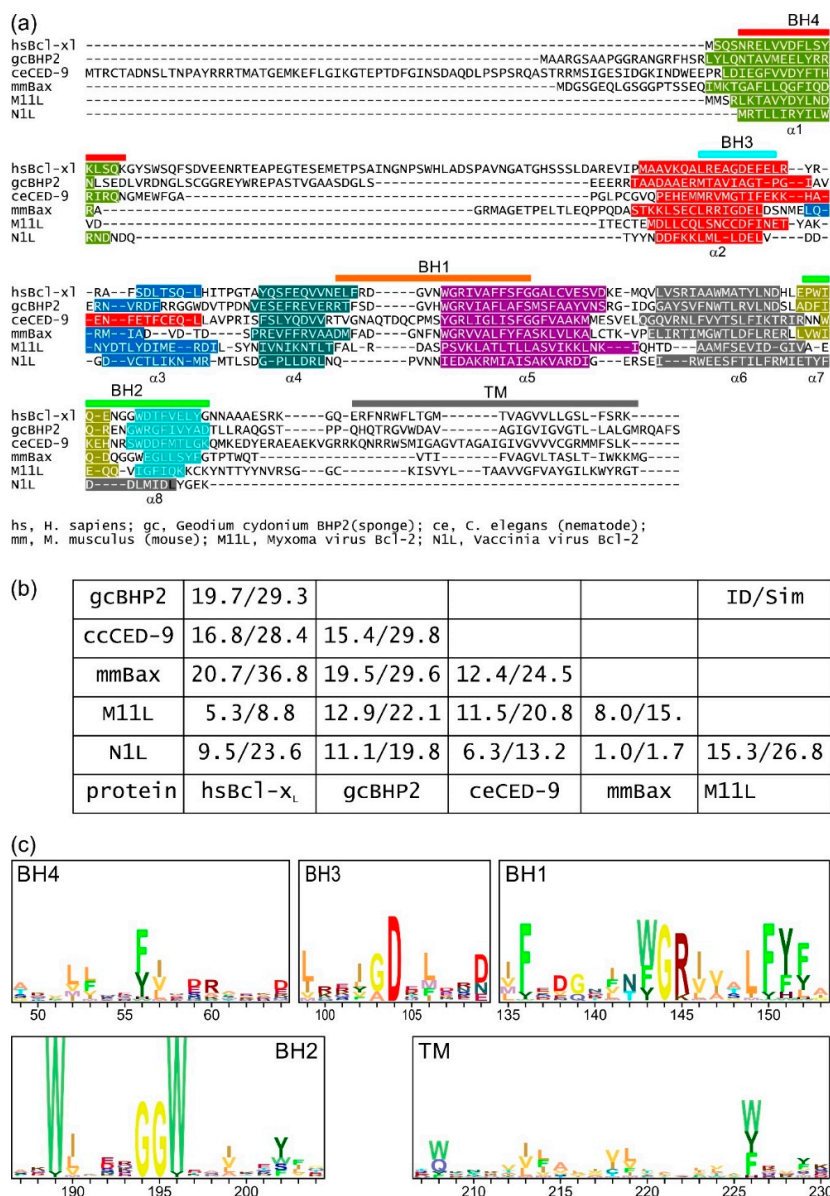
Figure 2. Sequence-structure analysis of Bcl-2 family members from sponges to man. (**a**) Structure-based sequence alignment of metazoan and viral Bcl-2 family members. Structurally equivalent residues are aligned. In (**a**), sequence–structure alignment shows prosurvival and proapoptotic Bcl-2 proteins share key sequence features. Sequences aligned: *H. sapiens* Bcl-x$_L$; *G. cydonium* BHP2; *C. elegans* CED-9; *Mus musculus* Bax; Myxoma virus M11L; Vaccinia virus N1L. Sequence–structure alignment was performed using Dali [85] and the secondary structure is indicated by the colored bars. The extent of the Bcl-2 homology (BH) motifs and transmembrane region (TM) is indicated by bars above the sequence and the helices below the sequences. (**b**) Table of sequence identities and similarities for the sequences in (**a**) given as percentage sequence identity/sequence similarity in each entry. Notably, the viral Bcl-2 proteins have little recognizable shared sequence identity with mammalian Bcl-2 proteins. (**c**) Profiles of BH and TM regions from Bax sequences representing bilaterians (*Lepisosteus oculatis, Strongylocentrotus purpuratus, Ciona intestinalis*), cnidarians (*H. vulgaris, Acropora digitifera*), placozoa (*T. adhaerens*), and porifera (*A queenslandica*). The height of each stack represents the conservation and the residue frequencies are represented by their height as determined by the program Skylign [86]. These indicate that the BH4 motif is a relatively weak and poorly conserved motif when compared to the BH1–BH3 motifs. Uniprot sequence and PDB IDs, hsBcl-x$_L$: Q07817, 1R2D; gcBHP2: Q967D2, 5TWA; ceCED-9: P41958, 1OHU; mmBax: Q07813, 5W62; Myxoma virus M11L: Q77PA8, 2JBX; Vaccinia virus N1L: P21054, 2I39.

The Bcl-2 proteins fold to form a distinct helical bundle structure where the core of the α–helical bundle is composed of a central hydrophobic helix (helix α5) that forms a scaffold for packing up to eight α-helices (Figures 2 and 3). In a feature maintained from sponges to man [9], the Bcl-2 fold brings the BH regions into close proximity to assemble the canonical BH3-binding groove where an antagonist BH3 motif binds (Figure 3b,c). Whilst this "in-groove" interaction mechanism appears to be the primary mode of interaction for Bcl-2-mediated control of apoptosis, alternative modes have been proposed including a site spanning helices α1 and 6 [87] and the BH4 motif [88]. Furthermore, nonapoptotic roles including modulation of NF-κB signaling are also not mediated via an in-groove mechanism [89]. BH motifs are recognizable from the earliest metazoan Bcl-2 proteins but may be absent in viral proteins. The sequence signatures of each of the four BH motifs (BH1–BH4) differ (Figure 2c) and are found in the order from the N-terminus: BH4, BH3, BH1, BH2 (Figure 2a) and for prosurvival proteins are normally located on the same exon while the gene structure for the proapoptotic proteins is more complex. The presence of a BH3 motif is a key feature of the proapoptotic proteins and required for their proapoptotic activity [9,90], whereas some of the prosurvival proteins do not feature the BH3 motif. In addition to the presence of the BH motifs, many Bcl-2 proteins bear a C-terminal transmembrane (TM) region that is located on a separate exon. The TM region targets these proteins to intracellular membranes including the nuclear envelope, mitochondrial inner and outer membranes, Golgi apparatus, lysosomes, ER, and peroxisomes [91]. However, it is Bcl-2 family action at the mitochondrial outer membrane (MOM) that is the most central mechanistic feature for intrinsic apoptosis. Both the gene structure and synteny of Bcl-2 proteins are well conserved across phyla [92].

Our current understanding of intrinsic apoptosis is mainly derived from investigations of mouse, human, nematode (*Caenorhabditis elegans*), and fly (*Drosophila melanogaster*) apoptosis. These studies have shown the Bcl-2 family consists of two phylogenetically distinct groups of proteins: those that share the Bcl-2 fold [90,93] that are either prosurvival or proapoptotic and the proapoptotic intrinsically disordered 'BH3-only' proteins, that bear only the BH3 motif [9]. The BH3-only proteins are upregulated in response to diverse apoptotic stimuli [94] and their principal role is to antagonize the prosurvival proteins [9], but apoptosis also occurs in their absence [95]. Notwithstanding the conservation in the Bcl-2 family, there are substantial differences in Bcl-2-regulated apoptosis mechanisms. In mammals, there are nine multimotif Bcl-2 paralogs (six prosurvival Bcl-2, Bcl-x_L, Bcl-w, Mcl-1, A1, Bcl-B, and three proapoptotic Bax, Bak, and Bok) and eight BH3-only proteins (Bim, Bad, Bmf, Bid, Bik, Noxa, Puma, Hrk) (Table 1) that regulate intrinsic apoptosis through a network of specific binding interactions that control the integrity of the MOM [7] (Figure 1). A key step is Bax, Bak, or Bok oligomerization at the mitochondrial membrane that results in formation of membrane pores releasing cytochrome *c* to activate the caspase cascade. In contrast to mammals, MOM permeabilization (MOMP) and cytochrome *c* do not play a role in initiation of apoptosis in ecdysozoans *C. elegans* (Figure 1) or *D. melanogaster* [7,42,96] (Figure 1). Combined, these results indicate the interactions of the Bcl-2 proteins have been maintained over the course of evolution.

The role of prosurvival Bcl-2 proteins is not limited to regulation of apoptosis; other functions have been proposed in processes as divergent as autophagy, calcium homeostasis regulation, and metabolism [97–99]. The most well-understood process at a molecular level of these nonapoptotic roles is that of autophagy. Both Bcl-2 and Bcl-x_L are able to bind the autophagy regulator Beclin-1 via a mechanism closely mimicking the canonical in-groove interaction with BH3-only proteins [49,100,101]. Beclin-1 has significant differences from the BH3-only proteins. In addition to being much longer (450 residues) than a typical BH3-only protein (54–198 residues for human BH3-only proteins), Beclin-1 has its BH3-like motif located in an unstructured N-terminal region [102] with the BH3 motif spread over the junction of two exons. In addition to its unstructured N-terminal region Beclin-1 bears a coiled coil domain and a folded evolutionary conserved domain [103]. The spread of the BH3 motif over two exons differentiates Beclin-1 from the BH3-only proteins where apart from Bid the BH3 occurs in the second-to-last exon. The molecular basis of Bcl-2 proteins in nonapoptotic functions remains to be delineated.
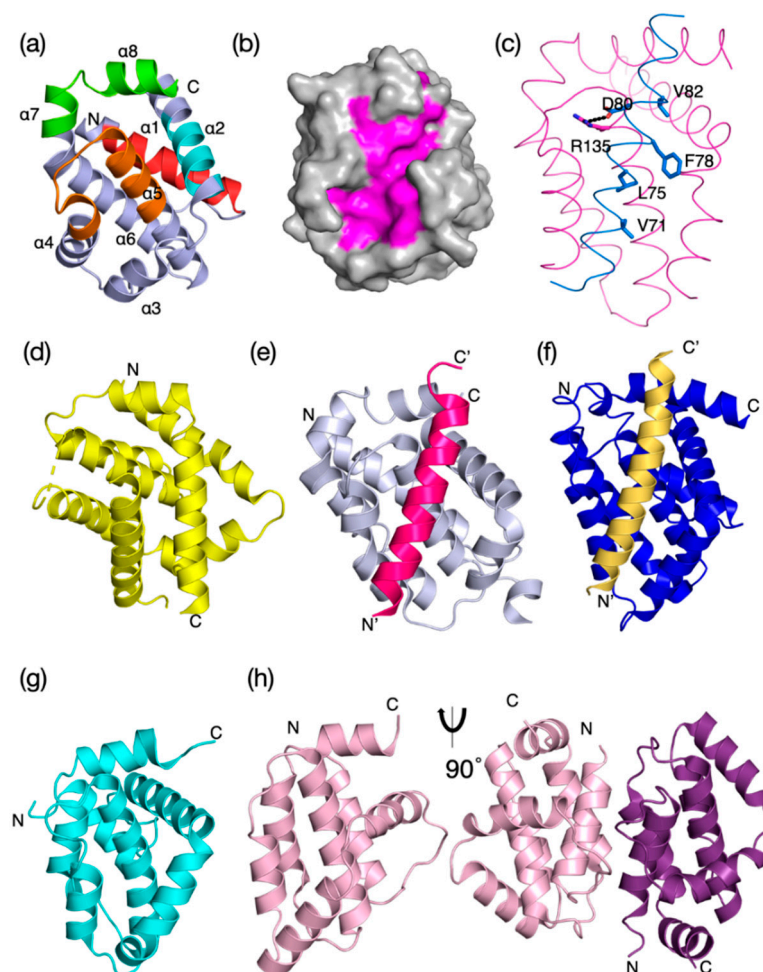
Figure 3. Evolutionary structure conservation in the Bcl-2 family and their complexes. Ribbon representation of the 3D structures of prosurvival and proapoptotic Bcl-2 family members and their complexes are shown. The helical bundle Bcl-2 structure occurred early in evolution and changed little over evolutionary time scales. (**a**) *H. sapiens* Bcl-x_L (PDB 1R2D) with BH1–4 motifs colored in orange, green, cyan, and red as shown in the sequence–structure alignment of Figure 2a, (**b**) *H. sapiens* Bcl–x_L (PDB 1R2D) shown as grey surface with canonical ligand-binding groove shaded in magenta, (**c**) BHP2 from the sponge *G. cydonium* Bcl-2, BHP2 (PDB 5TWA) magenta, LB–Bak sky blue. The canonical ionic interaction between the conserved Arg from prosurvival Bcl-2 and conserved Asp from the BH3 motif of prodeath Bcl-2 as well as the four conserved hydrophobic residues from the Bak BH3 motif are shown as sticks. (**d**) *M. musculus* Bax (PDB 5W62) yellow, (**e**) *H. sapiens* Bcl-b:Bim complex (PDB 4B4S), (**f**) *C. elegans* CED-9: EGL-1 complex, CED-9 (navy) with EGL–1 (sand) in the binding groove (PDB 1TY4). (**g**) Myxoma virus Bcl-2 M11L (PDB 2JBX) cyan, (**h**) Vaccinia virus N1L (PDB 2I39) salmon. Monomeric N1 is shown in the same orientation as in (**a**), and the functionally relevant dimer is shown rotated by 90° around the vertical axis. In (**a**), the extent of the BH motifs is indicated as ribbon colored as in Figure 2a and the helices α1–α8 are also indicated. The structures were aligned on human Bcl-x_L and the orientation for all structures is the same as that in (**a**). The N and C termini are indicated.

Dysfunctional apoptosis is one of the hallmarks of disease like cancer [104] and metazoans have coevolved with this disease [105]. While neoplasms in many vertebrates are well known [105], they have also been discovered in the early metazoans *H. vulgaris* [106], coral *Acropora palmata* [107], and molluscs [108], and in the case of hydra, occur as a result of dysregulation of apoptosis [106]. While some cancers are unique to a species, others occur across multiple species [109] and resistance to apoptosis is likely to be a central feature. There is strong interest in developing a molecular understanding in Bcl-2 function, interactions, and structures [7] but currently there is only a limited number of studies

on early metazoan Bcl-2-regulated apoptosis [6,110]. However, these initial studies strongly suggest conservation of structures and mechanisms across metazoan history. Exactly how intrinsic apoptosis is manifested at a molecular level varies according to the organism, but all mechanisms rely on loss of prosurvival activity to initiate apoptosis. Consequently, there has been a drive to explore the interactions of this family and elucidate the network of functions they regulate.

2. Virus-Encoded Bcl-2 Homologs

The importance of the Bcl-2 family in homeostatic regulation has been exploited by viruses with many viral genomes containing a Bcl-2 protein, and in some instances, multiple Bcl-2 proteins [8]. Sequence, structural, and functional homologs of Bcl-2 are found in *Herpesviridae* as well as Nucleocytoplasmic Large DNA Viruses (NCLDVs) such as *Asfarviridae* and *Iridoviridae* [8]. Many of these virus-encoded Bcl-2 family members display substantial differences with regards to their sequence (Figure 2a,b) and interaction profiles to their mammalian proapoptotic Bcl-2 family counterparts as well as their overall structure, owing to the more rapid pace at which these proteins have evolved as part of a host–pathogen interface [8,111]. The first viral Bcl-2 homologs were identified in adenovirus [112] and the γ-herpesvirus Epstein–Barr virus (EBV) [44]. Adenoviral E1B19K was shown to be a potent inhibitor of apoptosis and could be interchanged with Bcl-2 during cellular transformation [112]. Whilst the vast majority of virus-encoded apoptosis regulatory Bcl-2 proteins act by utilizing the canonical ligand-binding groove to sequester proapoptotic Bcl-2 family members, it has become apparent that this is not the sole mechanism utilized. In addition to binding proapoptotic proteins, viruses may target host prosurvival Bcl-2 proteins through the BH3-binding groove in a manner similar to but not identical to a BH3 motif, and Hepatitis B virus X protein was shown to engage the groove of Bcl-x$_L$ allowing viral replication to proceed [113].

2.1. Bcl-2 Homologs Encoded by Herpesviridae

Numerous *Herpesviridae* encode Bcl-2-like proteins such as BHRF1 from EBV, one of the earliest identified viral Bcl-2 homologs. BHRF1 adopts the classical Bcl-2 fold and utilizes the canonical ligand-binding groove to engage proapoptotic BH3 motif ligands [45,114]. BHRF1 was shown to prolong survival of cells [44,115], which is linked to its ability to engage proapoptotic Bcl-2 members Bim [116] and Bak [114]. An unusual herpesviral Bcl-2 homolog is found in murine γ–herpesvirus 68, M11 [117]. M11 is a potent inhibitor of TNFα and Fas-induced apoptosis, and was shown to bind multiple proapoptotic Bcl-2 proteins including Bim, Bak, and Bax [101]. However, M11 also binds the autophagy regulator Beclin-1, which bears a BH3-like motif, with nanomolar affinity (K$_D$ = 40 nM), which is bound via the canonical ligand-binding groove [101]. Indeed, functional studies suggest that autophagy may be the primary cell death pathway targeted by M11 [49]. Although the majority of herpesvirus-encoded Bcl-2 proteins target intrinsic apoptosis, γ68-encoded M11 clearly shows that other cell death pathways such as autophagy can also be viable targets. Indeed, M11 is not an exception, and adenoviral E1B19K was shown to be an autophagy inhibitor via engagement of Beclin-1 [118], as was the asfarvirus African swine fever virus (ASFV) A179L (see below).

2.2. Poxvirus Bcl-2 Homologs

The *Poxviridae* are a large superfamily of viruses amongst the NCLDVs comprising numerous families that are characterized by their relatively large genomes (130–360 kb) that frequently encode functional and structural homologs of Bcl-2. Most notable for human disease among the pox viruses are Variola virus, the causative agent of smallpox, and Vaccinia virus, which provides the basis for smallpox vaccine. Vaccinia virus (VACV) is the prototypical member of the *Orthopoxviridae* and encodes for prosurvival F1L. VACV F1L is a potent inhibitor of intrinsic apoptosis, but displays no detectable sequence identity with mammalian Bcl-2 [119,120]. Nevertheless, structural studies revealed that VACV F1L adopts a Bcl-2 fold, albeit with a previously not observed domain-swapped topology that rendered VACV F1L a constitutive dimer [53,121]. This unusual topology is paired

with a remarkably restricted ligand-binding profile, with VACV F1L only engaging Bim, Bak, and Bax. Interestingly, similar domain swapping was subsequently also observed during Bax and Bak oligomerization [122], suggesting that the structural plasticity observed amongst the virus-encoded Bcl-2 proteins is also pivotal for the function of metazoan family members. In the context of a live viral infection, F1L inhibits Bim to prevent premature host cell apoptosis [121] and replaces Mcl-1 activity [123]. An extended unstructured N-terminal section prior to the Bcl-2 fold [124] may be involved in apoptosis regulation but results are conflicting [124–126]. Despite being closely related to VACV F1L, the Variola virus (VAR) F1L homolog does not bind Bim; instead it binds Bid, Bak, and Bax [127], and only counters Bax-mediated apoptosis. The domain-swapped Bcl-2 topology is not restricted to the *Orthopoxviridae*, with deerpoxvirus-encoded DPV022 [55] also adopting this unusual fold [54]. Amongst the *Leoporipoxviridae*, myxomavirus encodes for antiapoptotic M11L (Figure 3d), a potent inhibitor of intrinsic apoptosis [128]. Despite lacking detectable sequence identity to cellular Bcl-2 or Bcl-x_L, M11L adopts a Bcl-2 fold [57,129] (Figure 2a,b and Figure 3g,h) and sequesters Bax and Bak to prevent apoptosis [57], unlike VACV F1L which operates via Bim neutralization [121]. Other poxvirus-encoded vBcl-2 members include fowlpox FPV039 [58,59] and canarypox virus (CNPV058) [61], sheep poxvirus [62], and orf virus ORFV125 [63]. Outside the *herpes* and *poxviridae*, ASFV encodes A179L [130], a Bcl-2 homolog that uses the canonical ligand-binding groove to engage all major host proapoptotic Bcl-2 members [51] as well as Beclin-1 [131], thus acting as a dual apoptosis/autophagy inhibitor [50,132]. Amongst the *Iridoviridae*, grouper iridovirus (GIV) harbors prosurvival GIV66 [65] that only binds Bim [64], and forms a novel noncovalent dimeric Bcl-2 architecture which leads to an occluded ligand-binding groove [64] and dimer dissociation upon Bim binding.

While numerous *Poxviridae* encode Bcl-2 homologs that inhibit apoptosis, it has become apparent that another subset of poxviral Bcl-2 proteins exists that also modulate other functions. This group includes VACV N1 which, like M11L, has little shared sequence identity with mammalian Bcl-2 proteins (Figure 2b) but is a structural homolog (Figure 3g). N1 is a dual inhibitor of intrinsic apoptosis that adopts a dimeric Bcl-2 fold (Figure 3h) [67,133] where an additional interaction site enables modulation of NF-κB signaling that is regulated independently of the canonical Bcl-2 groove [89]. Other VACV-encoded NF-κB modulatory Bcl-2 proteins include A46 [68,134], A49 [70], A52, B14 [72], and K7 [75]. Despite targeting NF-κB signaling, substantial structural and mechanistic differences are evident across this group of Bcl-2 proteins. Although A52 and B14 utilize helices α1 and α6 to form a similar interface [72] as N1, the angle of orientation between the constituent monomers varies between the three proteins.

Intriguingly, while apoptosis inhibitory Bcl-2 members are found in *Herpes*, *Pox*, *Asfar*, and *Iridoviridae*, more specialist functions are not widely found. Although several herpesviruses as well as ASFV harbor Bcl-2 homologs with autophagy inhibitory activity, no poxvirus has been shown to inhibit autophagy via a Bcl-2 homolog. Conversely, the NF-κB inhibitory activity found in poxvirus-encoded Bcl-2 homologs is not found outside the *Poxviridae*. Whether or not these differences are attributable to the unique and fundamentally different life cycles and primary sites of infection remains to be established. These findings differentiate the viral Bcl-2 proteins from those in metazoans but indicate the diversity of interactions possible with the Bcl-2 fold.

3. The Nonmammalian Bcl-2 Family

Of the four nonbilaterian basal clades of metazoans, Porifera, Placozoa, Cnidaria, and Ctenophora, multiple orthologous and paralogous Bcl-2 family members have been discovered in the genomes of organisms from Porifera, Placozoa and Cnidaria, but have not yet been identified in ctenophores. In contrast to higher organisms and viruses, experimental evidence for the function of the Bcl-2 family in basal metazoans is relatively sparse. Recent sequence, structural, and biochemical evidence gained from poriferan [6], placozoan [78], and cnidarian [110] Bcl-2 family members are elucidating the mechanisms of apoptosis in basal metazoans. Furthermore, these results strongly suggest the molecular

basis of intrinsic apoptosis determined by the structures, interactions, and intracellular localization of Bcl-2 proteins was foundational in metazoan evolution.

Sponges are currently considered the sister group to metazoans [135,136] and multiple Bcl-2 family proteins have been discovered in members of this phylum; for example, the genome of *Amphimedon queenslandica* contains seven potential Bcl-2 proteins [137], though little is known of their function. The demosponge *Lubomirskia baicalensis* harbors putative prosurvival and proapoptotic Bcl-2 proteins LB-Bcl-2 and LB-Bak-2 [76], and two Bcl-2 proteins, BHP1 and BHP2, have been identified in the sponge *Geodium cydonium* [77]. Structural and biochemical studies on BHP2 showed that a BH3 peptide derived from the BH3 region of *L. baicalensis* Bak-2 bound in the groove of BHP2 and many of the molecular features elucidated in mammalian Bcl-2 interactions were maintained [6]. Though the topology of BHP2 closely resembles those of other Bcl-2 proteins (Figures 2 and 3), a structure–phylogenetic analysis showed there were relatively subtle differences suggesting BHP2 has unique binding features when compared to mammalian and viral Bcl-2 proteins [6]. These findings not only indicate the structure conservation but the evolutionary conservation of the intermolecular interactions of the BH3 motif:Bcl-2-in-groove interaction between prosurvival and proapoptotic Bcl-2 proteins from sponges to man.

The placozoan *Trichoplax adhaerens* has four putative Bcl-2 fold proteins in its genome [138] including two putative proapoptotic proteins, Bax (trBcl-2L3 or trBax) and Bak (trBcl-2L4 or trBak), and two prosurvival proteins, trBcl-2L1 and trBcl-2L2 [78]. TrBax is inhibited by human Bcl-2, suggesting the BH3-in-groove interaction is conserved. The putative role of trBak in *T. adhaerens* is somewhat different from that in humans, where it antagonizes the prosurvival activity of trBcl-2L1 and trBcl-2L2 rather than inducing cytochrome *c* loss from mitochondria, and thus it has been hypothesized that trBak effectively adopts the role of a BH3-only protein in mammals; however, further investigation is required to establish this proposal as no detailed interaction studies were undertaken. As for the case of *G. cydonium*, the underlying conservation of the Bcl-2:Bax interaction was demonstrated by the inhibition of trBax by human prosurvival proteins.

The BH3-only proteins play a key role in mammalian apoptosis where they antagonize the action of prosurvival proteins (Figure 1), but their presence has not been detected in the genomes of Porifera or Placozoa. However, candidates for BH3-only proteins have been detected in the cnidarian *H. vulgaris* [139,140] in addition to Bcl-2 fold sharing prosurvival proapoptotic Bcl-2 proteins. Potential BH3-only proteins have been identified in *H. vulgaris* using a yeast two-hybrid screen [110]. The relatively short sequence of the BH3-only motif with essentially only a highly conserved Leu and absolutely conserved Asp four residues downstream has made it difficult to identify bona fide BH3-only sequences by sequence alone, making it necessary for biochemical verification [9,141]. In addition to the four proposed BH3-only proteins in *H. vulgaris*, there are nine putative Bcl-2 family members including two Bak-like and seven Bcl-2 like sequences [110]. Although further studies are required to establish the exact functional relationships for these proteins, the findings of Lasi et al. [110] point to a complex signaling network for the Bcl-2 proteins even in the earliest of metazoans.

The genetic [96] and molecular and structural [79,142] foundations of Bcl-2-regulated apoptosis were established in the ecdysozoan *C. elegans* (Figures 1, 2a and 3f). Since these discoveries, the basis of prosurvival, proapoptotic, and BH3-only protein interaction has been verified in other organisms. The genomes of the lophotrochozoans *Schmidtea mediterranea*, *S. japonicum,* and *S. mansoni* bear multiple Bcl-2-like proteins including BH3-only components [143,144]. Investigation of apoptosis in platyhelminths (*S. mediterranea* and *Dugesia dorotocephala*) identified Bak and Bcl-2 orthologs and experimental data mitochondrial cytochrome *c* release is associated with MOMP and caspase activation [144]. Binding between the Bcl-2 proteins and BH3-only proteins in *S. japonicum* was established using immunoprecipitation experiments [143]. Mutational, structural, and biochemical studies defined the binding mode as similar to other Bcl-2:BH3 interactions and cytochrome *c* release on treatment with a BH3 motif peptide [143]. Combined, these studies on lophotrochozoans indicate that, in contrast to ecdysozoans, a tripartite mechanism exists with prosurvival, proapoptotic, and

BH3-only proteins triggering MOMP and cytochrome *c* release to initiate intrinsic apoptosis in these organisms. The conclusion from these studies is that intrinsic apoptosis signaling in the protostomes has been modified by gene loss in some organisms but the underlying tripartite mechanism leading to MOMP is preserved in others and the MOM interaction remains central.

Experiments on the cytosolic extracts from the echinoderms *Strongylocentrotus purpuratus* (purple sea urchin) and *Dendraster excentricus* (sand dollar) indicate caspase activation could be induced with cytochrome *c*, suggesting mitochondrial-regulated apoptosis occurs in the deuterostomes in a similar way to that in the protostomes [144]. However, others have suggested that apoptosis activation in echinoderms may not involve cytochrome *c* release from mitochondria as cytochrome *c* is not apparently necessary for Apaf-1-activated apoptosis in the starfish *Asterina pectinifera* [145]. In the nonmammalian vertebrates, the molecular basis of apoptosis is probably best defined in zebrafish, *Danio rerio*, where all three groups of the tripartite Bcl-2 family have been identified [146]. *D. rerio* has an extensive network of Bcl-2 proteins, but as yet there are relatively few details on the mechanism of action even in this well-studied model organism [147]. Genome duplication events in teleost fish [148] have given rise to many Bcl-2 paralogs in *D. rerio* [97], but the molecular basis of apoptosis is likely similar to that in mammals [25]. Structural studies on *D. rerio* NRZ show the structure and mode of BH3 interaction is near identical to other organisms [25]. These studies establish Bcl-2 signaling in deuterostomes share many aspects with those from the protostomes and establish the basis for intrinsic apoptosis in the bilaterians.

4. The Role of Mitochondrial Membrane Interactions

The defining event of intrinsic apoptosis in mammals is release of cytochrome *c* from the mitochondrial intermembrane space through supramolecular pores formed by Bax, Bak, or Bok oligomerization on the MOM [149] (Figure 1). Crucial to this action is the presence of a TM anchor and most members of the Bcl-2 family bear tail anchors, including BH3-only proteins, [150] necessary both for their localization at the MOM [5] and apoptotic activity [151]. TM anchor deletion mutants of Bax and Bak lose their apoptotic abilities [152], suggesting the MOM as an activator of Bax/Bak [153]. Similarly, deletion of the TM region of prosurvival Bcl-x$_L$ decreases its prosurvival activity [151]. The most striking feature of the TM regions is their poor sequence conservation [154]. Figure 2c illustrates the relatively weak conservation of the TM region compared to the BH motifs in Bax sequences. In mammalian apoptosis, cofactors such as the β-barrel Voltage Dependent Anion Channel-2 (VDAC2) may be important in Bax/Bak membrane recruitment [155], but this has not yet been demonstrated in basal metazoan apoptosis. While most investigations have focused on apoptosis in the mouse or humans, MOM association has also been observed for Bcl-2 proteins from placozoans, hydra, and viral proteins, indicating the fundamental nature of this activity to Bcl-2 action.

The structures of the proapoptotic proteins Bax, [29] Bak, [27] and Bok [156,157] have an essentially identical core that suggests a common mode of action; however, their subcellular localization and dynamics differ significantly [91]. The crystal structure of mouse Bax shows that the TM region is helical and packed in the equivalent site as occupied by EGL-1-binding CED-9 (Figure 3d,f). Prior to apoptotic stimuli, Bax is largely cytosolic [158], with a fraction being shuttled to the mitochondrion surface [159], but subsequent to apoptotic stimuli, Bax accumulates at the MOM [160,161] via a process that is dependent on its TM residues [162]. In contrast to Bax, Bak is constitutively membrane-bound and Bok is only fractionally colocalized with mitochondria [163]. The prosurvival protein Bcl-x$_L$ translocates Bax from the MOM to the cytosol, and this process is dependent on the BH3-binding groove [159] and TM region of Bcl-x$_L$ [164]. Thus, the proapoptotic proteins have complex membrane interactions and dynamics and emerging data supports a similar view in basal metazoans.

Experimental details on the localization and dynamics of Bcl-2 proteins are now emerging for the placozoan *T. adhaerens,* and a similar picture of complex dynamic behavior to mammalian Bcl-2 family proteins is emerging [78]. *T. adhaerens* Bcl-2 proteins are differentially partitioned between mitochondria, ER, and the cytosol, and the TM region is necessary for its membrane localization [78].

TrBcl2L1 is tightly associated with the MOM, while trBcl-2L2 (trMcl-1) and trBcl-2L4 (trBak) are cytosolic and only loosely associated with intracellular membranes [78] in a manner that mirrors the mammalian Bcl-2 proteins. Mammalian prosurvival proteins like the proapoptotic proteins are differentially partitioned between cytosol and membranes. For example, Bcl-2 is membrane integrated and Bcl-x$_L$ partitioned between cytosol and membranes. Like its mammalian counterpart, Trichoplax Bax (Bcl-2L3) translocates to the mitochondria and induces cytochrome *c* release [78]. However, one caveat of these discoveries is that they have been performed in heterologous systems using expression of Trichoplax proteins in mammalian cells and have yet to be confirmed in homologous systems. The studies on *T. adhaerens* Bcl-2 proteins and their membrane interactions point to the fundamental nature of membrane interactions in their mechanism of action.

Although not all viral Bcl-2 proteins bear an obvious TM region, many do [165], and membrane interactions are necessary for their prosurvival activity. This trend closely mirrors what has been observed for mammalian proteins like Bcl-x$_L$. Similarly for the viral Bcl-2 protein F1L, association with mitochondria is necessary for its prosurvival behavior [52], and M11L localizes at the mitochondria [128] and colocalizes with Bak at the MOM [166]. ASFV A179L localizes to mitochondria and ER [132]. Although C-terminal anchoring of Bcl-2 proteins is often maintained, there are exceptions; for example, vMIA targets the MOM through its N-terminal region [167]. It appears likely that the interaction of Bcl-2 proteins with membranes is fundamental to Bcl-2 function and has been conserved from the earliest metazoans and maintained in viral Bcl-2 proteins.

While MOM localization of Bcl-2 proteins may be conserved, MOMP is not necessarily maintained as a mechanism of activating apoptosis. Ecdysozoans have undergone extensive gene loss [168] and have fewer Bcl-2 genes and mechanistic differences from mammalian apoptosis (Figure 1) [169]. For example, the sole Bcl-2 protein CED-9 in the nematode *C. elegans* is TM-anchored to mitochondria like its mammalian counterpart Bcl-2 and although they have closely related structures (Figures 2 and 3) and bind BH3-only proteins in their respective binding grooves, their role in apoptosis mechanisms is not identical [7]. CED-9 binds and antagonizes the apical caspase CED-4 and once released from its inhibition by the translationally upregulated BH3-only protein EGL-1 binding CED-9, CED-4 activates the caspase CED-3 [7,96]. In comparison, Bcl-2 is also localized to the MOM amongst other intracellular membranes [91] and binds BH3-only proteins but it does not bind Apaf-1, the mammalian caspase-activating protein corresponding to CED-4. Distinct from the nematode, the role of Bcl-2 proteins in the fly *D. melanogaster* is less well understood [170]. BH3-only proteins have not been found in the genome of *D. melanogaster* but two Bcl-2 proteins, Debcl and Buffy, have been recognized and it has been shown they interact [42] and both localize to the MOM with Buffy additionally found at the ER [171]. Thus, although the sequences, structure, and membrane binding may all be conserved elements in the Bcl-2 family, there are key differences in how they are manifested in the activation of caspases.

5. Conclusions

It is not clear how the Bcl-2 family arose; one hypothesis is that it occurred through horizontal gene transfer from a symbiont [172], but multiple Bcl-2 genes occurred early in metazoan evolution. Even in the sponges, a phylum considered to be the sister group of all metazoans [135], multiple Bcl-2 fold proteins have been identified in genomes, such as that of *A. queenslandica* [137] where seven such proteins were recognized. In contrast to the early appearance of Bcl-2 fold proteins, BH3-only proteins have not yet been identified in Porifera or Placozoa. Ctenophores appear to have lost the genes required for Bcl-2-regulated apoptosis altogether (Figure 4a). Emerging results from biophysical and biochemical measurements performed on the nonmammalian Bcl-2 family including those from sponges [6], placozoans [78] and cnidarians [110] indicate that the basic architecture of intrinsic apoptosis is maintained for these basal metazoans. Structural studies have shown that the molecular details of interactions have been conserved from sponges to man [6] and viruses have assimilated Bcl-2 proteins [111]. A key difference between sponges, placozoans, and cnidarians is an apparent absence

of BH3-only proteins in sponges and placozoans. The essential role of the BH3-only proteins, at least in mammals, is to neutralize the prosurvival proteins to allow the MOM to activate the proapoptotic Bcl-2 proteins [153]. Based on these results, a hypothesis for a simple model for intrinsic apoptosis in the absence of BH3-ony proteins could be envisaged as the prosurvival proteins keeping the proapoptotic proteins in check. Alternately, as recently proposed, the Bak-like protein may partially fulfill the role of BH3-only proteins [78] (Figure 4b). The investigation of the more evolutionary distant members of the Bcl-2 family has exposed the substantial complexity in Bcl-2-mediated signaling at the foundation of metazoan evolution and underscores the pivotal role these proteins play in biology. Functional and mechanistic studies to date have only just begun to unravel the role Bcl-2 has played during the early stages of metazoan life, and future studies are likely to discover new twists to Bcl-2 signaling.
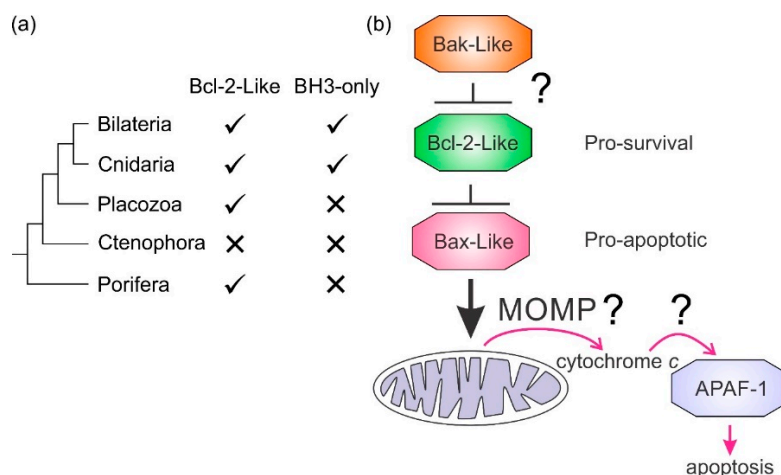
Figure 4. Bcl-2-like proteins in basal metazoan clades and potential apoptosis model. (**a**) Metazoan phylogenetic relationships and the presence or absence of Bcl-2 proteins. The presence or absence of Bcl-2 family members is indicated. (**b**) A simple model for intrinsic apoptosis in Porifera and Placozoa where BH3-only proteins have not been identified. Experiments have yet to delineate the roles of MOMP and adaptor protein initiation of caspases in their entirety.

Conflicts of Interest: The authors declare no conflict of interest.

References

1.　Koonin, E.V.; Aravind, L. Origin and evolution of eukaryotic apoptosis: The bacterial connection. *Cell Death Differ.* **2002**, *9*, 394–404. [CrossRef]

2.　Huettenbrenner, S.; Maier, S.; Leisser, C.; Polgar, D.; Strasser, S.; Grusch, M.; Krupitza, G. The evolution of cell death programs as prerequisites of multicellularity. *Mutat. Res.* **2003**, *543*, 235–249. [CrossRef]

3.　Singh, R.; Letai, A.; Sarosiek, K. Regulation of apoptosis in health and disease: The balancing act of BCL-2 family proteins. *Nat. Rev. Mol. Cell Biol.* **2019**, *20*, 175–193. [CrossRef]

4.　Strasser, A.; Vaux, D.L. Viewing BCL2 and cell death control from an evolutionary perspective. *Cell Death Differ.* **2018**, *25*, 13–20. [CrossRef]

5.　Shamas-Din, A.; Kale, J.; Leber, B.; Andrews, D.W. Mechanisms of action of bcl-2 family proteins. *Cold Spring Harb. Perspect. Biol.* **2013**, *5*. [CrossRef]

6. Caria, S.; Hinds, M.G.; Kvansakul, M. Structural insight into an evolutionarily ancient programmed cell death regulator—The crystal structure of marine sponge BHP2 bound to LB-Bak-2. *Cell Death Dis.* **2017**, *8*, e2543. [CrossRef]

7. Kvansakul, M.; Hinds, M.G. The Bcl-2 family: Structures, interactions and targets for drug discovery. *Apoptosis* **2015**, *20*, 136–150. [CrossRef]

8. Kvansakul, M.; Caria, S.; Hinds, M.G. The Bcl-2 Family in Host-Virus Interactions. *Viruses* **2017**, *9*, 290. [CrossRef] [PubMed]

9. Kvansakul, M.; Hinds, M.G. The structural biology of BH3-only proteins. *Methods Enzymol.* **2014**, *544*, 49–74. [PubMed]

10. Petros, A.M.; Medek, A.; Nettesheim, D.G.; Kim, D.H.; Yoon, H.S.; Swift, K.; Matayoshi, E.D.; Oltersdorf, T.; Fesik, S.W. Solution structure of the antiapoptotic protein bcl-2. *Proc. Natl. Acad. Sci. USA* **2001**, *98*, 3012–3017. [CrossRef] [PubMed]

11. Vaux, D.L.; Cory, S.; Adams, J.M. Bcl-2 gene promotes haemopoietic cell survival and cooperates with c-myc to immortalize pre-B cells. *Nature* **1988**, *335*, 440–442. [CrossRef] [PubMed]

12. Denisov, A.Y.; Madiraju, M.S.; Chen, G.; Khadir, A.; Beauparlant, P.; Attardo, G.; Shore, G.C.; Gehring, K. Solution structure of human BCL-w: Modulation of ligand binding by the C-terminal helix. *J. Biol. Chem.* **2003**, *278*, 21124–21128. [CrossRef] [PubMed]

13. Gibson, L.; Holmgreen, S.P.; Huang, D.C.; Bernard, O.; Copeland, N.G.; Jenkins, N.A.; Sutherland, G.R.; Baker, E.; Adams, J.M.; Cory, S. bcl-w, a novel member of the bcl-2 family, promotes cell survival. *Oncogene* **1996**, *13*, 665–675. [PubMed]

14. Hinds, M.G.; Lackmann, M.; Skea, G.L.; Harrison, P.J.; Huang, D.C.; Day, C.L. The structure of Bcl-w reveals a role for the C-terminal residues in modulating biological activity. *EMBO J.* **2003**, *22*, 1497–1507. [CrossRef] [PubMed]

15. Boise, L.H.; Gonzalez-Garcia, M.; Postema, C.E.; Ding, L.; Lindsten, T.; Turka, L.A.; Mao, X.; Nunez, G.; Thompson, C.B. bcl-x, a bcl-2-related gene that functions as a dominant regulator of apoptotic cell death. *Cell* **1993**, *74*, 597–608. [CrossRef]

16. Muchmore, S.W.; Sattler, M.; Liang, H.; Meadows, R.P.; Harlan, J.E.; Yoon, H.S.; Nettesheim, D.; Chang, B.S.; Thompson, C.B.; Wong, S.L.; et al. X-ray and NMR structure of human Bcl-xL, an inhibitor of programmed cell death. *Nature* **1996**, *381*, 335–341. [CrossRef]

17. Rinkenberger, J.L.; Horning, S.; Klocke, B.; Roth, K.; Korsmeyer, S.J. Mcl-1 deficiency results in peri-implantation embryonic lethality. *Genes Dev.* **2000**, *14*, 23–27.

18. Day, C.L.; Chen, L.; Richardson, S.J.; Harrison, P.J.; Huang, D.C.; Hinds, M.G. Solution structure of prosurvival Mcl-1 and characterization of its binding by proapoptotic BH3-only ligands. *J. Biol. Chem.* **2005**, *280*, 4738–4744. [CrossRef]

19. Smits, C.; Czabotar, P.E.; Hinds, M.G.; Day, C.L. Structural plasticity underpins promiscuous binding of the prosurvival protein A1. *Structure* **2008**, *16*, 818–829. [CrossRef]

20. Karsan, A.; Yee, E.; Kaushansky, K.; Harlan, J.M. Cloning of human Bcl-2 homologue: Inflammatory cytokines induce human A1 in cultured endothelial cells. *Blood* **1996**, *87*, 3089–3096. [CrossRef]

21. Ke, N.; Godzik, A.; Reed, J.C. Bcl-B, a novel Bcl-2 family member that differentially binds and regulates Bax and Bak. *J. Biol. Chem.* **2001**, *276*, 12481–12484. [CrossRef] [PubMed]

22. Rautureau, G.J.; Yabal, M.; Yang, H.; Huang, D.C.; Kvansakul, M.; Hinds, M.G. The restricted binding repertoire of Bcl-B leaves Bim as the universal BH3-only prosurvival Bcl-2 protein antagonist. *Cell Death Dis.* **2012**, *3*, e443. [CrossRef] [PubMed]

23. Rautureau, G.J.; Day, C.L.; Hinds, M.G. The structure of Boo/Diva reveals a divergent Bcl-2 protein. *Proteins* **2010**, *78*, 2181–2186. [CrossRef] [PubMed]

24. Arnaud, E.; Ferri, K.F.; Thibaut, J.; Haftek-Terreau, Z.; Aouacheria, A.; Le Guellec, D.; Lorca, T.; Gillet, G. The zebrafish bcl-2 homologue Nrz controls development during somitogenesis and gastrulation via apoptosis-dependent and -independent mechanisms. *Cell Death Differ.* **2006**, *13*, 1128–1137. [CrossRef]

25. Suraweera, C.D.; Caria, S.; Jarva, M.; Hinds, M.G.; Kvansakul, M. A structural investigation of NRZ mediated apoptosis regulation in zebrafish. *Cell Death Dis.* **2018**, *9*, 967. [CrossRef]

26. Chittenden, T.; Flemington, C.; Houghton, A.B.; Ebb, R.G.; Gallo, G.J.; Elangovan, B.; Chinnadurai, G.; Lutz, R.J. A conserved domain in Bak, distinct from BH1 and BH2, mediates cell death and protein binding functions. *EMBO J.* **1995**, *14*, 5589–5596. [CrossRef]

27. Moldoveanu, T.; Liu, Q.; Tocilj, A.; Watson, M.; Shore, G.; Gehring, K. The X-ray structure of a BAK homodimer reveals an inhibitory zinc binding site. *Mol. Cell* **2006**, *24*, 677–688. [CrossRef]

28. Oltvai, Z.N.; Milliman, C.L.; Korsmeyer, S.J. Bcl-2 heterodimerizes in vivo with a conserved homolog, Bax, that accelerates programmed cell death. *Cell* **1993**, *74*, 609–619. [CrossRef]

29. Suzuki, M.; Youle, R.J.; Tjandra, N. Structure of Bax: Coregulation of dimer formation and intracellular localization. *Cell* **2000**, *103*, 645–654. [CrossRef]

30. Hsu, S.Y.; Kaipia, A.; McGee, E.; Lomeli, M.; Hsueh, A.J. Bok is a pro-apoptotic Bcl-2 protein with restricted expression in reproductive tissues and heterodimerizes with selective anti-apoptotic Bcl-2 family members. *Proc. Natl. Acad. Sci. USA* **1997**, *94*, 12401–12406. [CrossRef]

31. Yang, E.; Zha, J.; Jockel, J.; Boise, L.H.; Thompson, C.B.; Korsmeyer, S.J. Bad, a heterodimeric partner for Bcl-XL and Bcl-2, displaces Bax and promotes cell death. *Cell* **1995**, *80*, 285–291. [CrossRef]

32. Wang, K.; Yin, X.M.; Chao, D.T.; Milliman, C.L.; Korsmeyer, S.J. BID: A novel BH3 domain-only death agonist. *Genes Dev.* **1996**, *10*, 2859–2869. [CrossRef] [PubMed]

33. Han, J.; Sabbatini, P.; White, E. Induction of apoptosis by human Nbk/Bik, a BH3-containing protein that interacts with E1B 19K. *Mol. Cell Biol.* **1996**, *16*, 5857–5864. [CrossRef] [PubMed]

34. O'Connor, L.; Strasser, A.; O'Reilly, L.A.; Hausmann, G.; Adams, J.M.; Cory, S.; Huang, D.C. Bim: A novel member of the Bcl-2 family that promotes apoptosis. *EMBO J.* **1998**, *17*, 384–395. [CrossRef]

35. Puthalakath, H.; Villunger, A.; O'Reilly, L.A.; Beaumont, J.G.; Coultas, L.; Cheney, R.E.; Huang, D.C.; Strasser, A. Bmf: A proapoptotic BH3-only protein regulated by interaction with the myosin V actin motor complex, activated by anoikis. *Science* **2001**, *293*, 1829–1832. [CrossRef]

36. Inohara, N.; Ding, L.; Chen, S.; Nunez, G. harakiri, a novel regulator of cell death, encodes a protein that activates apoptosis and interacts selectively with survival-promoting proteins Bcl-2 and Bcl-X(L). *EMBO J.* **1997**, *16*, 1686–1694. [CrossRef]

37. Hijikata, M.; Kato, N.; Sato, T.; Kagami, Y.; Shimotohno, K. Molecular cloning and characterization of a cDNA for a novel phorbol-12-myristate-13-acetate-responsive gene that is highly expressed in an adult T-cell leukemia cell line. *J. Virol.* **1990**, *64*, 4632–4639. [CrossRef]

38. Nakano, K.; Vousden, K.H. PUMA, a novel proapoptotic gene, is induced by p53. *Mol. Cell* **2001**, *7*, 683–694. [CrossRef]

39. Liang, X.H.; Kleeman, L.K.; Jiang, H.H.; Gordon, G.; Goldman, J.E.; Berry, G.; Herman, B.; Levine, B. Protection against fatal Sindbis virus encephalitis by beclin, a novel Bcl-2-interacting protein. *J. Virol.* **1998**, *72*, 8586–8596. [CrossRef]

40. Prudent, J.; Gillet, G.; Popgeorgiev, N. Nrz but not zBcl-xL antagonizes Bcl-wav pro-apoptotic activity in zebrafish. *Commun. Integr. Biol.* **2014**, *7*, e28008. [CrossRef]

41. Prudent, J.; Popgeorgiev, N.; Bonneau, B.; Thibaut, J.; Gadet, R.; Lopez, J.; Gonzalo, P.; Rimokh, R.; Manon, S.; Houart, C.; et al. Bcl-wav and the mitochondrial calcium uniporter drive gastrula morphogenesis in zebrafish. *Nat. Commun.* **2013**, *4*, 2330. [CrossRef] [PubMed]

42. Quinn, L.; Coombe, M.; Mills, K.; Daish, T.; Colussi, P.; Kumar, S.; Richardson, H. Buffy, a Drosophila Bcl-2 protein, has anti-apoptotic and cell cycle inhibitory functions. *EMBO J.* **2003**, *22*, 3568–3579. [CrossRef] [PubMed]

43. Colussi, P.A.; Quinn, L.M.; Huang, D.C.; Coombe, M.; Read, S.H.; Richardson, H.; Kumar, S. Debcl, a proapoptotic Bcl-2 homologue, is a component of the Drosophila melanogaster cell death machinery. *J. Cell Biol.* **2000**, *148*, 703–714. [CrossRef] [PubMed]

44. Henderson, S.; Huen, D.; Rowe, M.; Dawson, C.; Johnson, G.; Rickinson, A. Epstein-Barr virus-coded BHRF1 protein, a viral homologue of Bcl-2, protects human B cells from programmed cell death. *Proc. Natl. Acad. Sci. USA* **1993**, *90*, 8479–8483. [CrossRef] [PubMed]

45. Huang, Q.; Petros, A.M.; Virgin, H.W.; Fesik, S.W.; Olejniczak, E.T. Solution structure of the BHRF1 protein from Epstein-Barr virus, a homolog of human Bcl-2. *J. Mol. Biol.* **2003**, *332*, 1123–1130. [CrossRef]

46. Sarid, R.; Sato, T.; Bohenzky, R.A.; Russo, J.J.; Chang, Y. Kaposi's sarcoma-associated herpesvirus encodes a functional Bcl-2 homologue. *Nat. Med.* **1997**, *3*, 293–298. [CrossRef]

47. White, E.; Sabbatini, P.; Debbas, M.; Wold, W.S.; Kusher, D.I.; Gooding, L.R. The 19-kilodalton adenovirus E1B transforming protein inhibits programmed cell death and prevents cytolysis by tumor necrosis factor alpha. *Mol. Cell Biol.* **1992**, *12*, 2570–2580. [CrossRef]

48. Wang, G.H.; Garvey, T.L.; Cohen, J.I. The murine gammaherpesvirus-68 M11 protein inhibits Fas- and TNF-induced apoptosis. *J. Gen. Virol.* **1999**, *80 Pt 10*, 2737–2740. [CrossRef]

49. Sinha, S.; Colbert, C.L.; Becker, N.; Wei, Y.; Levine, B. Molecular basis of the regulation of Beclin 1-dependent autophagy by the gamma-herpesvirus 68 Bcl-2 homolog M11. *Autophagy* **2008**, *4*, 989–997. [CrossRef]

50. Brun, A.; Rivas, C.; Esteban, M.; Escribano, J.M.; Alonso, C. African swine fever virus gene A179L, a viral homologue of Bcl-2, protects cells from programmed cell death. *Virology* **1996**, *225*, 227–230. [CrossRef]

51. Banjara, S.; Caria, S.; Dixon, L.K.; Hinds, M.G.; Kvansakul, M. Structural Insight into African Swine Fever Virus A179L-Mediated Inhibition of Apoptosis. *J. Virol.* **2017**, *91*, e02228-16. [CrossRef] [PubMed]

52. Stewart, T.L.; Wasilenko, S.T.; Barry, M. Vaccinia virus F1L protein is a tail-anchored protein that functions at the mitochondria to inhibit apoptosis. *J. Virol.* **2005**, *79*, 1084–1098. [CrossRef] [PubMed]

53. Kvansakul, M.; Yang, H.; Fairlie, W.D.; Czabotar, P.E.; Fischer, S.F.; Perugini, M.A.; Huang, D.C.; Colman, P.M. Vaccinia virus anti-apoptotic F1L is a novel Bcl-2-like domain-swapped dimer that binds a highly selective subset of BH3-containing death ligands. *Cell Death Differ.* **2008**, *15*, 1564–1571. [CrossRef] [PubMed]

54. Burton, D.R.; Caria, S.; Marshall, B.; Barry, M.; Kvansakul, M. Structural basis of Deerpox virus-mediated inhibition of apoptosis. *Acta Crystallogr. D Biol. Crystallogr.* **2015**, *71*, 1593–1603. [CrossRef]

55. Banadyga, L.; Lam, S.C.; Okamoto, T.; Kvansakul, M.; Huang, D.C.; Barry, M. Deerpox virus encodes an inhibitor of apoptosis that regulates Bak and Bax. *J. Virol.* **2011**, *85*, 1922–1934. [CrossRef] [PubMed]

56. Opgenorth, A.; Graham, K.; Nation, N.; Strayer, D.; McFadden, G. Deletion analysis of two tandemly arranged virulence genes in myxoma virus, M11L and myxoma growth factor. *J. Virol.* **1992**, *66*, 4720–4731. [CrossRef]

57. Kvansakul, M.; van Delft, M.F.; Lee, E.F.; Gulbis, J.M.; Fairlie, W.D.; Huang, D.C.; Colman, P.M. A structural viral mimic of prosurvival Bcl-2: A pivotal role for sequestering proapoptotic Bax and Bak. *Mol. Cell* **2007**, *25*, 933–942. [CrossRef]

58. Banadyga, L.; Gerig, J.; Stewart, T.; Barry, M. Fowlpox virus encodes a Bcl-2 homologue that protects cells from apoptotic death through interaction with the proapoptotic protein Bak. *J. Virol.* **2007**, *81*, 11032–11045. [CrossRef]

59. Anasir, M.I.; Caria, S.; Skinner, M.A.; Kvansakul, M. Structural basis of apoptosis inhibition by the fowlpox virus protein FPV039. *J. Biol. Chem.* **2017**, *292*, 9010–9021. [CrossRef]

60. Tulman, E.R.; Afonso, C.L.; Lu, Z.; Zsak, L.; Kutish, G.F.; Rock, D.L. The genome of canarypox virus. *J. Virol.* **2004**, *78*, 353–366. [CrossRef]

61. Anasir, M.I.; Baxter, A.A.; Poon, I.K.H.; Hulett, M.D.; Kvansakul, M. Structural and Functional Insight into Canarypox Virus CNP058 Mediated Regulation of Apoptosis. *Viruses* **2017**, *9*, 305. [CrossRef] [PubMed]

62. Okamoto, T.; Campbell, S.; Mehta, N.; Thibault, J.; Colman, P.M.; Barry, M.; Huang, D.C.; Kvansakul, M. Sheeppox Virus SPPV14 Encodes a Bcl-2-like Cell Death Inhibitor that Counters a Distinct Set of Mammalian Pro-apoptotic Proteins. *J. Virol.* **2012**, *15*, 11501–11511. [CrossRef] [PubMed]

63. Westphal, D.; Ledgerwood, E.C.; Tyndall, J.D.; Hibma, M.H.; Ueda, N.; Fleming, S.B.; Mercer, A.A. The orf virus inhibitor of apoptosis functions in a Bcl-2-like manner, binding and neutralizing a set of BH3-only proteins and active Bax. *Apoptosis* **2009**, *14*, 1317–1330. [CrossRef] [PubMed]

64. Banjara, S.; Mao, J.; Ryan, T.M.; Caria, S.; Kvansakul, M. Grouper iridovirus GIV66 is a Bcl-2 protein that inhibits apoptosis by exclusively sequestering Bim. *J. Biol. Chem.* **2018**, *293*, 5464–5477. [CrossRef]

65. Lin, P.W.; Huang, Y.J.; John, J.A.; Chang, Y.N.; Yuan, C.H.; Chen, W.Y.; Yeh, C.H.; Shen, S.T.; Lin, F.P.; Tsui, W.H.; et al. Iridovirus Bcl-2 protein inhibits apoptosis in the early stage of viral infection. *Apoptosis* **2008**, *13*, 165–176. [CrossRef]

66. Bartlett, N.; Symons, J.A.; Tscharke, D.C.; Smith, G.L. The vaccinia virus N1L protein is an intracellular homodimer that promotes virulence. *J. Gen. Virol.* **2002**, *83*, 1965–1976. [CrossRef]

67. Cooray, S.; Bahar, M.W.; Abrescia, N.G.; McVey, C.E.; Bartlett, N.W.; Chen, R.A.; Stuart, D.I.; Grimes, J.M.; Smith, G.L. Functional and structural studies of the vaccinia virus virulence factor N1 reveal a Bcl-2-like anti-apoptotic protein. *J. Gen. Virol.* **2007**, *88*, 1656–1666. [CrossRef]

68. Fedosyuk, S.; Grishkovskaya, I.; de Almeida Ribeiro, E., Jr.; Skern, T. Characterization and structure of the vaccinia virus NF-kappaB antagonist A46. *J. Biol.Chem.* **2014**, *289*, 3749–3762. [CrossRef]

69. Gonzalez, J.M.; Esteban, M. A poxvirus Bcl-2-like gene family involved in regulation of host immune response: Sequence similarity and evolutionary history. *Virol. J.* **2010**, *7*, 59. [CrossRef]

70. Neidel, S.; Maluquer de Motes, C.; Mansur, D.S.; Strnadova, P.; Smith, G.L.; Graham, S.C. Vaccinia virus protein A49 is an unexpected member of the B-cell Lymphoma (Bcl)-2 protein family. *J. Biol. Chem.* **2015**, *290*, 5991–6002. [CrossRef]

71. Mansur, D.S.; Maluquer de Motes, C.; Unterholzner, L.; Sumner, R.P.; Ferguson, B.J.; Ren, H.; Strnadova, P.; Bowie, A.G.; Smith, G.L. Poxvirus targeting of E3 ligase beta-TrCP by molecular mimicry: A mechanism to inhibit NF-kappaB activation and promote immune evasion and virulence. *PLoS Pathog.* **2013**, *9*, e1003183. [CrossRef] [PubMed]

72. Graham, S.C.; Bahar, M.W.; Cooray, S.; Chen, R.A.; Whalen, D.M.; Abrescia, N.G.; Alderton, D.; Owens, R.J.; Stuart, D.I.; Smith, G.L.; et al. Vaccinia virus proteins A52 and B14 Share a Bcl-2-like fold but have evolved to inhibit NF-kappaB rather than apoptosis. *PLoS Pathog.* **2008**, *4*, e1000128. [CrossRef] [PubMed]

73. Chen, R.A.; Jacobs, N.; Smith, G.L. Vaccinia virus strain Western Reserve protein B14 is an intracellular virulence factor. *J. Gen. Virol.* **2006**, *87*, 1451–1458. [CrossRef] [PubMed]

74. Schroder, M.; Baran, M.; Bowie, A.G. Viral targeting of DEAD box protein 3 reveals its role in TBK1/IKKepsilon-mediated IRF activation. *EMBO J.* **2008**, *27*, 2147–2157. [CrossRef]

75. Kalverda, A.P.; Thompson, G.S.; Vogel, A.; Schroder, M.; Bowie, A.G.; Khan, A.R.; Homans, S.W. Poxvirus K7 protein adopts a Bcl-2 fold: Biochemical mapping of its interactions with human DEAD box RNA helicase DDX3. *J. Mol. Biol.* **2009**, *385*, 843–853. [CrossRef]

76. Wiens, M.; Belikov, S.I.; Kaluzhnaya, O.V.; Schroder, H.C.; Hamer, B.; Perovic-Ottstadt, S.; Borejko, A.; Luthringer, B.; Muller, I.M.; Muller, W.E. Axial (apical-basal) expression of pro-apoptotic and pro-survival genes in the lake baikal demosponge Lubomirskia baicalensis. *DNA Cell Biol.* **2006**, *25*, 152–164. [CrossRef]

77. Wiens, M.; Diehl-Seifert, B.; Muller, W.E. Sponge Bcl-2 homologous protein (BHP2-GC) confers distinct stress resistance to human HEK-293 cells. *Cell Death Differ.* **2001**, *8*, 887–898. [CrossRef]

78. Popgeorgiev, N.; Jabbour, L.; Nguyen, T.T.M.; Ralchev, N.; Gadet, R.; Manon, S.; Osigus, H.-J.; Schierwater, B.; Rimokh, R.; Gillet, G. Pleiotropy of Bcl-2 family proteins is an ancient trait in the metazoan evolution. *bioRxiv* **2019**. [CrossRef]

79. Yan, N.; Gu, L.; Kokel, D.; Chai, J.; Li, W.; Han, A.; Chen, L.; Xue, D.; Shi, Y. Structural, biochemical, and functional analyses of CED-9 recognition by the proapoptotic proteins EGL-1 and CED-4. *Mol. Cell* **2004**, *15*, 999–1006. [CrossRef]

80. Conradt, B.; Horvitz, H.R. The C. elegans protein EGL-1 is required for programmed cell death and interacts with the Bcl-2-like protein CED-9. *Cell* **1998**, *93*, 519–529. [CrossRef]

81. Hengartner, M.O.; Horvitz, H.R. C. elegans cell survival gene ced-9 encodes a functional homolog of the mammalian proto-oncogene bcl-2. *Cell* **1994**, *76*, 665–676. [CrossRef]

82. Woo, J.S.; Jung, J.S.; Ha, N.C.; Shin, J.; Kim, K.H.; Lee, W.; Oh, B.H. Unique structural features of a BCL-2 family protein CED-9 and biophysical characterization of CED-9/EGL-1 interactions. *Cell Death Differ.* **2003**, *10*, 1310–1319. [CrossRef] [PubMed]

83. Goldmacher, V.S.; Bartle, L.M.; Skaletskaya, A.; Dionne, C.A.; Kedersha, N.L.; Vater, C.A.; Han, J.W.; Lutz, R.J.; Watanabe, S.; Cahir McFarland, E.D.; et al. A cytomegalovirus-encoded mitochondria-localized inhibitor of apoptosis structurally unrelated to Bcl-2. *Proc. Natl. Acad. Sci. USA* **1999**, *96*, 12536–12541. [CrossRef] [PubMed]

84. Ma, J.; Edlich, F.; Bermejo, G.A.; Norris, K.L.; Youle, R.J.; Tjandra, N. Structural mechanism of Bax inhibition by cytomegalovirus protein vMIA. *Proc. Natl. Acad. Sci. USA* **2012**, *109*, 20901–20906. [CrossRef] [PubMed]

85. Holm, L.; Laakso, L.M. Dali server update. *Nucleic Acids Res.* **2016**, *44*, W351–W355. [CrossRef]

86. Wheeler, T.J.; Clements, J.; Finn, R.D. Skylign: A tool for creating informative, interactive logos representing sequence alignments and profile hidden Markov models. *BMC Bioinform.* **2014**, *15*, 7. [CrossRef]

87. Gavathiotis, E.; Suzuki, M.; Davis, M.L.; Pitter, K.; Bird, G.H.; Katz, S.G.; Tu, H.C.; Kim, H.; Cheng, E.H.; Tjandra, N.; et al. BAX activation is initiated at a novel interaction site. *Nature* **2008**, *455*, 1076–1081. [CrossRef]

88. Lalle, P.; Aouacheria, A.; Dumont-Miscopein, A.; Jambon, M.; Venet, S.; Bobichon, H.; Colas, P.; Deleage, G.; Geourjon, C.; Gillet, G. Evidence for crucial electrostatic interactions between Bcl-2 homology domains BH3 and BH4 in the anti-apoptotic Nr-13 protein. *Biochem. J.* **2002**, *368*, 213–221. [CrossRef]

89. De Motes, C.M.; Cooray, S.; Ren, H.; Almeida, G.M.F.; McGourty, K.; Bahar, M.W.; Stuart, D.I.; Grimes, J.M.; Graham, S.C.; Smith, G.L. Inhibition of Apoptosis and NF-kB Activation by Vaccinia Protein N1 Occur via Distinct Binding Surfaces and Make Different Contributions to Virulence. *PLoS Pathog.* **2011**, *7*, e1002430.

90. Huang, D.C.; Strasser, A. BH3-Only proteins-essential initiators of apoptotic cell death. *Cell* **2000**, *103*, 839–842. [CrossRef]

91. Popgeorgiev, N.; Jabbour, L.; Gillet, G. Subcellular Localization and Dynamics of the Bcl-2 Family of Proteins. *Front. Cell Dev. Biol.* **2018**, *6*, 13. [CrossRef] [PubMed]

92. Aouacheria, A.; Brunet, F.; Gouy, M. Phylogenomics of life-or-death switches in multicellular animals: Bcl-2, BH3-Only, and BNip families of apoptotic regulators. *Mol. Biol. Evol.* **2005**, *22*, 2395–2416. [CrossRef] [PubMed]

93. Day, C.L.; Smits, C.; Fan, F.C.; Lee, E.F.; Fairlie, W.D.; Hinds, M.G. Structure of the BH3 domains from the p53-inducible BH3-only proteins Noxa and Puma in complex with Mcl-1. *J. Mol. Biol.* **2008**, *380*, 958–971. [CrossRef] [PubMed]

94. Bouillet, P.; Strasser, A. BH3-only protein—Sevolutionarily conserved proapoptotic Bcl-2 family members essential for initiating programmed cell death. *J. Cell Sci.* **2002**, *115*, 1567–1574.

95. Huang, K.; O'Neill, K.L.; Li, J.; Zhou, W.; Han, N.; Pang, X.; Wu, W.; Struble, L.; Borgstahl, G.; Liu, Z.; et al. BH3-only proteins target BCL-xL/MCL-1, not BAX/BAK, to initiate apoptosis. *Cell Res.* **2019**. [CrossRef]

96. Metzstein, M.M.; Stanfield, G.M.; Horvitz, H.R. Genetics of programmed cell death in C. elegans: Past, present and future. *Trends Genet.* **1998**, *14*, 410–416. [CrossRef]

97. Prudent, J.; Popgeorgiev, N.; Bonneau, B.; Gillet, G. Bcl-2 proteins, cell migration and embryonic development: Lessons from zebrafish. *Cell Death Dis.* **2015**, *6*, e1910. [CrossRef]

98. Hardwick, J.M.; Chen, Y.B.; Jonas, E.A. Multipolar functions of BCL-2 proteins link energetics to apoptosis. *Trends Cell Biol.* **2012**, *22*, 318–328. [CrossRef]

99. Aouacheria, A.; Baghdiguian, S.; Lamb, H.M.; Huska, J.D.; Pineda, F.J.; Hardwick, J.M. Connecting mitochondrial dynamics and life-or-death events via Bcl-2 family proteins. *Neurochem. Int.* **2017**, *109*, 141–161. [CrossRef]

100. Oberstein, A.; Jeffrey, P.D.; Shi, Y. Crystal structure of the Bcl-XL-Beclin 1 peptide complex: Beclin 1 is a novel BH3-only protein. *J. Biol. Chem.* **2007**, *282*, 13123–13132. [CrossRef]

101. Ku, B.; Woo, J.S.; Liang, C.; Lee, K.H.; Hong, H.S.; E, X.; Kim, K.S.; Jung, J.U.; Oh, B.H. Structural and biochemical bases for the inhibition of autophagy and apoptosis by viral BCL-2 of murine gamma-herpesvirus 68. *PLoS Pathog.* **2008**, *4*, e25. [CrossRef] [PubMed]

102. Lee, E.F.; Perugini, M.A.; Pettikiriarachchi, A.; Evangelista, M.; Keizer, D.W.; Yao, S.; Fairlie, W.D. The BECN1 N-terminal domain is intrinsically disordered. *Autophagy* **2016**, *12*, 460–471. [CrossRef] [PubMed]

103. Huang, W.; Choi, W.; Hu, W.; Mi, N.; Guo, Q.; Ma, M.; Liu, M.; Tian, Y.; Lu, P.; Wang, F.L.; et al. Crystal structure and biochemical analyses reveal Beclin 1 as a novel membrane binding protein. *Cell Res.* **2012**, *22*, 473–489. [CrossRef] [PubMed]

104. Hanahan, D.; Weinberg, R.A. Hallmarks of cancer: The next generation. *Cell* **2011**, *144*, 646–674. [CrossRef]

105. Aktipis, C.A.; Boddy, A.M.; Jansen, G.; Hibner, U.; Hochberg, M.E.; Maley, C.C.; Wilkinson, G.S. Cancer across the tree of life: Cooperation and cheating in multicellularity. *Philos. Trans. R. Soc. Lond. B Biol. Sci.* **2015**, *370*. [CrossRef] [PubMed]

106. Domazet-Loso, T.; Klimovich, A.; Anokhin, B.; Anton-Erxleben, F.; Hamm, M.J.; Lange, C.; Bosch, T.C. Naturally occurring tumours in the basal metazoan Hydra. *Nat. Commun.* **2014**, *5*, 4222. [CrossRef] [PubMed]

107. Peters, E.C.; Halas, J.C.; McCarty, H.B. Calicoblastic neoplasms in Acropora palmata, with a review of reports on anomalies of growth and form in corals. *J. Natl. Cancer Inst.* **1986**, *76*, 895–912.

108. Hesselman, D.M.; Blake, N.J.; Peters, E.C. Gonadal neoplasms in hard shell clams Mercenaria spp., from the Indian River, Florida: Occurrence, prevalence, and histopathology. *J. Invertebr. Pathol.* **1988**, *52*, 436–446. [CrossRef]

109. Albuquerque, T.A.F.; Drummond do Val, L.; Doherty, A.; de Magalhaes, J.P. From humans to hydra: Patterns of cancer across the tree of life. *Biol. Rev. Camb. Philos. Soc.* **2018**, *93*, 1715–1734. [CrossRef]

110. Lasi, M.; Pauly, B.; Schmidt, N.; Cikala, M.; Stiening, B.; Kasbauer, T.; Zenner, G.; Popp, T.; Wagner, A.; Knapp, R.T.; et al. The molecular cell death machinery in the simple cnidarian Hydra includes an expanded caspase family and pro- and anti-apoptotic Bcl-2 proteins. *Cell Res.* **2010**, *20*, 812–825. [CrossRef]

111. Kvansakul, M.; Hinds, M.G. Structural biology of the Bcl-2 family and its mimicry by viral proteins. *Cell Death Dis.* **2013**, *4*, e909. [CrossRef] [PubMed]

112. Chiou, S.K.; Tseng, C.C.; Rao, L.; White, E. Functional complementation of the adenovirus E1B 19-kilodalton protein with Bcl-2 in the inhibition of apoptosis in infected cells. *J. Virol.* **1994**, *68*, 6553–6566. [CrossRef] [PubMed]

113. Zhang, T.Y.; Chen, H.Y.; Cao, J.L.; Xiong, H.L.; Mo, X.B.; Li, T.L.; Kang, X.Z.; Zhao, J.H.; Yin, B.; Zhao, X.; et al. Structural and functional analyses of hepatitis B virus X protein BH3-like domain and Bcl-xL interaction. *Nat. Commun.* **2019**, *10*, 3192. [CrossRef] [PubMed]

114. Kvansakul, M.; Wei, A.H.; Fletcher, J.I.; Willis, S.N.; Chen, L.; Roberts, A.W.; Huang, D.C.; Colman, P.M. Structural basis for apoptosis inhibition by Epstein-Barr virus BHRF1. *PLoS Pathog.* **2010**, *6*, e1001236. [CrossRef]

115. Fitzsimmons, L.; Cartlidge, R.; Chang, C.; Sejic, N.; Galbraith, L.C.A.; Suraweera, C.D.; Croom-Carter, D.; Dewson, G.; Tierney, R.J.; Bell, A.I.; et al. EBV BCL-2 homologue BHRF1 drives chemoresistance and lymphomagenesis by inhibiting multiple cellular pro-apoptotic proteins. *Cell Death Differ.* **2019**. [CrossRef]

116. Desbien, A.L.; Kappler, J.W.; Marrack, P. The Epstein-Barr virus Bcl-2 homolog, BHRF1, blocks apoptosis by binding to a limited amount of Bim. *Proc. Natl. Acad. Sci. USA* **2009**, *106*, 5663–5668. [CrossRef]

117. Virgin, H.W.T.; Latreille, P.; Wamsley, P.; Hallsworth, K.; Weck, K.E.; Dal Canto, A.J.; Speck, S.H. Complete sequence and genomic analysis of murine gammaherpesvirus 68. *J. Virol.* **1997**, *71*, 5894–5904. [CrossRef]

118. Piya, S.; White, E.J.; Klein, S.R.; Jiang, H.; McDonnell, T.J.; Gomez-Manzano, C.; Fueyo, J. The E1B19K oncoprotein complexes with Beclin 1 to regulate autophagy in adenovirus-infected cells. *PLoS ONE* **2011**, *6*, e29467. [CrossRef]

119. Wasilenko, S.T.; Stewart, T.L.; Meyers, A.F.; Barry, M. Vaccinia virus encodes a previously uncharacterized mitochondrial-associated inhibitor of apoptosis. *Proc. Natl. Acad. Sci. USA* **2003**, *100*, 14345–14350. [CrossRef]

120. Fischer, S.F.; Ludwig, H.; Holzapfel, J.; Kvansakul, M.; Chen, L.; Huang, D.C.; Sutter, G.; Knese, M.; Hacker, G. Modified vaccinia virus Ankara protein F1L is a novel BH3-domain-binding protein and acts together with the early viral protein E3L to block virus-associated apoptosis. *Cell Death Differ.* **2006**, *13*, 109–118. [CrossRef]

121. Campbell, S.; Thibault, J.; Mehta, N.; Colman, P.M.; Barry, M.; Kvansakul, M. Structural insight into BH3 domain binding of vaccinia virus antiapoptotic F1L. *J. Virol.* **2014**, *88*, 8667–8677. [CrossRef]

122. Czabotar, P.E.; Westphal, D.; Dewson, G.; Ma, S.; Hockings, C.; Fairlie, W.D.; Lee, E.F.; Yao, S.; Robin, A.Y.; Smith, B.J.; et al. Bax crystal structures reveal how BH3 domains activate Bax and nucleate its oligomerization to induce apoptosis. *Cell* **2013**, *152*, 519–531. [CrossRef]

123. Campbell, S.; Hazes, B.; Kvansakul, M.; Colman, P.; Barry, M. Vaccinia virus F1L interacts with Bak using highly divergent Bcl-2 homology domains and replaces the function of Mcl-1. *J. Biol. Chem.* **2010**, *285*, 4695–4708. [CrossRef] [PubMed]

124. Caria, S.; Marshall, B.; Burton, R.L.; Campbell, S.; Pantaki-Eimany, D.; Hawkins, C.J.; Barry, M.; Kvansakul, M. The N Terminus of the Vaccinia Virus Protein F1L Is an Intrinsically Unstructured Region That Is Not Involved in Apoptosis Regulation. *J. Biol. Chem.* **2016**, *291*, 14600–14608. [CrossRef] [PubMed]

125. Yu, E.; Zhai, D.; Jin, C.; Gerlic, M.; Reed, J.C.; Liddington, R. Structural determinants of caspase-9 inhibition by the vaccinia virus protein, F1L. *J. Biol. Chem.* **2011**, *286*, 30748–30758. [CrossRef] [PubMed]

126. Zhai, D.; Yu, E.; Jin, C.; Welsh, K.; Shiau, C.W.; Chen, L.; Salvesen, G.S.; Liddington, R.; Reed, J.C. Vaccinia virus protein F1L is a caspase-9 inhibitor. *J. Biol. Chem.* **2010**, *285*, 5569–5580. [CrossRef]

127. Marshall, B.; Puthalakath, H.; Caria, S.; Chugh, S.; Doerflinger, M.; Colman, P.M.; Kvansakul, M. Variola virus F1L is a Bcl-2-like protein that unlike its vaccinia virus counterpart inhibits apoptosis independent of Bim. *Cell Death Dis.* **2015**, *6*, e1680. [CrossRef]

128. Everett, H.; Barry, M.; Lee, S.F.; Sun, X.; Graham, K.; Stone, J.; Bleackley, R.C.; McFadden, G. M11L: A novel mitochondria-localized protein of myxoma virus that blocks apoptosis of infected leukocytes. *J. Exp. Med.* **2000**, *191*, 1487–1498. [CrossRef]

129. Douglas, A.E.; Corbett, K.D.; Berger, J.M.; McFadden, G.; Handel, T.M. Structure of M11L: A myxoma virus structural homolog of the apoptosis inhibitor, Bcl-2. *Protein Sci.* **2007**, *16*, 695–703. [CrossRef]

130. Neilan, J.G.; Lu, Z.; Afonso, C.L.; Kutish, G.F.; Sussman, M.D.; Rock, D.L. An African swine fever virus gene with similarity to the proto-oncogene bcl-2 and the Epstein-Barr virus gene BHRF1. *J. Virol.* **1993**, *67*, 4391–4394. [CrossRef]

131. Banjara, S.; Shimmon, G.L.; Dixon, L.K.; Netherton, C.L.; Hinds, M.G.; Kvansakul, M. Crystal Structure of African Swine Fever Virus A179L with the Autophagy Regulator Beclin. *Viruses* **2019**, *11*, 789. [CrossRef] [PubMed]

132. Hernaez, B.; Cabezas, M.; Munoz-Moreno, R.; Galindo, I.; Cuesta-Geijo, M.A.; Alonso, C. A179L, a new viral Bcl2 homolog targeting Beclin 1 autophagy related protein. *Curr. Mol. Med.* **2013**, *13*, 305–316. [CrossRef] [PubMed]

133. Aoyagi, M.; Zhai, D.; Jin, C.; Aleshin, A.E.; Stec, B.; Reed, J.C.; Liddington, R.C. Vaccinia virus N1L protein resembles a B cell lymphoma-2 (Bcl-2) family protein. *Protein Sci.* **2007**, *16*, 118–124. [CrossRef] [PubMed]

134. Kim, Y.; Lee, H.; Heo, L.; Seok, C.; Choe, J. Structure of vaccinia virus A46, an inhibitor of TLR4 signaling pathway, shows the conformation of VIPER motif. *Protein Sci.* **2014**, *23*, 906–914. [CrossRef] [PubMed]

135. Simion, P.; Philippe, H.; Baurain, D.; Jager, M.; Richter, D.J.; Di Franco, A.; Roure, B.; Satoh, N.; Queinnec, E.; Ereskovsky, A.; et al. A Large and Consistent Phylogenomic Dataset Supports Sponges as the Sister Group to All Other Animals. *Curr. Biol.* **2017**, *27*, 958–967. [CrossRef]

136. Feuda, R.; Dohrmann, M.; Pett, W.; Philippe, H.; Rota-Stabelli, O.; Lartillot, N.; Worheide, G.; Pisani, D. Improved Modeling of Compositional Heterogeneity Supports Sponges as Sister to All Other Animals. *Curr. Biol.* **2017**, *27*, 3864–3870. [CrossRef]

137. Srivastava, M.; Simakov, O.; Chapman, J.; Fahey, B.; Gauthier, M.E.; Mitros, T.; Richards, G.S.; Conaco, C.; Dacre, M.; Hellsten, U.; et al. The Amphimedon queenslandica genome and the evolution of animal complexity. *Nature* **2010**, *466*, 720–726. [CrossRef]

138. Srivastava, M.; Begovic, E.; Chapman, J.; Putnam, N.H.; Hellsten, U.; Kawashima, T.; Kuo, A.; Mitros, T.; Salamov, A.; Carpenter, M.L.; et al. The Trichoplax genome and the nature of placozoans. *Nature* **2008**, *454*, 955–960. [CrossRef]

139. Lasi, M.; David, C.N.; Bottger, A. Apoptosis in pre-Bilaterians: Hydra as a model. *Apoptosis* **2010**, *15*, 269–278. [CrossRef]

140. Chapman, J.A.; Kirkness, E.F.; Simakov, O.; Hampson, S.E.; Mitros, T.; Weinmaier, T.; Rattei, T.; Balasubramanian, P.G.; Borman, J.; Busam, D.; et al. The dynamic genome of Hydra. *Nature* **2010**, *464*, 592–596. [CrossRef]

141. Aouacheria, A.; Combet, C.; Tompa, P.; Hardwick, J.M. Redefining the BH3 Death Domain as a 'Short Linear Motif'. *Trends Biochem. Sci.* **2015**, *40*, 736–748. [CrossRef] [PubMed]

142. Yan, N.; Chai, J.; Lee, E.S.; Gu, L.; Liu, Q.; He, J.; Wu, J.W.; Kokel, D.; Li, H.; Hao, Q.; et al. Structure of the CED-4-CED-9 complex provides insights into programmed cell death in Caenorhabditis elegans. *Nature* **2005**, *437*, 831–837. [CrossRef] [PubMed]

143. Lee, E.F.; Clarke, O.B.; Evangelista, M.; Feng, Z.; Speed, T.P.; Tchoubrieva, E.B.; Strasser, A.; Kalinna, B.H.; Colman, P.M.; Fairlie, W.D. Discovery and molecular characterization of a Bcl-2-regulated cell death pathway in schistosomes. *Proc. Natl. Acad. Sci. USA* **2011**, *108*, 6999–7003. [CrossRef] [PubMed]

144. Bender, C.E.; Fitzgerald, P.; Tait, S.W.; Llambi, F.; McStay, G.P.; Tupper, D.O.; Pellettieri, J.; Sanchez Alvarado, A.; Salvesen, G.S.; Green, D.R. Mitochondrial pathway of apoptosis is ancestral in metazoans. *Proc. Natl. Acad. Sci. USA* **2012**, *109*, 4904–4909. [CrossRef]

145. Tamura, R.; Takada, M.; Sakaue, M.; Yoshida, A.; Ohi, S.; Hirano, K.; Hayakawa, T.; Hirohashi, N.; Yura, K.; Chiba, K. Starfish Apaf-1 activates effector caspase-3/9 upon apoptosis of aged eggs. *Sci. Rep.* **2018**, *8*, 1611. [CrossRef]

146. Eimon, P.M.; Ashkenazi, A. The zebrafish as a model organism for the study of apoptosis. *Apoptosis* **2010**, *15*, 331–349. [CrossRef]

147. Kratz, E.; Eimon, P.M.; Mukhyala, K.; Stern, H.; Zha, J.; Strasser, A.; Hart, R.; Ashkenazi, A. Functional characterization of the Bcl-2 gene family in the zebrafish. *Cell Death Differ.* **2006**, *13*, 1631–1640. [CrossRef]

148. Glasauer, S.M.; Neuhauss, S.C. Whole-genome duplication in teleost fishes and its evolutionary consequences. *Mol. Genet. Genom.* **2014**, *289*, 1045–1060. [CrossRef]

149. Kuwana, T.; Mackey, M.R.; Perkins, G.; Ellisman, M.H.; Latterich, M.; Schneiter, R.; Green, D.R.; Newmeyer, D.D. Bid, Bax, and lipids cooperate to form supramolecular openings in the outer mitochondrial membrane. *Cell* **2002**, *111*, 331–342. [CrossRef]

150. Wilfling, F.; Weber, A.; Potthoff, S.; Vogtle, F.N.; Meisinger, C.; Paschen, S.A.; Hacker, G. BH3-only proteins are tail-anchored in the outer mitochondrial membrane and can initiate the activation of Bax. *Cell Death Differ.* **2012**, *19*, 1328–1336. [CrossRef]

151. Wilson-Annan, J.; O'Reilly, L.A.; Crawford, S.A.; Hausmann, G.; Beaumont, J.G.; Parma, L.P.; Chen, L.; Lackmann, M.; Lithgow, T.; Hinds, M.G.; et al. Proapoptotic BH3-only proteins trigger membrane integration of prosurvival Bcl-w and neutralize its activity. *J. Cell Biol.* **2003**, *162*, 877–887. [CrossRef] [PubMed]

152. Wattenberg, B.W.; Clark, D.; Brock, S. An artificial mitochondrial tail signal/anchor sequence confirms a requirement for moderate hydrophobicity for targeting. *Biosci. Rep.* **2007**, *27*, 385–401. [CrossRef] [PubMed]

153. O'Neill, K.L.; Huang, K.; Zhang, J.; Chen, Y.; Luo, X. Inactivation of prosurvival Bcl-2 proteins activates Bax/Bak through the outer mitochondrial membrane. *Genes Dev.* **2016**, *30*, 973–988. [CrossRef] [PubMed]

154. Gomez-Fernandez, J.C. Functions of the C-terminal domains of apoptosis-related proteins of the Bcl-2 family. *Chem Phys. Lipids* **2014**, *183*, 77–90. [CrossRef] [PubMed]

155. Chin, H.S.; Li, M.X.; Tan, I.K.L.; Ninnis, R.L.; Reljic, B.; Scicluna, K.; Dagley, L.F.; Sandow, J.J.; Kelly, G.L.; Samson, A.L.; et al. VDAC2 enables BAX to mediate apoptosis and limit tumor development. *Nat. Commun.* **2018**, *9*, 4976. [CrossRef] [PubMed]

156. Ke, F.F.S.; Vanyai, H.K.; Cowan, A.D.; Delbridge, A.R.D.; Whitehead, L.; Grabow, S.; Czabotar, P.E.; Voss, A.K.; Strasser, A. Embryogenesis and Adult Life in the Absence of Intrinsic Apoptosis Effectors BAX, BAK, and BOK. *Cell* **2018**, *173*, 1217–1230. [CrossRef] [PubMed]

157. Zheng, J.H.; Grace, C.R.; Guibao, C.D.; McNamara, D.E.; Llambi, F.; Wang, Y.M.; Chen, T.; Moldoveanu, T. Intrinsic Instability of BOK Enables Membrane Permeabilization in Apoptosis. *Cell Rep.* **2018**, *23*, 2083–2094. [CrossRef]

158. Hsu, Y.T.; Youle, R.J. Bax in murine thymus is a soluble monomeric protein that displays differential detergent-induced conformations. *J. Biol. Chem.* **1998**, *273*, 10777–10783. [CrossRef]

159. Edlich, F.; Banerjee, S.; Suzuki, M.; Cleland, M.M.; Arnoult, D.; Wang, C.; Neutzner, A.; Tjandra, N.; Youle, R.J. Bcl-x(L) retrotranslocates Bax from the mitochondria into the cytosol. *Cell* **2011**, *145*, 104–116. [CrossRef]

160. Wolter, K.G.; Hsu, Y.T.; Smith, C.L.; Nechushtan, A.; Xi, X.G.; Youle, R.J. Movement of Bax from the cytosol to mitochondria during apoptosis. *J. Cell Biol.* **1997**, *139*, 1281–1292. [CrossRef]

161. Hsu, Y.T.; Wolter, K.G.; Youle, R.J. Cytosol-to-membrane redistribution of Bax and Bcl-X(L) during apoptosis. *Proc. Natl. Acad. Sci. USA* **1997**, *94*, 3668–3672. [CrossRef] [PubMed]

162. Nechushtan, A.; Smith, C.L.; Hsu, Y.T.; Youle, R.J. Conformation of the Bax C-terminus regulates subcellular location and cell death. *EMBO J.* **1999**, *18*, 2330–2341. [CrossRef] [PubMed]

163. Echeverry, N.; Bachmann, D.; Ke, F.; Strasser, A.; Simon, H.U.; Kaufmann, T. Intracellular localization of the BCL-2 family member BOK and functional implications. *Cell Death Differ.* **2013**, *20*, 785–799. [CrossRef] [PubMed]

164. Todt, F.; Cakir, Z.; Reichenbach, F.; Youle, R.J.; Edlich, F. The C-terminal helix of Bcl-x(L) mediates Bax retrotranslocation from the mitochondria. *Cell Death Differ.* **2013**, *20*, 333–342. [CrossRef]

165. Cuconati, A.; White, E. Viral homologs of BCL-2: Role of apoptosis in the regulation of virus infection. *Genes Dev.* **2002**, *16*, 2465–2478. [CrossRef]

166. Wang, G.; Barrett, J.W.; Nazarian, S.H.; Everett, H.; Gao, X.; Bleackley, C.; Colwill, K.; Moran, M.F.; McFadden, G. Myxoma virus M11L prevents apoptosis through constitutive interaction with Bak. *J. Virol.* **2004**, *78*, 7097–7111. [CrossRef]

167. Poncet, D.; Larochette, N.; Pauleau, A.L.; Boya, P.; Jalil, A.A.; Cartron, P.F.; Vallette, F.; Schnebelen, C.; Bartle, L.M.; Skaletskaya, A.; et al. An anti-apoptotic viral protein that recruits Bax to mitochondria. *J. Biol. Chem.* **2004**, *279*, 22605–22614. [CrossRef]

168. Kortschak, R.D.; Samuel, G.; Saint, R.; Miller, D.J. EST analysis of the cnidarian Acropora millepora reveals extensive gene loss and rapid sequence divergence in the model invertebrates. *Curr. Biol.* **2003**, *13*, 2190–2195. [CrossRef]

169. Fuchs, Y.; Steller, H. Programmed cell death in animal development and disease. *Cell* **2011**, *147*, 742–758. [CrossRef]

170. Clavier, A.; Rincheval-Arnold, A.; Colin, J.; Mignotte, B.; Guenal, I. Apoptosis in Drosophila: Which role for mitochondria? *Apoptosis* **2016**, *21*, 239–251. [CrossRef]

171. Doumanis, J.; Dorstyn, L.; Kumar, S. Molecular determinants of the subcellular localization of the Drosophila Bcl-2 homologues DEBCL and BUFFY. *Cell Death Differ.* **2007**, *14*, 907–915. [CrossRef] [PubMed]

172. Kroemer, G. Mitochondrial implication in apoptosis. Towards an endosymbiont hypothesis of apoptosis evolution. *Cell Death Differ.* **1997**, *4*, 443–456. [CrossRef] [PubMed]

Chapter 1B

Poxvirus Bcl-2 Modulated Apoptosis Inhibition

1B.1 Introduction

Apoptosis playing a pivotal role in development and tissue homeostasis in multicellular organisms apoptosis selectively removes unwanted, damaged or pathogen infected cells (3) (4). Initially, apoptosis probably arose as a defence mechanism against pathogens and subsequently was modified for tissue morphogenesis during development (1, 6). While necessary for homeostasis and other regulatory roles, subversion of apoptosis underlies several diseases, such as cancers and autoimmune diseases (7). Their importance in regulating cell death and immune responses has seen many apoptotic regulatory genes assimilated by viruses. Poxviruses, in particular, have captured various genes for manipulating apoptosis such as viral Bcl-2 homologs, serpin protease inhibitors, dsRNA inhibitors, NF-κB inhibitors (8, 9).

The mechanism underlying apoptosis is evolutionarily a well conserved process and has been conserved from the earliest metazoans to humans (2, 10). Metazoans share homologous genes that regulate both intrinsic and extrinsic apoptosis such as Bcl-2 proteins, caspases and adaptor genes (1). Both intrinsic and extrinsic apoptosis initiation is governed by activation of the caspase cascade, cysteine aspartyl proteases that degrade intracellular targets (11). However, there are significant differences in how the caspase cascade is initiated in intrinsic apoptosis compared with extrinsic apoptosis.

Intrinsic apoptosis is initiated by intracellular signals and primarily regulated by Bcl-2 family genes (3, 7). Bcl-2 proteins play crucial roles not only in apoptosis regulation but also have functions in autophagy (12, 13) and cytosolic Ca^{2+} regulation in higher organisms (14). The Bcl-2 family consists of both pro- and anti-apoptotic Bcl-2 members (2, 15) and share up to four conserved regions or Bcl-2 homology motifs (BH1-BH4) that are central to Bcl-2 action as either pro-survival or pro-apoptotic function. The pro-apoptotic Bcl-2 proteins are subdivided into two groups, either multi-motif pro-apoptotic

26

Bcl-2 (whose members include Bax, Bak and Bok) or BH3-only proteins (Bad, Bid, Bim, Bik, Bmf, Hrk, Noxa and Puma). Controversially, the BH3-only proteins have been further divided into two groups either activator BH3-only proteins (Bim and Bid) or sensitizer BH3-only proteins (Bad, Noxa, Bik, Bmf and Hrk). However, Puma has been characterised as either activator (16-18) or sensitizer (19, 20) in different studies. Other studies have questioned these findings as there does not appear to be a strong preference for Bax or Bak binding by BH3-motifs (21). So, Bax/Bak mediated apoptosis is maintained in the absence of all BH3-only proteins (22, 23), leading to the conclusion that BH3-only Proteins sole function is to inhibit the pro-survival Bcl-2 members (24). However they are classified, BH3-only proteins are major apoptosis inducers which are activated in response to various cellular damaging conditions and upregulate the cell death process initiating Bak and Bax oligomerization and mitochondria outer membrane permeabilization (MOMP) (25). MOMP leads to release of cytochrome c and other apoptosis inducing factors from mitochondria into the cytoplasm from the mitochondria inter membrane space to activate the subsequent caspase cascade and cell death (26).

The pro-survival Bcl-2 proteins exist as a globular helical bundle with 7 or 8 alpha helices and helices $\alpha 2$-$\alpha 5$ form the canonical hydrophobic ligand binding groove which provides the interaction site for BH3 motif of pro-apoptotic Bcl-2 proteins (4). Similarly, cellular pro-apoptotic proteins Bax, Bak and Bok have essentially the same structure as the pro-survival proteins (15), but their cellular localization differs, Bak is primarily resident in the mitochondria outer membrane or endoplasmic reticulum (ER) membrane (27), Bax is localized to the cytosol and translocates to mitochondria during apoptosis induction (28) and Bok is primarily localized to the ER (29).

As apoptosis plays an important front-line defence mechanism against invading pathogens (3, 15), viruses have evolved multiple strategies to block host apoptosis

mechanisms (9, 30) to enable successful infection and viral replication in the host-cell (31).
Most large DNA viruses, including the poxviruses, utilize protective responses during
infection to keep the host cells alive by molecular mimicry. During the infection of these
viruses produce structural, functional and sequence homologs of cellular pro-survival
proteins including Bcl-2 proteins to overturn host cell apoptosis. Pro-survival genes,
including those of the Bcl-2 family have been assimilated by viruses (2, 4). While Bcl-2
genes are not the only pro-survival factors in viral genomes, they are probably the most
well understood at a molecular level (32). Not all Bcl-2 mimics share significant sequence
similarity with mammalian Bcl-2 proteins, some shared low sequence identity ($<$ 10%)
making them difficult to identify from their sequence alone (33-35). Thus, for example,
the Bcl-2 homolog of Epstein Barr Virus (EBV) BHRF1 has 17.5% shared identity with
human Bcl-x_L, with poor sequence homology between BH regions and the myxoma virus
homolog M11L shares only 9.6% and displays no detectable BH regions, yet both viral
Bcl-2 (vBcl-2) homologs obstruct premature host cell death and are critical for successful
infection and proliferation (36).

The earliest identified vBcl-2 homologs were those identified in several virus
families by the presence of their characteristic BH sequence motifs and these regions were
confirmed to be vital for their function (37). Viral Bcl-2 members that were included in
this group are E1B19K from adenovirus (38, 39), BHRF1 from Herpesviridae EBV (40,
41). Other easily recognizable Bcl-2 proteins are those from Kaposi sarcoma virus, KsBcl2
(42), turkey herpes virus vNR13 (a viral Bcl-B ortholog) (43), Herpesvirus saimiri ORF16
(44), murine γ-herpes virus 68/ M11 (45), African swine fever virus (*asfarviridae*) A179L
(46, 47), Grouper Iridovirus (*iridiviridae*) GIV66 (48) and several members of poxvirus
(*poxviridae*) family, such as well-known member of pox family, vaccinia virus F1L

(VACV F1L) (34, 49). The structures of a number of the virus Bcl-2 proteins either in apo form or as complexes with their potential cellular targets have been determined (Figure 1). Viral Bcl-2 subversion of host cell apoptosis employs the interactions between pro-survival viral Bcl-2 proteins and cellular pro-apoptotic Bax and Bak and BH3-only proteins similar to cellular Bcl-2 proteins (50) (Figure 1). These interactions have been widely studied and affinity measurements reported, and the major finding is that there are significant variations in the BH3 binding profile of the vBcl-2 proteins. For instance, A179L (African swine fever virus (ASFV) Bcl-2 homolog) and FPV039 (Fowl pox virus (FPV) encoded Bcl-2) bound to almost all peptides derived from the BH3 motif of BH3-only proteins with wide range of affinities spanning from nanomolar to the sub-micromolar range. Most of the other vBcl2 proteins show selectivity towards BH3 motif peptides and bind relatively few of them (15). GIV66 (Grouper iridovirus (GIV) Bcl-2) on the other hand showed a highly specific binding profile and bound Bim BH3 peptide alone (48). Bim is a universal Bcl-2 interactor, that binds to all cellular pro-survival proteins with significantly high affinity (51). However, in the context of vBcl-2 proteins Bim does not bind to all vBcl-2 proteins, for example no Bim binding was detected with variola virus (VARV) F1L (35). Combined, these findings suggested that viruses selectively mimic and agonise the action of particular pro-survival Bcl-2 proteins which are important during viral infection and proliferation.

Pox viruses have relatively large and complex genomes when compared to other viruses and utilize multiple strategies for modulating host-cell apoptosis. Frequently poxviruses contain multiple Bcl-2 mimics (eg VACV N1L and F1L have structures that are Bcl-2 mimics) that interfere with Bax-Bak regulated apoptosis that attests to the importance of manipulating this pathway. Other strategies employed by poxviruses include tumour necrosis factor (TNF) receptor homologs such as Cytokine response modifier

(CrmB, CrmC, CrmD and CrmE) (52), Serine protease inhibitors (cowpox virus (CPXV) CrmA, VACV B13) (53, 54), Golgi anti- apoptotic protein (GAAP) (55), double stranded RNA (dsRNA) induced apoptosis (eg VACV E3, MYXV M029, shope fibroma virus,
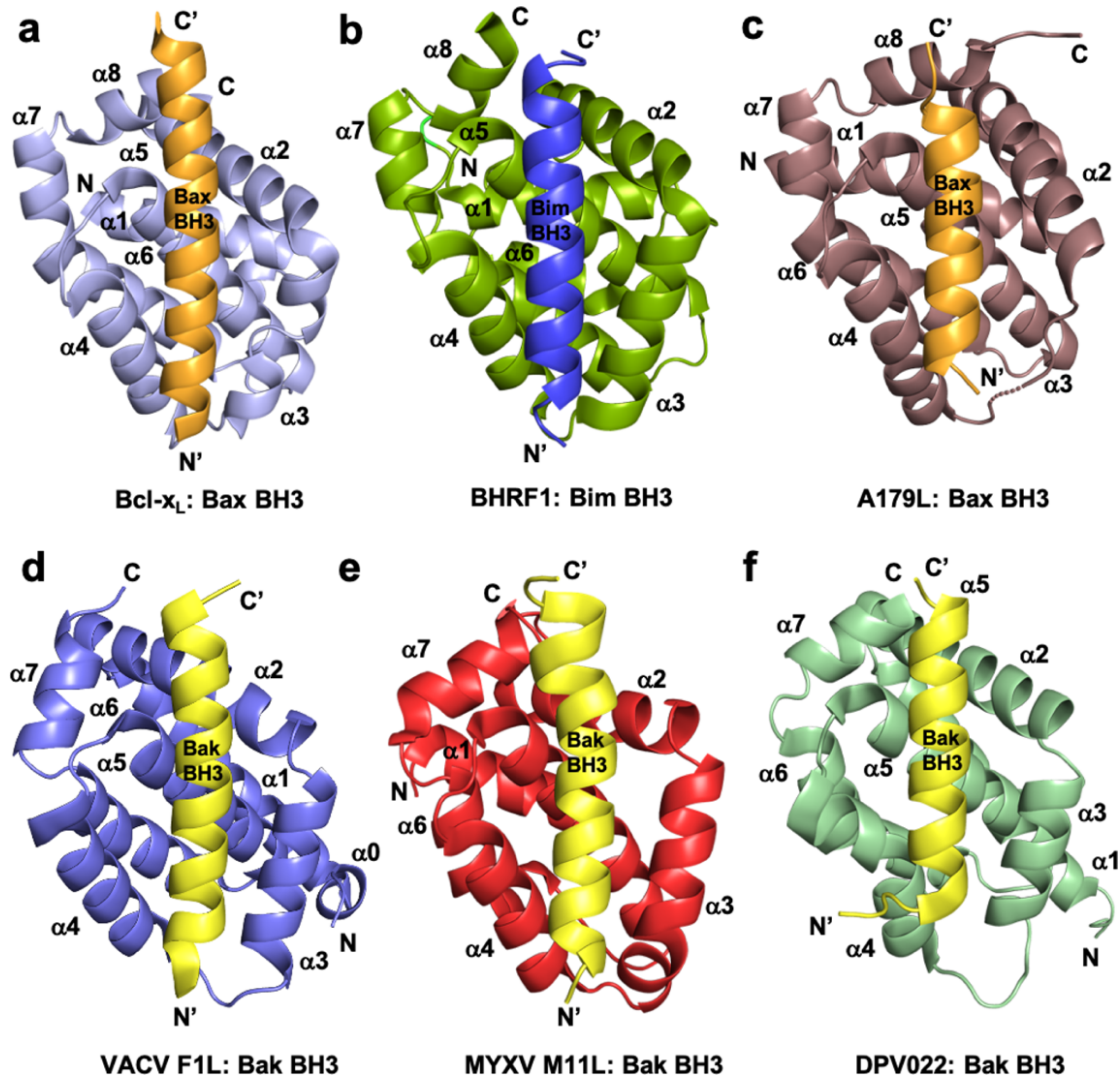
Figure 1: Cartoon representation of crystal structures of poxviral encoded Bcl-2 proteins and comparison with cellular Bcl-x_L and other viral Bcl-2 structures. a) human Bcl-x_L (light blue) in complex with Bax BH3 (tv orange) (PDB 3PL7) (56). All the helices are labelled as $\alpha1$-$\alpha7/8$ and the view is of the canonical ligand binding groove formed by helices $\alpha2$-$\alpha5$. b) EBV BHRF1 (split pea) in complex with Bim BH3 (blue) (PDB 2V6Q) (40), c) ASFV A179L (dirty violet) in complex with Bax BH3 (PDB 5UA5) (47) (tv orange), d) VACV F1L (slate) bound to Bak BH3 (yellow) (PDB 4D2L) (49), e) myxoma virus (MYXV) M11L (red) bound to Bak BH3 (yellow) (PDB 2JBY) (33) and f) deerpox virus (DPV) DPV022 (wheat) in complex with Bak BH3 (yellow) (PDB 4UF1) (57). All views (b-f) are as in a).

SFV032) (58-60) and Cu-Zn-Superoxide dismutase (SOD) induced apoptosis inhibition (M131, S131) (61). These strategies are summarized in Figure 2. However, there is significantly less structural and binding data available on these non-Bcl-2 mimics. Due to from potential health risk from pox viruses such as poxviral infections can be transmitted to human by infected animals (tanapox virus, ORF virus) or not having specific vaccine or treatments other than vaccination against smallpox virus would be a problem. Thus, current research is focusing on various immunomodulatory strategies encoded by various poxviruses against host immune system (9, 62). In this review we discuss details of the poxvirus Bcl-2 modulated host apoptosis inhibitory strategies to overcome the cellular apoptosis response.

1B.2   Pox virus inhibition of host intrinsic activated apoptosis with Bcl-2 homologs

Poxviridae are a numerous and diverse group of viruses that infect both vertebrates and invertebrates and subdivided into the *entomopoxviridae*, those that infect invertebrates such as insects, and *chordopoxviridae*, that infect vertebrates (63). Ten genera of *poxviridae* are currently identified and classified under *chordopoxviridae* (63). They are orthopoxvirus, capripoxvirus, cervidpoxvirus, suipoxvirus, leporipoxvirus, mollusicpoxvirus, yatapoxvirus, avipoxvirus, crocodylidpoxvirus and parapoxvirus. Among these phyla orthopoxvirus, molluscipoxvirus, yatapoxvirus and parapoxviruies have been shown to infect humans and cause disease (64). Monkeypox virus is an orthopoxvirus and classified as an emerging zoonotic disease and could have potentially significant impact on public health (65).

Poxviruses are large linear double stranded DNA viruses containing genomes of 135- 360 kbp in size, that encode up to 328 open reading frames (ORFs) (66) and exclusively replicate within the cytoplasm of the infected cells (63). For example, the causative agent responsible for Smallpox, Variola virus (VARV), is perhaps the most well-
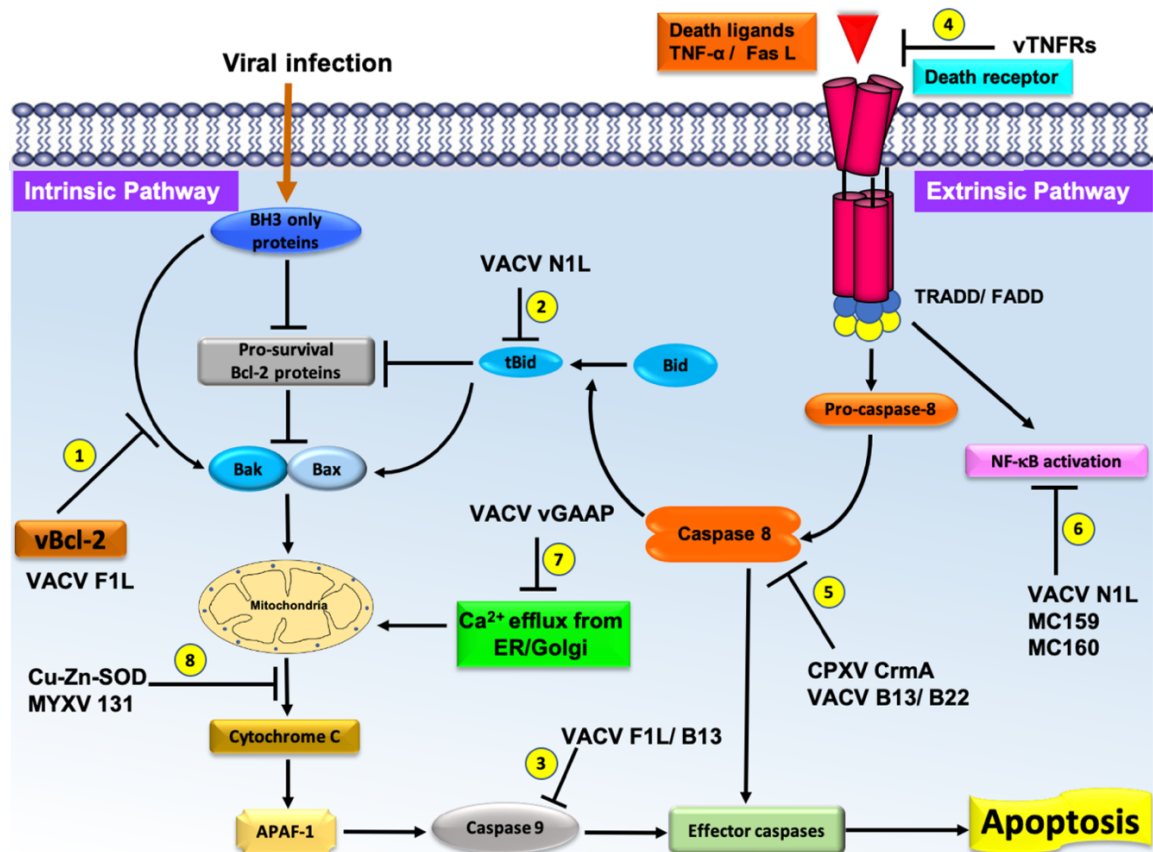
Figure 2: Schematic diagram of the major pathways to apoptosis and the pathways that are modulated by poxvirus encoded apoptosis inhibitors. All major apoptosis inhibition events caused by pox viruses are numbered as 1-8. The cellular intrinsic apoptosis pathway is initiated in the event of viral infection which activates the BH3-only proteins in the cytoplasm. These BH3 proteins interact with cellular pro-survival Bcl-2 proteins to neutralize their activity or directly interact with cellular pro-apoptotic Bcl-2 proteins releasing them to oligomerize at mitochondrial outer membrane to form pores. Release of cytochrome c and other factors through these mitochondrial pores activate the downstream events of intrinsic apoptosis such as APAF-1 activation. Virally encoded Bcl-2 proteins mimic the action of cellular pro-survival Bcl-2 proteins to block apoptosis by a variety of means. 1) VACV F1L interacts with BH3-only proteins to block their activity and subsequent activation of mitochondrial mediated apoptosis. 2) VACV N1L interacts with cellular BH3-only protein Bid to inhibit the downstream activation of apoptosis. 3) VACV F1L/ VACV B13 interact with caspase 9 and suppress the activation of caspase cascade and cell death. 4) poxvirus encoded vTNFRs mimic the cellular TNFR1/2 and block the initiation of extrinsic apoptosis. 5) poxvirus encoded CPXV CrmA/ VACV B13/B22 antagonize active caspase 8 and downstream activation of intrinsic or extrinsic apoptosis. 6) VACV N1L/ MC159/ MC160 inhibit the activation of NF-κB activation, 7) VACV GAAP blocks the Ca^{2+} efflux from Golgi/ER and 8) Cu-Zn-SOD encoded by MYXV inhibits the MOMP and subsequent activation of intrinsic apoptosis.

known member of pox family and was successfully eradicated globally by 1980 (67). Among those genes encoded by open reading frames (ORFs) of VARV there are genes important for host immune evasion that function by inhibiting both the adaptive and innate immune responses (68-70). Closely related to VARV is Vaccinia virus (VACV) and this virus encodes several proteins that mediate host immune evasion by targeting different apoptotic pathways, with the Bcl-2 homologs F1L and N1L that target host intrinsic apoptosis and NF-κB (nuclear factor-κB) inhibition respectively (34, 71). Almost all *poxviridae* of the chordopox families encode Bcl-2 like proteins and significantly no entomopox viruses have yet been identified with Bcl-2 homologs in their genomes. This observation is likely due to differences in Bcl-2 mediated apoptosis in invertebrates compared to vertebrates (2, 3).

Orthopoxviruses

Vaccinia virus (VACV), the prototypical member of *orthopoxviridiae,* expresses multiple proteins which have already been demonstrated or predicted to have Bcl-2-fold structures (72). Examples of structures of this class of protein have been given in Figure 3. Regardless of their structural similarity to Bcl-2 proteins, they do not all solely act via host cell apoptosis inhibition. Most of these proteins are associated with regulation of host innate immune response (73), largely by antagonizing Toll Like Receptor (TLR) signalling network (74, 75) (Figure 2). For example, VACV Bcl-2 like protein A46, A49, A52, B14, B15 and K7 have evolved to suppress different levels of TLR signalling network, in particular NF-κB inhibition (76, 77) which is a pro-inflammatory regulation mechanism activated through Tumour necrosis factor α (TNF-α) and interleukin 1 (IL-1) (78). Thus, similar Bcl-2 like ortholog genes were identified in almost all variants of vaccinia virus as well as in different genus of *chordopoxviridae* family (75).

VACV A46 was initially identified as a Bcl-2 like protein which does not engage in Bcl-2 like anti-apoptotic activity, instead A46 is an inhibitor of Toll/interleukin-1 receptor (TIR)-domain adaptor protein which is crucial for triggering innate immune responses against invading pathogens such as viruses (79, 80). Thus, VACV A46 particularly targets the BB-loop region of TIR, which is a well conserved short peptide sequence (30 amino acid residue) of TIR-domain proteins (81) and blocks the interactions between receptor and adaptor (82) and downstream activation of NF-κB signalling. The crystal structure of A46 showed it exists as a homodimer (Figure 04) with a Bcl-2 fold similar to that in VACV N1L, A52, B14 and K7 (Figure 3) (82) where the α2 helix of one protomer interacts with α6 helix of the neighbouring protomer to make the dimer interface (82, 83). A46 was shown to interact with TIR motif of adaptor protein MAL (MyD88-adaptor-like protein) with 13 uM affinity at the α1 helix of A46 and mutational analysis showed the mutant E97A reduces the affinity by around 36-fold and K88A reduces by 4-fold, in which E97 play an significant role (82). This suggested that charged residues at the protein binding site are crucial for interactions with TIR motif of adaptor proteins.

VACV A52 and B14 are intracellular 23 kDa and 17 kDa proteins, respectively, which are predicted to adopt the Bcl-2 fold and are expressed early in the infection cycle and important virulence factors of VACV that function by inhibiting the activation of NF-κB signalling (77, 84) (Figure 2). Structural analysis of VACV A52 and B14 (Figures 3d&e) showed them to homodimerize both *in vitro* as well as in the crystal structure as previously reported for VACV N1 and A46 (83). Neither A52 or B14 form a hydrophobic binding groove that is required for interaction with the BH3 motif of pro-apoptotic Bcl-2 proteins (77). An *in vivo* transfection based analysis reported that both A52 and B14 have a role in modulating NF-κB signalling (77). Nevertheless, structure based phylogenetic

analysis proposed that A52 and B14 are more similar to VACV N1 rather than Bcl-2 proteins although they follow the similar Bcl-2 fold (77).

VACV K7 is a 17 kDa intracellular protein that has a non-canonical Bcl-2 like protein fold (Figure 3) and has been shown to interact with IRAK2 and TRAF6 in *in vivo* transfected assays and downregulate the activation of TLR-dependent NF-κB (85). VACV K7 was shown to interact with DEAD-box RNA helicase (DDX3), which plays an important role in the innate immune response (86) and was shown to bind VACV K7 with 510 nM affinity in ITC experiments (86). The crystal structure of VACV K7 in complex with DDX3 revealed that the binding pocket of K7 is located in the region covered by N-terminus of α1 helix and the α6 helix and is largely unstructured (86). These data suggest vaccinia virus has captured a Bcl-2 like gene and over the evolution process this gene has been copied and adapted for utilization in various immunomodulatory functions.

VACV A49 is 19 kDa Bcl-2 like protein predominantly expressed in the cytosol. Despite having pro-survival function and a hydrophobic ligand binding groove which is unique to Bcl-2 proteins, A49 is closely related to MYXV M11L (87). However, homologs of A49 are only available in orthopoxviral genomes (88) and are shown to inhibit NF-κB activation and translocation into nucleus, with A49 knockout virus unable to block the NF-κB activation (89). Similar to VACV K7, A49 exists as a monomer in solution or in cells (89). These data suggest that VACV A49 features a monomeric Bcl-2 fold (Figure 3c) which lacks pro-survival function and is important for viral inhibition of NF-κB activation.

In addition to the previously discussed Bcl-2 homologs above, VACV also contains the Bcl-2 homolog F1L. VACV F1L was the first identified Bcl-2 like protein linked to mitochondria associated apoptosis inhibition in poxviruses (90) where there is no recognizable sequence identity to any mammalian Bcl-2 family members. Functional

studies of VACV F1L revealed that it is an essential element for survival of virus infected

cells and prevented staurosporin induced cell death and subsequent cytochrome c release
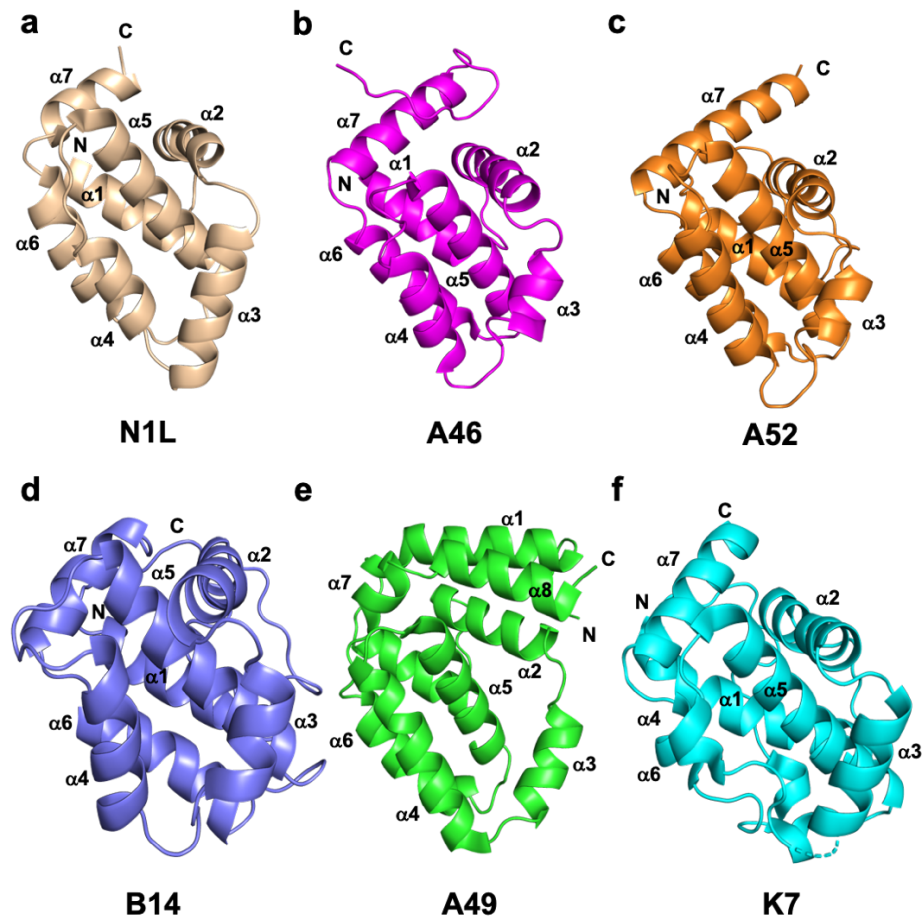
Figure 3: Cartoon representation of crystal structures of vaccinia virus encoded Bcl-2 like proteins. a) N1L (sand) (PDB 2I39), α-helices are labelled as α1-α7/8 with the view into the Bcl-2 ligand binding groove formed by α2-α5. b) structure of A46 (light magenta) (PDB 4LQK), c) structure of A52 (bright orange) (PDB 2VVW) d) structure of B14 (marine) (PDB 2VVY) e) cartoon representation of A49 (green) (PDB 4D5R) and f) structure of K7 (cyan) (PDB 3JRV). All views of b-f are as in a. The structures of figures a-d exist in a similar dimeric configuration to the crystal structure as of N1L (Figure 4b) and those of panels e and f exist as monomer in crystal structure. The dashed line in panel f represents the unstructured loop region in structure of K7.

from mitochondria in Jurkat cells (90). In comparison, an *f1l* deletion mutant,

VV811, underwent apoptosis and expression of F1L prevented all post-mitochondrial

events (90). Similar to other pro-survival Bcl-2 proteins VACV F1L was also shown to

localize to mitochondrial membranes through its hydrophobic C-terminal residues by a

fluorescence assay experiment using C-terminal sequence of pEGFP-F1L (199-226) in HeLa cells (90). Biochemical interaction studies of VACV F1L have shown that it has a highly selective BH3 binding profile and is only able to bind to peptides that span the BH3 regions from Bim, Bak and Bax with sub micromolar affinities (34). Interaction of VACV F1L with Bim is key to its pro-survival activity (49). In addition, F1L prevented Bak and Bax homo-oligomerization and subsequent cell death (91). Mutagenesis of the F1L binding groove residue, such as in F1L A115W, hindered the interactions with Bim_L, but not with Bak, and the mutant was unable to prevent host cell apoptosis (49). The crystal structure of F1L featured the conserved Bcl-2 fold with seven α-helices where $\alpha2$-$\alpha5$ form the canonical ligand binding grove, but the overall fold was a dimer with an unusual domain swap dimerization between $\alpha1$ helix of two neighbouring protomers (Figure 4). In contrast to F1L, mammalian pro-survival Bcl-2 protein possess 8 α-helices. In addition to the domain swapped dimer, F1L features a unique N-terminal extension spanning residues 1-15 (92), that is an intrinsically disordered region, and does not contribute to apoptosis regulation (34, 93). More recent functional analysis of VACV F1L indicates Caspase-9 inhibition (92) and inhibition of inflammasome activation by direct interaction with Nucleotide-binding domain and leucine-rich repeat containing receptors protein 1 (NLRP1), which is important for initiating innate immune responses against invading pathogens (94). VACV F1L was shown to interact with NLRP1 (Figure 1) in an immunoprecipitation experiment of cell transfection study (95). These results potentially imply direct regulation of inflammasome activity in the host by VACV F1L.

VACV also bears a second apoptosis inhibitory Bcl-2 like protein in its genome in addition to F1L, that encodes for the 117 residue protein N1L. N1L has been shown to interact with several cellular pro-apoptotic proteins including Bak, Bid and Bim with high affinity, similar to that observed previously for Bcl-x_L (71, 96). In contrast to other vBcl-

2 proteins, N1L is localized in the cytosol but not mitochondria (96). The crystal structure of VACV N1L revealed that it adopts an overall Bcl-2 fold with homodimeric topology, where α1 and α6 form the interface for dimerization (Figure 4b) (71). A structural comparison of VACV F1L and N1L shows that the proteins share a similar structure (Figure 4c). However, functionally VACV N1L inhibits NF-κB signalling during infection and it may be able to block the host intrinsic apoptosis pathway under specific conditions (72, 97). This has been confirmed in transiently transfected N1L immuno-co-precipitated with cellular Bax, Bid and Bad, where Bax was expressed by cellular transfection (96).

Unlike VACV F1L, Variola virus (VARV) the causative agent of smallpox infection in humans and an orthopoxvirus, also encodes an F1L homolog protein VARV F1L, which has almost identical structure and sequence into VACV F1L (35). However, functionally VARV F1L differs from VACV F1L. VARV F1L inhibits host apoptosis through interacting with only Bid, Bak and Bax but not with Bim. Compared with VACV F1L, VARV F1L could only inhibit Bax regulated cell death but not apoptosis via Bak inhibition (35). Other orthopox viruses have not been as well studied and the data available on their vBcl-2 function are more limited. Ectromelia virus for example is also an orthopoxvirus and the causative agent of Mousepox and expresses a protein that is a VACV F1L homolog, EMV025. EMV025 was found to interact with Bak, Bax and Bim, and blocked the host intrinsic apoptosis pathway by sequestering Bak (98, 99).

Leporipoxviruses

Leporipoxviruses (*Leporipoxviridae*) are pathogenic poxviruses that cause disease in species such as rabbits and squirrels. There are four identified poxviruses belonging to this genus and myxoma virus (MYXV) is considered the prototypical member of *leporipoxviridae* genus (64). MVXV is an infective agent of myxomatosis in European

rabbits (100) and encodes a vBcl-2 like protein, M11L, which is localized to the mitochondria outer membrane with its hydrophobic C-terminal trans-membrane (TM) region during virus infection. The crystal structure of M11L showed that it is monomeric and it was further confirmed by size exclusion chromatography where M11L eluted as a single peak in monomeric region (33, 101). The structure of M11L followed the overall Bcl-2 fold with seven α-helices and hydrophobic binding groove that engages with pro-apoptotic proteins, similar to that in other pro-survival proteins (33, 101). M11L displays very tight affinity towards the BH3-only protein Bim and was able to bind other pro-apoptotic proteins Bak (102), Bax, Bid and Bmf with high to moderate affinity (33).
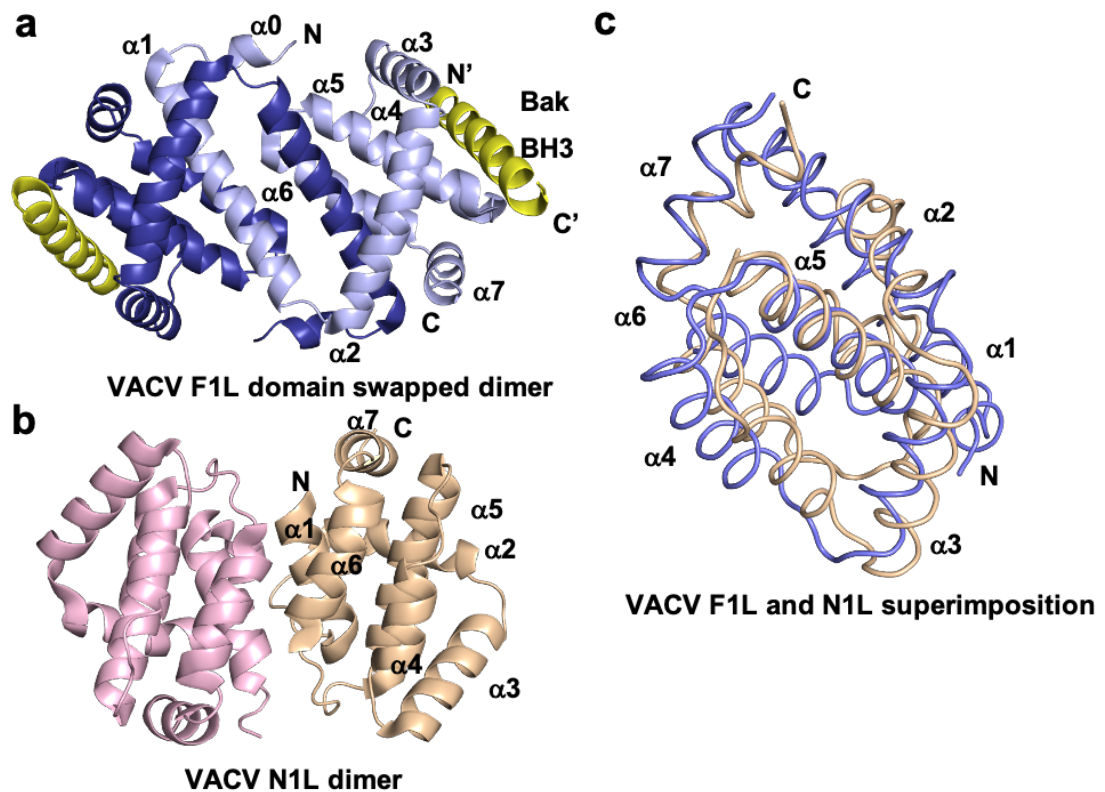
Figure 4: Cartoon representation of the different dimeric topologies of VACV F1L and VACV N1L. a) Crystal structure of dimer interface formed by VACV F1L (light blue) in complex with Bak BH3 (yellow) (PDB 4D2L) where α1 helix of one protomer is swapped with the α1 helix of a neighbouring protomer, b) dimeric interface formed by VACV N1L (beige) (PDB 2I39), where α1 helix of one protomer interact with α6 of the adjacent protomer in crystal contact. c) structural superimposition (RMSD value of 2.3 Å) of cartoon tube representation of VACV F1L and VACV N1L with the view into the hydrophobic binding groove formed by α2-α5. All helices are labelled as α1-α7.

In vivo studies confirmed that, unlike VACV F1L, M11L subverts the host cell apoptosis by primarily sequestering cellular Bak and Bax but not Bim (49). Myxoma virus infection initiates a rapid response from cellular Bax in which it is translocated to mitochondria (100). Interestingly, expression of M11L could inhibit the Fas-ligand induced apoptosis in HEK293 cells and downregulates the subsequent caspase cascade in virus infected cells (102). This data suggests that MYXV M11L could inhibit host apoptosis through both the intrinsic and extrinsic pathways.

Yatapoxviruses

Yatapoxviridae are primate specific poxviruses and there have been two identified members, the tanapoxvirus and yaba monkey tumour virus that can cause mild monkeypox like infections to human (64). Tanapox virus (TANV) encodes putative Bcl-2 like protein 16L (TANV16L). TANV16L displayed broad range of interactions towards pro-apoptotic Bcl-2 proteins by binding to almost all BH3 interactors except Bok and Noxa (Chapter 2, Table 1) (103). TANV16L was also shown inhibit yeast cell death induced by cellular Bax and Bax in a yeast model system (Chapter 2, Figure 3) (103). Surprisingly, the crystal structures of TANV16L adopt both monomeric and domain swapped dimeric Bcl-2 configurations where two complexes of TANV16L, with Bax BH3 and Bim BH3 crystallized as a domain swapped dimeric configuration, and TANV16L: Puma BH3 complex crystallized as a monomeric complex (Chapter 2, Figure 4) (103). This was further validated by analytical ultracentrifugation experiment where TANV16L exists in mainly monomeric and dimeric forms as well as very little amount of homotetrameric species also observed [103]. However, there no homotetrameric Bcl-2 protein structure has been reported to date (Chapter 2) (103). In TANV16L the dimeric state is similar to that

observed previously in vaccinia and variola virus Bcl-2 homologs (34, 35), and in its monomeric configuration α1 is folded back into its globular form.

Parapoxviruses

Parapoxviridae are also known as epitheliotropic viruses and cause skin infections in humans. ORF virus is the prototypical member of parapoxviruses and they commonly infect sheep, goats and humans (104). ORFV125 is a predicted anti-apoptotic Bcl-2 like gene encoded by ORF virus. Like other vBcl-2 proteins, ORFV125 lacks obvious Bcl-2 homology, while it antagonizes mitochondria mediated apoptosis and following cytochrome c release and caspase activation in virus infected cells (105). Furthermore, immunoprecipitation data of ORFV125 revealed that, it only engaged with a selective subset of pro-apoptotic proteins: Bim, Puma, Hrk, Bik, Noxa and active Bax but not Bak (106). While affinity measurements of those interactions have not been reported yet, this result implies that ORFV125 acts via suppression of Bax initiated apoptosis.

Capripoxviruses

Capripoxviruses are economically important pathogenic viruses which cause infections in domestic ruminants such as sheep and goats. Lumpy skin disease is a common disease which causes significant economic loss by terminating the wool production in sheep, and furthermore it is very difficult to control the infection (107). Sheeppox virus encoded SPPV14 is well characterized capripoxvirus anti-apoptotic vBcl-2 protein that adopts a monomeric Bcl-2 fold in nature (108) similar to the previously solved M11L (33), and features a broad range of interactions with all pro-apoptotic Bcl-2 proteins (109), except Noxa. The SPPV14 mutant Y46A significantly reduces binding affinities of Bak, Bax, Bim, Bmf, Hrk and Puma, but not for Bid, Bik, Bad and Bok (108).

Deerpox virus DPV022 is one of the first Bcl-2 like genes identified in poxviruses which does not have obvious BH motifs in its sequence. DPV022 was shown to block intrinsic apoptosis by interacting with highly selective subset of pro-apoptotic proteins Bak, Bax (110) and Bim. The structure of DPV022 resembles the domain swapped Bcl-2 fold (57) which has been previously seen in vaccinia and variola virus F1L (34, 35, 49).

Table 1: Summary of poxvirus Bcl-2 homolog binding data. Binding affinities of poxviral Bcl-2 proteins were measured by Isothermal Titration Calorimetry (ITC) or Surface Plasmon Resonance (SPR). All pox viral proteins have been shown to interact with cellular Bak, Bax and Bim except VARV F1L, which does not interact with Bim. This suggest that poxviruses are primarily targeting cellular Bak and Bax or Bim for inhibition and down regulate the subsequent activation of intrinsic apoptosis.

BH3 motif peptide	Binding affinities (nM)							
	VACV F1L* [34]	VARV F1L [35]	M11L* [33]	TANV16L [103]	SPPV14 [108,109]	DPV022 [57]	FPV039 [111]	CNP058 [112]
Bak	>1000	2640 ± 620.0	50	38 ± 4.0	48 ± 1.0	6930 ± 1460	76 ± 23	2442 ± 508.0
Bax	1850 ± 150.0	960 ± 90.0	75	70 ± 5.0	26 ± 3.0	4040 ± 520.0	76 ± 30	326 ± 140
Bok	N/A	N/A	N/A	NB	7580 ± 643.0	N/A	NB	NB
Bad	NB	NB	>1000	219 ± 34.0	5200 ± 523.0	NB	653 ± 277	NB
Bid	NB	3200 ± 590.0	100	719 ± 66.0	136 ± 23.0	NB	2 ± 0.2	50 ± 10
Bik	NB	NB	>1000	1250 ± 111.0	1760 ± 280.0	NB	30 ± 10	NB
Bim	250 ± 142	NB	5	180 ± 15.0	19 ± 3.0	340 ± 4.00	10 ± 6.0	353 ± 53.0
Bmf	NB	NB	100	606 ± 76.0	44 ± 5.0	NB	16 ± 1.5	294 ± 58.0
Hrk	NB	NB	>1000	3220 ± 301.0	39 ± 7.0	NB	24 ± 11	312 ± 69.0
Noxa	NB	NB	>1000	NB	NB	NB	28 ± 1.0	3280 ± 246.0
Puma	NB	NB	>1000	468 ± 47.0	56 ± 8.0	NB	24 ± 1.5	2480 ± 788.0

NB-No Binding, N/A- Not Available *affinity measured by SPR

Avipoxviruses

Avipoxviruses are the most prominent pathogenic virus among avian species, often causing slow growth (111) in birds. Two members of the *avipoxviridae* genus encode putative Bcl-2 like proteins, FPV039 from fowlpox virus and CNP059 from canarypox virus. Both of these proteins adopt the conserved monomeric Bcl-2 fold with eight alpha helices (112, 113). FPV039 is able to suppress the host apoptotic machinery by engaging with all pro-apoptotic Bcl-2 proteins (112), with FPV039 Bax interaction preventing Bax oligomerization and mitochondrial pore formation (114), whereas CNP058 interacts with

a distinct set of BH3 only proteins and did not show any detectable affinity towards Bok, Bad or Bik (113). Most likely, both of these viruses primary block host apoptosis by sequestering Bim along with direct interactions with cellular Bak and Bax (112, 113).

1B.3   Extrinsic apoptosis inhibition

The extrinsic apoptosis pathway is initiated through interaction of death ligand (Fas/ TNF) to their corresponding death receptors (Fas receptor/ TNF receptor1) (Figure 2) where TNF ligands function against microbial infections and stimulate the inflammatory response. Fas ligand involved in regulating activation of apoptosis of natural killer cells and peripheral lymphoma. Also, Fas is important for induction of apoptosis in virus infected cells or cancer cells (5). In the event of these death ligands binding a death receptor molecule a structural rearrangement of the receptor occurs and trimerization ensues, which initiates the activation of pro-caspase 8 through interaction with adaptor proteins FADD or TRADD (5). Subsequently pro-caspase 8 undergoes dimerization and changes into active caspase-8 (Figure 2). This ultimately leads to activation of the caspase cascade and subsequent apoptosis through either the extrinsic pathway or the intrinsic pathway via activation of Bid (115). Poxviruses have been shown to encode multiple inhibitors of extrinsic apoptosis and this includes caspase inhibitors, Tumour Necrosis Factor (TNF) homologs, and death effector proteins to evade the host immune system (9, 31) (Figure 2).

Poxvirus encoded caspase inhibitors

Cytokine response modifier A (CrmA) is a 38 kDa protein that was the first identified caspase inhibitor encoded by cowpox virus, and shares conserved sequence homology with serine protease inhibitors (serpin). CrmA is expressed during the early infection (116) and shown to suppress the activity of both cysteine and serine proteases (117) as well as inhibit

the function of caspase 1 (118) and caspase 8 (119), which are vital for both extrinsic and mitochondrial apoptosis pathways (Figure 2) (120). Thus, CrmA directly interacts with TNF and Fas receptors mediated pathways to inhibit the downstream activation of extrinsic apoptosis (121) but not intrinsic apoptosis (122). Nevertheless, CrmA has been shown to block Granzyme B, which is a serine protease secreted by cytotoxic T lymphocytes that activates the caspase cascade (123).

Vaccinia virus encodes a protein, B13 (SPI2), that is a homolog of CPXV CrmA that shares 92% sequence identity and was shown to have a similar function as CrmA and inhibit the action of several initiator caspases to block apoptosis (53, 124). MYXV was also shown to encode three serpin inhibitor homologs called as SERP-1, SERP-2 and SERP-3 (125). SERP-1 is an essential element of MYXV virulence (54), whereas SERP-2 functions by inhibiting caspase 1 and granzyme B (126, 127). However, the function of SERP-3 is still not known (128). This suggests that poxvirus encoded CrmA and their homologs are important for caspase and granzyme B inhibition for the blockade of apoptosis.

TNF homologs encoded by poxvirus

TNF receptor molecules are vital for initiating extrinsic apoptosis pathway (5) (Figure 2). Poxvirus encoded anti-apoptotic proteins mimic the action of TNF receptor or bind TNF receptors to inhibit their function (129). The first identified poxviral TNF receptor like proteins are myxoma virus M-T2 and shope fibroma virus S-T2 (130). Both of these proteins were shown to mimic the action of TNF and block the TNF induced extrinsic apoptosis in host (131, 132). It was reported that several other pox viruses also encode the TNF receptor homologs including vaccinia virus (CrmB, CrmC CrmE) (133), variola virus and ectromelia virus (134). Cowpox virus was also shown to encode for four unique TNF

receptor molecules and a distinct CD30 homolog (134), where CD30 is a member of TNFR family of proteins and initially identified in Hodkin's and Reed-Sternberg cells (135, 136). More recent work has shown that tanapox virus encoded 2L is a novel TNF binding protein which does not show significant sequence homology (13% identity) with its cellular counterpart TNF receptors. Despite having poor sequence homology, tanapoxvirus 2L was shown to bind TNF with very high affinity (43 pM) and block the subsequent activation of the caspase cascade of cell death (137).

Molluscum contagiosum virus (MCV) is the only known member of mulluscipoxvirus genus and one of the two specific human pox viruses other than variola virus (smallpox). MCV infection is commonly seen in the young and causes a skin rash (138). This virus was shown to utilize an alternative approach to block death receptor mediated apoptosis. MCV encodes two proteins, MC159 and MC160 which are 114 and 370 residues respectively, which have sequence homology for the death effector motif of adaptor proteins TRADD and FADD, and initiator caspase (139). Previous studies have shown that MC159 and MC160 interact with death effector motif of caspases and FADD in cell based transfection assays (30, 140). However, these interactions appear to be not potent enough for effective inhibition of apoptosis (141). Even though MC159 does not show apoptosis inhibition, another study has shown MC159 inhibition of NF-κB activation through degradation of iκBβ (142). Combined these studies show that poxviruses have utilized multiple strategies to successfully inhibit the host extrinsic apoptosis pathway to aid virus replication in the host cell.

The sections above describe poxvirus involvement in direct inhibition of host cell apoptosis. However, poxviruses also encode numerous other inhibitory proteins which are indirectly involved in inhibition of either intrinsic or extrinsic apoptosis. These include poxvirus expression of Golgi anti-apoptotic protein (GAAP) (143), Cu-Zn-superoxide

Table 2: Summary of poxvirus encoded inhibitors of apoptosis

Genus	Virus	Protein type	Protein	Function	Reference
Orthopoxviridae	VACV	Bcl-2 like	F1L	Pro-survival	(34)
			N1L	NF-κB inhibition	(71, 96)
			A46	NF-κB inhibition	(80, 82)
			A49	NF-κB inhibition	(89)
			A52	NF-κB inhibition	(77)
			B14	NF-κB inhibition	(77)
			B15	NF-κB inhibition	(76)
			K7	NF-κB inhibition IFN signalling	(86)
		Serpin	B22 (SPI-1)	Caspase inhibition	(144)
			B13 (SPI-2)	Caspase inhibition	(53, 124)
			SPI-3	Caspase inhibition	(145)
		vTNFR	CrmB	Mimic TNFR1/2	(133)
			CrmC	Mimic TNFR1/2	(133)
			CrmE	Mimic TNFR1/2	(133)
		Decapping enzymes	D9/ D10	PKR activation inhibitor	(60)
	VARV	Bcl-2 like	F1L	Pro-survival	(35)
	CPXV	Serpin	CrmA	Caspase inhibition	(117)
	CMLV	vGAAP	6L	Anti-apoptotic	(143)
	ECTV	Bcl-2 like	EMV025	Pro-survival	(98)
		vTNFR	CrmD	Mimic TNFR1/2	(146)
Leporipoxviridae	MYXV	Bcl-2 like	M11L	Pro-survival	(33)
		Serpin	SERP1	Caspase inhibition	(54)
			SERP2	Caspase inhibition	(127)
			SERP3	Caspase inhibition	(128)
		vTNFR	M-T2	Mimic TNFR1/2	(132)
		SOD homolog	M131	SOD induced anti-apoptosis	(147)
		E3 homolog	M029	PKR activation inhibitor	(148)
	SPV	vTNFR	T2	Mimic TNFR1/2	(131, 132)
		SOD homolog	S131	SOD induced anti-apoptosis	(147)
		E3 homolog	SPV032	PKR activation inhibitor	(149)
Yatapoxviridae	TANV	Bcl-2 like	16L	Pro-survival	(103)
		vTNFR	2L	Mimic TNFR1/2	(137)
Parapoxviridae	ORFV	Bcl-2 like	ORFV125	Pro-survival	(106)
Capripoxviridae	SPPV	Bcl-2 like	SPPV14	Pro-survival	(108, 109)
Cervidpoxviridae	DPV	Bcl-2 like	DPV022	Pro-survival	(57)
Avipoxviridae	FPV	Bcl-2 like	FPV039	Pro-survival	(112)
	CNP	Bcl-2 like	CNP058	Pro-survival	(113)
Molluscipoxviridae	MCV	SOD homolog	MC163	SOD induced anti-apoptosis	(150)
		vFLIP	MC159	Inhibitor TNF-α/ FasL induced apoptosis	(142)
			MC160	Inhibitor TNF-α/ induced NF-κB inhibition	(9)

dismutase (SOD) and double stranded RNA (dsRNA) induced apoptosis (9) (Figure 2). With host cells having evolved multiple cell death mechanisms, and apoptosis being triggered by multiple pathways, poxviruses have evolved to counteract a range of host cell death mechanisms via multiple inhibitory strategies as discussed above to successfullyestablish an infection and generate viral progeny. Table 2 summarizes the currently known poxvirus encoded inhibitors and their functions as well as their classification.

The initiation of apoptosis is a crucial frontline defence mechanism for a host cells against invading pathogens. A solid defence of host apoptosis is essential for maintaining healthy cells and defend against pathogen encoded immune modulatory proteins. Poxviruses with their large genomes have evolved a diverse array of anti-apoptotic strategies to block host cell suicide mechanisms. As outlined above poxviruses have evolved both direct and indirect inhibition mechanisms of host apoptosis for successful infections. The direct apoptosis inhibition includes viral Bcl-2 mediated mitochondrial apoptosis inhibition, caspase cascade inhibition and deactivation of death receptor molecules. Indirect inhibition includes inhibition of dsRNA induced apoptosis, mimicry of golgi anti-apoptotic protein and Cu-Zn-SOD inhibition. These features reveal the sophistication of poxviruses in targeting apoptosis. However, there is a paucity of direct molecular data or structures to indicate how these molecules involved function in detail. My current studies on structure and interactions of poxvirus encoded anti-apoptotic Bcl-2 proteins has attempted to provide a detailed understanding of apoptosis inhibition in poxviruses by these proteins.

Chapter 2

Paper II: Structural Insight into Tanapoxvirus-Mediated Inhibition of Apoptosis

2.1   Introduction

Tanapox virus (TANV) is a large double stranded DNA virus that belongs to genus *yatapoxviridae* and causes mild monkeypox like infections primarily in humans and primates (151). This virus has been shown to encode a putative viral Bcl-2 homolog TANV16L, that has poor sequence homology to cellular Bcl-2 proteins. The closest viral homolog is deerpox virus Bcl-2 protein DPV022 (57), that shares 32% sequence identity with TANV16L. However, little information is available about the mechanism of the potential apoptosis inhibition by tanapox virus upon infection to their host.

Here I examined the detailed molecular mechanism of TANV16L subversion of host cell apoptosis by measuring the binding interactions of TANV16L with its potential endogenous BH3 motif peptides from human pro-apoptotic Bcl-2 proteins. In order to delineate the molecular mechanisms of action I then determined the high resolution crystal structure of three complexes of TANV16L bound to Bax, Bim and Puma BH3 peptides (103). The results obtained from this work has been published in FEBS Journal (2020), under the manuscript title "Structural insight into tanapoxvirus-mediated inhibition of apoptosis" (103).

2.2 Co-author contribution

Chathura D. Suraweera	Protein Expression and purification
	Determination of TANV16L binding partners
	Protein crystallization, X-ray data collection
	Structure solution and refinement
	Structural analysis
	Manuscript writing (Introduction, Material and Methods
	Results and Discussion)
	Preparation of figures and tables in the manuscript
Mohd Ishtiaq Anasir	Protein Expression and purification
	Screening of BH3 interactions of TANV16L
Srishti Chugh	Performed the yeast cell death assay
Airah Javorsky	AUC data collection, analysis and interpretation
Rachael E. Impey	AUC data collection, analysis and interpretation
Mohammad Hasan Zadeh	Protein Expression and purification
Tatiana P. Soares da Costa	AUC data collection, analysis and interpretation, drafted and revised the manuscript
Mark G. Hinds	Overall scientific direction of the project
	Structural analysis and interpretation
	Drafted and revised the manuscript
Marc Kvansakul	Overall scientific direction of the project
	X-ray diffraction and data collection
	Structure solution and refinement
	Structural analysis
	drafted and revised the manuscript

Structural insight into tanapoxvirus-mediated inhibition of apoptosis

Chathura D. Suraweera[1] (iD), Mohd Ishtiaq Anasir[1,*], Srishti Chugh[1,†], Airah Javorsky[1], Rachael E. Impey[1], Mohammad Hasan Zadeh[1], Tatiana P. Soares da Costa[1] (iD), Mark G. Hinds[2] (iD) and Marc Kvansakul[1] (iD)

1 Department of Biochemistry and Genetics, La Trobe Institute for Molecular Science, La Trobe University, Melbourne, Australia
2 Bio21 Molecular Science and Biotechnology Institute, The University of Melbourne, Parkville, Australia

Premature programmed cell death or apoptosis of cells is a strategy utilized by multicellular organisms to counter microbial threats. Tanapoxvirus (TANV) is a large double-stranded DNA virus belonging to the *poxviridae* that causes mild monkeypox-like infections in humans and primates. TANV encodes for a putative apoptosis inhibitory protein 16L. We show that TANV16L is able to bind to a range of peptides spanning the BH3 motif of human proapoptotic Bcl-2 proteins and is able to counter growth arrest of yeast induced by human Bak and Bax. We then determined the crystal structures of TANV16L bound to three identified interactors, Bax, Bim and Puma BH3. TANV16L adopts a globular Bcl-2 fold comprising 7 α-helices and utilizes the canonical Bcl-2 binding groove to engage proapoptotic host cell Bcl-2 proteins. Unexpectedly, TANV16L is able to adopt both a monomeric and a domain-swapped dimeric topology where the α1 helix from one protomer is swapped into a neighbouring unit. Despite adopting two different oligomeric forms, the canonical ligand binding groove in TANV16L remains unchanged from monomer to domain-swapped dimer. Our results provide a structural and mechanistic basis for tanapoxvirus-mediated inhibition of host cell apoptosis and reveal the capacity of Bcl-2 proteins to adopt differential oligomeric states whilst maintaining the canonical ligand binding groove in an unchanged state.

Database

Structural data are available in the Protein Data Bank (PDB) under the accession numbers 6TPQ, 6TQQ and 6TRR.

Introduction

Tanapoxvirus [1] is a large double-stranded DNA virus and member of the genus yatapoxvirus, which belongs to the *poxviridae* family. Tanapoxvirus (TANV) causes mild monkeypox-like infections in humans as well as primates with symptoms that include fever and skin lesions [2]. Tanapoxvirus encodes a range of immune-modulatory proteins such as TNF inhibitors [3], as well as a putative B-cell lymphoma-2 (Bcl-2) homolog [4]. Bcl-2 proteins constitute a large family of proteins that primarily control programmed cell death, or apoptosis, in higher organisms [5] and are evolutionarily ancient [6]. The family comprises both prosurvival and proapoptotic members, which are characterized by the presence of one or more of four Bcl-2 homology

or BH motifs and a transmembrane anchor region [7]. The mammalian prosurvival Bcl-2 members comprise Bcl-2, Bcl-w, Bcl-x_L, Mcl-1, A1 and Bcl-b, and maintain host cell survival. In contrast, proapoptotic Bcl-2 family members are subdivided into two separate groups, the multimotif executors that comprise Bak, Bax and Bok, and a second group, the BH3-only proteins, which only feature a BH3 motif and include Bad, Bid, Bik, Bim, Bmf, Hrk, Noxa and Puma [8]. The BH3-only proteins modulate apoptosis by neutralizing the activity of prosurvival Bcl-2 through binding a surface groove [9]. After activation, Bak and Bax oligomerize to perforate the outer mitochondrial membrane leading to inner membrane herniation [10] and subsequent release of cytochrome *c* that triggers the formation of the apoptosome and activation of downstream caspases that dismantle the cell [11].

A number of large DNA viruses encode functional, sequence and structural homologs of Bcl-2 that promote infected host cell survival and viral proliferation [12]. Viral Bcl-2 homologs have been identified in *herpesviridae*, include those from Epstein–Barr virus BHRF1 [13,14] and Kaposi sarcoma virus KsBcl-2 [15–17]. Other major virus families that contain members encoding for prosurvival Bcl-2 proteins include the *asfarviridae* with African swine fever virus-encoded A179L [18–20], and grouper iridovirus-encoded GIV66 [21,22] from the *iridoviridae*. However, the largest number of Bcl-2 homologs is found in *poxviridae* [12] such as vaccinia and variola virus F1L [23–25] and myxomavirus M11L [26–28]. Whilst structural studies have shown [18,21,24,29–32] these virus-encoded Bcl-2 homologs that adopt a Bcl-2 fold, there is substantial diversity with regard to which proapoptotic host Bcl-2 proteins they bind. For example, vaccinia virus F1L binds Bim, Bak and Bax only [33], whereas sheeppoxvirus SPPV14 binds Bid, Bim, Bmf, Hrk, Puma, Bak and Bax [34], and African swine fever virus A179L binds all major proapoptotic Bcl-2 proteins [18]. The diversity observed amongst the proapoptotic ligand binding profiles for virus-encoded prosurvival Bcl-2 extends to the mechanisms of action too; for example, myxomavirus M11L primarily acts by sequestering Bak and Bax [28], whereas vaccinia virus F1L neutralizes host cell death by sequestering Bim during viral infections [23].

Tanapoxvirus-encoded TANV16L is a putative homolog of deerpoxvirus DPV022 [4] (Fig. 1), with which it shares 32% sequence identity. In order to understand the putative apoptosis regulatory function of TANV16L, we examined its ability to bind to peptides of host proapoptotic Bcl-2 proteins and determined crystal structures of TANV16L bound to its

interactors. We now show that TANV16L is a highly flexible Bcl-2 fold protein that is able to bind to BH3 motif peptides of host proapoptotic Bcl-2 proteins with high affinity both as a monomeric and domain-swapped dimeric form. These findings provide a mechanistic basis for tanapoxvirus-mediated inhibition of apoptosis and highlight the substantial structural flexibility in the Bcl-2 fold that allows multiple oligomeric topologies to engage proapoptotic interactors using the canonical ligand binding groove.

Results

In order to reveal the function for TANV16L, we recombinantly expressed and purified TANV16L lacking the C-terminal 23 residues and examined its ability to bind to peptides spanning the BH3 motif of all proapoptotic human Bcl-2 proteins using isothermal titration calorimetry (ITC). TANV16L bound to a number of BH3 motif peptides with high affinity, including those from the BH3-only proteins Bim, Bid, Hrk and Puma as well as those from the multimotif executor proteins Bak and Bax (Fig. 2, Table 1). We then utilized a yeast-based heterologous expression system for studying functional interactions of TANV16L with Bak and Bax [13]. Consistent with our ITC data, we observed that TANV16L could directly counter Bak and Bax induced yeast growth arrest when these proteins were overexpressed in yeast (Fig. 3).

To understand the structural basis for proapoptotic Bcl-2 binding by TANV16L, we then determined the crystal structures of TANV16L bound to the human Bax, Bim and Puma BH3 motifs (Fig. 4, Table 2). In the TANV16L:Bax BH3 complex, TANV16L adopts a globular Bcl-2 fold comprising 7 α-helices (Fig. 4A). Similar to vaccinia and variola virus F1L and deerpoxvirus DPV022, TANV16L adopts a domain-swapped dimeric topology where the α1 helix from one protomer is swapped with that of a second protomer in the complex, taking up the space vacated by the matching α1 helix (Fig. 4A,C). Superimposition of one chain of the TANV16L from the domain-swapped dimer TANV16L:Bax BH3 complex with the equivalent chain from the domain-swapped dimer VACV F1L from F1L:Bak BH3 [23] and the domain-swapped dimer DPV022 from DPV022:Bax BH3 [29] (Fig. 4C, G) yields an rmsd of 2.3 Å (superimposed over 122 Cα atoms) and 2.1 Å (superimposed over 131 Cα atoms), respectively, whereas superimposition of the entire domain-swapped dimer of TANV16L yields rmsd values of 2.2 and 2.7 Å, respectively. The position of the TANV16L α1 within the domain-swapped dimer is identical to VACV F1L and DPV022 (Fig. 4F).
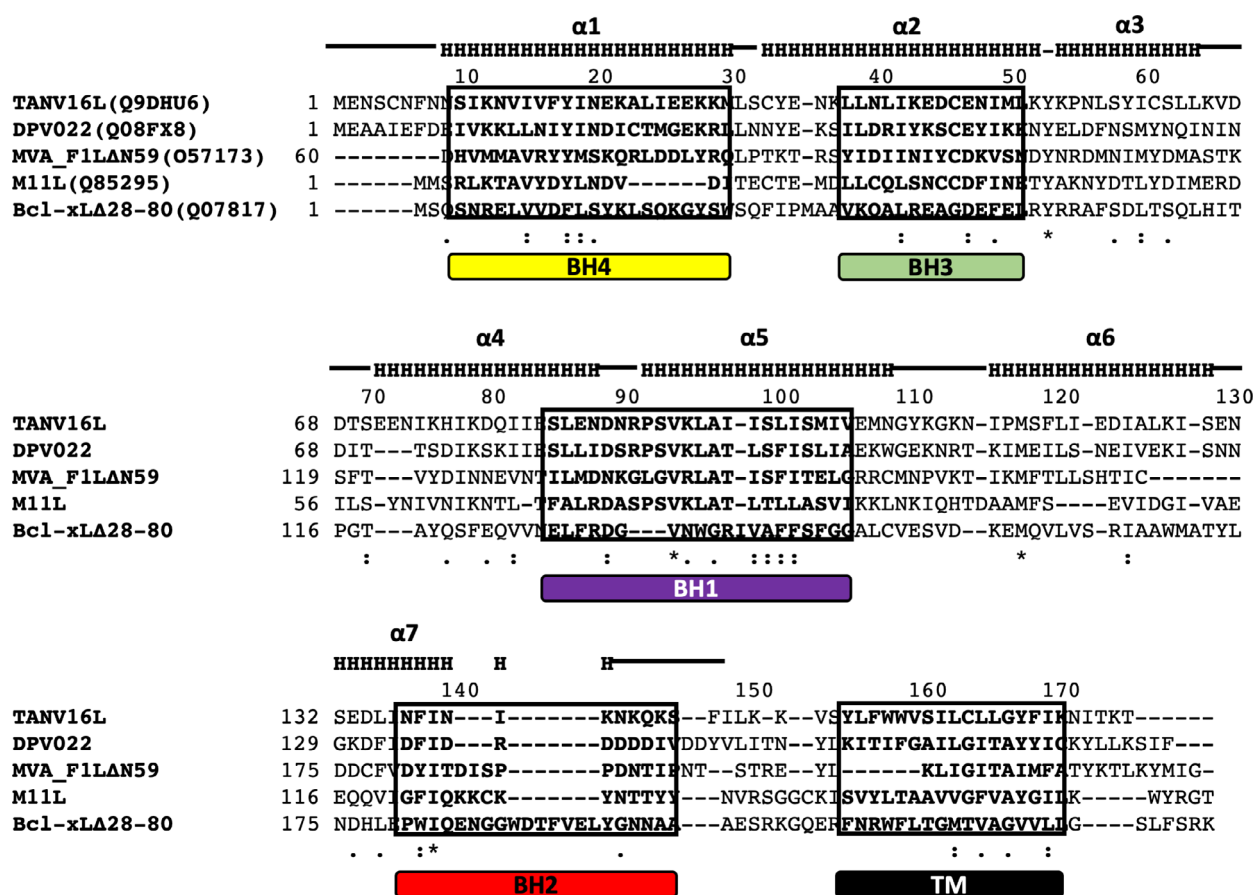
Fig. 1. Sequence alignment of TANV16L with prosurvival Bcl-2 family members. The sequences of tanapoxvirus 16L (UniProt accession number: A7XCC0), deerpoxvirus DPV022 (UniProt accession number: Q08FX8), vaccinia virus F1L (UniProt accession number: O57173), myxomavirus M11L (UniProt accession number: Q85295) and human Bcl-x$_L$ (UniProt accession number: Q07817) were aligned using MUSCLE [66]. Secondary structure elements are marked based on the crystal structure of TANV16L, and BH motifs are boxed and shown in bold [70]. The regions of helix are marked 'H' and unstructured loops with a bar above the sequence, conserved residues are denoted by '*', with highly conservative substitutions indicated by ':' and conserved substitutions indicated by '.'.

Similarly, TANV16L in the TANV16L:Bim BH3 complex adopts a domain-swapped dimeric configuration that is identical to the TANV16L:Bax BH3 complex (Fig. 4B).

Unexpectedly, TANV16L in the TANV16L: Puma BH3 complex adopts a monomeric Bcl-2 fold, where the α1 helix is folded back into the side of the globular Bcl-2 fold (Fig. 4D). A DALI analysis [35] indicated that the closest homolog in the PDB is myxomavirus M11L (Fig. 4E, PDB ID 2JBX [28]) with an rmsd of 2.1 Å (over 111 Cα), whereas the closest mammalian Bcl-2 structure is human Mcl-1 (PDB ID 5FC4 [36]) with an rmsd of 2.3 Å (over 126 Cα) (Fig. 4H). In the crystal structure of TPV16L:Puma BH3, one heterodimer contacts a neighbouring one via an interface formed by helices α1 and α2 from one chain and α7 as well as Puma BH3 from a neighbouring chain (Fig. 5D). PISA

(protein interfaces, surface and assembly) analysis of this interface yields a complexation significance score of 0, which suggests it is a crystallographic dimer and not a functionally relevant interface.

TANV16L utilized the canonical Bcl-2 ligand binding groove formed by α2–α5 to engage BH3 motif ligands (Fig. 5). In the TANV16L:Bax BH3 complex (Fig. 5A), Bax residues L59, L63, I66 and L70 protrude into the four hydrophobic pockets of TANV16L. In addition, ionic interactions are observed between TANV16L R90 guanidium group and Bax D68 carboxyl as well as TANV16L R90 guanidium group and Bax D71 carboxyl group, with a further two hydrogen bonds between the TANV16L S84 hydroxyl group and the Bax S60 hydroxyl group as well as TANV16L S92 hydroxyl group and the main chain amide group of Bax G67 (Fig. 5A).
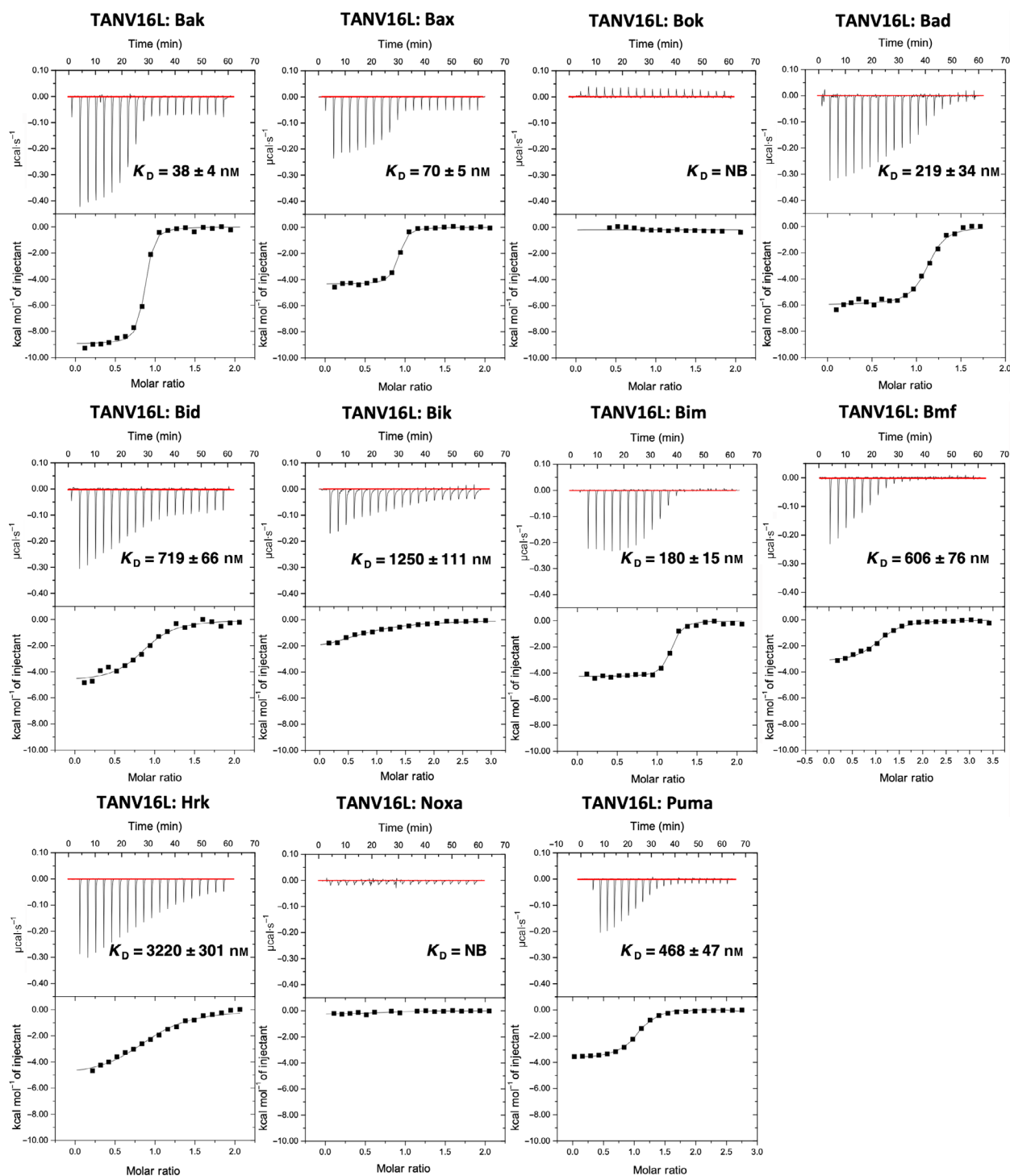
Fig. 2. TANV16L engages a broad spectrum of BH3 motif peptides of proapoptotic Bcl-2 proteins. The affinities of recombinant TANV16L for BH3 motif peptides (26-mers, except for a Bid 34-mer and Bax 28-mers) were measured using ITC and the raw thermograms shown. K_D values (in nM) are the means of three experiments $\pm$ SD. NB, no binding detected. The binding affinities are tabulated in Table 1.

In the TANV16L:Bim BH3 complex (Fig. 5B), Bim residues I148, L152, I155 and F159 are used to engage the four hydrophobic pockets in TANV16L.

Furthermore, there is one ionic interaction between TANV16L R90 guanidium group and Bim D157 carboxyl group and a hydrogen bond between TANV16L

Table 1. Interactions of TANV16L with proapoptotic BH3 motif peptides. All affinities were measured using ITC and K_D values given in nM as a mean of three independent experiments with SD. NB denotes no binding detectable, nd denotes that data obtained did not allow determination of affinity and thermodynamic parameters, and N denotes stoichiometry of the interaction.

| | WT 16L | | | 16L_R90A | | |
Peptide	K_D (nM)	ΔH	N	K_D (nM)	ΔH	N
Bak	38 ± 4	−4.27 ± 0.07	0.99 ± 0.08	2325 ± 261	−4.07 ± 0.26	0.95 ± 0.02
Bax	70 ± 5	−4.55 ± 0.2	1.01 ± 0.06	2301 ± 374	−7.36 ± 0.37	1.03 ± 0.03
Bok	NB	NB	NB	NB	NB	NB
Bad	219 ± 34	−6.3 ± 1.3	0.95 ± 0.07	10 206 ± 1570	−4.45 ± 0.20	0.87 ± 0.06
Bid	719 ± 66	−4.13 ± 0.5	1.02 ± 0.07	nd	nd	nd
Bik	1250 ± 111	−2.51 ± 0.31	0.85 ± 0.03	14 356 ± 1370	−3.17 ± 0.75	1.12 ± 0.05
Bim	180 ± 15	−4.93 ± 0.31	0.90 ± 0.03	1766 ± 320	−6.16 ± 0.63	0.98 ± 0.1
Bmf	606 ± 76	−5.83 ± 0.52	0.98 ± 0.06	nd	nd	nd
Hrk	3220 ± 301	−5.07 ± 0.10	1.02 ± 0.09	nd	nd	nd
Noxa	NB	NB	NB	NB	NB	NB
Puma	468 ± 47	−5.87 ± 0.15	0.88 ± 0.08	911 ± 39	−1.17 ± 0.1	0.99 ± 0.08

| | 16L_K52A | | |
Peptide	K_D (nM)	ΔH	N
Bak	113 ± 3	−8.24 ± 0.73	1.03 ± 0.04
Bax	266 ± 11	−6.23 ± 0.32	1.05 ± 0.04
Bok	NB	NB	NB
Bad	5857 ± 732	−3.63 ± 0.40	0.89 ± 0.04
Bid	976 ± 126	−5.8 ± 0.26	1.04 ± 0.03
Bik	3382 ± 85	−5.67 ± 0.11	0.97 ± 0.06
Bim	558 ± 27	−4.61 ± 0.29	1.01 ± 0.006
Bmf	nd	nd	nd
Hrk	nd	nd	nd
Noxa	NB	NB	NB
Puma	1010 ± 130	2.95 ± 0.15	1.04 ± 0.02
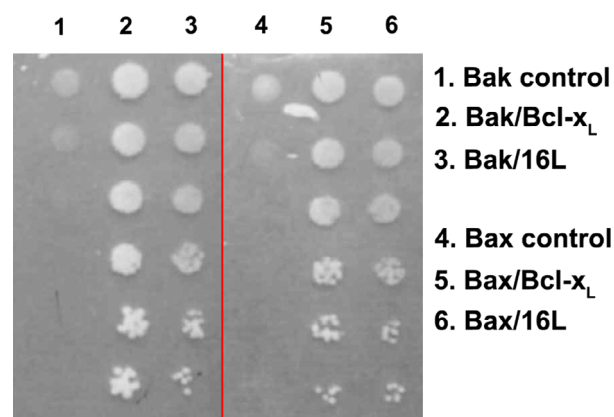
Fig. 3. TANV16L is able to prevent Bak and Bax induced yeast growth arrest. Yeast co-transformed with constructs encoding Bax or Bak and the indicated prosurvival proteins, each under the control of an inducible (GAL) promoter, were spotted onto inducing galactose ('ON') or repressing glucose ('OFF') plates as 5-fold serial dilutions. Images are representative of two independent experiments.

1. Bak control
2. Bak/Bcl-x$_L$
3. Bak/16L

4. Bax control
5. Bax/Bcl-x$_L$
6. Bax/16L

N87 amide and Bim R153 guanidium group. In the TANV16L: Puma BH3 complex (Fig. 5C), Puma utilizes the four hydrophobic residues I137, L141, M144 and L148 to engage the four hydrophobic pockets in TANV16L. These hydrophobic interactions are supplemented by ionic interactions between TANV16L R90 guanidium group and Puma D146 carboxyl group as well as TANV16L K52 ammonium group and Puma D146 carboxyl group. Furthermore, two hydrogen bonds are found between TANV16L Y53 hydroxyl and Puma D147 carboxyl group, and between the TANV16L N56 sidechain amide and Puma Q140 sidechain carbonyl groups. Superimposition of monomeric TANV16L from the complex with Puma BH3 with one of the chains from the domain-swapped dimeric form of TANV16L from the Bax BH3 complex yields an rmsd of 1.2 Å over α2–7 (117 Cα atoms), indicating that despite the topology change from monomer to domain-swapped dimer the regions of TANV16L not involved in the domain swap remain near identical.
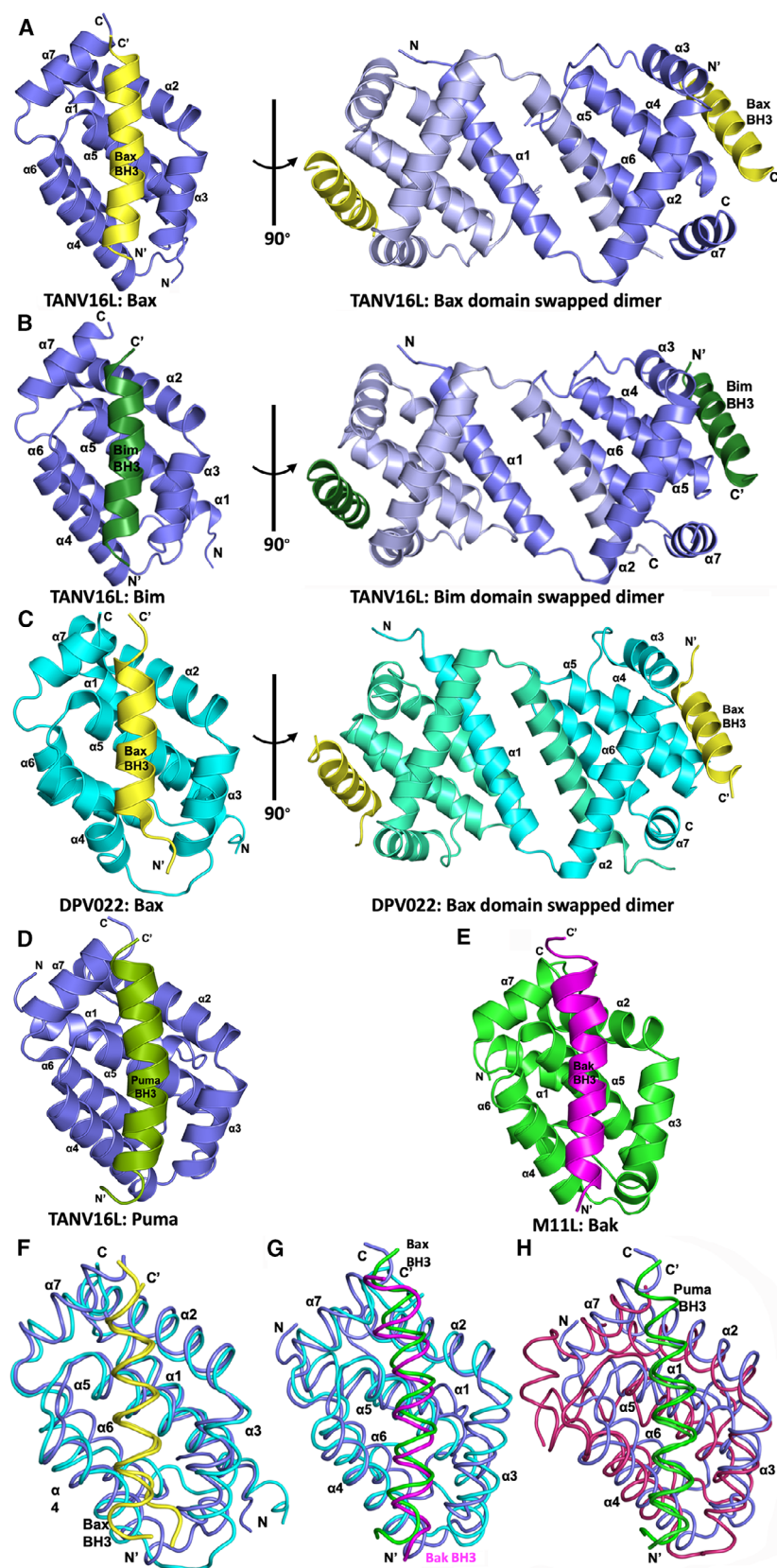
Fig. 4. Crystal structures of TANV16L bound to Bax, Puma and Bim BH3 motifs. (A) TANV16L (slate) in complex with the Bax BH3 motif (yellow). TANV16L helices are labelled α1–α7. The left-hand view is of the hydrophobic binding groove of one protomer formed by helices α3–α5, and the right-hand view is the domain-swapped dimer viewed along the 2-fold symmetry axis between the domain-swapped α1 helices. (B) TANV16L (slate) in complex with the Bim BH3 domain (dark green) (C) DPV022 (cyan) in complex with the Bax BH3 domain (yellow) [29]. The view is as in (A). (D) TANV16L (slate) in complex with the Puma BH3 domain (olive) (E) Myxoma virus M11L (green) in complex with Bak BH3 (magenta). All structures were aligned using DALI pairwise alignment [35], and the view is as in (A). The view in the right-hand panels in (B) and (C) is as in (A). (F) Superimposition of the Cα backbone of TANV16L:Bax BH3 (slate and yellow) with DPV022:Bax BH3 (cyan and yellow, PDB ID 4UF2). (G) TANV16L:Bax BH3 (slate and yellow) with DPV022:Bak BH3 (cyan and magenta, PDB ID 4UF1) (H) TANV16L:Puma BH3 (slate and green) (green) with human Mcl-1:Puma BH3 (raspberry and green, PDB ID 6QFM), the most similar structure to that of TANV16L:Puma BH3 identified using Dali. All views are into the canonical ligand binding groove formed by helices α2–5. Superimpositions were generated using pairwise Dali alignment [35]. Images were generated using the PYMOL Molecular Graphics System, Version 1.8 Schrödinger, LLC.

Table 2. X-ray data collection and refinement statistics. Values in parentheses are for the highest resolution shell.

	TANV16L: Bax BH3	TANV16L: Puma BH3	TANV16L: Bim BH3
Data collection			
Space group	P4₃2₁2	P2₁2₁2₁	P3₂21
Cell dimensions			
a, b, c (Å)	55.38, 55.38, 126.94	54.09, 54.87, 60.22	59.65, 59.65, 90.90
α, β, γ (°)	90, 90, 90	90, 90, 90	90, 90, 120
Wavelength (Å)	0.9537	0.9537	0.9537
Resolution (Å)	33.33–2.12 (2.19–2.12)	32.45–1.85 (1.91–1.85)	44.92–3.00 (3.11–3.00)
R_{sym} or R_{merge}	0.097 (2.67)	0.066 (1.55)	0.168 (1.50)
$I/\sigma I$	11.2 (0.8)	11.1 (0.9)	4.3 (0.7)
Completeness (%)	99.86 (99.65)	99.51 (97.62)	99.9 (100)
$CC_{1/2}$	0.99 (0.29)	0.99 (0.40)	0.99 (0.34)
Redundancy	8.6 (6.6)	5.5 (4.7)	4.7 (4.6)
Refinement			
No. reflections	11 838	15 799	7992
R_{work}/R_{free}	0.239/254	0.195/0.223	0.242/0.276
Clashscore	0.5	2.17	2.66
No. atoms			
Protein	1291	1369	1298
Ligand/ion	2	1	1
Water	23	91	8
B-factors			
Protein	65.68	51.74	72.84
Ligand/ion	84.20	86.29	63.59
Water	60.76	50.89	65.12
R.m.s. deviations			
Bond lengths (Å)	0.003	0.006	0.003
Bond angles (°)	0.44	0.67	0.51

Since we observed TANV16L in both a monomeric and domain-swapped dimeric topology, we subjected TANV16L and some of its complexes with BH3 motif peptides to analytical ultracentrifugation (AUC). AUC was performed on TANV16L alone as well as on TANV16L bound to Bim, Bax and Puma BH3 (Fig. 6). TANV16L alone revealed a mixture of monomeric and dimeric protein as well as a small amount of tetramers at concentrations ranging from 0.2 to 0.8 mg·mL^{-1}, with a ratio of monomer:dimer of ~ 3.5 : 1. Similarly, complexes of TANV16L with Bim, Bax and Puma BH3 at 0.2 mg·mL^{-1} also revealed a mixture of heterodimers and heterotetramers, with the ratio of TANV16L:Bim BH3 heterodimers vs heterotetramers being ~ 4 : 1, with TANV16L: Bax and Puma complexes displaying comparable ratios of ~ 3.5 : 1, respectively, closely matching the ratio observed for TANV16L alone (Fig. 6).

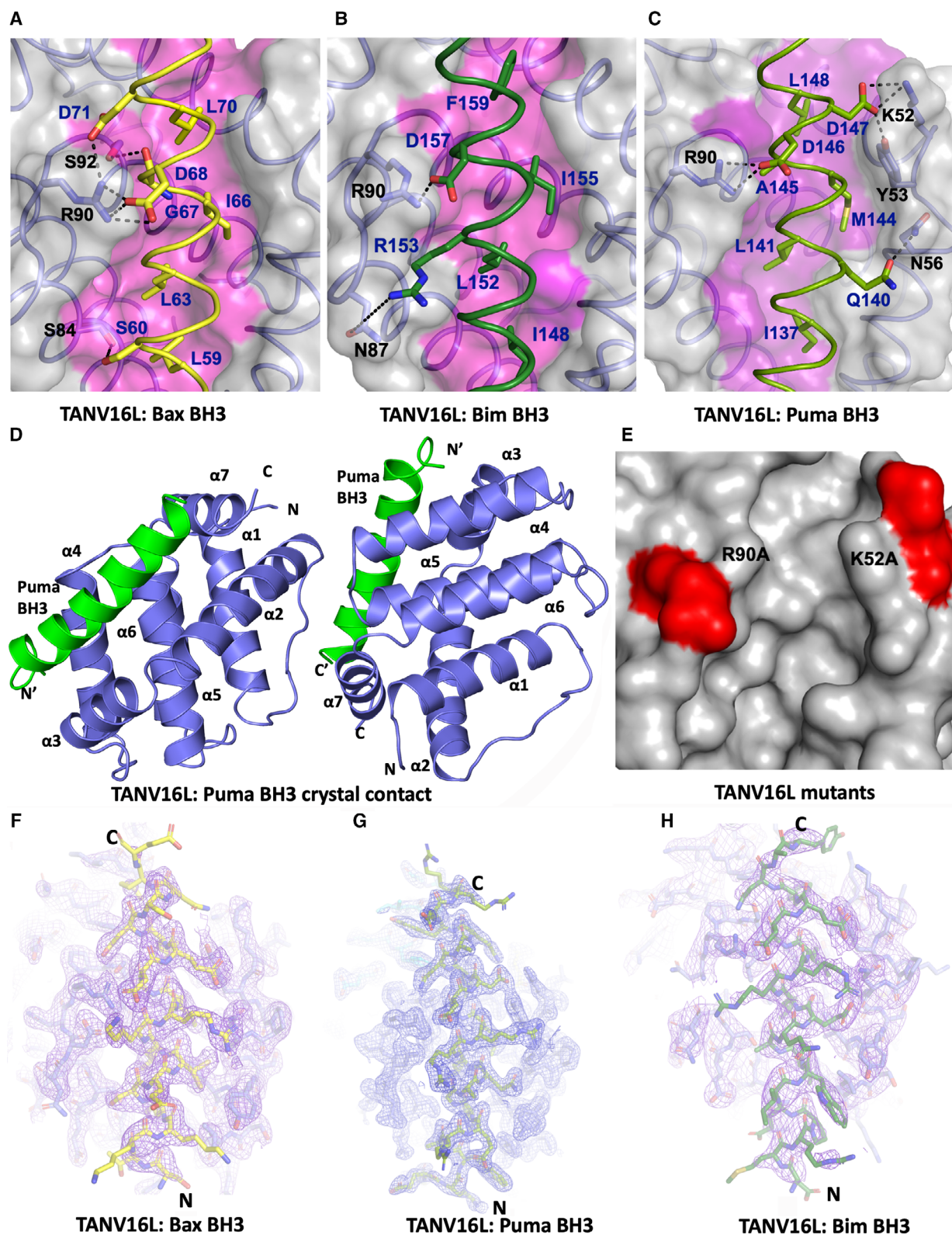To validate the crystal structures of TANV16L bound to Bim, Bax and Puma BH3, we performed structure-guided mutagenesis (Fig. 5E) and analysed the mutants for their ability to bind to proapoptotic BH3 motif peptides (Table 1). Mutation of the conserved R90 in TANV16L substantially impacts on its ability to bind BH3 motif peptides, with 10- to 80-fold reduction in affinities for Bim, Bad, Bid, Bik as well as Bak and Bax BH3 binding, whereas binding to Hrk and Puma BH3 is only reduced ~ 2-fold (Fig. 7). In contrast, whilst mutation of K52 to Ala also led to a 2- to 4-fold reduction in binding affinities for many interactors, binding to Bid BH3 was largely unaffected. Binding to Bad and Bmf BH3 was reduced by 27- and 20-fold, respectively (Fig. 8).

Discussion

Altruistic death of an infected cell is a potent mechanism to restrict viral infections. Viruses have evolved numerous strategies to prevent premature host cell death to establish productive infections [12]. Tanapoxvirus encodes TANV16L, a putative Bcl-2 homolog, and we now show that TANV16L adopts both a classical monomeric form as well as a domain-swapped dimer. Dimeric TANV16L is able to bind both BH3-only proteins and the BH3 motifs of Bak and Bax. TANV16L harbours a broad proapoptotic BH3 ligand binding profile when compared to other poxvirus-encoded domain-swapped prosurvival Bcl-2 proteins. The poxvirus-encoded prosurvival Bcl-2 homologs VACV F1L [33], VARV F1L [24] and deerpoxvirus DPV022 [29] all have similar dimeric topologies to TANV16L dimer but feature more restricted interaction and affinity profiles. VACV F1L [33] and DPV022 [29] only bind to Bim, Bak and Bak whereas VARV F1L binds Bid, Bak and Bax [24]. In all three cases, these interactions are characterized by lower affinities, in particular for Bak and Bax which bind with only micromolar affinities to VACV F1L, VARV F1L and DPV022. In contrast, TANV16L displays much tighter affinities including 38 nM for Bak and 70 nM for Bax BH3 (Table 1). Intriguingly, TANV16L is able to adopt both monomeric and domain-swapped dimer topologies; however, the domain swap does not impact significantly on the configuration of the canonical ligand binding groove. Superimposition of monomeric and dimeric TANV16L reveals there are virtually no differences in the respective ligand binding grooves. However, no thermodynamic analysis has been performed to examine such effects on ligand binding. When performing AUC analysis, we observed a small amount of a homotetrameric species of TANV16L in addition to monomeric and dimeric

A TANV16L: Bax BH3

B TANV16L: Bim BH3

C TANV16L: Puma BH3

D TANV16L: Puma BH3 crystal contact

E TANV16L mutants

F TANV16L: Bax BH3

G TANV16L: Puma BH3

H TANV16L: Bim BH3

TANV16L, However, no homotetrameric structures of Bcl-2 proteins have been determined to date. Coupled with the identification of other unexpected avenues for multimerization such as a groove-in-groove dimer as shown recently for GIV66 [21], we are unable to speculate as to what a potential homotetrameric species of TANV16L may look like with regard to the overall topology and multimerization route.

A comparison of the overall dimeric structures of TANV16L with other domain-swapped poxviral Bcl-2 dimers reveals that dimeric TANV16L superimposes on a VACV F1L dimer with an rmsd of 2.2 Å (over 266 Cα atoms) and on dimeric DPV022 with 2.7 Å (over 274 Cα atoms). This high level of similarity is achieved despite low overall sequence identity (8% between TANV16L and VACV F1L and 31% between TANV16L and DPV022). A detailed comparison of the interactions formed by TANV16L and DPV022 when bound to Bax reveals that the hallmark interaction between the conserved Asp from Bax BH3 with an Arg from TANV16L or DPV022 BH1 is preserved, as are hydrogen bonds between Bax Ser60 and Asp169 with TANV16L S84 or DPV022 E80. As expected, loss of the hallmark ionic interaction severely impacts TANV16L ability to bind to proapoptotic Bcl-2 interactors, with a TANV16L R90A mutation displaying up to 80-fold reduction in affinity (Table 1), as previously observed for mammalian prosurvival Bcl-2 [37]. Unlike in the DPV022 complex with Bax [29], the bulk of the BH3 peptides are engaged in the TANV16L ligand binding groove resulting in buried surface areas of 2343–3142 Å² for the complexes with Bax, Bim and Puma, whereas in DPV022:Bax BH3 only 4 helical turns are engaged that bury 2117 Å², which may contribute to the more modest affinity of the interaction. The more extensive engagement of the TANV16L binding groove with a BH3 peptide thus provides a possible rational for the substantially tighter binding observed compared with DPV022.

Virus-encoded Bcl-2 proteins are not limited to domain-swapping for dimer formation (Fig. 9). Vaccinia virus has been shown to encode for a suite of Bcl-2 fold proteins that modulate NF-κB signalling, with several of them adopting different dimeric topologies. N1 [38], B14 and A52 [39] utilize an interface formed by helices α1 and α6, whereas A46 forms a dimer via an α4 and α6 interface [40]. In contrast, grouper iridovirus-encoded GIV66 forms dimers that occlude the canonical ligand binding groove, with binding of BH3 motif peptides dissociating the dimers [21]. Domain swapping is not limited to virus-encoded Bcl-2 proteins and is also observed in mammalian Bcl-2 proteins. Bcl-xL has been shown to adopt domain-swapped topologies featuring either α5–α8 or α1 swaps. However, these swaps were induced by exposure to extreme pH [41] or temperature environments [42] or by truncation of the loop connecting α1 and α2 [43], respectively. In contrast, recombinantly expressed Bcl-w lacking its C-terminal tail adopts both a monomeric state and a domain-swapped dimeric state where α3–α4 are swapped [44,45]. Such a swap impacts the canonical ligand binding groove and leads to differential binding affinities between monomeric and dimeric Bcl-w [45]. Domain swapping has also been shown for human proapoptotic Bak [46] and Bax [47], where the formation of an extended single helix comprising helices α5 and α6 leads to a core/latch configuration, where a core domain formed by α1–4 partners the latch domain formed by α6–α8 from a second protomer. In contrast, catfish Bax features a domain-swapped α9 helix [48]. This significant number of topological variances across dimeric Bcl-2 proteins underscores the inherent flexibility in this fold and potentially enables additional layers of functionality to modulate function in addition to direct interactions.

Fig. 5. Detailed view of the TANV16L: Bax, Bim and Puma BH3 interfaces and mutation sites. (A) Surface depiction of the TANV16L: Bax BH3 complex. The TANV16L surface, backbone and floor of the binding groove are shown in grey and pink, respectively, whilst Bax BH3 is shown as a yellow ribbon. The four key hydrophobic residues of Bax BH3 (L59, L63, I66 and L70) are protruding into the binding groove, and the conserved salt bridge formed by Bax D68 and TANV16L R90 is labelled, as well as residues involved in hydrogen bonds. (B) TANV16L:Bim BH3 with the surface of TANV16L is shown as in (a), and Bim BH3 is shown in dark green. The four key hydrophobic residues of Bim BH3 (I148, L152, I155 and F159) are protruding into the binding groove, and the conserved salt bridge formed by Bim D157 and TANV16L R90 is labelled, as well as residues involved in hydrogen bonds. Interactions are denoted as black dotted lines. (C) TANV16L: Puma BH3 is shown as in (A), with Puma BH3 shown in olive. The four key hydrophobic residues of Puma BH3 (I137, L141, M144 and L148) are protruding into the binding groove, and the conserved salt bridge formed by Puma D146 and TANV16L R90 is labelled, as well as residues involved in hydrogen bonds. Interactions are denoted as black dotted lines. (D) Crystal packing of TANV16L:Puma BH3 complex. (E) TANV16L is shown as a grey surface, with locations of mutations used to investigate the binding site shaded in red. The views were selected for the clearest view of the groove interactions in each case. (F) 2Fo-Fc electron density maps of TANV16L:Bax BH3 complex interface. (G) 2Fo-Fc electron density maps of TANV16L:Puma BH3 complex interface. (H) 2Fo-Fc electron density maps of TANV16L:Bim BH3 complex interface. All maps were contoured at 1.5 σ. The N and C termini of the BH3 peptides are labelled and the structures aligned as in Fig. 4. The view was selected for clarity of the BH3 peptide side chains. Images were generated using the PYMOL Molecular Graphics System, Version 1.8 Schrödinger, LLC.
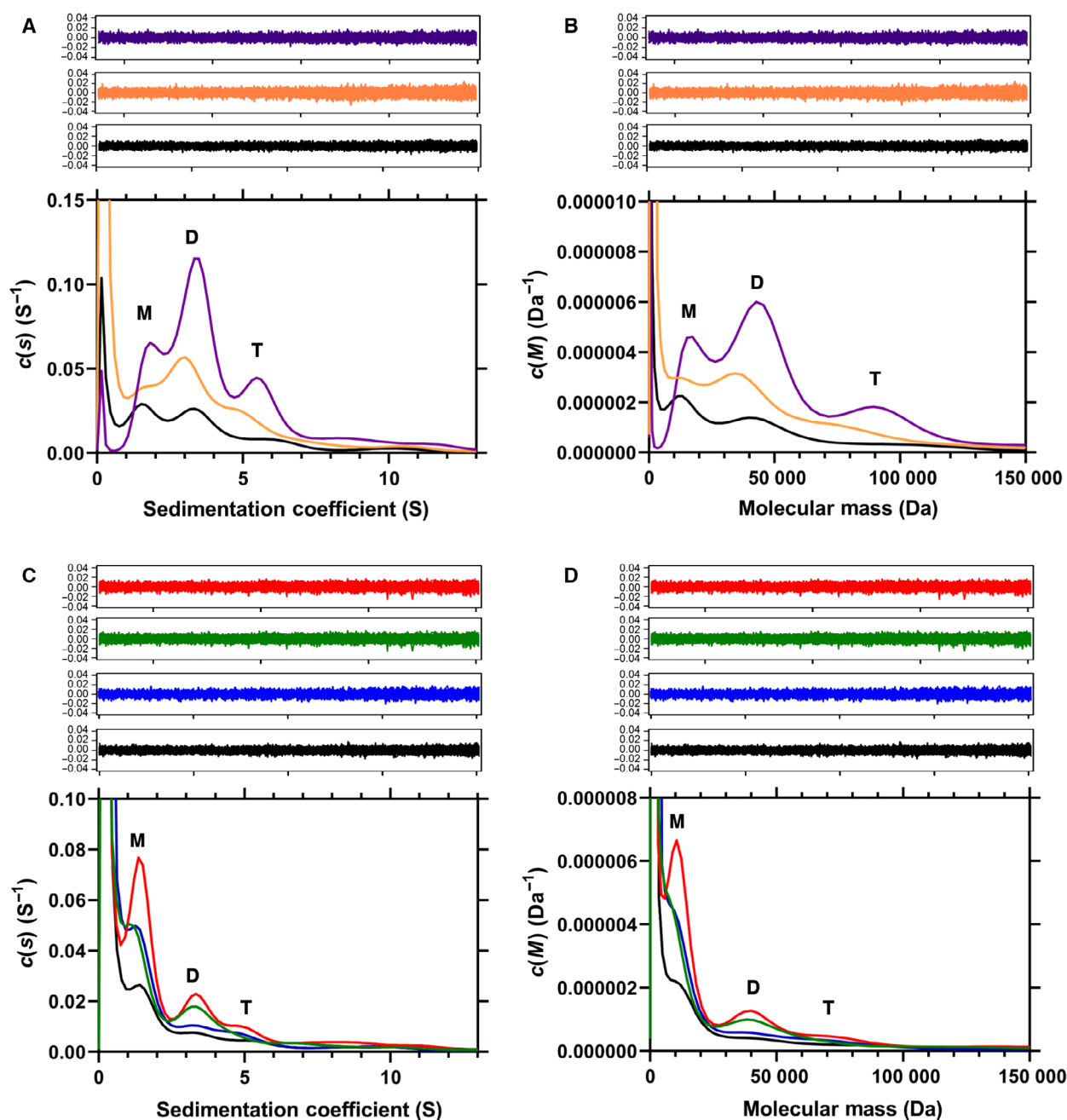
Fig. 6. Sedimentation velocity AUC analysis of (A, B) TANV16L on its own at initial concentrations of 0.2 mg·mL^{-1} (black), 0.4 mg·mL^{-1} (orange) and 0.8 mg·mL^{-1} (purple) and (C, D) TANV16L at an initial concentration of 0.2 mg·mL^{-1} unliganded (black) and in complex with Bim (blue), Bax (green) or Puma (red). *Top panels* – Residuals resulting from the sedimentation coefficient distribution *c*(*s*) (A, C) and distribution of molar masses *c*(*M*) (B, D) best fits are plotted as a function of radial position. The residuals for the given curves are shown in the same colour above the plots. M denotes monomeric, D dimeric and T tetrameric species.

In summary, we report the biochemical and structural analysis of tanapoxvirus 16L, which revealed a broad high affinity binding profile for mammalian proapoptotic Bcl-2 proteins. Furthermore, our crystal structures of TANV16L bound to Bax and Puma BH3 indicate that

TANV16L displays substantial structural plasticity, being able to adopt both a classical monomeric Bcl-2 fold and a domain-swapped dimeric Bcl-2 fold. Overall, our findings provide a mechanistic platform for dissecting the role of 16L for tanapoxvirus replication and infectivity.
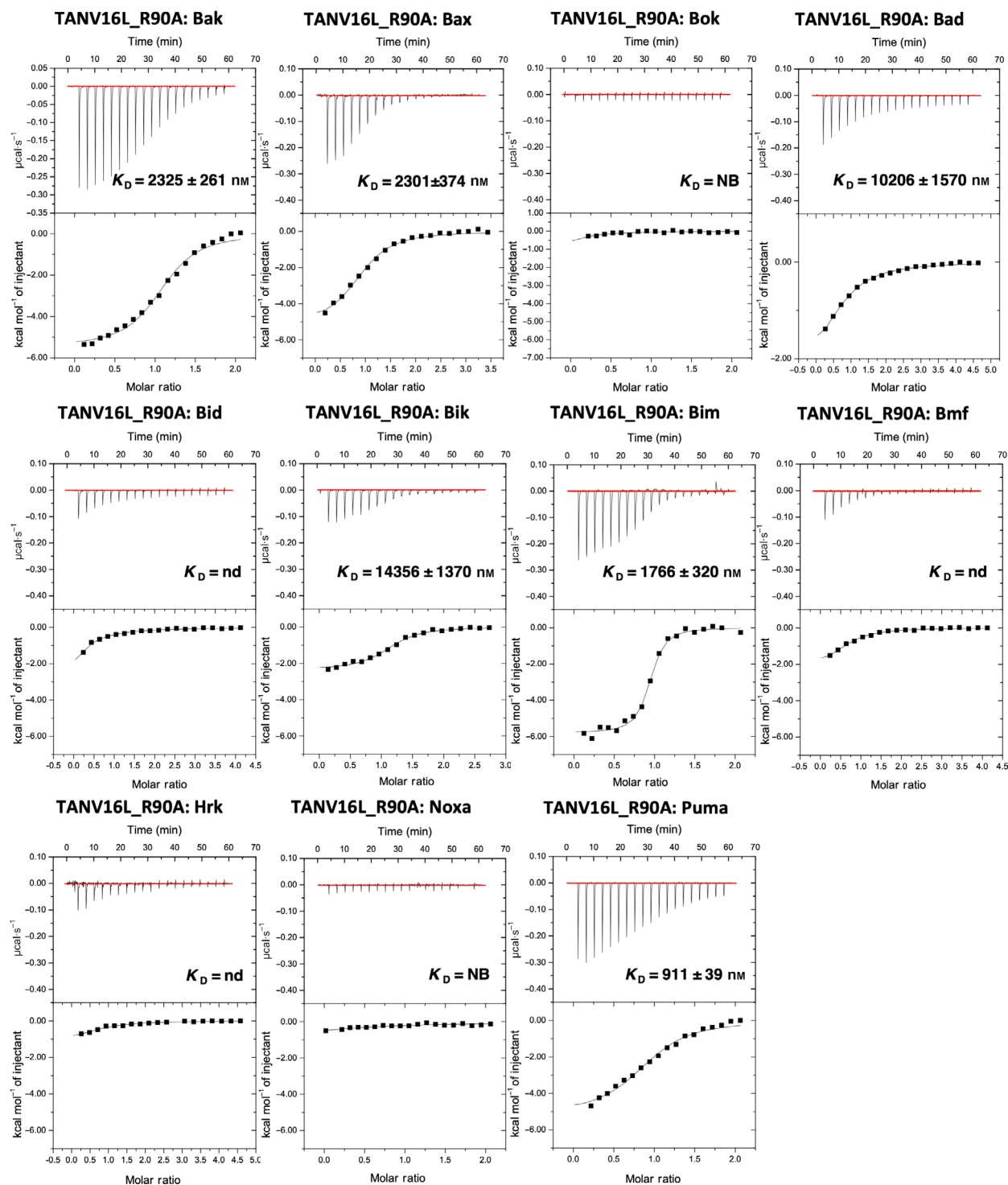
Fig. 7. The affinities of recombinant TANV16L_R90A mutant for BH3 motif peptides (26-mers, except for a Bid 34-mer and Bax 28-mers) were measured using ITC and the raw thermograms shown. K_D values (in nM) are the means of 3 experiments $\pm$ SD. NB: no binding detected. nd: not determined with data obtained not suitable for precise determination of affinities and thermodynamic parameters. The binding affinities are tabulated in Table 1.

TANV16L_K52A: Bak

$K_D = 113 \pm 3$ nM

TANV16L_K52A: Bax

$K_D = 266 \pm 11$ nM

TANV16L_K52A: Bok

$K_D = $ NB

TANV16L_K52A: Bad

$K_D = 5857 \pm 732$ nM

TANV16L_K52A: Bid

$K_D = 976 \pm 126$ nM

TANV16L_K52A: Bik

$K_D = 3382 \pm 85$ nM

TANV16L_K52A: Bim

$K_D = 558 \pm 27$ nM

TANV16L_K52A: Bmf

$K_D = $ nd

TANV16L_K52A: Hrk

$K_D = $ nd

TANV16L_K52A: Noxa

$K_D = $ NB

TANV16L_K52A: Puma

$K_D = 1010 \pm 130$ nM

Fig. 8. The affinities of recombinant TANV16L_K52A mutant for BH3 motif peptides (26-mers, except for a Bid 34-mer and Bax 28-mers) were measured using ITC and the raw thermograms shown. K_D values (in nM) are the means of three experiments $\pm$ SD. NB: no binding detected. nd: not determined with data obtained not suitable for precise determination of affinities and thermodynamic parameters. The binding affinities are tabulated in Table 1.

Materials and methods

Protein expression and purification

Synthetic cDNA encoding for codon-optimized wild-type TANV16L (UniProt accession number: Q9DHU6) as well as two mutants TANV16L (K52A and R90A) lacking 23 C-terminal residues was cloned into the bacterial expression vector pGex-6p-1 (GenScript, Piscataway, NJ, USA). Recombinant TANV16L was expressed in C41(DE3) cells in 2YT medium supplemented with 1 mg·mL^{-1} ampicillin at 37 °C in a shaking incubator until an OD$_{600}$ of 0.6 was reached. The protein expression was induced by adding isopropyl β-D-1-thiogalactopyranoside (IPTG) to final concentration of 0.75 mM for 18 h at 20 °C. Bacterial cells were harvested by centrifugation at 5180 *g* (JLA 9.1000 rotor, Beckman Coulter Avanti J-E, Brea, CA, USA) for 20 min and re-suspended in 100 mL lysis buffer A [50 mM Tris pH 8.0, 300 mM NaCl and 10 mM DTT (dithiothreitol)]. The cells were homogenized using an Aves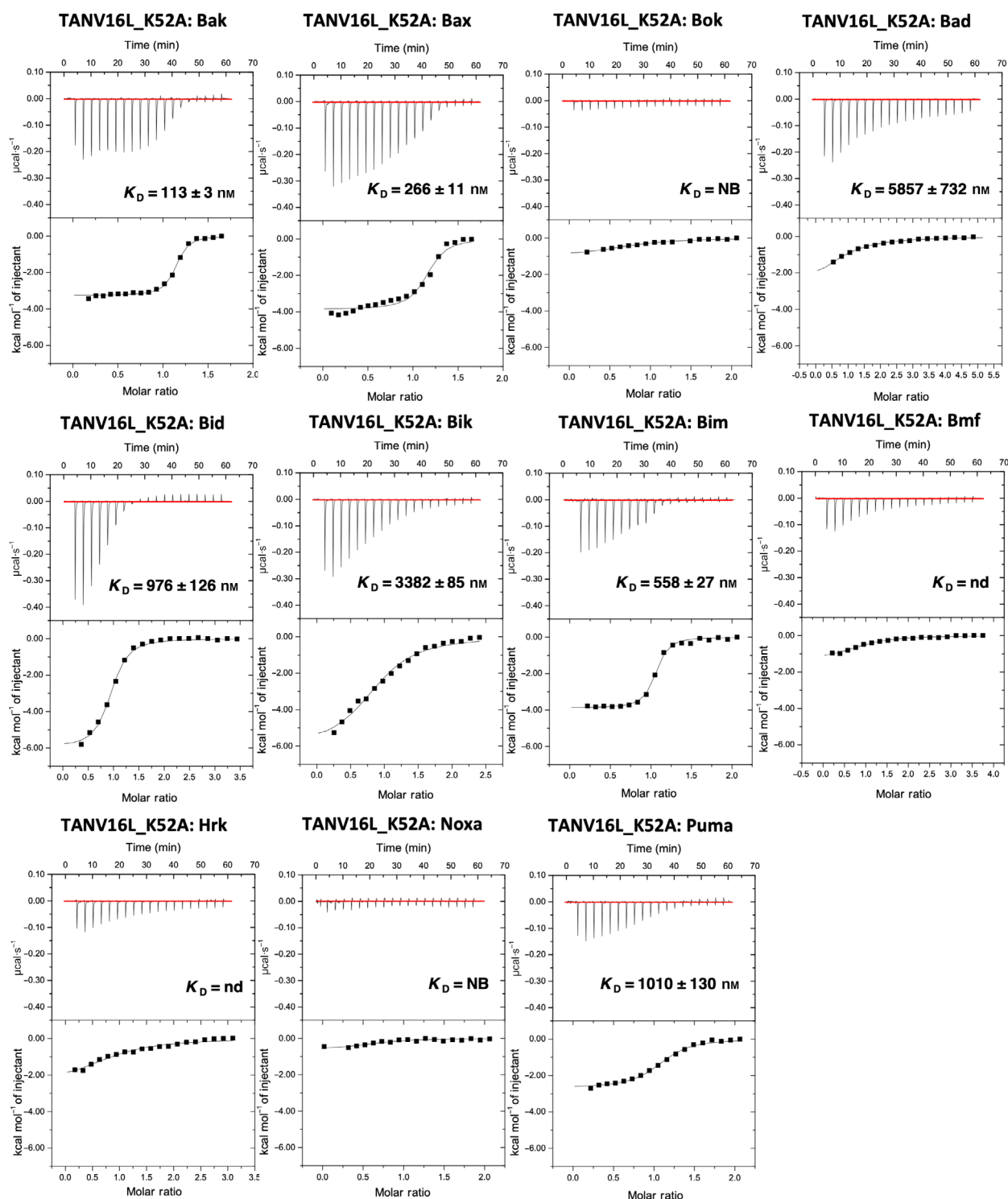tin EmulsiFlex homogenizer and lysed using sonication (programme 7; Fisher Scientific™ Model 705 Sonic Dismembrator, Waltham, MA, USA), and the resultant lysate was transferred into SS34 tubes for further centrifugation at 39 190 *g* (JA-25.50 rotor, Beckman Coulter Avanti J-E) for 30 min. The supernatant was loaded onto 5 mL of glutathione sepharose 4B (GE Healthcare, Chicago, IL, USA) equilibrated with buffer A. After sample application, the column was washed with 150 mL of buffer A and protein on-column cleavage was achieved by adding HRV 3C protease overnight at 4 °C. The cleaved protein was eluted using buffer A, with the remaining protein being concentrated using a centrifugal concentrator with 3 kDa molecular weight cut-off (Amicon® Ultra 15, Merck Millipore, Kenilworth, NJ, USA) to a final volume of 2 mL. Concentrated TANV16L was subjected to size-exclusion chromatography using a Superdex S200 increase 10/300 column mounted on an ÄKTA Pure system (GE Healthcare) equilibrated in 25 mM HEPES pH 7.5, 150 mM NaCl and 5 mM TCEP (Tris(2-carboxyethyl)phosphine hydrochloride), and fractions analysed using SDS/PAGE. The final sample purity was estimated to be greater than 95% based on SDS/PAGE analysis. Appropriate fractions were pooled and concentrated using a centrifugal concentrator with 3 kDa molecular weight cut-off (Amicon® Ultra 15) to final concentration of 5.4 mg·mL^{-1}.

Analytical ultracentrifugation

Sedimentation velocity experiments were performed in a Beckman Coulter XL-A analytical ultracentrifuge as described previously [49–52]. Briefly, double-sector quartz cells were loaded with 400 μL of buffer (25 mM HEPES pH 7.5, 150 mM NaCl, 5 mM TCEP) and 380 μL of sample (solubilized in buffer). For the runs with apoprotein, initial concentrations of 0.2, 0.4 and 0.8 mg·mL^{-1} were employed. For the runs with the complexes, the protein and peptide concentrations were kept at 0.2 mg·mL^{-1}. The cells were loaded into an An50-Ti rotor and the experiments conducted at 25 °C. Initial scans were carried out at 4146 *g* to determine the optimal wavelength and radial positions. Final scans were performed at 80 000 *g*, and data were collected continuously at 230 nm using a step size of 0.003 cm without averaging. Solvent density, solvent viscosity and estimates of the partial specific volume of *apo*-TANV16L, TANV16L:Bim, TANV16L:Puma and TANV16L:Bax at 25 °C were calculated using SEDNTERP [53]. Data were fitted using the SEDFIT software (www.analyticalultracentrifugation.com) to a continuous size-distribution model [54–56].

Measurement of dissociation constants

Binding affinities were measured using a MicroCal iTC200 system (GE Healthcare) at 25 °C using wild-type TANV16L as well as two mutants TANV16L K52A and R90A in 25 mM HEPES pH 7.5, 150 mM NaCl and 5 mM TCEP. Measurements were performed at a range of different concentrations for BH3 motif peptide and TANV16L proteins, which are summarized below in Table 3. All affinity measurements were performed in triplicate. Protein concentrations were measured using a Nanodrop UV spectrophotometer (Thermo Fisher Scientific, Waltham, MA, USA) at a wavelength of 280 nm. Peptide concentrations were calculated based on the dry peptide weight after synthesis. The BH3 motif peptides used were commercially synthesized and were purified to a final purity of 95% (GenScript) and based on the human sequences as previously described [57].

Crystallization and structure determination

Crystals for TANV16L: Bax BH3, TANV16L: Puma BH3 or TANV16L: Bim BH3 complexes were obtained by mixing TANV16L with human Bax BH3 28-mer or Puma BH3 26-mer peptide into 1 : 1.25 molar ratio as described previously [58] and concentrated using a centrifugal concentrator with 3 kDa molecular weight cut-off (Amicon® Ultra 0.5) to 5 mg·mL^{-1}, and concentrated protein was immediately used for crystallization trials. Initial high-throughput sparse matrix screening was performed using 96-well sitting drop trays (Swissci, Neuheim, Switzerland) using 200 nL of protein mixed with 200 nL of reservoir solution.

TANV16L: Bax BH3 crystals were grown by the sitting drop vapour diffusion method at 20 °C in 1.0 M LiCl, 0.1 M Citrate pH 4.0, and 20 % W/V PEG 6000. The crystals were flash cooled at −173 °C in mother liquor supplemented with 20% ethylene glycol. Diffraction data were collected at the Australian Synchrotron MX2 beamline using an Eiger detector with an oscillation range 0.1° per frame with a wavelength of 0.9537 Å, integrated using XDS [59] and scaled using AIMLESS [60]. Molecular replacement was carried out using PHASER [61] with the previously solved
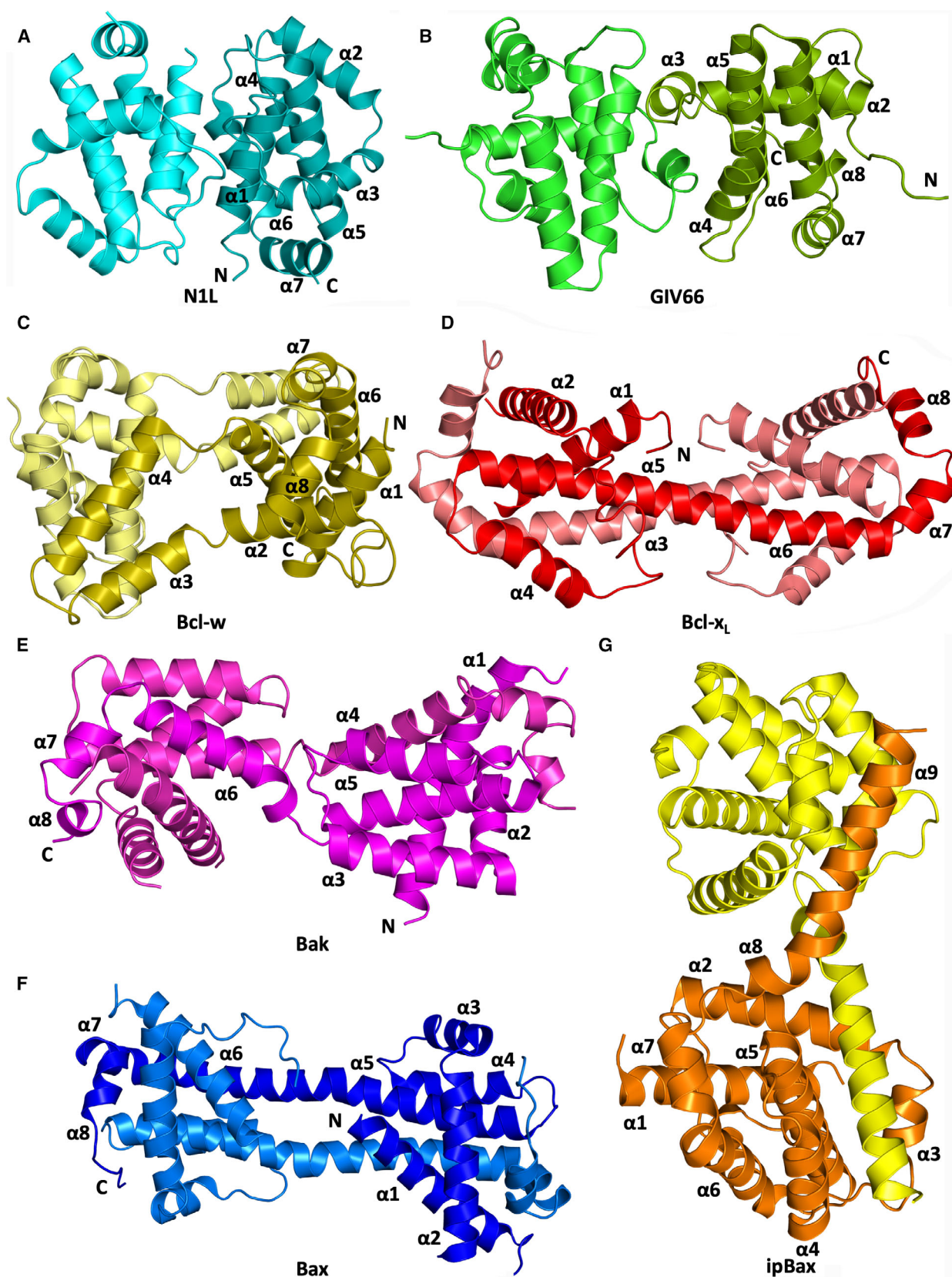
Table 3. Summary of protein and ligand concentrations used in ITC measurements.

Interaction	Protein concentration (μm)	BH3 motif peptide concentration (μm)
TANV16L:Bak BH3	60	600
TANV16L:Bax BH3	60	600
TANV16L:Bok BH3	60	600
TANV16L:Bad BH3	60	550
TANV16L:Bid BH3	60	600
TANV16L:Bik BH3	60	750
TANV16L:Bim BH3	60	600
TANV16L:Bmf BH3	60	800
TANV16L:Hrk BH3	60	600
TANV16L:Noxa BH3	60	600
TANV16L:Puma BH3	60	700
TANV16L_R90A:Bak BH3	60	600
TANV16L_R90A:Bax BH3	60	800
TANV16L_R90A:Bok BH3	60	600
TANV16L_R90A:Bad BH3	60	950
TANV16L_R90A:Bid BH3	60	900
TANV16L_R90A:Bik BH3	60	700
TANV16L_R90A:Bim BH3	60	600
TANV16L_R90A:Bmf BH3	60	900
TANV16L_R90A:Hrk BH3	65	900
TANV16L_R90A:Noxa BH3	60	600
TANV16L_R90A:Puma BH3	60	600
TANV16L_K52A:Bak BH3	60	550
TANV16L_K52A:Bax BH3	60	550
TANV16L_K52A:Bok BH3	60	600
TANV16L_K52A:Bad BH3	60	1000
TANV16L_K52A:Bid BH3	60	800
TANV16L_K52A:Bik BH3	60	650
TANV16L_K52A:Bim BH3	60	600
TANV16L_K52A:Bmf BH3	60	850
TANV16L_K52A:Hrk BH3	65	600
TANV16L_K52A:Noxa BH3	60	600
TANV16L_K52A:Puma BH3	60	600

structure of DPV022 (PDB ID: 4UF1 [29]) as a search model. TANV16L: Bax BH3 crystals contained one molecule of TANV16L and one Bax BH3 peptide in the asymmetric unit, with 46.3% solvent content and final TFZ and LLG values of 8.0 and 52.79, respectively. The final model of TANV16L: Bax BH3 was built manually over several cycles using COOT [62] and refined using PHENIX [63].

TANV16L: Puma BH3 crystals were grown as the TANV16L: Bax BH3 crystals and were obtained in 0.1 M potassium thiocyanate, 30% PEG 2000MME. The crystals were flash cooled at −173 °C in mother liquor. Diffraction data collection, integration and scaling were performed as described above. The molecular replacement was carried out using PHASER with the previously solved structure of TANV16L: Bax BH3 as a search model. TANV16L: Puma BH3 crystals contain one molecule of TANV16L and one Puma BH3 peptide, with 46.3% solvent content and final TFZ and LLG values of 13.2 and 133.15, respectively. The final model of TANV16L: Puma BH3 was built manually over several cycles using COOT and refined using PHENIX.

TANV16L: Bim BH3 crystals were grown similar to other two complexes as above and in 0.1 M MIB buffer pH 8.0, 25% PEG 1500. The crystals were flash cooled at −173 °C in mother liquor. Diffraction data collection, integration and scaling were performed as described above. Molecular replacement was carried out using PHASER with the previously solved structure of TANV16L: Bax BH3 as a search model. TANV16L: Bim BH3 crystals contain one molecule of TANV16L and one Bim BH3 peptide, with 44.01% solvent content and final TFZ and LLG values of 15.8 and 208.64, respectively. The final model of TANV16L: Bim BH3 was built manually and refined as described above. Coordinate files have been deposited in the Protein Data Bank under the accession codes 6TPQ, 6TQQ and 6TRR. All images were generated using the PYMOL Molecular Graphics System, Version 1.8 Schrödinger, LLC. All software was accessed using the SBGrid suite [64]. All raw diffraction images were deposited on the SBGrid Data Bank [65] using their PDB accession code 6TPQ, 6TQQ and 6TRR.

Sequence alignment and interface analysis

Sequence alignments were performed using MUSCLE [66] (https://www.ebi.ac.uk/Tools/msa/muscle/) with the default settings, and sequence identities were calculated based on the total number of conserved residues in TANV16L against the full sequence. Protein interfaces were analysed using PISA [67].

Yeast colony assays

Saccharomyces cerevisiae W303α cells were co-transformed with pGALL(TRP) vector only, pGALL(TRP)-Bcl-x_L, or pGALL(TRP)-TANV16L and pGALL(Leu)-Bak or pGALL(Leu)-Bax. pGALL(TRP) and pGALL(Leu) places

Fig. 9. Cartoon diagrams of dimeric topologies in the Bcl-2 family (A) Vaccinia virus N1L homodimer (cyan, PDB ID 2UXE) [38]. (B) Grouper iridovirus GIV66 (green, PDB ID 5VMN) [21]. (C) Human Bcl-w (sand, PDB ID 2Y6W) [45]. (D) Human Bcl-x_L (red, PDB ID 1R2D) [41]. (E) Human Bak core-latch dimer (magenta, PDB ID 4U2U) [46]. (F) Human Bax core-latch dimer (blue, PDB ID 4ZIE) [47]. (G) Catfish Bax groove-tail dimer (yellow and orange, PDB ID 5W63) [48]. Images were generated using the PYMOL Molecular Graphics System, Version 1.8 Schrödinger, LLC.

genes under the control of a galactose-inducible promoter [68]. Cells were subsequently spotted as a 5-fold serial dilution series onto medium supplemented with 2% w/v galactose (inducing, 'ON') to induce protein expression, or 2% w/v glucose (repressing, 'OFF'), which prevents protein expression, as previously described [69]. Plates were incubated for 48 h at 30 °C and then photographed.

Acknowledgements

Conflict of interest

The authors declare no conflict of interest.

Author contributions

CDS and TPSC acquired, analysed and interpreted the data, and drafted and revised the manuscript. MIA, AJ, SC, REI and MHZ acquired, analysed and interpreted the data. MGH conceived and designed the study, analysed and interpreted the data, and drafted and revised the manuscript. MK conceived and designed the study; acquired, analysed and interpreted the data; and drafted and revised the manuscript.

References

1 Downie AW, Taylor-Robinson CH, Caunt AE, Nelson GS, Manson-Bahr PE & Matthews TC (1971) Tanapox: a new disease caused by a pox virus. *Br Med J* **1**, 363–368.

2 Knight JC, Novembre FJ, Brown DR, Goldsmith CS & Esposito JJ (1989) Studies on tanapox virus. *Virology* **172**, 116–124.

3 Brunetti CR, Paulose-Murphy M, Singh R, Qin J, Barrett JW, Tardivel A, Schneider P, Essani K & McFadden G (2003) A secreted high-affinity inhibitor of human TNF from tanapox virus. *Proc Natl Acad Sci USA* **100**, 4831–4836.

4 Nazarian SH, Barrett JW, Frace AM, Olsen-Rasmussen M, Khristova M, Shaban M, Neering S, Li Y, Damon

IK, Esposito JJ *et al.* (2007) Comparative genetic analysis of genomic DNA sequences of two human isolates of tanapox virus. *Virus Res* **129**, 11–25.

5 Kvansakul M & Hinds MG (2015) The Bcl-2 family: structures, interactions and targets for drug discovery. *Apoptosis* **20**, 136–150.

6 Banjara S, Suraweera CD, Hinds MG & Kvansakul M (2020) The Bcl-2 family: ancient origins, conserved structures, and divergent mechanisms. *Biomolecules* **10**, 128.

7 Kvansakul M & Hinds MG (2013) Structural biology of the Bcl-2 family and its mimicry by viral proteins. *Cell Death Dis* **4**, e909.

8 Kvansakul M & Hinds MG (2014) The structural biology of BH3-only proteins. *Methods Enzymol* **544**, 49–74.

9 Shamas-Din A, Kale J, Leber B & Andrews DW (2013) Mechanisms of action of bcl-2 family proteins. *Cold Spring Harb Perspect Biol* **5**, a008714.

10 McArthur K, Whitehead LW, Heddleston JM, Li L, Padman BS, Oorschot V, Geoghegan ND, Chappaz S, Davidson S, San Chin H *et al.* (2018) BAK/BAX macropores facilitate mitochondrial herniation and mtDNA efflux during apoptosis. *Science* **359**, eaao6047.

11 Tait SW & Green DR (2010) Mitochondria and cell death: outer membrane permeabilization and beyond. *Nat Rev Mol Cell Biol* **11**, 621–632.

12 Kvansakul M, Caria S & Hinds MG (2017) The Bcl-2 family in host-virus interactions. *Viruses* **9**, 290.

13 Kvansakul M, Wei AH, Fletcher JI, Willis SN, Chen L, Roberts AW, Huang DC & Colman PM (2010) Structural basis for apoptosis inhibition by Epstein-Barr virus BHRF1. *PLoS Pathog* **6**, e1001236.

14 Henderson S, Huen D, Rowe M, Dawson C, Johnson G & Rickinson A (1993) Epstein-Barr virus-coded BHRF1 protein, a viral homologue of Bcl-2, protects human B cells from programmed cell death. *Proc Natl Acad Sci USA* **90**, 8479–8483.

15 Huang Q, Petros AM, Virgin HW, Fesik SW & Olejniczak ET (2002) Solution structure of a Bcl-2 homolog from Kaposi sarcoma virus. *Proc Natl Acad Sci USA* **99**, 3428–3433.

16 Sarid R, Sato T, Bohenzky RA, Russo JJ & Chang Y (1997) Kaposi's sarcoma-associated herpesvirus encodes a functional bcl-2 homologue. *Nat Med* **3**, 293–298.

17 Cheng EH, Nicholas J, Bellows DS, Hayward GS, Guo HG, Reitz MS & Hardwick JM (1997) A Bcl-2 homolog encoded by Kaposi sarcoma-associated virus, human herpesvirus 8, inhibits apoptosis but does not heterodimerize with Bax or Bak. *Proc Natl Acad Sci USA* **94**, 690–694.

18 Banjara S, Caria S, Dixon LK, Hinds MG & Kvansakul M (2017) Structural insight into African swine fever virus A179L-mediated inhibition of apoptosis. *J Virol* **91**, e02228-16.

19 Brun A, Rivas C, Esteban M, Escribano JM & Alonso C (1996) African swine fever virus gene A179L, a viral homologue of bcl-2, protects cells from programmed cell death. *Virology* **225**, 227–230.

20 Banjara S, Shimmon GL, Dixon LK, Netherton CL, Hinds MG & Kvansakul M (2019) Crystal structure of African swine fever virus A179L with the autophagy regulator Beclin. *Viruses* **11**, 789.

21 Banjara S, Mao J, Ryan TM, Caria S & Kvansakul M (2018) Grouper iridovirus GIV66 is a Bcl-2 protein that inhibits apoptosis by exclusively sequestering Bim. *J Biol Chem* **293**, 5464–5477.

22 Lin PW, Huang YJ, John JA, Chang YN, Yuan CH, Chen WY, Yeh CH, Shen ST, Lin FP, Tsui WH *et al.* (2008) Iridovirus Bcl-2 protein inhibits apoptosis in the early stage of viral infection. *Apoptosis* **13**, 165–176.

23 Campbell S, Thibault J, Mehta N, Colman PM, Barry M & Kvansakul M (2014) Structural insight into BH3 domain binding of vaccinia virus antiapoptotic F1L. *J Virol* **88**, 8667–8677.

24 Marshall B, Puthalakath H, Caria S, Chugh S, Doerflinger M, Colman PM & Kvansakul M (2015) Variola virus F1L is a Bcl-2-like protein that unlike its vaccinia virus counterpart inhibits apoptosis independent of Bim. *Cell Death Dis* **6**, e1680.

25 Wasilenko ST, Stewart TL, Meyers AF & Barry M (2003) Vaccinia virus encodes a previously uncharacterized mitochondrial-associated inhibitor of apoptosis. *Proc Natl Acad Sci USA* **100**, 14345–14350.

26 Opgenorth A, Graham K, Nation N, Strayer D & McFadden G (1992) Deletion analysis of two tandemly arranged virulence genes in myxoma virus, M11L and myxoma growth factor. *J Virol* **66**, 4720–4731.

27 Douglas AE, Corbett KD, Berger JM, McFadden G & Handel TM (2007) Structure of M11L: a myxoma virus structural homolog of the apoptosis inhibitor, Bcl-2. *Protein Sci* **16**, 695–703.

28 Kvansakul M, van Delft MF, Lee EF, Gulbis JM, Fairlie WD, Huang DC & Colman PM (2007) A structural viral mimic of prosurvival Bcl-2: a pivotal role for sequestering proapoptotic Bax and Bak. *Mol Cell* **25**, 933–942.

29 Burton DR, Caria S, Marshall B, Barry M & Kvansakul M (2015) Structural basis of Deerpox virus-mediated inhibition of apoptosis. *Acta Crystallogr D* **71**, 1593–1603.

30 Anasir MI, Baxter AA, Poon IKH, Hulett MD & Kvansakul M (2017) Structural and functional insight into canarypox virus CNP058 mediated regulation of apoptosis. *Viruses* **9**, 305.

31 Anasir MI, Caria S, Skinner MA & Kvansakul M (2017) Structural basis of apoptosis inhibition by the fowlpox virus protein FPV039. *J Biol Chem* **292**, 9010–9021.

32 Suraweera CD, Burton DR, Hinds MG & Kvansakul M (2020) Crystal structures of the sheeppoxvirus encoded inhibitor of apoptosis SPPV14 bound to Hrk and Bax BH3 peptides. *FEBS Lett*. https://doi.org/10.1002/1873-3468.13807

33 Kvansakul M, Yang H, Fairlie WD, Czabotar PE, Fischer SF, Perugini MA, Huang DC & Colman PM (2008) Vaccinia virus anti-apoptotic F1L is a novel Bcl-2-like domain-swapped dimer that binds a highly selective subset of BH3-containing death ligands. *Cell Death Differ* **15**, 1564–1571.

34 Okamoto T, Campbell S, Mehta N, Thibault J, Colman PM, Barry M, Huang DC & Kvansakul M (2012) Sheeppox virus SPPV14 encodes a Bcl-2-like cell death inhibitor that counters a distinct set of mammalian proapoptotic proteins. *J Virol* **86**, 11501–11511.

35 Holm L & Rosenstrom P (2010) Dali server: conservation mapping in 3D. *Nucleic Acids Res* **38**, W545–W549.

36 Pelz NF, Bian Z, Zhao B, Shaw S, Tarr JC, Belmar J, Gregg C, Camper DV, Goodwin CM, Arnold AL *et al.* (2016) Discovery of 2-indole-acylsulfonamide myeloid cell leukemia 1 (Mcl-1) inhibitors using fragment-based methods. *J Med Chem* **59**, 2054–2066.

37 Sattler M, Liang H, Nettesheim D, Meadows RP, Harlan JE, Eberstadt M, Yoon HS, Shuker SB, Chang BS, Minn AJ *et al.* (1997) Structure of Bcl-xL-Bak peptide complex: recognition between regulators of apoptosis. *Science* **275**, 983–986.

38 Cooray S, Bahar MW, Abrescia NG, McVey CE, Bartlett NW, Chen RA, Stuart DI, Grimes JM & Smith GL (2007) Functional and structural studies of the vaccinia virus virulence factor N1 reveal a Bcl-2-like anti-apoptotic protein. *J Gen Virol* **88**, 1656–1666.

39 Graham SC, Bahar MW, Cooray S, Chen RA, Whalen DM, Abrescia NG, Alderton D, Owens RJ, Stuart DI, Smith GL *et al.* (2008) Vaccinia virus proteins A52 and B14 Share a Bcl-2-like fold but have evolved to inhibit NF-kappaB rather than apoptosis. *PLoS Pathog* **4**, e1000128.

40 Fedosyuk S, Grishkovskaya I, de Almeida Ribeiro E Jr & Skern T (2014) Characterization and structure of the vaccinia virus NF-kappaB antagonist A46. *J Biol Chem* **289**, 3749–3762.

41 O'Neill JW, Manion MK, Maguire B & Hockenbery DM (2006) BCL-XL dimerization by three-dimensional domain swapping. *J Mol Biol* **356**, 367–381.

42 Denisov AY, Sprules T, Fraser J, Kozlov G & Gehring K (2007) Heat-induced dimerization of BCL-xL through alpha-helix swapping. *Biochemistry* **46**, 734–740.

43 Oberstein A, Jeffrey PD & Shi Y (2007) Crystal structure of the Bcl-XL-Beclin 1 peptide complex: Beclin 1 is a novel BH3-only protein. *J Biol Chem* **282**, 13123–13132.

44 Hinds MG, Lackmann M, Skea GL, Harrison PJ, Huang DC & Day CL (2003) The structure of Bcl-w reveals a role for the C-terminal residues in modulating biological activity. *EMBO J* **22**, 1497–1507.

45 Lee EF, Dewson G, Smith BJ, Evangelista M, Pettikiriarachchi A, Dogovski C, Perugini MA, Colman PM & Fairlie WD (2011) Crystal structure of a BCL-W domain-swapped dimer: implications for the function of BCL-2 family proteins. *Structure* **19**, 1467–1476.

46 Brouwer JM, Westphal D, Dewson G, Robin AY, Uren RT, Bartolo R, Thompson GV, Colman PM, Kluck RM & Czabotar PE (2014) Bak core and latch domains separate during activation, and freed core domains form symmetric homodimers. *Mol Cell* **55**, 938–946.

47 Czabotar PE, Westphal D, Dewson G, Ma S, Hockings C, Fairlie WD, Lee EF, Yao S, Robin AY, Smith BJ *et al.* (2013) Bax crystal structures reveal how BH3 domains activate Bax and nucleate its oligomerization to induce apoptosis. *Cell* **152**, 519–531.

48 Robin AY, Iyer S, Birkinshaw RW, Sandow J, Wardak A, Luo CS, Shi M, Webb AI, Czabotar PE, Kluck RM *et al.* (2018) Ensemble properties of Bax determine its function. *Structure* **26**, 1346–1359, e5.

49 Soares da Costa TP, Yap MY, Perugini MA, Wallace JC, Abell AD, Wilce MC, Polyak SW & Booker GW (2014) Dual roles of F123 in protein homodimerization and inhibitor binding to biotin protein ligase from *Staphylococcus aureus*. *Mol Microbiol* **91**, 110–120.

50 Soares da Costa TP, Patel M, Desbois S, Gupta R, Faou P & Perugini MA (2017) Identification of a dimeric KDG aldolase from *Agrobacterium tumefaciens*. *Proteins* **85**, 2058–2065.

51 Soares da Costa TP, Desbois S, Dogovski C, Gorman MA, Ketaren NE, Paxman JJ, Siddiqui T, Zammit LM, Abbott BM, Robins-Browne RM *et al.* (2016) Structural determinants defining the allosteric inhibition of an essential antibiotic target. *Structure* **24**, 1282–1291.

52 Soares da Costa TP, Christensen JB, Desbois S, Gordon SE, Gupta R, Hogan CJ, Nelson TG, Downton MT, Gardhi CK, Abbott BM *et al.* (2015) Quaternary structure analyses of an essential oligomeric enzyme. *Methods Enzymol* **562**, 205–223.

53 Laue TM, Shah B, Ridgeway TM & Pelletier SL. (1992) Computer-aided interpretation of analytical sedimentation data for proteins. In Analytical Ultracentrifugation in Biochemistry and Polymer Science (Harding SE, Horton JC & Rowe AJ, eds), pp. 90–125. Royal Society of Chemistry, Cambridge, UK.

54 Schuck P, Perugini MA, Gonzales NR, Howlett GJ & Schubert D (2002) Size-distribution analysis of proteins by analytical ultracentrifugation: strategies and application to model systems. *Biophys J* **82**, 1096–1111.

55 Schuck P (2000) Size-distribution analysis of macromolecules by sedimentation velocity ultracentrifugation and lamm equation modeling. *Biophys J* **78**, 1606–1619.

56 Perugini MA, Schuck P & Howlett GJ (2002) Differences in the binding capacity of human apolipoprotein E3 and E4 to size-fractionated lipid emulsions. *Eur J Biochem* **269**, 5939–5949.

57 Caria S, Hinds MG & Kvansakul M (2017) Structural insight into an evolutionarily ancient programmed cell death regulator – the crystal structure of marine sponge BHP2 bound to LB-Bak-2. *Cell Death Dis* **8**, e2543.

58 Kvansakul M & Czabotar PE (2016) Preparing samples for crystallization of Bcl-2 family complexes. *Methods Mol Biol* **1419**, 213–229.

59 Kabsch W (2010) Xds. *Acta Crystallogr D* **66**, 125–132.

60 Evans P (2006) Scaling and assessment of data quality. *Acta Crystallogr D* **62**, 72–82.

61 McCoy AJ (2007) Solving structures of protein complexes by molecular replacement with Phaser. *Acta Crystallogr D* **63**, 32–41.

62 Emsley P, Lohkamp B, Scott WG & Cowtan K (2010) Features and development of Coot. *Acta Crystallogr D* **66**, 486–501.

63 Echols N, Grosse-Kunstleve RW, Afonine PV, Bunkoczi G, Chen VB, Headd JJ, McCoy AJ, Moriarty NW, Read RJ, Richardson DC *et al.* (2012) Graphical tools for macromolecular crystallography in PHENIX. *J Appl Crystallogr* **45**, 581–586.

64 Morin A, Eisenbraun B, Key J, Sanschagrin PC, Timony MA, Ottaviano M & Sliz P (2013) Collaboration gets the most out of software. *Elife* **2**, e01456.

65 Meyer PA, Socias S, Key J, Ransey E, Tjon EC, Buschiazzo A, Lei M, Botka C, Withrow J, Neau D *et al.* (2016) Data publication with the structural biology data grid supports live analysis. *Nat Commun* **7**, 10882.

66 Edgar RC (2004) MUSCLE: multiple sequence alignment with high accuracy and high throughput. *Nucleic Acids Res* **32**, 1792–1797.

67 Krissinel E & Henrick K (2007) Inference of macromolecular assemblies from crystalline state. *J Mol Biol* **372**, 774–797.

68 Hawkins CJ, Wang SL & Hay BA (1999) A cloning method to identify caspases and their regulators in yeast: identification of *Drosophila* IAP1 as an inhibitor of the *Drosophila* caspase DCP-1. *Proc Natl Acad Sci USA* **96**, 2885–2890.

69 Jabbour AM, Puryer MA, Yu JY, Lithgow T, Riffkin CD, Ashley DM, Vaux DL, Ekert PG & Hawkins CJ (2006) Human Bcl-2 cannot directly inhibit the *Caenorhabditis elegans* Apaf-1 homologue CED-4, but can interact with EGL-1. *J Cell Sci* **119**, 2572–2582.

70 Petros AM, Olejniczak ET & Fesik SW (2004) Structural biology of the Bcl-2 family of proteins. *Biochim Biophys Acta* **1644**, 83–94.

Chapter 3

Paper III: Monkeypox virus C7L is a Bcl-2-fold protein that binds human pro-apoptotic Bcl-2 proteins

3.1   Introduction

Monkeypox virus (MPXV) is emergent zoonotic virus belonging to the genus *orthopoxviridae* that is the infective agent in smallpox like disease in humans (62). Sequence analysis of the monkeypox genome identified a potential viral Bcl-2 like protein, MPXV C7L, an ortholog of VACV F1L, that shares 85% sequence identity with MPXV C7L. At the time I initiated my studies there was nothing known of the structure or function of MPXV C7L. To address this research question of the potential mechanisms of MPXV C7L driven apoptosis inhibition I examined the detailed binding profile of MPXV C7L to peptides spanning the human BH3 motifs of pro-apoptotic Bcl-2 proteins followed by crystal structure determination of MPXV C7L in complex with Bax and Bim BH3 peptides.

The data acquired from this project are presented as a manuscript entitled "Monkeypox virus C7L is a Bcl-2-fold protein that binds human pro-apoptotic Bcl-2 proteins" that is under review in the journal Viruses.

3.2   Co-author contribution

Chathura D. Suraweera	Protein Expression and purification
	Determination of MPXV C7L binding partners
	Protein crystallization, X-ray diffraction and data collection
	Structure solution and refinement
	Structural analysis
	Manuscript writing (Introduction, Material and Methods Results and Discussion)
	Preparation of figures and tables in the manuscript
Sofia Caria	Protein Expression and purification
	Screening of BH3 interactions of MPXV C7L
Mark G. Hinds	Overall scientific direction of the project
	Structural analysis and interpretation
	Drafted and revised the manuscript
Marc Kvansakul	Overall scientific direction of the project
	X-ray diffraction and data collection
	Structure solution and refinement
	Structural analysis
	drafted and revised the manuscript

Monkeypox virus C7L is a Bcl-2-fold protein that binds human pro-apoptotic Bcl-2 proteins

Chathura D. Suraweera [1], Sofia Caria [1&], Mark G. Hinds [2,*] and Marc Kvansakul [1,*]

[1]   La Trobe Institute for Molecular Science, Department of Biochemistry and Genetics, La Trobe University, VIC 3086, Australia; m.kvansakul@latrobe.edu.au

[2]   Bio21 Molecular Science and Biotechnology Institute, The University of Melbourne, Parkville, Australia ; hinds.mark.g@gmail.com

[&]   Current address: Evotec Ltd, Abingdon, UK

[*]   Correspondence: m.kvansakul@latrobe.edu.au (M.K.); hinds.mark.g@gmail.com (M.G.H.)

Abstract: Poxviruses harbor a suite of immune modulatory effector proteins including inhibitors of apoptosis to counter host immune responses. Monkeypox virus (MPXV) encodes for C7L, a putative Bcl-2 homolog. Deletion mutants of MPXV lacking a genomic region comprising 15 ORFs including C7L revealed a substantially attenuated phenotype for mutant, however the function of C7L on its own has not been defined. Here we report the biochemical and structural analysis of MPXV C7L. We show that recombinant C7L is able to bind to a diverse set of BH3 motif peptides of human proapoptotic Bcl-2 proteins including Bim, Puma, Bak and Bax. Unexpectedly, C7L bound a broader range of host proapoptotic ligands compared to its closely related homolog in vaccinia virus, F1L, and furthermore these interactions were of a higher affinity. We then determined the crystal structures of C7L bound to Bim and Bax BH3. Our crystallographic analysis reveals that MPXV C7L engages human Bim BH3 using its four canonical hydrophobic residues. However, unlike its vaccinia virus F1L counterpart, C7L also forms a network of additional ionic and hydrogen bonds to supplement the conserved hydrophobic interactions, thus providing a rationale for the higher affinities and broader ligand binding spectrum observed.

Keywords: Bcl-2; monkeypox virus; apoptosis; X-ray crystallography

1. Introduction

Programmed cell death forms part of suite of immune response strategies utilized by multicellular organisms to clear invading pathogens [1]. In order to counter host cell death-based defence mechanisms viruses have acquired genes to either to counter or enhance host programmed cell death to ensure their proliferation and survival [2]. One such strategy for viral manipulation of the host-cell programmed cell death response to invasion has been the acquisition of pro-survival homologs of the B-cell lymphoma 2 (Bcl-2) family that mediate intrinsic apoptosis [3]. Bcl-2 proteins are critical arbiters of intrinsic or mitochondrially mediated apoptosis and are characterized by the presence of one or more conserved Bcl-2 homology (BH) sequence motifs, though the viral Bcl-2 homologs frequently lack any sequence conservation with their mammalian counterparts [4].

The mammalian Bcl-2 family can be divided into pro-survival or pro-apoptotic members. Mammalian pro-survival members comprise Bcl-2, Bcl-x_L, Mcl-1, A1 and Bcl-B all of which harbor multiple BH motifs in addition to a C-terminal transmembrane region that targets them to the outer mitochondrial membrane. The other members of the family are pro-death Bcl-2 proteins and these are subdivided into two groups: those that feature multiple BH motifs such as Bak, Bax and Bok; and others that contain only the BH3 motif and are denoted as BH3-only proteins [5]. The mammalian

44 BH3-only proteins include Bad, Bid, Bik, Bim, Bmf, Hrk, Noxa and Puma, and act either by countering
45 the ability of pro-survival Bcl-2 proteins to hold Bak and Bax in check, or they may directly activate
46 Bak and Bax [6]. A number of poxviruses have been found to have acquired pro-survival Bcl-2
47 homologs among their survival genes [7]. Interactions between prosurvival Bcl-2 proteins and the
48 BH3 motif of pro-apoptotic proteins occur via a conserved hydrophobic ligand binding groove on
49 pro-survival Bcl-2. Key to the cell death are the pro-apoptotic Bcl-2 members Bax and Bak. After
50 activation, Bax and Bak multimerize on the mitochondrial outer membrane to form large pores [8]
51 that results in the release of pro-apoptotic factors including cytochrome c. Cytochrome c together
52 with the adapter protein APAF-1 forms the apoptosome [9], which enables activation downstream
53 caspases and subsequent dismantling of the cell. The presence of pro-survival viral Bcl-2 homologs
54 inhibits the action of Bax and Bak to preserve the cell for viral replication[10].

55 Monkeypox (MPXV) virus is an emergent zoonotic virus of the poxviridae family belonging to the
56 genus orthopoxviridae. Other members of orthopoxviridae include the closely related variola (VAR),
57 vaccinia (VAC) [11] as well as cowpox (CPV) viruses [12], rabbitpox virus [13]and akhmeta virus
58 (APXV) [14]. MPXV is endemic to central Africa [15] and infects rodents and apes as well as humans.
59 Individuals with MPXV infections display symptoms similar to smallpox infections including fever,
60 swollen lymph nodes and rashes and there is an associated mortality rate of 10- 40% for those infected
61 [12]. MPXV is a large double stranded DNA virus whose genome features ~197 open reading frames
62 [12] that encode a number of immunomodulatory genes [16] including homologs of the dual
63 apoptosis/NF-kB inhibitor N1L [17] as well as the apoptosis inhibitory serpin B13R [18]. Sequence
64 analysis identified the presence of the ORF *c7l* that encodes a 219 residue protein C7L [12]. C7L
65 displays sequence homology to vaccinia virus F1L, a Bcl-2 mimetic that shares the Bcl-2 fold, but lacks
66 any significant shared sequence identity with mammalian Bcl-2 proteins [19]. Although MPXV
67 encodes for a putative Bcl-2 homolog, the ability of MPXV to modulate Bcl-2 mediated apoptosis
68 remains to be clarified. Deletion of a genomic region of MPXV comprising of several reading frames
69 including C7L resulted in virus displaying strong attenuation in vivo as well as reduced pathogenesis
70 [20]. Here we report the structural and biochemical characterization of MPXV C7L and its potential
71 role in modulating apoptosis in human. MPXV C7L shares 85% identity with its vaccinia virus
72 homolog F1L, and like F1L is able to bind to peptides spanning the BH3 motif of human pro-apoptotic
73 Bcl-2 proteins including those of Bax, Bak, Bim, Bid and Bik. Furthermore, we show C7L adopts a
74 domain swapped dimeric structure similar to other poxvirus encoded Bcl-2 homologs, and is able to
75 bind BH3 motif peptides using the canonical Bcl-2 ligand binding groove. Combined, these findings
76 establish C7L as a novel inhibitor of apoptosis in monkeypox virus.

77 **2. Materials and Methods**

78 *Protein expression and purification*

79 Synthetic cDNA codon optimized for *Escherichia coli* encoding for MPXV C7L from the viral isolate
80 Congo 1990 [21] (Uniprot Accession number Q3I8Y3) lacking the N-terminal 36 residues as well as
81 the C-terminal 35 residues (spanning residues 37-184) was cloned into the bacterial expression vector
82 pGEX-6P3 (Genscript) and transformed into *E. coli* C41(DE3). Cells were grown in 2YT medium
83 containing 1 mg ml^{-1} ampicillin at 37°C in a shaker incubator until an OD$_{600}$ of 0.6 was reached, and
84 C7L expression was induced by adding isopropyl β-D-1-thiogalactopyranoside (IPTG) to a final
85 concentration of 0.75 mM for 20 hours at 22°C. Cells were harvested by ultracentrifugation at 6000
86 rev min^{-1} (JLA 9.1000 rotor, Beckman Coulter Avanti J-E) for 20 min prior to resuspension in 100 ml
87 lysis buffer A (50 mM Tris pH 8.0, 200 mM NaCl and 10 mM DTT (dithiothreitol). Harvested cells
88 were lysed via sonication (Model 705 Sonic Dismembrator, Fisher Scientific, Hampton, New
89 Hampshire, US). The resultant lysate was transferred to SS34 tubes for centrifugation at 20,000 rev
90 min^{-1} (JA-25.50 rotor, Beckman Coulter Avanti J-E) for 30 min. The supernatant was decanted and
91 loaded onto 4 ml of Glutathione Sepharose 4B resin in a gravity flow column (GE Healthcare)
92 equilibrated with buffer A. Following sample application, the column was washed with 15 column

93   volumes of buffer A followed by HRV 3C protease cleavage overnight at 4°C. The liberated target
94   protein was eluted using 5 column volumes of buffer A and concentrated to a 3.0 mg ml^{-1} using a
95   centrifugal concentrator with a 3 kDa molecular weight cut-off (Amicon® Ultra 15). Concentrated
96   C7L was subjected to size-exclusion chromatography using a Superdex S200 10/300 column mounted
97   on an ÄKTApure system (GE Healthcare) equilibrated in 25 mM HEPES pH 7.5, 150 mM NaCl, 5 mM
98   TCEP (Tris(2-carboxyethyl)phosphine hydrochloride), where it eluted as a single peak. The final
99   sample purity was estimated to be higher than 95% based on SDS–PAGE analysis.

100 *Measurement of dissociation constants*

101 Binding affinities were measured using a MicroCal iTC200 system (GE Healthcare) at 25°C using C7L
102 in 25 mM HEPES pH 7.5, 150 mM NaCl at a final concentration of 30 μM as previously described [22].
103 All affinity measurements were performed in triplicate. Protein concentrations were measured using
104 a Nanodrop UV spectrophotometer (Thermo Scientific) at a wavelength of 280 nm. Peptide
105 concentrations were calculated based on the dry peptide weight after synthesis. The BH3-motif
106 peptides used were commercially synthesized using liquid-phase peptide synthesis (GenScript) and
107 were purified to a final purity of 95%. Peptide sequences have been described previously [23].

108 *Analytical Size-exclusion chromatography*

109 Analytical size-exclusion chromatography was performed using a Superdex S75 3.2/300 column as
110 described above. The column was calibrated using three protein molecular weight markers (1 mg ml^{-1}
111 Albumin (66 kDa), 2 mg ml^{-1} carbonic anhydrase (29 kDa) and 2 mg ml^{-1} cytochrome c (12 kDa))
112 (Sigma-Aldrich) dissolved in the same gel filtration buffer as C7L. C7L at a concentration of 5.6 mg
113 ml^{-1} was then injected, and all elution profiles of the chromatograms were recorded.

114 *Crystallization and data collection*

115 A complex of C7L with Bax BH3 was reconstituted as previously described [24] by adding Bax BH3-
116 motif peptide at a 1:1.25 molar ratio to C7L. The reconstituted complex was concentrated to 5.6 mg
117 ml^{-1} using a centrifugal concentrator with a 3 kDa molecular weight cut-off (Amicon ® Ultra 0.5),
118 flash-cooled and stored under liquid nitrogen. Crystals of C7L: Bax BH3 were obtained at a protein
119 concentration of 5.6 mg ml^{-1} using the sitting-drop method at 20°C in 0.2 M Magnesium acetate
120 tetrahydrate, 25% W/V PEG 3350. The crystals were flash cooled at -173°C in mother liquor
121 supplemented with 20% (v/v) ethylene glycol. The C7L: Bax BH3 complex formed cuboidal shaped
122 crystals belonging to space group P2$_1$ with a=61.58 Å, b=91.26 Å, c=70.33 Å, α=90.00 Å, β=105.91 Å,
123 γ=90.00 Å in the monoclinic crystal system. Diffraction data were collected on the MX2 beamline at
124 the Australian Synchrotron using an EIGER 16M detector at a wavelength of 0.9537 Å and an
125 oscillation range of 0.1° per frame. Diffraction data were integrated using XDS [25] and scaled using
126 AIMLESS [26]. Crystals of C7L: Bax BH3 contained four chains of C7L and four chains of Bax BH3 in
127 the asymmetric unit, with a calculated solvent content of 46.12%. The structure was phased by
128 molecular replacement using VARV F1L as a search model (PDB accession code 5AJJ [27]). The final
129 C7L:Bax BH3 complex was manually built using Coot [28] and refined using PHENIX [29] with final
130 Rwork/Rfree of 20.1/22.9 %, with 98.1 % of residues in Ramachandran favoured region of the plot and
131 no outliers.

132 C7L: Bim BH3 crystals were grown as described above for the C7L: Bax BH3 complex. Crystals were
133 obtained in 1.5M sodium chloride, 10% v/v ethanol. The crystals were flash cooled at -173°C in mother
134 liquor supplemented with 20% ethylene glycol as a cryo-protectant. The C7L: Bim BH3 complex
135 formed single cube shaped very small (2 um, 2 um, 1 um) crystals belong to space group I2 with
136 a=61.33 Å, b=74.18 Å, c=80.17 Å, α=90.00 Å, β=111.45 Å, γ=90.00 Å in the monoclinic crystal system
137 and significant signal of translational Non-Crystallographic Symmetry (t-NCS) was present.
138 Diffraction data collection, integration and scaling were performed as described above. The

139 molecular replacement was carried out using PHASER with the previously solved structure of C7L:
140 Bax BH3 as a search model. C7L: Bim BH3 crystals contain two molecules of C7L and two Bim BH3
141 peptide, with 39.3% solvent content and final TFZ and LLG values of 22.6 and 475.75 respectively.
142 The final model of C7L_Bim BH3 was built manually over several cycles using Coot and refined using
143 PHENIX with final Rwork/Rfree of 21.6/26.1 %, with 99.7 % of residues in Ramachandran favoured
144 region of the plot and no outliers.

145 Details of the data-collection and refinement statistics are summarized in Table 2. All images were
146 generated using PyMOL. All software was accessed via SBGrid [30]. Raw images were deposited
147 with the SBGrid Data Bank [31].

148 *Sequence search, alignment and interface analysis*

149 A BLAST [32] search of the NCBI sequence database [33] was performed using the MPXV C7L
150 sequence (Uniprot Q3I8Y3) as a seed . Hidden Markov Model (HMM) searches were performed with
151 HMMER [34] or the MPI bioinformatics tookit, HHBlits [35]. Sequence alignments were performed
152 using MUSCLE [36] with the default settings, and sequence identities were calculated based on the
153 total number of conserved residues in MPV C7L against the full sequence. Protein interfaces were
154 analysed using PISA [37].

155 **3. Results**

156 A BLAST [32] search of the NCBI standard nucleotide database [33] using MPXV C7L as a bait shows
157 there is is strong sequence identity with many other homologs from chordopox viruses including
158 vaccinia, variola, akhmeta cowpox, ectromelia and yokapox [38], and thus likely constitutes a
159 putative MPXV encoded Bcl-2 homolog (Figure 1a). No entomopox sequence homologs of C7L were
160 identified by our searches. It is significant that no mammalian Bcl-2 homologues are found in simple
161 BLAST search. Sequence searches for low sequence identity C7L homologs using HMM [34] or the
162 MPI bioinformatics tookit, HHBlits [35] found and more distantly related sequences such as tanapox
163 virus 16L [39], yaba monkey Tumour virus 16L, but again no entomopox or mammalian Bcl-2
164 proteins were found using these methods. This finding is consistent with the low shared sequence
165 identity observed between these viral proteins and the mammalian Bcl-2 family members (Figure 1c).
166 Indeed, sequence analysis of MPXV C7L indicates that the hallmark BH motifs are absent.

Figure 1. Sequence comparisons of MPXV and related proteins a) Sequence alignment of MPXV C7L with its orthologs from vaccinia virus, variola virus F1L, rabbitpox virus, cowpox virus, and akhmeta virus. Sequence substitutions of MPXV C7L compared to vaccinia F1L are highlighted in yellow. Sequence identities of the different orthopoxvirus C7L homologs are: VARV F1L (78%), VACV F1L (85.5%), RPXV 029 (87.6%), CPXV 048 (78 %), APXV F1 (82.3%). b) Positions of the sequence substitutions (blue) of MPXV C7L compared to vaccinia F1L shown on the molecular surface of MPXV C7L. c) Sequence alignment of MPXV C7L with pro-survival Bcl-2 family members. The sequences of monkeypox virus C7L (uniprot accession number: Q3I8Y3), vaccinia virus F1L (uniprot: O57173), myxomavirus M11L (uniprot: Q85295) and human Bcl-xL (uniprot: Q07817) were aligned using MUSCLE [36]. Secondary structure elements are marked based on the crystal structure of MPXV C7L, and BH motifs of Bcl-xL highlighted (BH4 (yellow), BH3 (bright green), BH1 (turquoise), BH2 (pink)) and shown in bold [40]. The regions of helix are marked 'H' and unstructured loops with a bar above the sequence, conserved residues are denoted by '*', with highly conservative substitutions indicated by ':' and conserved substitutions indicated by '.'.

To determine if MPXV C7L is able to interfere with Bcl-2 mediated apoptosis by engaging host proapoptotic Bcl-2, we expressed and purified recombinant C7L lacking the N-terminal 36 residues encoding for a putative flexible region as well as the C-terminal 35 residues comprising the transmembrane motif. We then examined the ability of recombinant C7L to bind BH3 motif peptides

185   from all human proapoptotic Bcl-2 proteins using isothermal titration calorimetry (ITC). ITC revealed
186   a broad interaction spectrum for C7L with nanomolar affinities for BH3 motifs from Bax, Bak, Bim,
187   Bid and Bik as well as micromolar affinities for those from Puma, Bok and Hrk with a stoichiometry
188   of 1:1. In contrast, no interactions were detected with Bad, Bmf or Noxa BH3 motifs (Table 1). A
189   comparison of the relative affinities of BH3-peptides for MXPV and the closely related viruses VACV
190   F1L and VARV F1L is given in Figure 2. MPXV C7L has a much broader spectrum of BH3 binding
191   than VACV F1L and VARV F1L. To establish the structural basis for BH3 ligand engagement by C7L
192   we then determined the crystal structure of C7L complexes with two of the identified high affinity
193   interactors, Bax and Bim BH3 (Figure 2). Clear and continous electron density was observed for C7L
194   residues 46-183 and Bax residues 56-76 in the C7L: Bax BH3 complex, as well as C7L residues 48-184
195   and Bim residues 143-166 in the C7L:Bim BH3 complex (Figure 3). The crystal structure of a C7L:Bax
196   BH3 complex revealed that as previously seen for the related VACV[41] and VARV F1L[27], C7L
197   adopts a typical Bcl-2 fold with dimeric topology via a domain-swap where the α1 helices of two
198   neighbouring chains are swapped (Figure 2).

Peptide	K_D (nM)
Bak	401 ± 31.0
Bax	22 ± 5.0
Bok	1370 ± 194.0
Bad	NB
Bid	560 ± 30.0
Bik	930 ± 88.0
Bim	131 ± 20.0
Bmf	NB
Hrk	1285 ± 221.0
Noxa	NB
Puma	2605 ± 308.0

199   **Table 1.** Affinity measurements of C7L and BH3 motif peptides from human pro-apoptotic Bcl-2
200   proteins. C7L interacts with BH3 motif peptides of human pro-apoptotic Bcl-2 proteins. Isothermal
201   titration calorimetry measurements of monkey pox virus Bcl-2 homolog C7L and its two mutants X
202   and Y with human pro-apoptotic BH3 motif peptides. All K_D values (in nM) are the means of three
203   replicates with standard error. NB denotes no binding.

204

MPXV C7L: Bax BH3

MPXV C7L: Bax BH3 domain swapped dimer

MPXV C7L: Bim BH3

MPXV C7L: Bim BH3 domain swapped dimer

VACV F1L: Bak BH3

VACV F1L: Bak BH3 domain swapped dimer

DPV022: Bax BH3

DPV022: Bax BH3 domain swapped dimer

TANV16L: Bax BH3

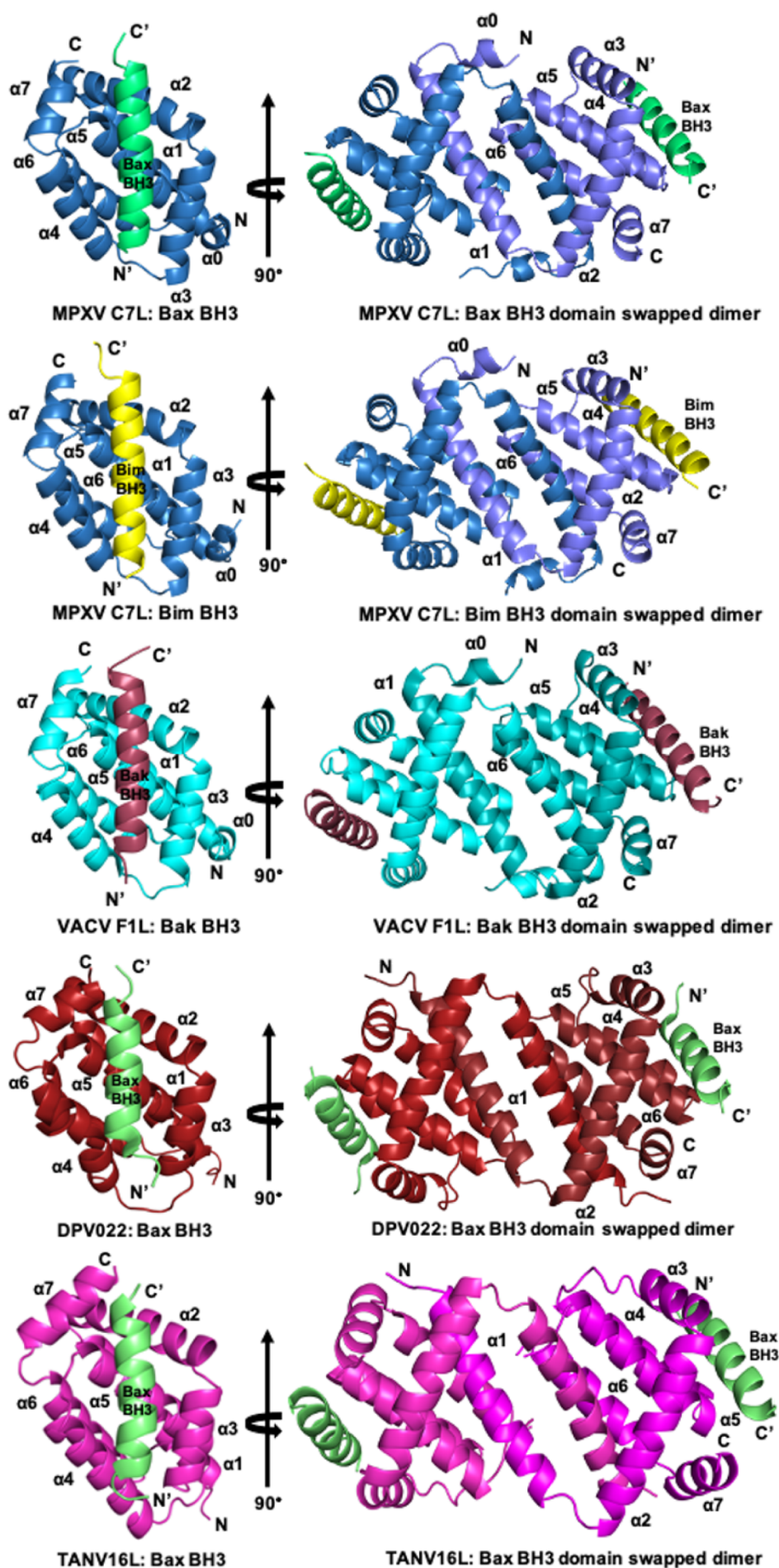TANV16L: Bax BH3 domain swapped dimer

205

206 **Figure 2.** Ribbon representation and comparison of viral Bcl-2 protein structures in complex with
207 BH3-motif peptides. a) Crystal structure of MPXV C7L bound to human Bax BH3 peptide. MPXV C7L
208 (sky blue) in complex with the Bax BH3 peptide (lime). C7L helices are labeled α0-α7. The view in (a)
209 is into the hydrophobic binding groove formed by helices α2-a5 and C7L: Bax BH3 view down the 2-
210 fold symmetry axis between the domain-swapped α1 helices. b) MPXV C7L (sky blue) in complex
211 with the Bim BH3 peptide (yellow) c) VACV F1L (cyan) in complex with the Bak BH3 domain
212 (raspberry) [41]. d) TANV16L (magenta) in complex with the Bax BH3 domain (lime) e) DPV022
213 (firebrick) in complex with the Bax BH3 domain (orange). The views in b-d as in (a). In all cases the
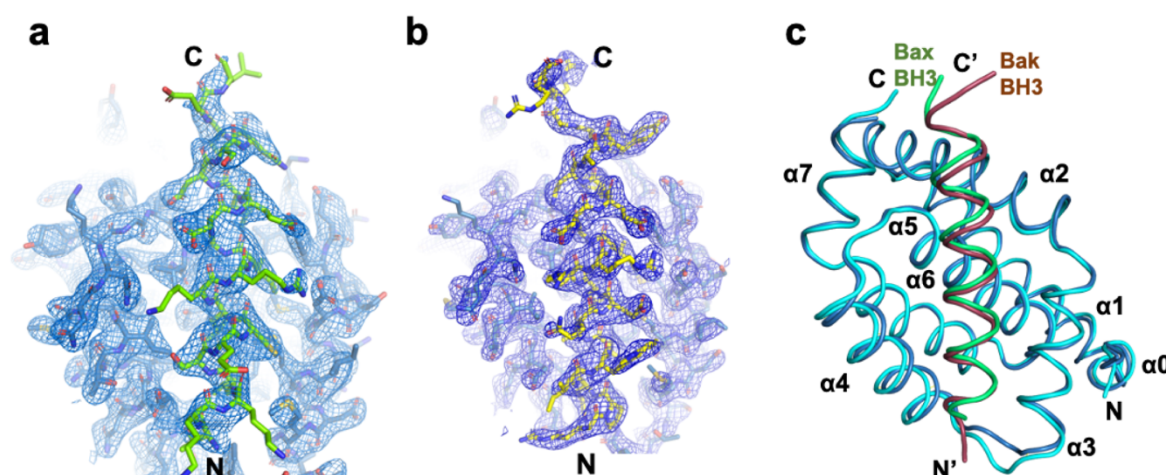214 view on the left is a single protomer and the right view the dimer.

215
216 **Figure 3.** a) 2Fo-Fc electron density maps of MPXV C7L: Bax BH3 complex interface contoured at 1.5
217 σ, b) 2Fo-Fc electron density maps of MPXV C7L: Bim BH3 complex interface contoured at 1.5 σ and
218 c) Cartoon representation of MPXV C7L (sky blue): Bax (lime) superimposed onto VACV F1L (cyan):
219 Bak (raspberry) BH3 complex. The view is into the canonical hydrophobic binding groove formed by
220 α2–α5.

221

222 To validate the dimeric topology of C7L, we performed analytical size exclusion chromatography
223 (Figure 4). This revealed that C7L eluted at a volume commensurate with a dimeric assembly and
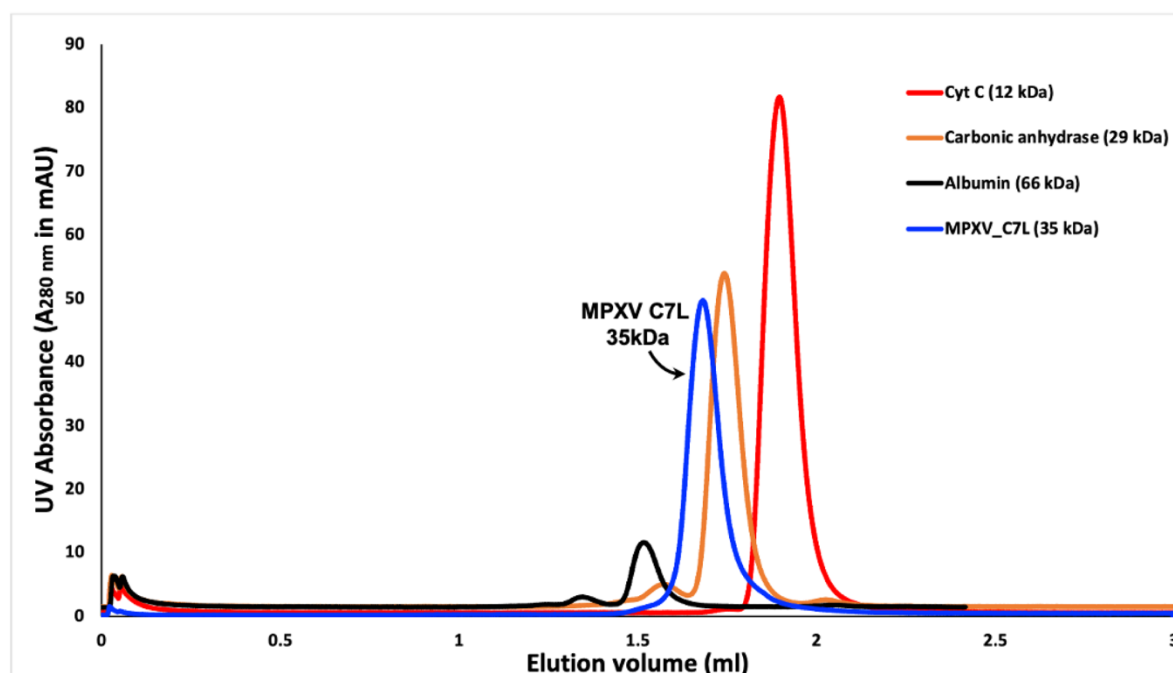224 supports the dimeric structure observed in our crystals.

Figure 4. MPXV C7L is a dimer in solution. Size exclusion chromatography of MPXV C7L using a Superdex S75 3.2/300 column. The elution profile of the peak of interest (MPXV C7L) is 1.69 mL (blue line). The molecular weight standards shown are albumin (66 kDa) (black), carbonic anhydrase (29 kDa) (orange) and cytochrome *c* (Cyt *c*) (12 kDa) (red), AU: absorbance units at wavelength 280 nm.

A comparison of a single chain of C7L with a single protomer of other domain swapped dimeric viral Bcl-2 proteins including VACV F1L, VARV F1L, deerpoxvirus DPV022 [42] and TANV16L (Figure 2b-e) [39] revealed that the C7L Cα backbone superimposes with rmsd values of 0.52, 0.38, 2.09 and 1.42 Å respectively. Dimeric C7L superimposes with the corresponding dimeric VACV and VARC F1L, DPV022 and TANV16L with rmsd values of 0.53, 0.41, 2.18 and 1.83 Å respectively. As expected, the backbone structure of C7L is highly similar for both the monomeric protomer as well as the domain-swapped dimer to its homologous counterparts amongst the orthopoxviridae, as well as the cervidpox homolog DPV022.

Binding of Bax BH3 peptide to C7L occurs via the canonical ligand binding groove that is formed by helices α2-α5 (Figure 2). The four canonical BH3 motif defining residues from Bax, L59, L63 and I66 and L70, are bound in four hydrophobic pockets of the canonical C7L ligand binding groove (Figure 5a). Furthermore, Bax M74 occupies a fifth hydrophobic pocket in C7L. The hallmark ionic interaction between pro-survival Bcl-2 proteins and pro-apoptotic BH3 motif ligands between a conserved arginine in the BH1 motif and apartate of the BH3-motif [4] is absent. However, an ionic interaction is formed between R65[BAX] and D105[C7L] , and this interaction is supplemented by hydrogen bonds between E69[BAX] and Y102[C7L] as well as between D71[BAX] and G138[C7L] (Figure 5a). Similarly, in the C7L:Bim BH3 complex Bim residues I148, L152, I155 And F159 protrude into four hydrophobic pockets in the C7L ligand binding groove, and an ionic interaction is formed by R154[BIM] and D105[C7L]. Additional hydrogen bonds are found between E158[BIM] and Y102[C7L] , N160[Bim] and G138[C7L] as well as between D71[BAX] and G138[C7L] (Figure 5b).
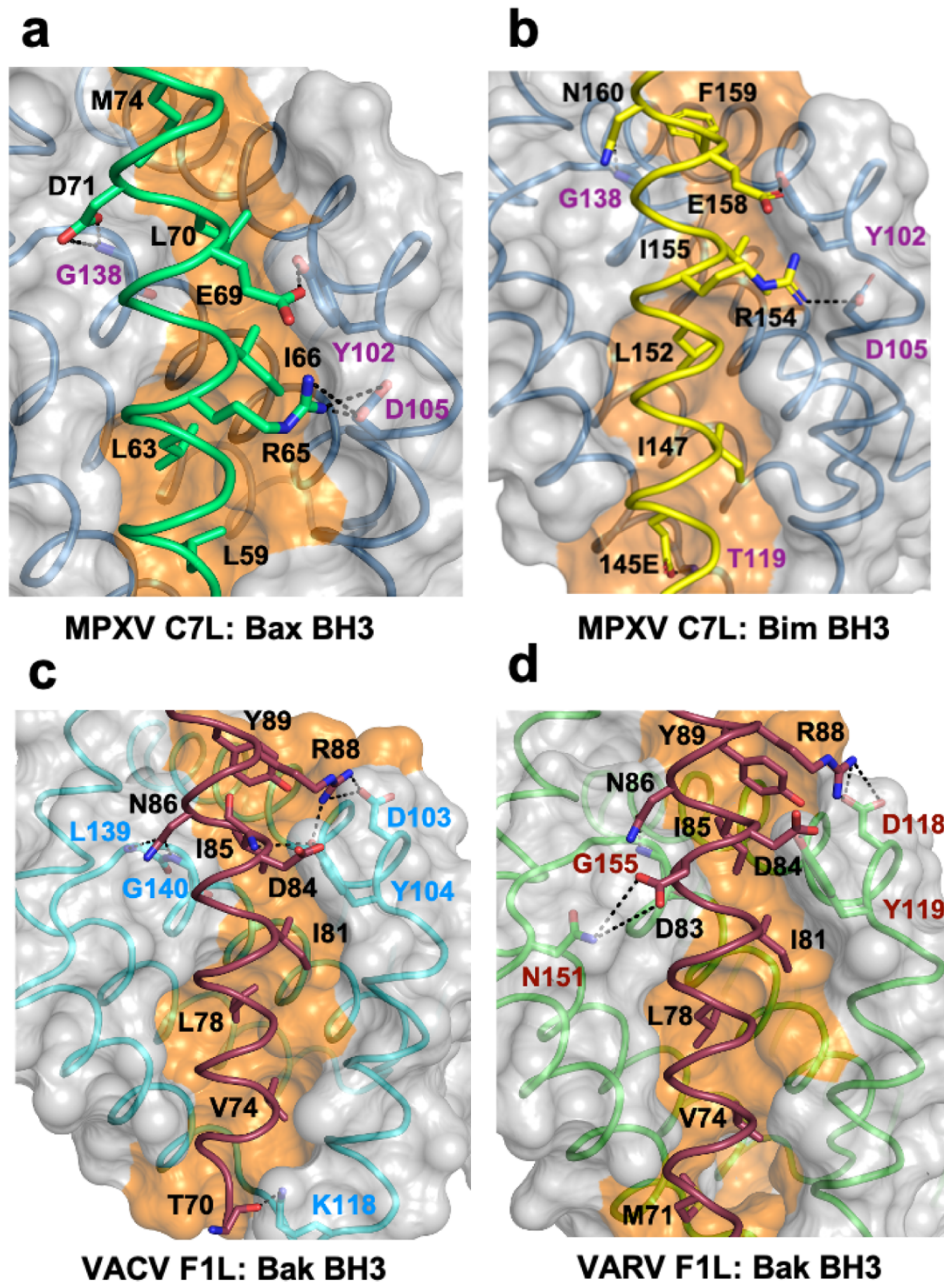
Figure 5. Detailed views of the MPXV C7L: Bax BH3, MPXV C7L: Bim BH3, VACV F1L: Bak BH3 and VARV F1L: Bak BH3 interfaces. a) The C7L surface, backbone and binding groove are shown in grey, sky blue and marine respectively, while Bax BH3 is shown in lime. The five key interacting residues of Bax L59, L63, I66, L70 and (additionally M74), are protruding into the binding groove. b) The C7L surface, backbone and binding groove are shown as a, while Bim BH3 is shown in yellow. The four key interacting residues of Bim I147, L152, I155 and F159, are protruding into the binding groove. c) The VACV F1L surface, backbone and binding groove are shown in grey, cyan and orange respectively, while Bak BH3 is shown in raspberry. The five key interacting residues of Bax V74, L78, I81, I85 and Y89, are protruding into the binding groove. d) The VARV F1L surface, backbone and binding groove are shown in grey, green and pale yellow respectively, while Bak BH3 is shown in raspberry. The six?? key interacting residues of Bak M71, V74, L78, I81, I85 and Y89, are protruding into the binding groove. Residues involved in ionic interactions and hydrogen bonds (shown as dotted black lines) are labelled.

265   **Table 2.** Crystallographic data collection and refinement statistics

	C7L: Bax BH3	C7L: Bim BH3
Data collection		
Space group	P2$_1$	I121
Cell dimensions		
a, b, c (Å)	61.65, 91.26, 70.33	61.33, 74.18, 80.17
α, β, γ (°)	90, 105.90, 90	90.00, 111.45, 90.00
Wavelength (Å)	0.9537	0.9537
Resolution (Å)	33.61 - 2.10 (2.18 - 2.10) *	38.98 - 2.48 (2.56 - 2.48) *
R$_{sym}$ or R$_{merge}$	0.032 (1.07)	0.108 (0.47)
I / σI	9.5 (0.6)	3.21 (1.05)
Completeness (%)	99.8 (99.3)	96.8 (97.2)
CC$_{1/2}$	1.00 (0.42)	0.98 (0.72)
Redundancy	3.5 (3.3)	1.8 (1.7)
Refinement		
Resolution (Å)	33.61 - 2.10 (2.18 - 2.10)	49.87 - 2.48 (3.04 - 2.88)
No. reflections	43416	11574
R$_{work}$ / R$_{free}$	0.210/0.236	0.226/0.274
Clashscore	2.15	0.37
No. atoms		
Protein	5023	2641
Ligand/ion	12	8
Water	130	65
B-factors		
Protein	80.48	53.46
Ligand/ion	101.23	62.67
Water	77.94	46.08
R.m.s. deviations		
Bond lengths (Å)	0.003	0.002
Bond angles (°)	0.47	0.37

266   * Values in parentheses are for the highest resolution shell

267   **4. Discussion**

268   Bcl-2 homologs are a widely used amongst large DNA viruses to ensure viral proliferation and/or
269   survival ref. Amongst the *poxviridae,* the majority of generae have been shown to encode apoptosis
270   inhibiting Bcl-2 homologs including the *orthopoxviridae* vaccinia, variola and ectromelia viruses
271   [27,41,43-45], *leporipoxviridae* myxomavirus [46,47], *cervidpoxviridae* deerpoxvirus [42,48],
272   *capripoxviridae* sheeppoxvirus [49,50], *avipoxviridae* fowlpox and canarypoxvirus [51,52] and
273   *parapoxviridae* orf virus [53]. Whilst many *poxviridae* encode for sequence, structural or functional
274   prosurvival Bcl-2 homologs, considerable diversity exists amongst these proteins (Figure 1). There
275   are widely differing interaction profiles with host proapoptotic Bcl-2 and differences in overall
276   structure and topology as well as detailed interactions at the atomic level, as might be expected from
277   these highly sequence divergent Bcl-2 fold sequences. Here we report that the *orthopoxviridae*
278   monkeypoxvirus C7L encodes a potent binder of mammalian apoptosis inducers. C7L adopts a
279   domain swapped dimeric Bcl-2 fold (Figure 2), and binds to a number of BH3 motif peptides from

280   human proapoptotic Bcl-2 proteins including those from Bax, Bak and Bim (Table 1). Analytical size-
281   exclusion chromatography confirmed that the dimeric topology we observed in our crystal structures
282   was recapitulated in solution (Figure 5). In contrast to the tanapox virus encoded TANV16L[39],
283   which displays both monomeric and domain-swapped dimeric topologies, we did not detect other
284   oligomeric states for C7L. This suggests that C7L may be less flexible in terms of its ability to
285   reorganize its helical elements compared to TANV16L. Superimpositions of the domain swapped
286   dimeric poxvirus encoded prosurvival Bcl-2 proteins whose structures have been determined to date
287   reveals that the dimeric forms all superimpose very closely with rmsd values below 2.2 Å, with little
288   variation in the lengths of the helical elements and geometry of helical arrangements (Figure 2). This
289   may suggest that structural constraints are imposed on how these dimers are constructed that do not
290   leave significant scope for variations to the fold. Interestingly, tanapoxvirus encoded 16L that adopts
291   both domain swapped dimeric and monomeric topologies revealed that the ligand binding groove
292   that mediates interactions with proapoptotic host proteins is nearly identical in both oligomeric forms
293   [39]. Consequently, the absence of significant differences in the manner in which the domain
294   swapped dimeric poxviral Bcl-2 proteins are assembled may be a response to the evolutionary
295   pressure to maintain the canonical ligand binding groove in a particular configuration.
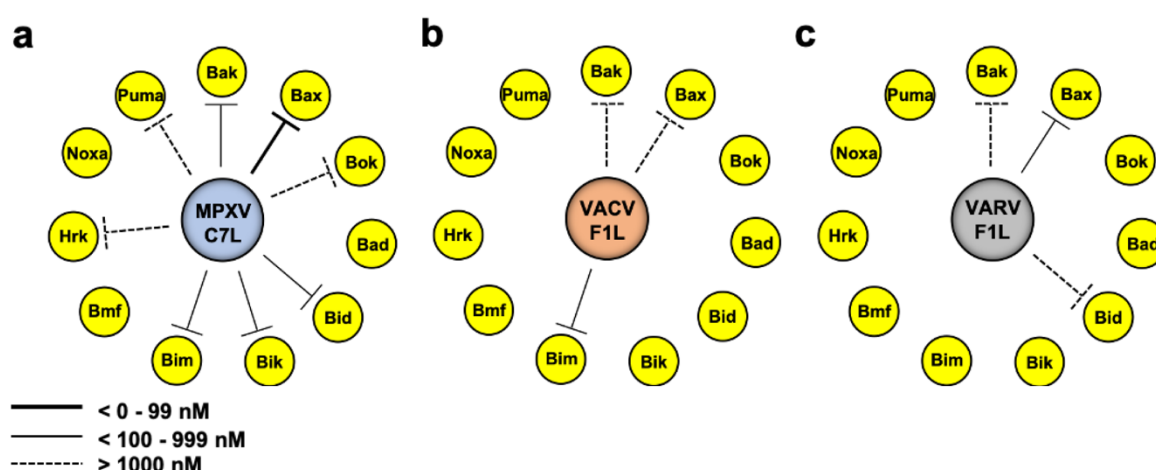

Figure 6. Comparison of the BH3 binding profile of MPXV C7L with its closest homologs from vaccinia virus F1L (VACV F1L) and variola virus F1L (VARV F1L). a) Binding profile of MPXV C7L with BH3 motif peptides (b) binding profile of VACV F1L and (c) binding profile of VARV F1L, the sequences of all BH3 motif peptides used in (a)(b) and (c) are of human origin. The line weight of the bars indicates the binding affinity ranges from 0-99 nM, < 999 nM, and < 1000 nM, as shown in the inset.

303   Although the closely related orthopoxviruses vaccinia, variola and ectromelia virus encode the highly
304   homologous F1L that adopts a near identical overall structure (Figure 2), intriguing differences can
305   be seen in the ability of the different orthopox virus F1L homologs to bind host cell proapoptotic
306   Bcl-2. Vaccinia virus F1L is only able to bind to Bim, Bak and Bax [43], and has been shown to
307   functionally act by replacing Mcl-1 [54] and neutralize Bim [41]. In contrast, variola virus F1L is
308   unable to bind Bim and binds to Bid, Bak and Bax instead [27]. Functionally, variola virus F1L was
309   only able to counter Bax, but not Bak mediated apoptosis. Ectromeliavirus F1L bound to Bim, Bak
310   and Bax, and inhibited both Bak and Bax mediated apoptosis [45]. Considering the 90 % primary
311   sequence identity within the Bcl-2 fold of each of these proteins amongst the orthopoxviruses, the
312   substantial differences in proapoptotic interaction spectra are unexpected (Figure 6). Despite the high
313   degree of sequence identity, MPXV C7L displays a spectrum of proapoptotic ligands and associated
314   affinities that much more resembles those from other monomeric poxviral prosurvival Bcl-2 proteins
315   such as sheeppoxvirus SPPV14 [49,50], myxomavirus M11L [46] or the avipoxvirus fowlpoxvirus
316   FPV039 [52] and canarypoxvirus CNP058 [51]. Whilst sequence differences between all identified
317   orthopoxvirus prosurvival Bcl-2 proteins are subtle, significant differences exist at the N-termini of
318   the respective proteins. Vaccinia, variola and ectromelia F1L feature long repeat sequences at their

N-termini, which are absent in monkeypox C7L (Figure 1a) [55]. The function of these N-terminal extensions remains to be fully clarified. Initial reports for vaccinia virus F1L suggested a role of the extreme N-terminus in apoptosis inhibition via a caspase dependent mechanism [56]. However, subsequent data showed no effect of the F1L N-terminus on apoptosis inhibition [55].

A comparison of the crystal structures of vaccinia and variola virus F1L [27,41,43] with monkeypox virus C7L reveals that the sites of primary sequence variations within the Bcl-2 fold occur in sites distant from the canonical ligand binding groove (Figure 1c). Nonetheless, significant differences exist in the manner in which VACV F1L and MPXV C7L engage human Bim BH3. F1L binding to Bim is primarily mediated by hydrophobic interactions via the four canonical hydrophobic residues in Bim as well as van der Waals contacts, with no hydrogen bonds between F1L and Bim residues present [41]. In contrast, MPXV formed an ionic interaction with R154[BIM] via D105[C7L] as well as two hydrogen between E158[BIM] and Y102[C7L] , and D71[BAX] and G138[C7L]. The ability of C7L to form additional interactions with bound BH3 motif peptides is likely a contributing factor to the broader proapoptotic ligand binding profile of MPXV C7L compared to VACV F1L, as well as the tighter binding affinities observed, suggesting that the remote amino acid substitutions impact ligand binding. However, detailed cell-based studies are required to probe the contribution of each of the interactions with proapoptotic Bcl-2 proteins to establish which ones are the primary drivers for apoptosis suppression during virus infection, and whether or not MPXV primarily targets Bim in a manner similar to VACV.

Analysis of the detailed interaction between the different orthopox virus encoded Bcl-2 proteins and host pro-apoptotic Bcl-2 reveals that whilst the BH1 motif is not conserved in these proteins, residues that occupy the positions of the NWGR motif of the BH1 region in, for example, Bcl-x_L still perform important roles. In both MPXV C7L complexes as well as in VACV F1L and VARV F1L a Gly residue is structurally conserved where one would normally find the NWGR motif, and in each orthopoxvirus Bcl-2 protein it forms a hydrogen bond with the bound BH3 motif peptide. Whilst the hallmark interaction between the Arg residue from the NWGR motif and the Asp from the BH3 motif peptide is absent, the equivalent region of the BH1 motif in orthopox virus prosurvival Bcl-2 proteins still contribute to binding and specificity. A similar observation was made for both sheeppox virus SPPV14 [50] and tanapox virus 16L [39], which utilize a different Arg to recapitulate the hallmark ionic interaction observed for mammalian prosurvival Bcl-2 proteins bound to BH3 motif bearing interactors [4]. These observations underscore the continued importance of the BH1 equivalent region for determining interactions between Bcl-2 family proteins, even in the absence of the canonical motifs.

In summary, we show that C7L is a dimeric Bcl-2 protein with domain-swapped topology that is able to bind important host pro-apoptotic Bcl-2 members and potentially interfere with host cell apoptosis signalling in infected cells. Our findings provide a structural basis for dissecting the role of C7L in monkeypox virus infection and to define the contribution that suppression of Bcl-2 mediated apoptosis makes to the viral life cycle.

References

371 1. Jorgensen, I.; Rayamajhi, M.; Miao, E.A. Programmed cell death as a defence against infection. *Nat Rev*
372 *Immunol* **2017**, *17*, 151-164, doi:10.1038/nri.2016.147.

373 2. Galluzzi, L.; Brenner, C.; Morselli, E.; Touat, Z.; Kroemer, G. Viral control of mitochondrial apoptosis.
374 *PLoS Pathog* **2008**, *4*, e1000018, doi:10.1371/journal.ppat.1000018.

375 3. Kvansakul, M.; Hinds, M.G. Structural biology of the Bcl-2 family and its mimicry by viral proteins.
376 *Cell Death Dis* **2013**, *4*, e909, doi:10.1038/cddis.2013.436.

377 4. Banjara, S.; Suraweera, C.D.; Hinds, M.G.; Kvansakul, M. The Bcl-2 Family: Ancient Origins, Conserved
378 Structures, and Divergent Mechanisms. *Biomolecules* **2020**, *10*, 128,
379 doi:https://doi.org/10.3390/biom10010128.

380 5. Kvansakul, M.; Hinds, M.G. The structural biology of BH3-only proteins. *Methods Enzymol* **2014**, *544*,
381 49-74, doi:10.1016/B978-0-12-417158-9.00003-0.

382 6. Shamas-Din, A.; Kale, J.; Leber, B.; Andrews, D.W. Mechanisms of action of bcl-2 family proteins. *Cold*
383 *Spring Harb Perspect Biol* **2013**, *5*, doi:10.1101/cshperspect.a008714.

384 7. Nichols, D.B.; De Martini, W.; Cottrell, J. Poxviruses Utilize Multiple Strategies to Inhibit Apoptosis.
385 *Viruses* **2017**, *9*, doi:10.3390/v9080215.

386 8. Czabotar, P.E.; Westphal, D.; Dewson, G.; Ma, S.; Hockings, C.; Fairlie, W.D.; Lee, E.F.; Yao, S.; Robin,
387 A.Y.; Smith, B.J., et al. Bax crystal structures reveal how BH3 domains activate Bax and nucleate its
388 oligomerization to induce apoptosis. *Cell* **2013**, *152*, 519-531, doi:10.1016/j.cell.2012.12.031.

389 9. Dorstyn, L.; Akey, C.W.; Kumar, S. New insights into apoptosome structure and function. *Cell Death*
390 *Differ* **2018**, *25*, 1194-1208, doi:10.1038/s41418-017-0025-z.

391 10. Neumann, S.; El Maadidi, S.; Faletti, L.; Haun, F.; Labib, S.; Schejtman, A.; Maurer, U.; Borner, C. How
392 do viruses control mitochondria-mediated apoptosis? *Virus Res* **2015**, *209*, 45-55,
393 doi:10.1016/j.virusres.2015.02.026.

394 11. Shchelkunov, S.N.; Resenchuk, S.M.; Totmenin, A.V.; Blinov, V.M.; Marennikova, S.S.; Sandakhchiev,
395 L.S. Comparison of the genetic maps of variola and vaccinia viruses. *FEBS Lett* **1993**, *327*, 321-324,
396 doi:10.1016/0014-5793(93)81013-p.

397 12. Shchelkunov, S.N.; Totmenin, A.V.; Safronov, P.F.; Mikheev, M.V.; Gutorov, V.V.; Ryazankina, O.I.;
398 Petrov, N.A.; Babkin, I.V.; Uvarova, E.A.; Sandakhchiev, L.S., et al. Analysis of the monkeypox virus
399 genome. *Virology* **2002**, *297*, 172-194, doi:10.1006/viro.2002.1446.

400 13. Li, G.; Chen, N.; Roper, R.L.; Feng, Z.; Hunter, A.; Danila, M.; Lefkowitz, E.J.; Buller, R.M.L.; Upton, C.
401 Complete coding sequences of the rabbitpox virus genome. *J Gen Virol* **2005**, *86*, 2969-2977,
402 doi:10.1099/vir.0.81331-0.

403 14. Gao, J.; Gigante, C.; Khmaladze, E.; Liu, P.; Tang, S.; Wilkins, K.; Zhao, K.; Davidson, W.; Nakazawa,
404 Y.; Maghlakelidze, G., et al. Genome Sequences of Akhmeta Virus, an Early Divergent Old World
405 Orthopoxvirus. *Viruses* **2018**, *10*, doi:10.3390/v10050252.

406   15.   Kugelman, J.R.; Johnston, S.C.; Mulembakani, P.M.; Kisalu, N.; Lee, M.S.; Koroleva, G.; McCarthy, S.E.;
407   Gestole, M.C.; Wolfe, N.D.; Fair, J.N., et al. Genomic variability of monkeypox virus among humans,
408   Democratic Republic of the Congo. *Emerg Infect Dis* **2014**, *20*, 232-239, doi:10.3201/eid2002.130118.
409   16.   Weaver, J.R.; Isaacs, S.N. Monkeypox virus and insights into its immunomodulatory proteins.
410   *Immunological Reviews* **2008**, *225*, 96-113, doi:10.1111/j.1600-065X.2008.00691.x.
411   17.   de Motes, C.M.; Cooray, S.; Ren, H.; Almeida, G.M.F.; McGourty, K.; Bahar, M.W.; Stuart, D.I.; Grimes,
412   J.M.; Graham, S.C.; Smith, G.L. Inhibition of Apoptosis and NF-kB Activation by Vaccinia Protein N1
413   Occur via Distinct Binding Surfaces and Make Different Contributions to Virulence. *PLoS Pathog* **2011**,
414   *7*, e1002430.
415   18.   Kettle, S.; Alcami, A.; Khanna, A.; Ehret, R.; Jassoy, C.; Smith, G.L. Vaccinia virus serpin B13R (SPI-2)
416   inhibits interleukin-1beta-converting enzyme and protects virus-infected cells from TNF- and Fas-
417   mediated apoptosis, but does not prevent IL-1beta-induced fever. *J Gen Virol* **1997**, *78 (Pt 3)*, 677-685,
418   doi:10.1099/0022-1317-78-3-677.
419   19.   Chen, N.; Li, G.; Liszewski, M.K.; Atkinson, J.P.; Jahrling, P.B.; Feng, Z.; Schriewer, J.; Buck, C.; Wang,
420   C.; Lefkowitz, E.J., et al. Virulence differences between monkeypox virus isolates from West Africa and
421   the Congo basin. *Virology* **2005**, *340*, 46-63, doi:10.1016/j.virol.2005.05.030.
422   20.   Lopera, J.G.; Falendysz, E.A.; Rocke, T.E.; Osorio, J.E. Attenuation of monkeypox virus by deletion of
423   genomic regions. *Virology* **2015**, *475*, 129-138, doi:10.1016/j.virol.2014.11.009.
424   21.   Likos, A.M.; Sammons, S.A.; Olson, V.A.; Frace, A.M.; Li, Y.; Olsen-Rasmussen, M.; Davidson, W.;
425   Galloway, R.; Khristova, M.L.; Reynolds, M.G., et al. A tale of two clades: monkeypox viruses. *J Gen*
426   *Virol* **2005**, *86*, 2661-2672, doi:10.1099/vir.0.81215-0.
427   22.   Suraweera, C.D.; Caria, S.; Jarva, M.; Hinds, M.G.; Kvansakul, M. A structural investigation of NRZ
428   mediated apoptosis regulation in zebrafish. *Cell Death Dis* **2018**, *9*, 967, doi:10.1038/s41419-018-0992-0.
429   23.   Kvansakul, M.; Wei, A.H.; Fletcher, J.I.; Willis, S.N.; Chen, L.; Roberts, A.W.; Huang, D.C.; Colman,
430   P.M. Structural basis for apoptosis inhibition by Epstein-Barr virus BHRF1. *PLoS Pathog* **2010**, *6*,
431   e1001236, doi:10.1371/journal.ppat.1001236 [doi].
432   24.   Kvansakul, M.; Czabotar, P.E. Preparing Samples for Crystallization of Bcl-2 Family Complexes.
433   *Methods Mol Biol* **2016**, *1419*, 213-229, doi:10.1007/978-1-4939-3581-9_16.
434   25.   Kabsch, W. Xds. *Acta Crystallogr D Biol Crystallogr* **2010**, *66*, 125-132, doi:10.1107/S0907444909047337.
435   26.   Evans, P. Scaling and assessment of data quality. *Acta Crystallogr D Biol Crystallogr* **2006**, *62*, 72-82,
436   doi:10.1107/S0907444905036693.
437   27.   Marshall, B.; Puthalakath, H.; Caria, S.; Chugh, S.; Doerflinger, M.; Colman, P.M.; Kvansakul, M.
438   Variola virus F1L is a Bcl-2-like protein that unlike its vaccinia virus counterpart inhibits apoptosis
439   independent of Bim. *Cell Death Dis* **2015**, *6*, e1680, doi:10.1038/cddis.2015.52.
440   28.   Emsley, P.; Lohkamp, B.; Scott, W.G.; Cowtan, K. Features and development of Coot. *Acta Crystallogr D*
441   *Biol Crystallogr* **2010**, *66*, 486-501, doi:10.1107/S0907444910007493.
442   29.   Afonine, P.V.; Grosse-Kunstleve, R.W.; Echols, N.; Headd, J.J.; Moriarty, N.W.; Mustyakimov, M.;
443   Terwilliger, T.C.; Urzhumtsev, A.; Zwart, P.H.; Adams, P.D. Towards automated crystallographic
444   structure refinement with phenix.refine. *Acta Crystallogr D Biol Crystallogr* **2012**, *68*, 352-367,
445   doi:10.1107/S0907444912001308.
446   30.   Morin, A.; Eisenbraun, B.; Key, J.; Sanschagrin, P.C.; Timony, M.A.; Ottaviano, M.; Sliz, P. Collaboration
447   gets the most out of software. *Elife* **2013**, *2*, e01456, doi:10.7554/eLife.01456.

448   31.   Meyer, P.A.; Socias, S.; Key, J.; Ransey, E.; Tjon, E.C.; Buschiazzo, A.; Lei, M.; Botka, C.; Withrow, J.;
449   Neau, D., et al. Data publication with the structural biology data grid supports live analysis. *Nat*
450   *Commun* **2016**, *7*, 10882, doi:10.1038/ncomms10882.

451   32.   Johnson, M.; Zaretskaya, I.; Raytselis, Y.; Merezhuk, Y.; McGinnis, S.; Madden, T.L. NCBI BLAST: a
452   better web interface. *Nucleic Acids Res* **2008**, *36*, W5-9, doi:10.1093/nar/gkn201.

453   33.   Coordinators, N.R. Database resources of the National Center for Biotechnology Information. *Nucleic*
454   *Acids Res* **2016**, *44*, D7-19, doi:10.1093/nar/gkv1290.

455   34.   Potter, S.C.; Luciani, A.; Eddy, S.R.; Park, Y.; Lopez, R.; Finn, R.D. HMMER web server: 2018 update.
456   *Nucleic Acids Res* **2018**, *46*, W200-W204, doi:10.1093/nar/gky448.

457   35.   Zimmermann, L.; Stephens, A.; Nam, S.Z.; Rau, D.; Kubler, J.; Lozajic, M.; Gabler, F.; Soding, J.; Lupas,
458   A.N.; Alva, V. A Completely Reimplemented MPI Bioinformatics Toolkit with a New HHpred Server
459   at its Core. *J Mol Biol* **2018**, *430*, 2237-2243, doi:10.1016/j.jmb.2017.12.007.

460   36.   Edgar, R.C. MUSCLE: multiple sequence alignment with high accuracy and high throughput. *Nucleic*
461   *Acids Res* **2004**, *32*, 1792-1797, doi:10.1093/nar/gkh340.

462   37.   Krissinel, E.; Henrick, K. Inference of macromolecular assemblies from crystalline state. *J Mol Biol* **2007**,
463   *372*, 774-797, doi:10.1016/j.jmb.2007.05.022.

464   38.   Zhao, G.; Droit, L.; Tesh, R.B.; Popov, V.L.; Little, N.S.; Upton, C.; Virgin, H.W.; Wang, D. The genome
465   of Yoka poxvirus. *J Virol* **2011**, *85*, 10230-10238, doi:10.1128/JVI.00637-11.

466   39.   Suraweera, C.D.; Anasir, M.I.; Chugh, S.; Javorsky, A.; Impey, R.E.; Hasan Zadeh, M.; Soares da Costa,
467   T.P.; Hinds, M.G.; Kvansakul, M. Structural insight into tanapoxvirus-mediated inhibition of apoptosis.
468   *FEBS J* **2020**, 10.1111/febs.15365, doi:10.1111/febs.15365.

469   40.   Petros, A.M.; Olejniczak, E.T.; Fesik, S.W. Structural biology of the Bcl-2 family of proteins. *Biochim*
470   *Biophys Acta* **2004**, *1644*, 83-94, doi:10.1016/j.bbamcr.2003.08.012

471   41.   Campbell, S.; Thibault, J.; Mehta, N.; Colman, P.M.; Barry, M.; Kvansakul, M. Structural insight into
472   BH3 domain binding of vaccinia virus antiapoptotic F1L. *J Virol* **2014**, *88*, 8667-8677,
473   doi:10.1128/JVI.01092-14.

474   42.   Burton, D.R.; Caria, S.; Marshall, B.; Barry, M.; Kvansakul, M. Structural basis of Deerpox virus-
475   mediated inhibition of apoptosis. *Acta Crystallogr D Biol Crystallogr* **2015**, *71*, 1593-1603,
476   doi:10.1107/S1399004715009402.

477   43.   Kvansakul, M.; Yang, H.; Fairlie, W.D.; Czabotar, P.E.; Fischer, S.F.; Perugini, M.A.; Huang, D.C.;
478   Colman, P.M. Vaccinia virus anti-apoptotic F1L is a novel Bcl-2-like domain-swapped dimer that binds
479   a highly selective subset of BH3-containing death ligands. *Cell Death Differ* **2008**, *15*, 1564-1571,
480   doi:cdd200883

481   44.   Wasilenko, S.T.; Banadyga, L.; Bond, D.; Barry, M. The vaccinia virus F1L protein interacts with the
482   proapoptotic protein Bak and inhibits Bak activation. *J Virol* **2005**, *79*, 14031-14043,
483   doi:10.1128/JVI.79.22.14031-14043.2005.

484   45.   Mehta, N.; Taylor, J.; Quilty, D.; Barry, M. Ectromelia virus encodes an anti-apoptotic protein that
485   regulates cell death. *Virology* **2015**, *475*, 74-87, doi:10.1016/j.virol.2014.10.023.

486   46.   Kvansakul, M.; van Delft, M.F.; Lee, E.F.; Gulbis, J.M.; Fairlie, W.D.; Huang, D.C.; Colman, P.M. A
487   structural viral mimic of prosurvival Bcl-2: a pivotal role for sequestering proapoptotic Bax and Bak.
488   *Mol Cell* **2007**, *25*, 933-942.

489   47.   Douglas, A.E.; Corbett, K.D.; Berger, J.M.; McFadden, G.; Handel, T.M. Structure of M11L: A myxoma
490   virus structural homolog of the apoptosis inhibitor, Bcl-2. *Protein Sci* **2007**, *16*, 695-703.

48. Banadyga, L.; Lam, S.C.; Okamoto, T.; Kvansakul, M.; Huang, D.C.; Barry, M. Deerpox virus encodes an inhibitor of apoptosis that regulates Bak and Bax. *J Virol* **2011**, *85*, 1922-1934, doi:JVI.01959-10

49. Okamoto, T.; Campbell, S.; Mehta, N.; Thibault, J.; Colman, P.M.; Barry, M.; Huang, D.C.; Kvansakul, M. Sheeppox virus SPPV14 encodes a Bcl-2-like cell death inhibitor that counters a distinct set of mammalian proapoptotic proteins. *J Virol* **2012**, *86*, 11501-11511, doi:10.1128/JVI.01115-12.

50. Suraweera, C.D.; Burton, D.R.; Hinds, M.G.; Kvansakul, M. Crystal structures of the sheeppox virus encoded inhibitor of apoptosis SPPV14 bound to the proapoptotic BH3 peptides Hrk and Bax. *FEBS Lett* **2020**, *594*, 2016-2026, doi:10.1002/1873-3468.13807.

51. Anasir, M.I.; Baxter, A.A.; Poon, I.K.H.; Hulett, M.D.; Kvansakul, M. Structural and Functional Insight into Canarypox Virus CNP058 Mediated Regulation of Apoptosis. *Viruses* **2017**, *9*, 305, doi:10.3390/v9100305.

52. Anasir, M.I.; Caria, S.; Skinner, M.A.; Kvansakul, M. Structural basis of apoptosis inhibition by the fowlpox virus protein FPV039. *J Biol Chem* **2017**, *292*, 9010-9021, doi:10.1074/jbc.M116.768879.

53. Westphal, D.; Ledgerwood, E.C.; Hibma, M.H.; Fleming, S.B.; Whelan, E.M.; Mercer, A.A. A novel Bcl-2-like inhibitor of apoptosis is encoded by the parapoxvirus ORF virus. *J Virol* **2007**, *81*, 7178-7188, doi:10.1128/JVI.00404-07.

54. Campbell, S.; Hazes, B.; Kvansakul, M.; Colman, P.; Barry, M. Vaccinia virus F1L interacts with Bak using highly divergent Bcl-2 homology domains and replaces the function of Mcl-1. *J Biol Chem* **2010**, *285*, 4695-4708, doi:M109.053769

55. Caria, S.; Marshall, B.; Burton, R.L.; Campbell, S.; Pantaki-Eimany, D.; Hawkins, C.J.; Barry, M.; Kvansakul, M. The N Terminus of the Vaccinia Virus Protein F1L Is an Intrinsically Unstructured Region That Is Not Involved in Apoptosis Regulation. *J Biol Chem* **2016**, *291*, 14600-14608, doi:10.1074/jbc.M116.726851.

56. Zhai, D.; Yu, E.; Jin, C.; Welsh, K.; Shiau, C.W.; Chen, L.; Salvesen, G.S.; Liddington, R.; Reed, J.C. Vaccinia virus protein F1L is a caspase-9 inhibitor. *J Biol Chem* **2010**, *285*, 5569-5580, doi:10.1074/jbc.M109.078113.

Chapter 4

Paper IV: Crystal Structures of the Sheeppox Virus Encoded Inhibitor of Apoptosis SPPV14 Bound to the Proapoptotic BH3 Peptides Hrk and Bax

4.1 Introduction

Sheeppox virus SPPV14 was initially identified as an myxoma virus M11L ortholog by database mining. Similar to M11L, SPPV14 lacks recognizable conserved BH motifs in its sequence whilst it was shown to block cellular apoptosis induced by multiple agents, such as UV irradiation or in viral infection (109). Consistent with the cellular data, SPPV14 was shown to interact with Bak and Bax *in vivo* and suppress the downstream activation of mitochondrial apoptosis (109). However, the detailed molecular mechanism underlaying SPPV14 mediated host intrinsic apoptosis had yet to be discovered.

To address this, I measured the extended binding interactions of SPPV14 to its interacting partners of BH3 motif peptides from endogenous human pro-apoptotic Bcl-2 proteins and determined the crystal structures of SPPV14 in complex with both Bax and Hrk BH3 motif peptides. The data obtained from this work are presented in the manuscript titled as "Crystal structures of the sheeppox virus encoded inhibitor of apoptosis SPPV14 bound to the proapoptotic BH3 peptides Hrk and Bax" that was published in FEBS Letters (2020) (108).

4.2 Co-author contribution

Chathura D. Suraweera	Protein Expression and purification
	Determination of SPPV14 binding partners
	Protein crystallization, X-ray diffraction and data collection
	Structure solution and refinement
	Structural analysis
	Manuscript writing (Introduction, Material and Methods Results and Discussion)
	Preparation of figures and tables in the manuscript
Denis R. Burton	Protein Expression and purification
	Protein crystallization
Mark G. Hinds	Overall scientific direction of the project
	Structural analysis and interpretation
	Drafted and revised the manuscript
Marc Kvansakul	Overall scientific direction of the project
	X-ray diffraction and data collection
	Structure solution and refinement
	Structural analysis
	drafted and revised the manuscript

Crystal structures of the sheeppox virus encoded inhibitor of apoptosis SPPV14 bound to the proapoptotic BH3 peptides Hrk and Bax

Chathura D. Suraweera[1] (iD), Denis R. Burton[1,*], Mark G. Hinds[2] (iD) and Marc Kvansakul[1] (iD)

1 Department of Biochemistry and Genetics, La Trobe Institute for Molecular Science, La Trobe University, Melbourne, Vic., Australia
2 Bio21 Molecular Science and Biotechnology Institute, The University of Melbourne, Parkville, Vic., Australia

Correspondence
M. Kvansakul, Department of Biochemistry and Genetics, La Trobe Institute for Molecular Science, La Trobe University, Melbourne, Vic. 3086, Australia
Tel: +61 3 9479 2263
E-mail: m.kvansakul@latrobe.edu.au

Present address
* Kaneka Eurogentec S.A, 14 Rue Bois Saint-Jean, Seraing, 4102, Belgium

Mark G. Hinds and Marc Kvansakul are Co-senior author

Programmed death of infected cells is used by multicellular organisms to counter viral infections. Sheeppox virus encodes for SPPV14, a potent inhibitor of Bcl-2-mediated apoptosis. We reveal the structural basis of apoptosis inhibition by determining crystal structures of SPPV14 bound to BH3 motifs of proapoptotic Bax and Hrk. The structures show that SPPV14 engages BH3 peptides using the canonical ligand-binding groove. Unexpectedly, Arg84 from SPPV14 forms an ionic interaction with the conserved Asp in the BH3 motif in a manner that replaces the canonical ionic interaction seen in almost all host Bcl-2:BH3 motif complexes. These results reveal the flexibility of virus-encoded Bcl-2 proteins to mimic key interactions from endogenous host signalling pathways to retain BH3 binding and prosurvival functionality.

Keywords: apoptosis; Bcl-2; isothermal titration calorimetry; poxvirus; sheeppox virus; X-ray crystallography

The altruistic death of infected host cells *via* programmed cell death or apoptosis is a potent feature of the first line of defence against invading pathogens [1]. The ability of multicellular hosts to eliminate infected cells *via* apoptosis forced viruses to evolve sophisticated strategies to counter host cell apoptotic defences, including the use of virus-encoded homologs of the B-cell lymphoma 2 or Bcl-2 family [2]. As primary modulators of the mitochondrially mediated or intrinsic apoptosis pathway, the Bcl-2 family can be divided into two factions: the prosurvival members and the proapoptotic members [3]. All mammalian Bcl-2 family members are characterized by the presence of one or more of the Bcl-2 homology or BH sequence

motifs. The prosurvival members, which include Bcl-2, Bcl-w, Bcl-x_L, A1, Mcl-1 and Bcl-b, all feature multiple BH motifs as well as a transmembrane region that enables localization to the outer mitochondrial membrane [4]. The proapoptotic family members can be further separated into two groups, the multi-BH motif proteins Bak, Bax and Bok, and the BH3-only proteins Bim, Bid, Puma, Bad, Bik, Bmf, Hrk and Noxa that only feature the BH3 motif [5]. Mechanistically, the BH3-only proteins act by either relieving the ability of prosurvival Bcl-2 to hold Bak and Bax in an inactive state or may directly activate Bak and Bax [6]. The interplay between the members is mediated by a helix-in-groove interaction, where a helical BH3 motif

is bound in the canonical hydrophobic ligand-binding groove on prosurvival Bcl-2 proteins [7]. Ultimately, it is the balance of the prosurvival and proapoptotic Bcl-2 members that determine the fate of a given cell.

Large DNA viruses encode a number of sequence and structural homologs of Bcl-2, including examples among the *adenoviridae* [8], *asfarviridae* [9,10], *herpesviridae* [11,12] and *iridoviridae* [13,14]. Among the *poxviridae*, the majority of genera have been shown to harbour one or more examples, including the *orthopoxviridae* [15,16], *leporipoxviridae* [17,18], *cervidpoxviridae* [19,20], *avipoxviridae* [21,22], *parapoxviridae* [23] and *chordopoxviridae* [24], with the vaccinia virus F1L and myxoma virus M11L the prototypical members of the family. Among the *capripoxviridae*, sheeppox virus has been shown to encode the potent apoptosis inhibitory protein SPPV14, a Bcl-2 homolog [25]. SPPV14 has been shown to inhibit apoptosis in transfected cells after treatment with etoposide, arabinose-C or UV irradiation. Furthermore, interaction studies revealed that SPPV14 is able to directly bind BH3 motif peptides of several mammalian proapoptotic Bcl-2 family members and functionally replaces F1L in the context of a recombinant vaccinia virus infection. However, the structural and biochemical basis for apoptosis inhibition by SPPV14 remained unclear. Here, we report the crystal structures and affinity data of SPPV14 bound to BH3 motifs of proapoptotic Bcl-2 family members. Our findings provide a structural and biochemical platform to understand sheeppox virus-mediated inhibition of apoptosis.

Materials and methods

Protein expression and purification

Recombinant SPPV14ΔC31 (UniProt accession number A0A2P1A8X8; SPPV14 residues 1-145 with a 31-residue C-terminal deletion and hereafter referred to as SPPV14) was expressed and purified as previously described [25]. SPPV14 mutants R84A and Y46A were synthesized as codon-optimized cDNA (GenScript), cloned into the bacterial expression vector pGEX-6P3 and purified as previously described [25]. Purified protein obtained using glutathione affinity chromatography was then subjected to size-exclusion chromatography using a Superdex S75 10/300 or 16/600 column mounted on an ÄKTA pure system (GE Healthcare, Chicago, IL, USA) equilibrated in 25 mM HEPES, pH 7.5, 150 mM NaCl and 10 mM TCEP (Tris(2-carboxyethyl)phosphine hydrochloride), and fractions analysed using SDS/PAGE. The final sample purity was estimated to be greater than 95% based on SDS/PAGE analysis, and appropriate fractions were pooled and concentrated using a centrifugal concentrator with 3 kDa molecular weight cut-off (Amicon ® Ultra-15) to final concentration of 10.0 mg·mL^{-1}. Recombinant SPPV14ΔC31:Bim BH3 complex was subjected to size-exclusion chromatography as described above for SPPV14ΔC31 alone. Molecular weight standards (Sigma-Aldrich, St. Louis, MO, USA) used for column calibration were as follows: bovine thyroglobulin (670 kDa), bovine γ-globulin (158 kDa), chicken ovalbumin (44 kDa), horse myoglobin (17 kDa) and vitamin B12 (1.350 kDa).

Measurement of dissociation constants

Binding affinities were measured by isothermal titration calorimetry (ITC) using a MicroCal iTC200 System (GE Healthcare) at 25 °C using wild-type truncated SPPV14 as well as two mutants SPPV14 Y46A and R84A in 25 mM HEPES, pH 7.5, 150 mM NaCl and 10 mM TCEP at a final concentration of 30 μM. BH3 motif peptides were used at a concentration of 300 μM and titrated using 19 injections of 2.0 μL of ligand solution. All affinity measurements were performed in triplicate. Protein concentrations were measured using a NanoDrop UV spectrophotometer (Thermo Fisher Scientific, Waltham, MA, USA) at a wavelength of 280 nm. Peptide concentrations were calculated based on the dry peptide weight after synthesis. The BH3-motif peptides used were commercially synthesized and were purified to a final purity of 95% (GenScript, Piscataway, NJ, USA) and based on the human sequences previously described [26] except for Bok BH3: VPGRLAEVCAVLLRLGDELE-MIRPSV (accession code Q9UMX3, residues 59–84).

Crystallization and structure determination

Crystals for SPPV14:Hrk BH3 and SPPV14:Bax BH3 complexes were obtained by mixing SPPV14 with human Hrk 26-mer or Bax 28-mer peptide using a 1 : 1.25 molar ratio as described [27] and concentrated using a centrifugal concentrator with 3 kDa molecular weight cut-off (Amicon ® Ultra 0.5) to 10.0 mg·mL^{-1}. Concentrated protein was immediately used for crystallization trials. Initial high-throughput sparse matrix screening was performed using 96-well sitting-drop trays (Swissci, Neuheim, Switzerland).

SPPV14:Hrk BH3 crystals were grown by the sitting-drop vapour diffusion method at 20 °C in 0.2 M sodium potassium tartrate, 0.1 M Bis-Tris propane, pH 6.5, and 20% poly(ethylene glycol) 3350. The crystals were flash-cooled at −173 °C in mother liquor supplemented with 25% glucose. The SPPV14:Hrk BH3 complex formed single cuboidal crystals, which belong to space group C222$_1$ with $a = 43.28$ Å, $b = 70.66$ Å, $c = 115.08$ Å, $\alpha = 90.00°$, $\beta = 90.00°$ and $\gamma = 90.00°$ in the orthorhombic crystal system.

All diffraction data were collected at the Australian Synchrotron MX2 [28] beamline using an Eiger detector with

an oscillation range 0.1° per frame at a wavelength of 0.9537 Å. The diffraction data were integrated using XDS [29] and scaled using AIMLESS [30]. A molecular replacement solution was obtained using the BALBES [31] automated pipeline and identified M11L (PDB code: 2BJY) [18] as the optimal model. SPPV14:Hrk BH3 crystals contained one molecule of SPPV14 and one Hrk BH3 peptide in the asymmetric unit, with a 43% solvent content, and gave final TFZ and LLG values of 32.2 and 1539, respectively. The final model of SPPV14:Hrk BH3 was built manually over several cycles using Coot [32] and refined using PHENIX [33] giving final R_{work}/R_{free} values of 0.221/0.235, with 99% of residues in the favoured region of the Ramachandran plot and no outliers.

SPPV14:Bax BH3 crystals were obtained in 1.0 M lithium chloride, 0.1 M citrate, pH 5.0, and 30% poly(ethylene glycol) 6000. The crystals were flash-cooled at −173 °C in mother liquor. The SPPV14:Bax BH3 complex formed single rod-shaped crystals, which belong to space group P2$_1$ with cell dimensions $a = 100.27$ Å, $b = 78.56$ Å, $c = 107.76$ Å, $\alpha = 90.00°$, $\beta = 110.96°$ and $\gamma = 90.00°$ in the monoclinic crystal system. Diffraction data collection, integration and scaling were performed as described above. The molecular replacement was performed using Phaser [34] with the previously solved structure of SPPV14:Hrk BH3 as a search model. SPPV14:Bax BH3 crystals contain eight molecules of SPPV14 and eight Bax BH3 peptides, with a 48.9% solvent content and final TFZ and LLG values of 11.2 and 1720, respectively. The final model of SPPV14:Bax BH3 was built manually as described above giving final R_{work}/R_{free} values of 0.238/0.288, with 99% of residues in Ramachandran favoured region and no outliers. All images for SPPV14:Hrk and SPPV14:Bax complexes were generated using PYMOL (Schrodinger, New York, NY, USA) molecular graphic system version 1.8.6.0 (Schrödinger, LLC, New York, NY, USA). The coordinates for the structures were deposited at the Protein Data Bank (PDB) using accession codes 6XY4 and 6XY6. All raw images were deposited at the SBGridDB using their PDB accession codes [35]. All software was accessed through the SBGrid suite [36].

Bioinformatics analyses

The closest structural homologs of SPPV14 were identified using the Dali server [37] by searching the entire PDB. Protein interaction interfaces were examined using the ePDB Proteins, Interactions, Surfaces, Assemblies program [38]. Sequence alignments were performed using MUSCLE [39].

Results

We previously showed sheeppox virus-encoded SPPV14 binds peptides spanning the BH3 motif of the proapoptotic Bcl-2 family members Bak and Bax as well as Bim, Bid, Bmf, Hrk and Puma as determined by surface plasmon resonance (SPR) [25]. To determine the BH3 peptide binding specificity, we performed ITC employing a recombinant protein, SPPV14ΔC31 (hereafter referred to as SPPV14), lacking the 31 C-terminal residues of the predicted transmembrane motif and BH3 motif peptides derived from human proapoptotic Bcl-2 proteins (Table 1). ITC confirmed BH3 peptides of Bak and Bax as well as Bim, Bid, Bmf, Hrk and Puma as high-affinity interactors, as previously reported [25]. In addition, we observed weaker affinities for BH3 peptides of Bad and Bok, with K_D values of 5.2 and 7.6 μM, respectively. To understand the structural basis for BH3 motif binding by SPPV14, we expressed and purified recombinant truncated SPPV14 and reconstituted SPPV14:Hrk BH3 and SPPV14:Bax BH3 complexes. Crystals of the SPPV14:Hrk BH3 complex diffracted to 2.05 Å (Table 2). After molecular replacement using M11L as a search model (PDB ID 2BJY) [18], clear and continuous electron density was observed for SPPV14 residues 5–139 and Hrk residues 26–50 (Fig. 1A), with the remaining residues presumed disordered. SPPV14 adopts a globular helical bundle structure comprising a central helix α5 around which six additional helices are scaffolded to form the classical Bcl-2 fold (Fig. 2A). A Dali structural similarity analysis identified deerpox virus DPV022 (PDB ID: 4UF3) [20] as the closest structural homolog of SPPV14 with an rmsd of 2.1 Å over 106 Cα atoms, with M11L the second closest match with an rmsd of 2.3 Å over 111 Cα atoms (Fig. 2C).

Table 1. Interactions of wild-type sheeppox virus SPPV14 and two mutants R84A and Y46A with human proapoptotic BH3 motif peptides. Measurements were performed using ITC. All K_D values (in nM) are the means of three independent measurements with standard error. 'NB' denotes no binding.

Peptide	WT K_D (nM)	R84A K_D (nM)	Y46A K_D (nM)
Bak	48 ± 1	139 ± 10	2553 ± 353
Bax	26 ± 3	182 ± 15	4645 ± 393
Bok	7580 ± 643	NB	NB
Bad	5197 ± 533	6700 ± 806	NB
Bid	136 ± 23	1698 ± 16	NB
Bik	1766 ± 280	9245 ± 701	NB
Bim	19 ± 3	44 ± 3	165 ± 18
Bmf	44 ± 7	97 ± 2	151 ± 18
Hrk	39 ± 5	132 ± 3	2250 ± 318
Noxa	NB	NB	NB
Puma	56 ± 8	95 ± 3	988 ± 142

Table 2. X-ray data collection and refinement statistics.

	SPPV14:Hrk BH3	SPPV14:Bax BH3
Data collection		
Space group	C222$_1$	P2$_1$
Cell dimensions		
a, b, c (Å)	43.28, 70.66, 115.08	100.28, 78.56, 107.77
α, β, γ (°)	90, 90, 90	90, 110.97, 90
Wavelength (Å)	0.9537	0.9537
Resolution (Å)	31.07–2.05 (2.12–2.05)[a]	37.61–2.91 (3.02–2.9)[a]
R_{sym} or R_{merge}	0.066 (1.12)[a]	0.15 (1.24)[a]
$I/\sigma I$	8.7 (0.9)[a]	5.2 (0.9)[a]
Completeness (%)	98.2 (90.3)[a]	99.6 (98.3)[a]
CC$_{1/2}$	0.99 (0.59)[a]	0.99 (0.54)[a]
Redundancy	5.0 (4.7)[a]	3.5 (3.6)[a]
Refinement		
Resolution (Å)	31.07–2.05 (2.12–2.05)[a]	37.61–2.91 (3.02–2.9)[a]
No. of reflections	11 232	34 323
R_{work}/R_{free}	0.221/0.235	0.238/0.288
Clashscore	0.40	5.14
No. of atoms		
Protein	1235	10 281
Ligand/ion	0	0
Water	28	44
B-factors		
Protein	59.40	66.91
Ligand/ion	0	0
Water	52.66	46.66
RMSD		
Bond lengths (Å)	0.003	0.004
Bond angles (°)	0.45	0.63

[a]Values in parentheses are for the highest resolution shell.

SPPV14 harbours the canonical ligand-binding groove formed by helices α2-α5, which engages Hrk BH3 (Figs 1A and 2A). The mode of binding of BH3 motif peptides observed for SPPV14 is nearly identical to what has been previously observed for M11L:Bak (Fig. 2C), with the SPPV14:Hrk complex superimposing onto the M11L:Bak complex with an rmsd of 1.8 Å over the entire SPPV14 chain. The three conserved hydrophobic residues L37, I40 and L44 as well as T35 from Hrk protrude into the SPPV14-binding groove and engage the resident four hydrophobic pockets (Fig. 3A). In addition to these hydrophobic interactions, SPPV14 forms an ionic interaction with Hrk *via* SPPV14 R84 and Hrk D42 carboxyl group. Furthermore, two hydrogen bonds are observed between SPPV14 Y46 hydroxyl and Hrk E43 carboxyl SPPV14 and T78 hydroxyl with Hrk A34 amide.

The SPPV14:Bax BH3 complex was solved by molecular replacement using the SPPV14 model obtained from the SPPV14:Hrk BH3 complex and refined to a resolution of 2.9 Å (Fig. 1B, Table 2). Clear and continuous density was observed for SPPV14 5–139 and Bax 52–74 (Fig. 2B). The four conserved hydrophobic residues L59, L63, I66 and L70 from Bax are nestled in the corresponding four hydrophobic pockets of the SPPV14-binding groove (Fig. 3B). Furthermore, Bax M74 also makes contact with the SPPV14-binding groove in a pocket formed by residues C38, V41, I42, F133 and N137. Additional interactions are observed as ionic interactions between SPPV14 R84 and the carboxyl groups of Hrk D68 and D71 as well as hydrogen bonds between SPPV14 S81 hydroxyl and Bax K64 lysyl, and the main chain carbonyl of SPPV14 I74 and Bax S60 hydroxyl group (Fig. 3B).

To validate our crystal structures, we performed size-exclusion chromatography to determine the oligomeric state of SPPV14 in solution. An SPPV14:Bim BH3 complex eluted at a volume commensurate with a heterodimeric species (Fig. 4). We next performed structure-guided mutagenesis to modulate the affinity of SPPV14 for BH3 motif ligands (Table 1). Indeed, the SPPV14 mutants Y46A and R84A display attenuated affinities, with SPPV14 Y46A binding BH3 peptides from Bak, Bax, Bim, Bmf, Hrk and Puma with lower affinity and losing binding to those of Bad, Bid, Bik and Bok, whilst SPPV14 R84A bound Bax, Bak, Bid, Bik and Hrk BH3 peptides with lower affinities and lost binding to Bok BH3 compared to wild-type protein.

Discussion

Subversion of premature host cell apoptosis is a frequently used strategy for many large DNA viruses, including the *poxviridae,* to evade the innate immune response [40]. It has previously been shown that sheeppox virus harbours the potent apoptosis inhibitor SPPV14, which acts by sequestering BH3-only proteins including Bim, Bid, Bmf, Hrk and Puma as well as Bak and Bax [25]. In addition to the known interactors, we observed previously unreported low micromolar affinities for Bad and Bok BH3 motifs. Previous studies had relied on the use of competition SPR spectroscopy measurements, which could not detect binding affinities weaker than IC$_{50}$ = 2 μM. These findings implicate Bad and Bok inhibition as a potential antiapoptotic strategy of SPPV14; however, considering the comparatively low affinity of the interaction the
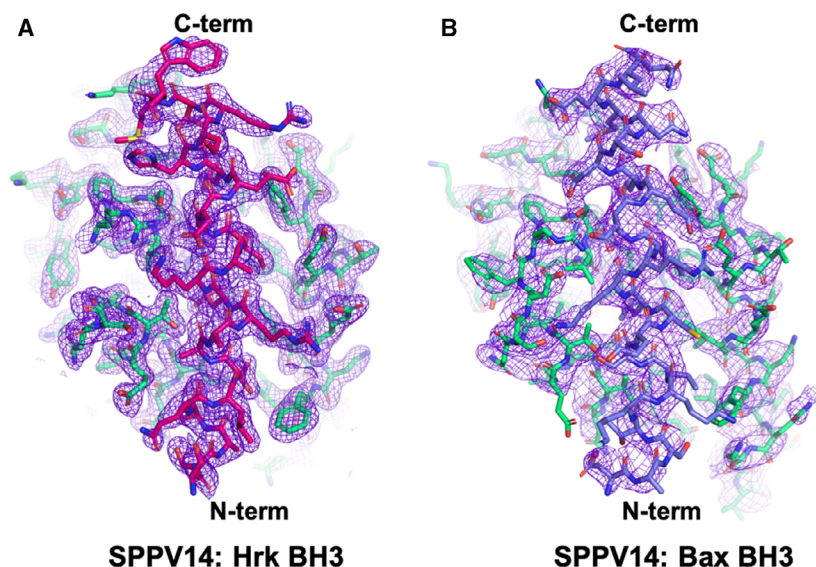
Fig. 1. Electron density maps of SPPV14: Hrk and Bax BH3 complexes (A) $2F_o$-F_c electron density maps of SPPV14:Hrk BH3 complex interface contoured at 1.5 σ. SPPV14 is shown as green sticks and Hrk as pink-coloured sticks. (B) 2Fo-Fc electron density maps of SPPV14:Bax BH3 complex interface contoured at 1.5 σ. SPPV14 is shown as green sticks and Bax as slate-coloured sticks. The N and C termini of the BH3 peptides are labelled.

functional relevance of Bad and Bok inhibition remains to be established.

Having identified potentially new BH3 ligands, we defined the structural basis for BH3 motif interactions with SPPV14 by determining the crystal structures of the SPPV14:Hrk BH3 and SPPV14:Bax BH3 complexes. SPPV14 binds both Hrk and Bax BH3 tightly with K_D values of 39 and 26 nM, respectively, and the interactions are mediated by the canonical hydrophobic interactions involving the four hydrophobic pockets in SPPV14 as well as several ionic interactions and hydrogen bonds (Figs 2 and 3). A comparison with other virus-encoded Bcl-2 proteins reveals that unlike the myxoma virus M11L and vaccinia virus F1L prosurvival Bcl-2 proteins, of which both feature low sequence identity to mammalian Bcl-2 [7], SPPV14 forms an ionic interaction using R84 with Hrk D42 or Bax D68 that is reminiscent of the highly conserved ionic interaction between a conserved Arg in the BH1 region of mammalian prosurvival Bcl-2 proteins and the conserved Asp of the BH3 motif (Fig. 5A). Such an ionic interaction is seen in all mammalian prosurvival Bcl-2 protein:BH3 peptide complexes exemplified by Bcl-x_L R139-Bax D68 (Fig. 5A). This Arg:Asp interaction is also observed in the complexes with BH3 peptides of the virus-encoded Bcl-2 homologs A179L [10,41], BHRF1 [12] and FPV039 [22]. Unlike the canonical ionic interaction [42,43], the geometric configuration of the ionic bond in SPPV14 is different, allowing SPPV14 to engage BH3 motifs in a manner that resembles the use of the BH1 motif in mammalian prosurvival Bcl-2 interactions despite the lack of a recognizable BH1 sequence motif (Fig. 5A,B).

Furthermore, loss of this ionic interaction substantially impacts SPPV14 affinities for BH3 peptide of proapoptotic host Bcl-2 proteins (Table 1), epitomising the behaviour of endogenous mammalian prosurvival Bcl-2 interactions [44].

The SPPV14:Bax BH3 complex revealed that an additional residue, M74, engages a fifth pocket in the canonical ligand-binding groove besides the four canonical hydrophobic residues that are already accommodated in their respective pockets. This observation mirrors previous findings for Bcl-x_L and Mcl-1 [45]. A further example of additional hydrophobic residues from a BH3 motif peptide engaging a pocket is the variola virus F1L:Bid BH3 complex, where I101 from Bid protrudes into a fifth pocket [46]. A comparison of the detailed architecture of these additional pockets (Fig. 5C–F) reveals that there is little conservation of residues that form the pockets. In Mcl-1, V216, F318 and F319 are involved, whereas in Bcl-x_L, it is A93 and Y195. In variola virus F1L, I101 from the Bid BH3 motif engages a fifth pocket formed by Y111, L154, L158 and I200. Interestingly, mutations affecting the binding of Bax M74 to Bcl-x_L or Mcl-1 resulted in increased sensitivity to the BH3 mimetic drug ABT-737 [45]. However, the functional consequences of disruption of M74-mediated binding of Bax to SPPV14 remain to be established. We note that binding of the Bax BH3 motif would require substantial structural rearrangements in the context of full-length Bax, since in folded cytosolic Bax, the BH3 motif is buried and not available for binding to SPPV14 or other prosurvival Bcl-2 proteins [47]. However, the molecular details of such structural changes
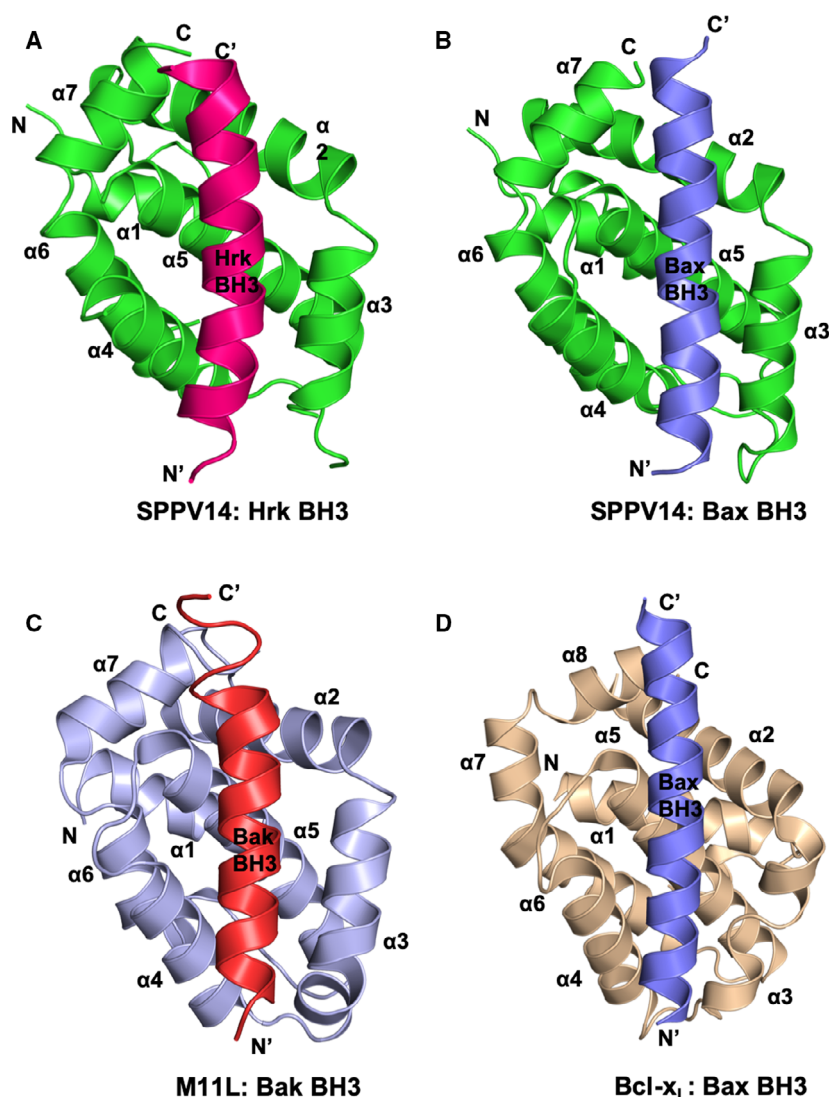
Fig. 2. SPPV14 binds to BH3 motif peptides of proapoptotic Bcl-2 proteins using the canonical ligand-binding groove ribbon representations of Bcl-2 protein BH3 peptide complexes. (A) SPPV14:Hrk BH3 complex. SPPV14 is shown in green and Hrk BH3 is shown in pink, and SPPV14 helices are labelled α1–α7. The view is into the hydrophobic binding groove formed by helices α2–α5. (B) SPPV14:Bax BH3 complex. SPPV14 is shown as in (A) with the Bax BH3 coloured slate. The view is as in (A). (C) M11L:Bak BH3 complex (PDB ID 2JBY) [18]. M11L is shown in light blue, and Bak BH3 is shown in red. (D) Bcl-x_L:Bax BH3 complex (PDB ID 1BXL) [45]. Bcl-x_L is shown as sand-coloured ribbon, and Bax BH3 is shown in slate. The views in C–D are as in (A).

remain to be defined. In contrast, Hrk is predicted to be an intrinsically unfolded protein, and thus, the BH3 motif interactions we observed with SPPV14 are likely to be recapitulated in the context of full-length Hrk [48].

Previously, several residues were predicted to be located in the binding groove of SPPV14 based on the M11L structure and thus designated as potential mediators of interactions with BH3 motif ligands [25]. A comparison of the predicted structure with our experimentally determined structures reveals that out of the six predicted residues, all six were indeed found in the SPPV14-binding groove, revealing the high degree of similarity between the SPPV14 and M11L canonical ligand-binding grooves despite an overall sequence identity of 22% [25]. However, whilst six key residues in the binding groove are conserved, the remaining

additional BH3 motif contacting residues influence the selectivity or affinity of the viral Bcl-2 for its mammalian targets, as seen by the differential ligand binding profiles and affinities of SPPV14 and M11L. For instance, SPPV14 utilizes Y46 to form a hydrogen bond with Hrk E46, and a similar hydrogen bond is formed by the equivalent tyrosine in M11L, Y41, with Bak D84. Indeed, SPPV14 Y46 is conserved across a number of putative Bcl-2-like proteins in poxviruses including deerpox, swinepox and rabbitpox [18,25], as well as in mammalian Bcl-2 proteins such as murine Bcl-x_L [42]. In contrast, SPPV14 R84, which forms a salt bridge with Hrk D42, is not recapitulated in M11L. Considering that the salt bridge formed by SPPV14 R84-Hrk D42 mimics other salt bridge interactions seen in many prosurvival Bcl-2 protein:BH3 motif interactions where the prosurvival Bcl-2 protein
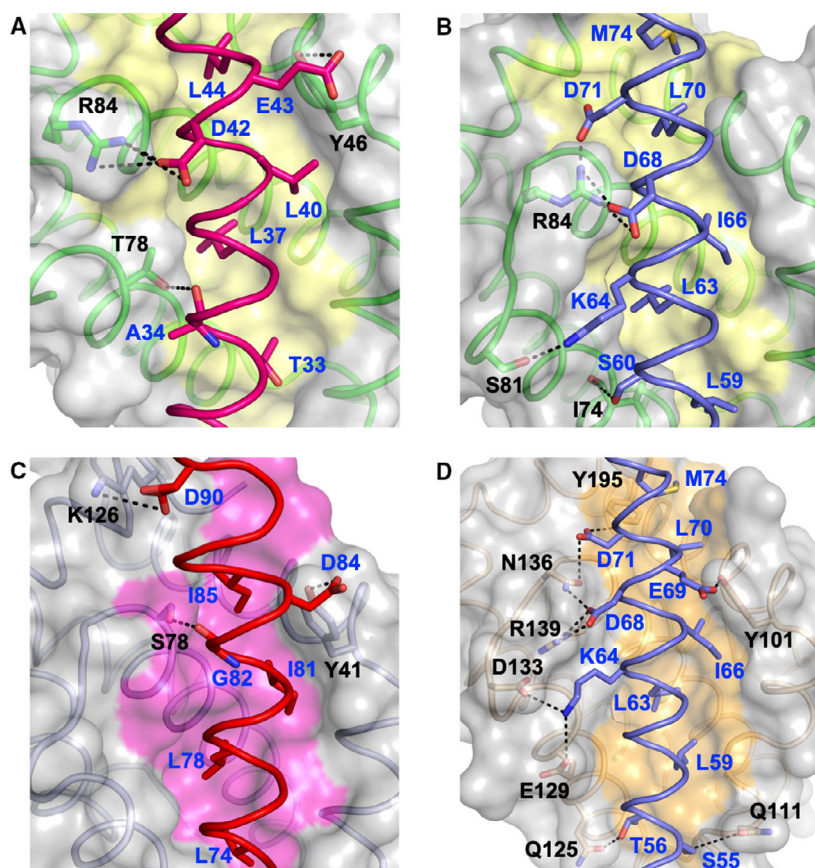
Fig. 3. Detailed view of the SPPV14:Hrk BH3, SPPV14:Bax BH3, M11L:Bak BH3 and Bcl-x$_L$:Bax BH3 interfaces. (A) The SPPV14 backbone, floor of the binding groove and surface are shown in green, yellow and grey, respectively, whilst the Hrk BH3 ribbon is shown in hot pink. The three hydrophobic residues of Hrk (L37, L40 and L44) as well as T35 are protruding into the binding groove, and the conserved ionic interaction formed by SPPV14 R84 and Hrk BH3 D42 is labelled, as well as all other residues involved in hydrogen bonds between protein and peptide. (B) SPPV14 is shown as in (A), whilst the Bax BH3 ribbon is shown in slate. The five hydrophobic residues of Bax BH3 (L59, L63, I66, L70 and M74) are protruding into the binding groove, and the conserved salt bridge interaction formed by SPPV14 R84 and Bax BH3 D68 is labelled, as well as other residues involved in additional ionic interactions and hydrogen bonds. (C) M11L (light blue) is shown as in (C), whilst the Bak BH3 ribbon is shown in red (PDB ID 1JBY). The four hydrophobic residues of Bak BH3 (L74, L78, I81 and I85) are protruding into the binding groove, and the ionic interaction formed by M11L K126 and Bak BH3 D90 is labelled, as well as other residues involved in protein:peptide hydrogen bonds. (D) Bcl-x$_L$ (wheat) is shown as in (A), whilst the Bax BH3 is shown as slate-coloured sticks (PDB ID 1BXL). The five hydrophobic residues of Bax BH3 (L59, L63, I66, L70 and M74) are protruding into the binding groove, and the conserved ionic interaction formed by Bcl-x$_L$ R139 and Bax BH3 D68 is labelled, as well as other residues involved in additional ionic interactions and hydrogen bonds. Ionic interactions and hydrogen bonds are shown as dotted black lines, and the participating residues are labelled.

features broad binding specificity, we speculate that R84 may be a feature that enables the broader binding specificity of SPPV14 when compared to M11L.

SPPV14 is able to directly sequester proapoptotic BH3-only proteins as well as Bax and Bak. Whilst numerous large DNA viruses encode for prosurvival Bcl-2 homologs to subvert host cell apoptosis by targeting Bax and Bak [18,41,46,49,50], mechanisms that do not rely on prosurvival Bcl-2 proteins for Bax/Bak neutralization have also been identified in other viruses. For instance, the herpesvirus human

cytomegalovirus encodes for vMIA [51], which has been shown to neutralize Bax by binding in a non-canonical site [52]. Intriguingly, only a short peptide sequence of vMIA is able to mediate the inhibitory effect on Bax. The murine counterpart murine cytome-galovirus (MCMV) encodes the Bax inhibitor m38.5 [53,54]; however, the structural basis of this inhibition remains to be established. Inhibition of Bak is achieved by MCMV-encoded m41.1 [55,56]. Strikingly, none of these CMV-encoded Bax/Bak inhibitors appear to be multimotif Bcl-2 homologs, underscoring
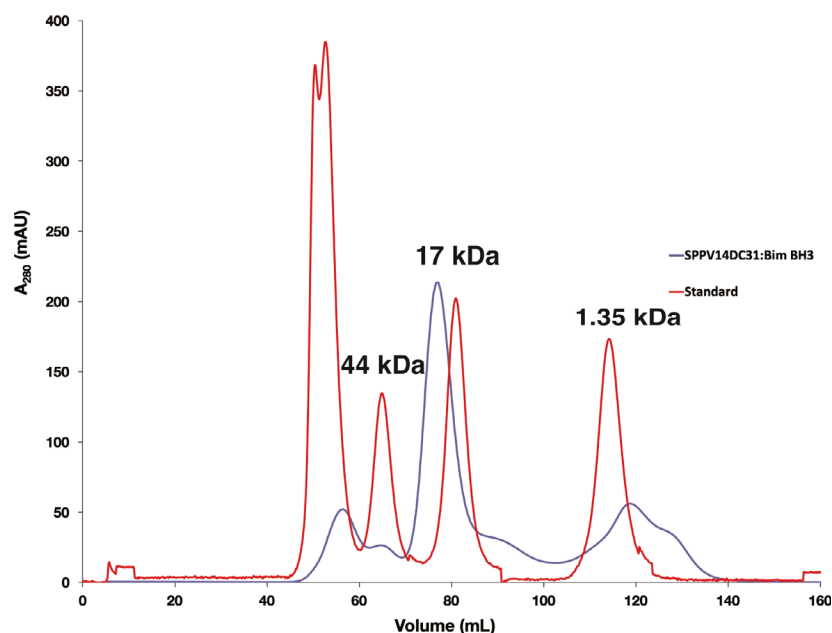
Fig. 4. Size-exclusion chromatography of SPPV14:Bim BH3 complex. Reconstituted recombinant SPPV14ΔC31:Bim BH3 complex was subjected to size-exclusion chromatography using a Superdex 75 16/600 column (blue trace). Molecular weight standards are labelled and indicated on the red trace.
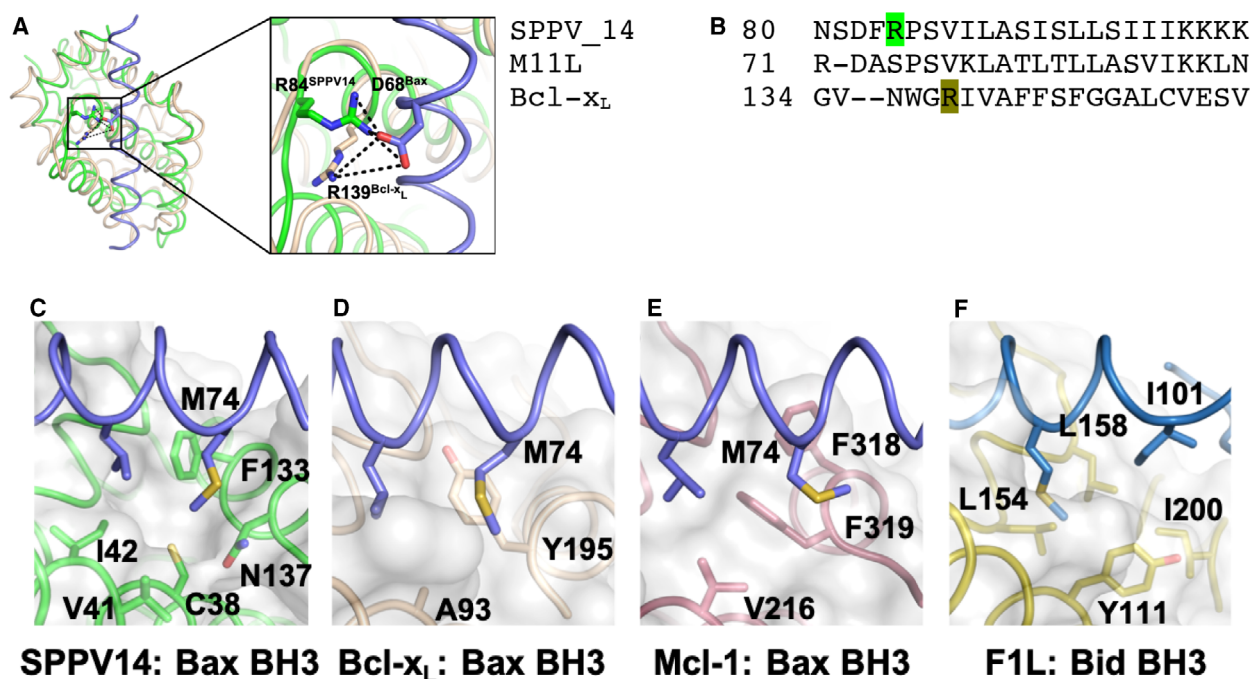

Fig. 5. Noncanonical interactions in the SPPV14:Bax BH3 complex. (A) SPPV14 R84 (green) forms an ionic bond with Bax BH3 D68 (slate) that resembles the canonical ionic interaction between Bcl-x_L R139 (sand) and Bax BH3 D68 (slate). For clarity, only Bax BH3 from the SPPV14:Bax BH complex is shown. (B) Sequence alignment of SPPV14, M11L and Bcl-x_L BH1 motifs. Arg residues involved in the ionic interactions with Bax BH3 shown in (A) are coloured. (C) Bax M74 protrudes into a fifth pocket in the SPPV14-binding groove formed by C38, V41, I42, F133 and N137. (D) Bax M74 bound in the equivalent pocket in Bcl-x_L [46]. (E) Bax M74 bound in the equivalent pocket in Mcl-1 [46]. (F) Bid I101 bound in the equivalent pocket in variola virus F1L [47].

the importance of Bax/Bak neutralization for the viral life cycle.

In both crystal structures of SPPV14 bound to BH3 motif peptides, SPPV14 appears to be monomeric. Analysis of contacts between SPPV14 chains in the crystal lattices scores all interfaces with a complex significance score of 0, suggesting that none of them are biologically relevant. Furthermore, during purification of C-terminally truncated SPPV14 using size-exclusion chromatography, SPPV14 bound to Bim BH3 elutes at a volume corresponding to a heterodimeric species comprising a single chain of SPPV14 (Fig. 4). Whilst we cannot exclude the possibility that SPPV14 forms homodimers in a cellular context, our data using recombinantly expressed protein suggest that the active form of SPPV14 is monomeric. Interestingly, a Dali analysis identified DPV022 as the closest structural homolog, even though DPV022 adopts a domain-swapped dimeric topology [20]. Whether or not SPPV14 is able to form similar domain-swapped dimers such as DPV022 or other poxvirus-encoded domain-swapped dimers such as vaccinia and variola virus F1L is unclear. To date, no clear molecular signature that is indicative of an ability to form domain-swapped dimers has been identified in Bcl-2 proteins. It has previously been shown that truncation of the loop connecting helices α1 and 2 in Bcl-x_L triggers domain swapping [57], and in DPV022 and F1L, the corresponding α1/2 loops are very short and only 2–3 amino acids in length.

In summary, we show that SPPV14 is a monomeric prosurvival Bcl-2 protein that utilizes the canonical ligand-binding groove to engage BH3 motif peptides of proapoptotic Bcl-2 proteins. Our structures provide a mechanistic basis to delineate detailed intermolecular interactions and the importance of neutralizing different proapoptotic Bcl-2 proteins for sheeppox virus infectivity and proliferation.

Acknowledgements

Funding

Author contributions

References

1 Galluzzi L, Brenner C, Morselli E, Touat Z and Kroemer G (2008) Viral control of mitochondrial apoptosis. *PLoS Pathog* **4**, e1000018.

2 Kvansakul M, Caria S and Hinds MG (2017) The Bcl-2 Family in Host-Virus Interactions. *Viruses* **9**, 290.

3 Adams JM and Cory S (1998) The Bcl-2 protein family: arbiters of cell survival. *Science* **281**, 1322–1326.

4 Banjara S, Suraweera CD, Hinds MG and Kvansakul M (2020) The Bcl-2 family: ancient origins, conserved structures, and divergent mechanisms. *Biomolecules* **10**, 128.

5 Kvansakul M and Hinds MG (2014) The structural biology of BH3-only proteins. *Methods Enzymol* **544**, 49–74.

6 Shamas-Din A, Kale J, Leber B and Andrews DW (2013) Mechanisms of action of bcl-2 family proteins. *Cold Spring Harb Perspect Biol* **5**, a008714.

7 Kvansakul M and Hinds MG (2013) Structural biology of the Bcl-2 family and its mimicry by viral proteins. *Cell Death Dis* **4**, e909.

8 White E, Sabbatini P, Debbas M, Wold WS, Kusher DI and Gooding LR (1992) The 19-kilodalton adenovirus E1B transforming protein inhibits programmed cell death and prevents cytolysis by tumor necrosis factor alpha. *Mol Cell Biol* **12**, 2570–2580.

9 Neilan JG, Lu Z, Afonso CL, Kutish GF, Sussman MD and Rock DL (1993) An African swine fever virus gene with similarity to the proto-oncogene bcl-2 and the Epstein-Barr virus gene BHRF1. *J Virol* **67**, 4391–4394.

10 Banjara S, Shimmon GL, Dixon LK, Netherton CL, Hinds MG and Kvansakul M (2019) Crystal structure of african swine fever virus A179L with the autophagy regulator beclin. *Viruses* **11**, 789.

11 Henderson S, Huen D, Rowe M, Dawson C, Johnson G and Rickinson A (1993) Epstein-Barr virus-coded BHRF1 protein, a viral homologue of Bcl-2, protects human B cells from programmed cell death. *Proc Natl Acad Sci USA* **90**, 8479–8483.

12 Kvansakul M, Wei AH, Fletcher JI, Willis SN, Chen L, Roberts AW, Huang DC and Colman PM (2010) Structural basis for apoptosis inhibition by Epstein-Barr virus BHRF1. *PLoS Pathog* **6**, e1001236.

13 Lin PW, Huang YJ, John JA, Chang YN, Yuan CH, Chen WY, Yeh CH, Shen ST, Lin FP, Tsui WH *et al.* (2008) Iridovirus Bcl-2 protein inhibits apoptosis in the early stage of viral infection. *Apoptosis* **13**, 165–176.

14 Banjara S, Mao J, Ryan TM, Caria S and Kvansakul M (2018) Grouper iridovirus GIV66 is a Bcl-2 protein that inhibits apoptosis by exclusively sequestering Bim. *J Biol Chem* **293**, 5464–5477.

15 Wasilenko ST, Stewart TL, Meyers AF and Barry M (2003) Vaccinia virus encodes a previously uncharacterized mitochondrial-associated inhibitor of apoptosis. *Proc Natl Acad Sci USA* **100**, 14345–14350.

16 Kvansakul M, Yang H, Fairlie WD, Czabotar PE, Fischer SF, Perugini MA, Huang DC and Colman PM (2008) Vaccinia virus anti-apoptotic F1L is a novel Bcl-2-like domain-swapped dimer that binds a highly selective subset of BH3-containing death ligands. *Cell Death Differ* **15**, 1564–1571.

17 Graham KA, Opgenorth A, Upton C and McFadden G (1992) Myxoma virus M11L ORF encodes a protein for which cell surface localization is critical in manifestation of viral virulence. *Virology* **191**, 112–124.

18 Kvansakul M, van Delft MF, Lee EF, Gulbis JM, Fairlie WD, Huang DC and Colman PM (2007) A structural viral mimic of prosurvival Bcl-2: a pivotal role for sequestering proapoptotic Bax and Bak. *Mol Cell* **25**, 933–942.

19 Banadyga L, Lam SC, Okamoto T, Kvansakul M, Huang DC and Barry M (2011) Deerpox virus encodes an inhibitor of apoptosis that regulates Bak and Bax. *J Virol* **85**, 1922–1934.

20 Burton DR, Caria S, Marshall B, Barry M and Kvansakul M (2015) Structural basis of Deerpox virus-mediated inhibition of apoptosis. *Acta Crystallogr D Biol Crystallogr* **71**, 1593–1603.

21 Banadyga L, Gerig J, Stewart T and Barry M (2007) Fowlpox virus encodes a Bcl-2 homologue that protects cells from apoptotic death through interaction with the proapoptotic protein Bak. *J Virol* **81**, 11032–11045.

22 Anasir MI, Caria S, Skinner MA and Kvansakul M (2017) Structural basis of apoptosis inhibition by the fowlpox virus protein FPV039. *J Biol Chem* **292**, 9010–9021.

23 Westphal D, Ledgerwood EC, Hibma MH, Fleming SB, Whelan EM and Mercer AA (2007) A novel Bcl-2-like inhibitor of apoptosis is encoded by the parapoxvirus ORF virus. *J Virol* **81**, 7178–7188.

24 Suraweera CD, Ishtiaq Anasir M, Chugh S, Javorsky A, Impey RA, Hasan Zadeh M, Soares da Costa TP, Hinds MG and Kvansakul M (2020) Structural insight into tanapoxvirus mediated inhibition of apoptosis. *FEBS J*, doi: 10.1111/febs.15365

25 Okamoto T, Campbell S, Mehta N, Thibault J, Colman PM, Barry M, Huang DC and Kvansakul M (2012) Sheeppox virus SPPV14 encodes a Bcl-2-like cell death inhibitor that counters a distinct set of mammalian proapoptotic proteins. *J Virol* **86**, 11501–11511.

26 Caria S, Hinds MG and Kvansakul M (2017) Structural insight into an evolutionarily ancient programmed cell death regulator - the crystal structure of marine sponge BHP2 bound to LB-Bak-2. *Cell Death Dis* **8**, e2543.

27 Kvansakul M and Czabotar PE (2016) Preparing samples for crystallization of Bcl-2 family complexes. In Programmed Cell Death: Methods and Protocols (Puthalakath H and Hawkins CJ, eds), pp. 213–229. Springer New York, New York, NY.

28 Aragao D, Aishima J, Cherukuvada H, Clarken R, Clift M, Cowieson NP, Ericsson DJ, Gee CL, Macedo S, Mudie N *et al.* (2018) MX2: a high-flux undulator microfocus beamline serving both the chemical and macromolecular crystallography communities at the Australian Synchrotron. *J Synchrotron Radiat* **25**, 885–891.

29 Kabsch W (2010) XDS. *Acta Crystallogr D* **66**, 125–132.

30 Evans P (2006) Scaling and assessment of data quality. *Acta Crystallogr D* **62**, 72–82.

31 Long F, Vagin AA, Young P and Murshudov GN (2008) BALBES: a molecular-replacement pipeline. *Acta Crystallogr D Biol Crystallogr* **64**, 125–132.

32 Emsley P, Lohkamp B, Scott WG and Cowtan K (2010) Features and development of Coot. *Acta Crystallogr D* **66**, 486–501.

33 Afonine PV, Grosse-Kunstleve RW, Echols N, Headd JJ, Moriarty NW, Mustyakimov M, Terwilliger TC, Urzhumtsev A, Zwart PH and Adams PD (2012) Towards automated crystallographic structure refinement with phenix.refine. *Acta Crystallogr D* **68**, 352–367.

34 McCoy A (2007) Solving structures of protein complexes by molecular replacement with Phaser. *Acta Crystallogr D* **63**, 32–41.

35 Meyer PA, Socias S, Key J, Ransey E, Tjon EC, Buschiazzo A, Lei M, Botka C, Withrow J, Neau D *et al.* (2016) Data publication with the structural biology data grid supports live analysis. *Nat Commun* **7**, 10882.

36 Morin A, Eisenbraun B, Key J, Sanschagrin PC, Timony MA, Ottaviano M and Sliz P (2013) Collaboration gets the most out of software. *eLife* **2**, e01456.

37 Holm L and Rosenstrom P (2010) Dali server: conservation mapping in 3D. *Nucleic Acids Res* **38**, W545–W549.

38 Krissinel E and Henrick K (2007) Inference of macromolecular assemblies from crystalline state. *J Mol Biol* **372**, 774–797.

39 Edgar RC (2004) MUSCLE: multiple sequence alignment with high accuracy and high throughput. *Nucleic Acids Res* **32**, 1792–1797.

40 Nichols DB, De Martini W and Cottrell J (2017) Poxviruses utilize multiple strategies to inhibit apoptosis. *Viruses* **9**, 215.

41 Banjara S, Caria S, Dixon LK, Hinds MG and Kvansakul M (2017) Structural insight into African swine fever virus A179L-mediated inhibition of apoptosis. *J Virol* **91**, e02228–16.

42 Liu X, Dai S, Zhu Y, Marrack P and Kappler JW (2003) The structure of a Bcl-xL/Bim fragment complex: implications for Bim function. *Immunity* **19**, 341–352.

43 Kvansakul M and Hinds MG (2015) The Bcl-2 family: structures, interactions and targets for drug discovery. *Apoptosis* **20**, 136–150.

44 Sattler M, Liang H, Nettesheim D, Meadows RP, Harlan JE, Eberstadt M, Yoon HS, Shuker SB, Chang BS, Minn AJ *et al.* (1997) Structure of Bcl-xL-Bak peptide complex: recognition between regulators of apoptosis. *Science* **275**, 983–986.

45 Czabotar PE, Lee EF, Thompson GV, Wardak AZ, Fairlie WD and Colman PM (2011) Mutation to Bax beyond the BH3 domain disrupts interactions with pro-survival proteins and promotes apoptosis. *J Biol Chem* **286**, 7123–7131.

46 Marshall B, Puthalakath H, Caria S, Chugh S, Doerflinger M, Colman PM and Kvansakul M (2015) Variola virus F1L is a Bcl-2-like protein that unlike its vaccinia virus counterpart inhibits apoptosis independent of Bim. *Cell Death Dis* **6**, e1680.

47 Suzuki M, Youle RJ and Tjandra N (2000) Structure of Bax: coregulation of dimer formation and intracellular localization. *Cell* **103**, 645–654.

48 Hinds MG, Smits C, Fredericks-Short R, Risk JM, Bailey M, Huang DC and Day CL (2007) Bim, Bad and Bmf: intrinsically unstructured BH3-only proteins that undergo a localized conformational change upon binding to prosurvival Bcl-2 targets. *Cell Death Differ* **14**, 128–136.

49 Anasir MI, Baxter AA, Poon IKH, Hulett MD and Kvansakul M (2017) Structural and functional insight into canarypox virus CNP058 mediated regulation of apoptosis. *Viruses* **9**, 305.

50 Campbell S, Thibault J, Mehta N, Colman PM, Barry M and Kvansakul M (2014) Structural insight into BH3 domain binding of vaccinia virus antiapoptotic F1L. *J Virol* **88**, 8667–8677.

51 Goldmacher VS, Bartle LM, Skaletskaya A, Dionne CA, Kedersha NL, Vater CA, Han JW, Lutz RJ, Watanabe S, Cahir McFarland ED *et al.* (1999) A cytomegalovirus-encoded mitochondria-localized inhibitor of apoptosis structurally unrelated to Bcl-2. *Proc Natl Acad Sci USA* **96**, 12536–12541.

52 Ma J, Edlich F, Bermejo GA, Norris KL, Youle RJ and Tjandra N (2012) Structural mechanism of Bax inhibition by cytomegalovirus protein vMIA. *Proc Natl Acad Sci USA* **109**, 20901–20906.

53 Arnoult D, Skaletskaya A, Estaquier J, Dufour C and Goldmacher VS (2008) The murine cytomegalovirus cell death suppressor m38.5 binds Bax and blocks Bax-mediated mitochondrial outer membrane permeabilization. *Apoptosis* **13**, 1100–1110.

54 Manzur M, Fleming P, Huang DC, Degli-Esposti MA and Andoniou CE (2009) Virally mediated inhibition of Bax in leukocytes promotes dissemination of murine cytomegalovirus. *Cell Death Differ* **16**, 312–320.

55 Cam M, Handke W, Picard-Maureau M and Brune W (2010) Cytomegaloviruses inhibit Bak- and Bax-mediated apoptosis with two separate viral proteins. *Cell Death Differ* **17**, 655–665.

56 Fleming P, Kvansakul M, Voigt V, Kile BT, Kluck RM, Huang DC, Degli-Esposti MA and Andoniou CE (2013) MCMV-mediated inhibition of the pro-apoptotic Bak protein is required for optimal *in vivo* replication. *PLoS Pathog* **9**, e1003192.

57 Oberstein A, Jeffrey PD and Shi Y (2007) Crystal structure of the Bcl-XL-Beclin 1 peptide complex: Beclin 1 is a novel BH3-only protein. *J Biol Chem* **282**, 13123–13132.

Chapter 5

Concluding Remarks and Future Directions

Apoptosis is a powerful defence mechanism utilized by higher organisms against invading pathogens such as viruses (152). However, viruses have evolved impressive strategies to hijack host cell suicide mechanisms to secure successful infection, subsequent replication and survival (50, 153). Several large DNA viruses encode Bcl-2 like genes that have been shown to be vital virulence factors during early stage infection to counteract the host intrinsic apoptotic pathway and prevent premature cell death (50). Gene knockout studies have shown that a failure to express viral Bcl-2 homologues during early infection permits the host cell to undergo apoptosis, for example, deletion of *f1l* in vaccinia virus (90) or *m11l* in myxoma virus (102) allows host cell apoptosis to proceed.

Remarkably, these viral Bcl-2 proteins may be highly sequence divergent from their host counterpart Bcl-2 homologues with no obvious shared sequence identity, including the BH motifs, while other viral Bcl-2 homologues share these motifs. The common feature of these viral Bcl-2 proteins is that they are structurally conserved. Generally, the shared sequence identity between viral Bcl-2 proteins and human Bcl-x_L is significantly low and varies between 5-20 %. Examples of viral Bcl-2 homologs that have BH motifs include those from adenovirus E1B19K (39), EBV BHRF1 (40), ASFV A179L (47) and FPV039 (112). More sequence divergent Bcl-2 homologues include most poxvirus encoded Bcl-2 proteins, which do not have recognizable BH motifs such as myxoma virus M11L (33), vaccinia virus F1L (34), sheeppox virus SPPV14 (109) and deerpox virus DPV022 (57). Though these divergent Bcl-2 proteins share approximately the same amount of sequence identity when aligned with human Bcl-x_L, they do not bear obvious BH motifs.

The main focus of this thesis has been the structural and biochemical characterization of poxvirus encoded Bcl-2 like proteins. This field of study was initiated more than two decades ago when Han et al. investigated EBV BHRF1 (39) and is still

continuing to uncover important aspects related to these proteins. Specifically, their functions during viral infection and mechanism of action. While most pox virus encoded Bcl-2 proteins do not show any detectable sequence identity with their host counterparts they share the Bcl-2 fold (33, 34). For instance, this structural similarity can be
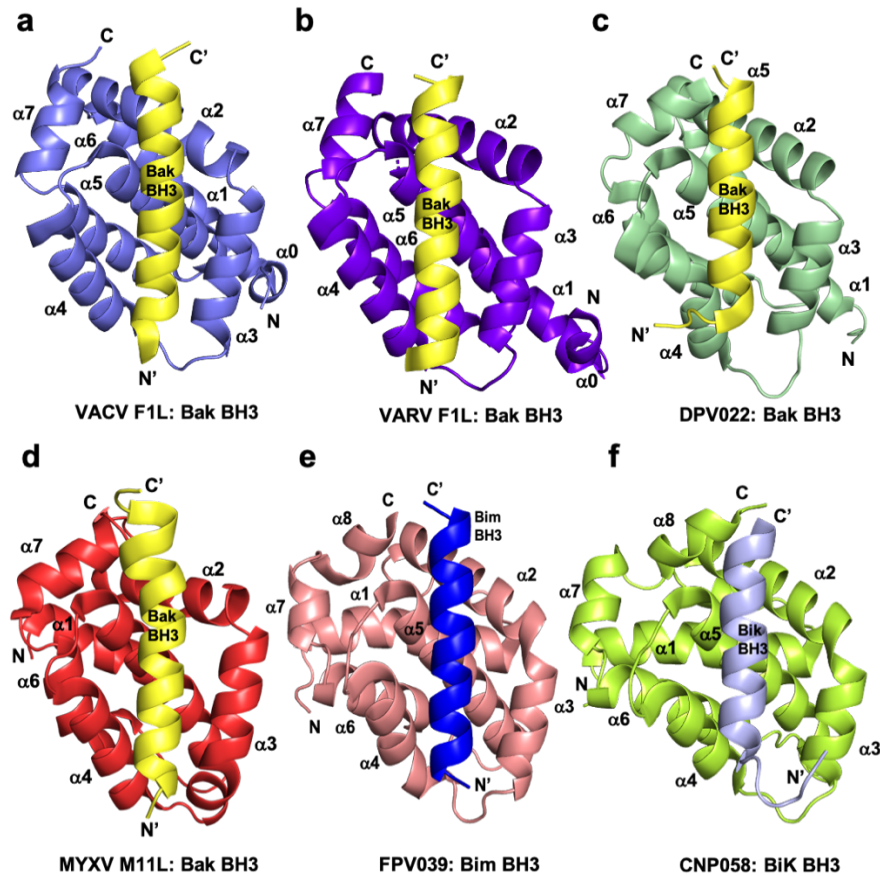
Figure 1: Cartoon representation of previously characterized poxviral encoded Bcl-2 proteins. a) ribbon diagram of VACV F1L (slate): Bak BH3 (tv_yellow) in view of hydrophobic ligand binding groove made by α2-α5. b) ribbon diagram of VARV F1L (purple blue): Bak BH3 (tv_yellow), c) DPV022 (wheat)in complex with Bak BH3 (tv_yellow), d) MYXV M11L (tv_red): Bak BH3 (tv_yellow) complex, e) FPV039 (salmon): Bim BH3 (blue) complex and f) CNP058 (limon): Bik BH3 (light blue) complex. The N and C termini of the Bcl-2 protein are labelled N and C and the ligand N' and C' respectively.

seen with the previously characterized vaccinia and variola virus F1L (34), deerpox virus DPV022 (57), myxoma virus M11L (33) FPV039 and CNP058 (112, 113) and these structures are depicted in Figure 1. The structures of Bcl-2 complexes with their ligands

depicted in Figure 1 show the structural similarity of both the Bcl-2 protein and mechanism of engagement with the ligand in the canonical binding groove. While these studies have provided valuable and detailed insight into the mechanisms by which certain viruses modulate Bcl-2 regulated apoptosis, there is little information on the structural and functional relationships of poxvirus Bcl-2 like genes of tanapox virus 16L (TANV16L), monkeypox virus C7L (MPXV C7L) or sheeppox virus SPPV14, which are emerging zoonotic diseases with a potential impact on public health (62).

In this thesis I characterized the structure-activity relationship of TANV16L, MPXV C7L and SPPV14 in relation to their possible mechanisms of host immune modulation by using a combination of structural, biophysical, biochemical approaches employing X-ray crystallography, Isothermal Titration Calorimetry (ITC) and protein functional assays.

5.1   Tanapox virus

5.1.1   TANV16L is a poxviral Bcl-2 protein encoded by Tanapox virus

TANV16L is a recently identified putative viral Bcl-2 (vBcl-2) protein encoded by Tanapox virus and the first characterized intrinsic apoptosis inhibitor from the *Yatapoxvirus* family (103). TANV16L lacks detectable sequence identity with its cellular counterparts. For example, sequence identity of TANV16L into cellular Bcl-x_L or Bcl-2 are 8.6% and 13.2%. however, when TANV16L is expressed in a yeast model system it protects against apoptosis induced by human Bax and Bak in a cell death assay (103). To evaluate the underlying molecular mechanism of TANV16L mediated host cell death inhibition, we systematically performed a series of binding assays between TANV16L and BH3 motif peptides derived from human pro-apoptotic proteins. Using ITC, I showed that TANV16L engaged a broad spectrum of pro-apoptotic BH3 proteins with a wide range of

affinities from the nanomolar to sub micromolar range but did not bind either Noxa or Bok (103).

With the BH3-motif peptides from the determined interactors of TANV16L, I crystallized and solved the structures of three complexes of TANV16L with Bax, Bim and Puma BH3 motifs. The first structure of TANV16L in complex with Bax BH3 peptide, TANV16L:BaxBH3, was solved by molecular replacement using the previously solved structure of deerpox virus DPV022 (57) as a search model. Likewise, the TANV16L:BimBH3 and TANV16L:PumaBH3 were solved by molecular replacement using TANV16L: Bax BH3 as a search model. TANV16L:BaxBH3 and TANV16L:BimBH3 complexes exist as domain swapped dimers in crystal structure and adopt the Bcl-2 fold similar to that observed previously in vaccinia and variola virus F1L and DPV022 (34, 57), where these dimers have very limited and weak binding BH3-peptide profiles. Surprisingly, the TANV16L: Puma complex exists as a monomer in crystal structure, and the structure showed the α1 helix of the dimer interface in TANV16L:BaxBH3 and TANV16L:BimBH3 is folded back into its globular core. However, TANV16L dimerization does not change the local fold of the canonical ligand binding groove (103). I examined the monomer-dimer equilibrium using analytical ultracentrifugation and found that *apo*-TANV16L also exists in a homotetrameric species in solution but with low abundance (Paper 1 (103), chapter 2). Homotetrameric Bcl-2 species have not been previously reported for Bcl-2 proteins.

To further investigate the BH3-peptide binding profile of TANV16L and evaluate the significance of local residues at the binding site I also measured the binding affinity of BH3 peptides against TANV16L mutants, R90A and K52A. These two specific mutants were selected based on their significance to make interactions with BH3 motif peptide. TANV16L R90A substantially lost affinity for BH3-peptides with a 10-80-fold reduction

for Bim, Bid, Bik, Bad as well as Bax and Bak BH3 peptides, while affinity for Puma and Hrk BH3 motifs showed an approximately 2-fold reduction. Although the TANV16L mutant K52A did not show significant loss of affinity for most of its interactors, its affinity for Bmf and Bad BH3 peptides was reduced by 20 and 27-fold respectively (Paper 1 (103), chapter 2).

I conclude from this work that the likely mechanism of TANV16L action is via the blockade of the mammalian host apoptosis pathway through sequestration of cellular Bak and Bax in addition to the BH3-only protein Bim. Intriguingly, TANV16L appears to be able to bind BH3-peptides as either a monomer or a domain swapped dimer. The crystal structure of TANV16L shows it exists in globular monomeric form in the case of the Puma BH3 complex, with the Puma BH3 peptide in the canonical groove. However, in the BaxBH3 complex TANV16L exists as a domain swapped dimer. Where the $\alpha 1$ helix of a one protomer is swapped with the $\alpha 1$ helix of neighbouring protomer (34). Thus, multiple forms of TANV16L are able to engage BH3-peptides with high affinity.

5.1.2 Future directions for the tanapox virus 16L project

Further experiments are required to be performed to confirm the effect of apoptosis inhibition by TANV16L *in-vivo*. Also, gene knockout experiments would be beneficial to analyse the virulence of TANV16L mediated apoptosis inhibition. Poxviral Bcl-2 proteins have been shown to be involved in targeting other cell death inhibitory pathways, such as NF-κB signalling (71) and caspase 9 inhibition (154). Further functional assays are required to evaluate the effect of 16L on those pathways and there is no structural data to describe the molecular interactions. In addition, TANV16L was shown to interact with Bad BH3 peptide with moderate affinity (103). It was previously reported that ABT737 is a peptido mimetic drug which successfully mimics the action of the BH3-only protein Bad

and selectively interacts with the cellular pro-survival Bcl-2 proteins Bcl-2, Bcl-x_L and Bcl-w with very high affinity (155) to alter the cell death mechanism inhibited by those proteins. Currently there is no vaccine or drug that can target tanapox virus infection in humans and the potential exits that ABT737 will target TANV16L. Such an interaction between TANV16L and ABT737 could make it a potential drug against tanapox virus.

5.2 Monkeypox Virus

5.2.1 MPXV C7L is a novel viral Bcl-2 protein encoded by Monkeypox virus

Monkeypox virus (MPXV) encoded C7L is a hypothetical viral Bcl-2 protein, that shares little sequence identity with cellular Bcl-2 proteins. Whereas, MPXV C7L has well conserved sequence identity (>85%) to vaccinia virus F1L or variola virus F1L (34);(35), the well-known Bcl-2 homologues of the poxvirus family. Unlike vaccinia or variola virus F1L, there is little information about how MPXV C7L mediates apoptosis. To address this question, I systematically investigated the MPXV C7L ability to interact with BH3 motif peptides from human pro-apoptotic Bcl-2 proteins. Interestingly, MPXV C7L shows a broad range of affinities towards BH3 motif peptides, including very strong affinity to Bax (22 nM), moderate affinity to Bim (131 nM), Bak (401 nM), Bid (560 nM), Bik (930 nM), low affinity to Hrk (1286 nM), Bok (1370 nM), and Puma (2605 nM) and it did not bind to either Bad or Noxa BH3 peptides. In contrast, vaccinia virus (VACV) or variola virus (VARV) F1L only showed very weak and restricted binding affinity towards pro-apoptotic BH3-motif peptides and were able to bind only three BH3 peptides. VACV F1L was able to bind Bak, Bax or Bim (34) and VARV F1L bound only for Bak, Bax or Bid (35). However, sequence alignment of MPXV C7L with VACV F1L shows that, there are six substitutions located in helices that comprise the canonical ligand binding groove of VACV F1L that differ from those in MPXV C7L, including $I95_{F1L}$ to $T93_{C7L}$, $S101_{F1L}$ to

N99$_{C7L}$, 106R$_{F1L}$ to S104$_{C7L}$, Y112$_{F1L}$ to 110C$_{C7L}$, 118K$_{F1L}$ to 116E$_{C7L}$ and D131$_{F1L}$ to N133$_{C7L}$ (Chapter 3, page 5 , Figure 1b). Interestingly, these residues of VACV F1L or MPXV C7L are not involved in making close contacts with BH3 motif peptides, and face away from the binding groove. Notably, MPXV C7L residue D105 forms an ionic interaction with BH3 motif peptide, which is not seen in VACV F1L or VARV F1L complexes with BH3 motif peptides. The variation of the binding profiles of VACV F1L, VARV F1L and MPXV C7L may suggest the differential molecular mechanism acquired by pox viruses to subvert host premature cell death during infection, even though these three evolutionarily related proteins share near identical sequences, with shared sequence identities between MPXV C7L and VACV F1L or VARV F1L being 85% and 78% respectively.

With the BH3 interactors of MPXV C7L characterized, I turned to determining their crystal structures, and solved two complexes of MPXV C7L with its tightest interactors Bax and Bim BH3 peptides. The MPXV C7L: BaxBH3 complex was solved by molecular replacement using the previously determined VACV F1L structure (34) as a search model and MPXV C7L: Bim BH3 was solved by using previously solved MPXV C7L: Bax BH3 as a search model. As expected, MPXV C7L exists as a domain swapped dimer where α1 helix of one protomer exchanged with α1 helix of a neighbouring protomer and features a Bcl-2 fold with 7 α-helices where the α2-α5 helices form the canonical ligand binding groove. This structure resembles those of poxvirus encoded Bcl-2 proteins such as VACV F1L (34), VARV F1L (35), TANV16L and DPV022 (57).

A structural comparison of MPXV C7L with each of the domain swapped of VACV F1L, VARV F1L, TANV16L and DPV022 dimers was performed by generating superimpositions of MPXV C7L with individual proteins. Interestingly, all structures showed a near identical fold with MPXV C7L. Variola virus F1L and Vaccinia virus F1L

superimpositions over the Cα backbone yielded Root Mean Square Deviations (RMSDs) of 0.44 Å and 0.50 Å over 135 and 136 Cα atoms, respectively. Similarly, deerpox virus DPV022 showed a RMSD of 2.2 Å over 117 Cα atoms and Tanapox virus TANV16L domain swapped dimer aligned with an RMSD of 2.1 Å over 92 Cα atoms, whilst TANV16L monomeric form yield RMSD 1.4 Å over 92 Cα atoms. These RMSD values demonstrate the structural similarity between all of these vBcl-2 proteins but there is some variation in the structures.

In summary, my data suggest that like TANV16L, MPXV C7L primarily inhibits host cell apoptosis via direct interactions with cellular mitochondrial apoptosis mediators Bak and Bax and BH3-only protein Bim. All of these MPXV:BH3 peptide complexes are structurally conserved. Furthermore, I was able to perform the structural and functional analysis of MPXV C7L, a Bcl-2 homologue that showed a broad binding profile for peptides spanning BH3 motifs of cellular pro-death Bcl-2 proteins. The result of these studies provides structural insight to MPXV C7L modulated cell death inhibition in the human host (paper 2 [103], Chapter 2).

5.2.2 Future directions for the monkeypox virus C7L project

My analysis of MPXV C7L inhibition of apoptosis focussed on biochemical and structural aspects, however it is important to analyse those interactions in an *in vivo* setting. Consequently, the results of cell-based apoptosis assays using C7L would be very interesting. Also, structure guided site-directed mutagenesis of important interactions of MPXV C7L with BH3 ligands should be performed, and these data could then be validated in cell-based apoptosis assays. Examining interactions of those mutants in both *in-vitro* and *in-vivo* context could then form the basis for defining a detailed mechanism underlying

MPXV C7L apoptosis inhibition and may potentially aid drug discovery for this emergent virus.

5.3   Sheeppox virus

5.3.1   SPPV14 is a poxviral Bcl-2 protein encoded by sheeppox virus

SPPV14 is encoded by sheeppox virus and it has been shown to protect cells from multiple apoptotic signals (109). Initially, SPPV14 was identified as an M11L ortholog that could potentially inhibit apoptosis in a Bcl-2 proteins dependent manner (109). Despite the poor sequence similarity of SPPV14 with cellular Bcl-2 proteins, it has been shown to engage directly with cellular Bak and Bax as well as BH3 only protein Bim, Bid, Puma, Hrk and Bmf to down regulate the host intrinsic apoptotic pathway (109).

To investigate the binding specificity of a complete set of BH3 peptides derived from human pro-apoptotic Bcl-2 proteins towards SPPV14, I performed ITC using recombinant protein SPPV14 (1-145) a protein that lacks 31 residues at C terminus, and purified it as previously described (109). In addition to the previously reported tight BH3 interactors (Bak, Bax, Bim, Bid, Puma, Hrk) of SPPV14 (109), I observed additional weak BH3 interactions with Bad, Bok and Bik, which bind SPPV14 with sub micromolar affinities (Figure 3b)(108).

To understand the detailed molecular basis of SPPV14 modulated apoptosis I crystallized two complexes of SPPV14 bound to BH3 peptides, those of Bax and Hrk. The SPPV14: Hrk BH3 structure was solved using a model suggested by the Balbes molecular replacement programme (156). The SPPV14: Bax BH3 complex was solved by molecular replacement using SPPV14: Hrk as a search model. The crystal structure of SPPV14 revealed it to be a monomer with the conserved globular Bcl-2 fold consisting of 7 α-helices and $\alpha2$-$\alpha5$ forming the canonical ligand binding groove. Surprisingly, a salt bridge

interaction made by Arg84 $_{SPPV14}$ at the beginning of $\alpha 5$ helix and Asp in the BH3 motif peptide replaces the canonical ionic interaction between a conserved Arg in the BH1 motif and the Asp of the BH3 motif ligand (108) (Chapter 3, Figure 5a), an interaction seen in almost all mammalian Bcl-2: BH3 complexes (4). Superimposition of SPPV14: Hrk BH3 with M11L: Bak BH3 backbone yielded a near-identical structure with an RMSD of 1.8 Å over the complete SPPV14 chain.

Site directed mutagenesis was performed to validate the SPPV14 structure and its interactions with BH3 motif peptides and affinity measurements recorded for two SPPV14 mutants, R84A and Y46A, in which R84 and Y46 formed the ionic and hydrogen bond interactions with BH3 motif peptide, respectively. Among those two mutants, Y46A significantly reduced its binding affinity to Bak, Bax, Puma, Bmf, Hrk and Bim BH3 peptides and decreased the interaction with Bid, Bik, Bok and Bad BH3 peptides. In contrast, R84A lost the interaction only for Bok BH3 and showed reduced affinity for the other BH3 interactors, but the reduction in affinities where not as large as those observed for the mutant Y46A (108). This result suggests that SPPV14 Y46 plays an important role in inhibiting host cell apoptosis during sheeppox virus infection.

5.3.2 Future directions for the sheeppox virus SPPV14 project

The characterisation of affinity measurements and acquisition of crystal structure of SPPV14 is a key element in the analysis of SPPV14 function as an anti-apoptotic protein. Sheeppox virus infection is emerging transboundary disease that results in huge economic loss in the sheep industry (157). Unlike TANV16L or MPXV C7L, SPPV14 was shown to exist as a monomer in solution (108). However, SPPV14 is able to directly interact with cellular human Bak and Bax with high affinity similar to TANV16L or MPXV C7L (108, 109) and potentially able to block host mitochondrial apoptosis. To address these

similarities and differences, more experiments are required to be performed under *in vivo* conditions. Similar to TANV16L, SPPV14 is also able to interact with Bad BH3 peptide and further experiments are needed to characterise interactions between SPPV14 and the BH3 mimetic drug ABT737.

5.4   Comparison of poxvirus Bcl-2 proteins

5.4.1   Poxvirus Bcl-2 proteins lack conserved BH motifs

Bcl-2 family proteins can be recognized by the presence of at least one out of four short conserved regions of sequence known as Bcl-2 homology (BH) motifs. These BH motifs are structurally and functionally important to regulate the intrinsic apoptotic pathway (4, 158). The cellular pro-survival Bcl-2 proteins feature to up to four BH (BH1-BH4) motifs in their sequences. These conserved BH motifs, BH1-BH4, approximately align with secondary structural elements and can be seen in $\alpha 1$ (BH4), $\alpha 7$ (BH2), $\alpha 2$ (BH3) and $\alpha 5$ (BH1) helices of Bcl-2 proteins and contribute to the BH3-binding groove $\alpha 2$-$\alpha 5$ (Figure 2a) (15, 158). The BH1 motif plays a crucial structural role during cell death inhibition and can be easily recognized by a short well conserved signature sequence motif "NWGR". The Gly (G) and Arg (R), residues of 'NWGR" motif are important for protein-protein interactions within the Bcl-2 family proteins (159, 160) (Figure 2b). The Arg residue is usually located at the beginning of the core $\alpha 5$ helix of the Bcl-2 protein and forms the canonical ionic/ salt bridge interaction with the conserved Asp (D) residue of BH3 motif of the pro-apoptotic Bcl-2 proteins. This ionic interaction can be seen in almost all cellular Bcl-2: BH3 interactions (4) and the Gly is involved in making a hydrogen bond interaction with BH3 motif peptides of cellular pro-apoptotic Bcl-2 proteins (159, 160).

As discussed above poxvirus encoded Bcl-2 proteins often do not bear recognizable BH motifs in their sequences (Figure 2c), though they have closely related structures

(Figure 1) (9) (50). Fowlpox virus FPV039 (112) and canarypox virus CNP058 (113) bear BH1 signature motifs as a "NWGR" in FPV039 and "TWGR" in CNP058 and form the conserved salt bridge interaction as explained above (Figure 2b) (112, 113). Despite lacking the characteristic BH1 "NWGR" motif in poxvirus encoded Bcl-2 proteins, TANV16L (R90) "NDNR" (103), SPPV14 (R84) "INSR" (108) and DPV022 (R87) "IDSR" (57) have a conserved Arg residue at the start of the α5 helix and form an ionic interaction with the conserved Asp residue of the BH3 motif peptide (Figure 2b). The ionic interaction in SPPV14 is made by SPPV14 (R84) and replaces the canonical interaction
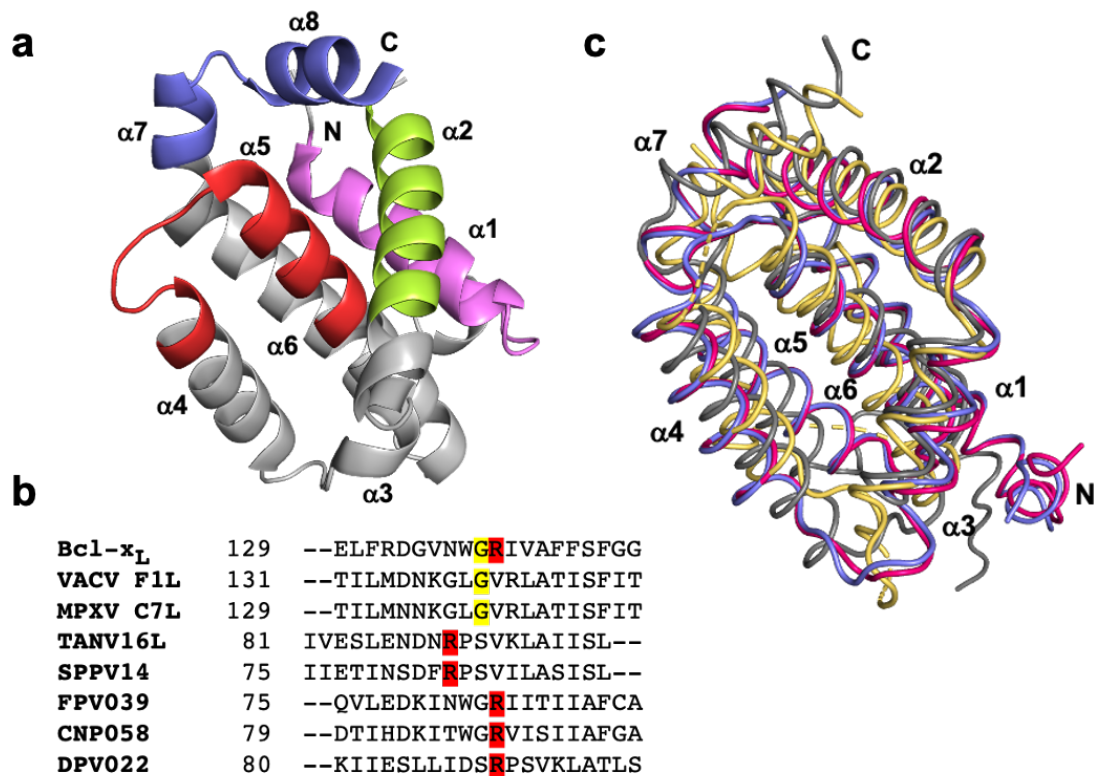
Figure 2: a) cartoon representation of Bcl-x$_L$ (grey 80) (PDB 4QVF) with conserved BH1-BH4 motifs are coloured as red, magenta, green and light blue and helices are labelled as α1-α8. b) sequence alignment of BH1 motifs sequences of Bcl-x$_L$, VACV F1L, MPXV C7L, TANV 16L, SPPV14, FPV039, CNP058 and DPV022. Arg residues involved the salt bridge interactions with BH3 motif peptides are shown in red and the conserved Gly residue of BH1 motif is highlighted in yellow. c) structural alignment of MPXV C7L (hot pink), VACV F1L (slate), TANV16L (grey 50) and SPPV14 (olive) as view into the hydrophobic binding groove formed by α2-α5.

(108) seen in other Bcl-2:BH3 complexes. In contrast, vaccinia and variola virus F1L or monkeypox virus C7L are unable to make the canonical ionic interaction with BH3 motif of pro-apoptotic Bcl-2 protein (35, 49) as these proteins lack the Arg residue in an appropriate position. Structure based sequence alignment analysis of vaccinia and variola virus F1L or monkeypox virus C7L with prototypical cellular Bcl-2 protein Bcl-x$_L$ shows that these three poxviral Bcl-2 proteins lack the BH1 "NWGR" motif which is replaced by the sequence "GLGV" motif at the N-terminal end of the α5 helix where the BH1 Gly is conserved but the BH1 Arg is replaced by a Val residue (Figure 2b). However, the conserved second Gly of the GLGV motif maintains the hydrogen bonding interactions with the BH3 motif of pro-death Bcl-2 proteins as in the NWGR motif (35, 49). This has led to the suggestion that the Gly in this region plays an important role in structure and interaction of Bcl-2 proteins (159, 160). Even though, most of poxviral encoded Bcl-2 proteins lack conserved BH motifs, their molecular surface still forms the extended hydrophobic ligand binding groove constructed by the α2-α5 helices, that can be seen in all pro-survival Bcl-2 proteins (Figure 2c).

5.4.2 Poxvirus Bcl-2 proteins can be classified into two structural folds

The three different poxvirus Bcl-2 structures, TANV16L, MPXV C7L and SPPV14 are discussed in this thesis. The determination of these structures has enhanced our understanding of the structural diversity of poxvirus Bcl-2 homologues central to their pro-survival action. I observed a range of behaviours for poxviral Bcl-2 proteins. Sheeppox SPPV14 exist as a monomer (108), Monkeypox MPXV C7L exist as a dimer in solution, which were confirmed by size-exclusion chromatography and Tanapox TANV16L exist as both monomeric and dimeric configuration in crystal structure (103). The combination of my findings presented in this thesis with all other available poxvirus Bcl-2 proteins

structures, I propose that, poxvirus Bcl-2 proteins can be divided into two structural sub-classes:

1. The monomeric proteins that feature conserved Bcl-2 fold and showed high binding affinities for numerous BH3 ligands.

2. The domain swapped dimeric proteins that have comparatively low affinity and high selectivity for BH3 ligands.

According to this classification, the most noticeable features are, restricted BH3 ligand binding profile and weak binding affinities of dimeric poxvirus Bcl-2 proteins. For instance, VACV F1L and DPV022 only interacts with Bak, Bax and Bim with relatively low affinities (34, 57). whereas MPXV C7L show extended BH3 binding profile, even though it forms a dimer in solution. Consistently, these viral Bcl-2 proteins antagonize Bak, Bax and Bim. This would suggest that, interactions with Bak, Bax and Bim are sufficiently block host cell apoptosis for viral replication. However, many questions remain to be answered, for instance, why do poxvirus Bcl-2 proteins exist as monomeric and dimeric forms and what would be the advantage of being a dimer compared to monomer? This may be due to weaker affinities of dimeric poxviral proteins, which could lead to lower virulence compared to monomeric poxviral Bcl-2 proteins.

5.4.3 Poxvirus encoded Bcl-2 proteins do not interact with BH3-only protein Noxa

Cellular Bak and Bax are the key regulators of MOMP activated by BH3-only proteins (161). It has been reported that, BH3-only proteins Bim and Noxa play a vital role during viral infections to activate apoptosis (162). Bim is activated by endoplasmic reticulum (ER) stress, cytokine deprivation (163) or in response to viral infection (164) and Noxa is upregulated through NF-κB activation during accumulation of double stranded RNA (dsRNA) in viral infected cells (165). A previous study reported that a vaccinia virus Bcl-

2 inhibitor F1L deficient mutant largely protected cells from apoptosis in the absence of Noxa, whilst showing only a minor effect in the absence of Bim. Thus, loss of both Noxa and Bim in macrophages showed very strong protection against apoptosis (162). This suggested that Noxa is not a necessary BH3-only protein to inhibit during pox viral infection.

Bim acts as a promiscuous high affinity BH3 interactor, with the exception of variola virus F1L which does not interact with Bim, during viral infections (35). Noxa only binds FPV039 with high affinity (28 nM) (112) and has weaker interactions with CNP058 (3284 nM) (113) or M11L (>1000 nM) (33) and does not bind to any of the dimeric poxvirus Bcl-2 proteins. It was reported that, orf virus encoded Bcl-2 protein ORFV125 interacts with Noxa in immunoprecipitation experiment (106) however, affinity measurements were not reported.

Combined, these data may suggest that, cellular BH3 only protein Bim plays a crucial role in the action of pox virus encoded Bcl-2 proteins and the activation of intrinsic apoptosis. From the poxvirus point of view, targeting Bim for inactivation by virally encoded Bcl-2 proteins would be the first priority and inactivation of Bak and Bax would provide the added advantage of blocking host mitochondria mediated apoptosis as these proteins are necessary and probably the most important activators of apoptosis (166). Bim acts as a universal initiator of apoptosis in cellular Bcl-2 proteins (51) and interacts with almost all poxviral Bcl-2 proteins except VARV F1L (35) and logically would be a viral target to inhibit apoptosis. In contrast to Bim inhibition, the inhibition of Noxa appears to be relatively unimportant for viral suppression of apoptosis. The ability of viral Bcl-2 proteins to interact with BH3-only proteins other than Bim probably enhances their importance as virulence factors, but may not be their key function (50).

5.4.4 Summary and Overview of Poxvirus Bcl-2 subversion of host intrinsic apoptosis

Our current effort is focussed on understanding detailed molecular mechanism underlying poxvirus encoded Bcl-2 mediated cell death inhibition in host. To address this question, I used a combination of *in-vitro* and *in-vivo* characterization techniques using biochemical interactions and structural biology to support my hypothesis that sequestration of BH3-only proteins is a key function of viral Bcl-2 proteins, and in particular the most potent BH3-only protein Bim. By combining my findings with previous data from other researchers in the field of poxvirus Bcl-2 proteins I am able to describe the potential mechanism of action of poxvirus Bcl-2 mediated host immune evasion during infection. To date numerous poxvirus Bcl-2 proteins have been characterized that regulate host apoptosis (33, 34, 103, 109). The majority of these Bcl-2 like proteins subvert host intrinsic apoptosis, while others may regulate caspase 9 inhibition (154), NF-κB (71) and inflammasome signalling (95). However, affinity measurements and structural data for these alternative interactions have never been reported.

Based on my experimental findings and previous literature, I suggest that almost all poxviral encoded Bcl-2 proteins primarily act by sequestering the cellular BH3-only protein Bim to block the host intrinsic apoptosis by preventing subsequent activation of mitochondrial membrane permeabilization regulators Bak and Bax, or direct inactivation of cellular Bak and Bax. Figure 3 depicts possible mechanisms of action of viral Bcl-2 proteins. In the event of viral infection host apoptosis mechanism activated through BH3-only proteins and downstream activation depends on the interactions between pro-survival Bcl-2 proteins and pro-apoptotic Bcl-2 proteins (Figure 3). However, when virus starts to express and secrete vBcl-2 proteins, they are initiating the interactions with cellular BH3-only proteins and pro-apoptotic Bak and Bax to neutralize their activity. Primarily, vBcl-

2 binds the pro-apoptotic molecules Bax and Bim and therefore prevents apoptosis (Figure 3).
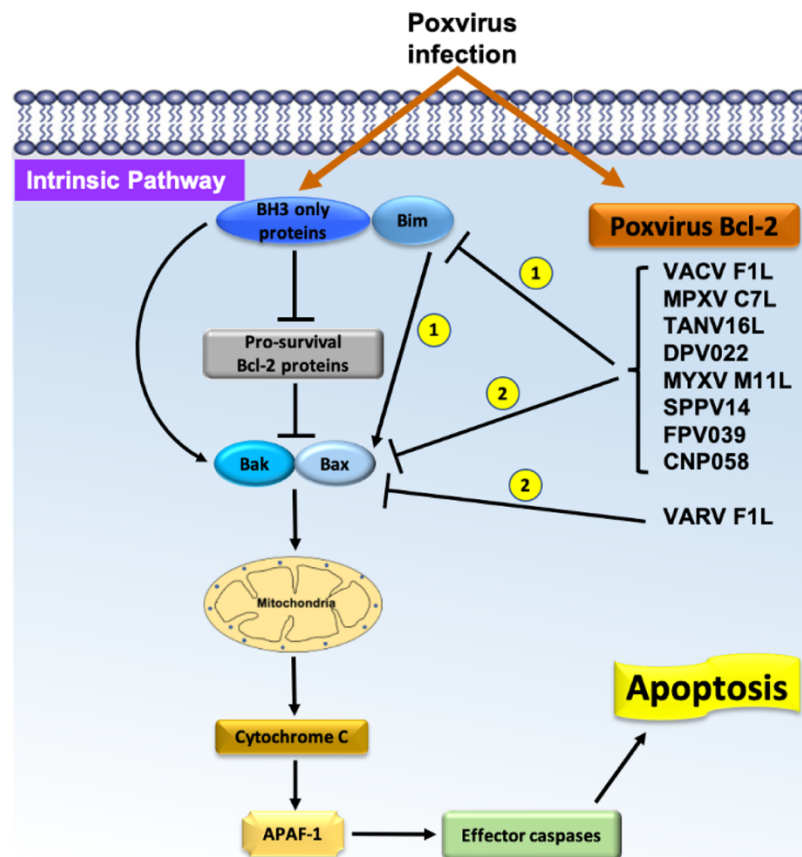

Figure 3: Schematic diagram summarizing the key steps involving the use of poxvirus encoded inhibitiors of the intrinsic apoptosis pathway. Mammalian intrinsic apoptosis is initiated when BH3-only proteins neutralize the cellular pro-survival Bcl-2 proteins and activate the pro-apoptotic Bcl-2 proteins Bak and Bax to oligomerize and form pores in the mitochondrial outer membrane. Release of cytochrome c from mitochondria activates cellular APAF-1 and subsequent activation of effector caspases and leads to cell death. Pox virus encoded Bcl-2 proteins downregulate this mechanism either by 1) interaction with BH3-only protein Bim and downregulate the subsequent Bak and Bax activation through their inhibition by cellular Bcl-2 proteins or 2) direct interactions with Bak and Bax and inhibit the downstream activation of mitochondrial apoptosis. All poxvirus Bcl-2 proteins primarily inhibit intrinsic apoptosis using either or both mechanism 1 and 2 with the possible exception of VARV F1L, that directly inhibits cellular Bak and Bax only.

Structural and biochemical analysis of TANV16L (103), MPXV C7L and SPPV14 (108, 109) revealed that all three potentially inhibit host apoptosis initiation pathways by direct interactions with cellular Bak, Bax and Bim. Each of these proteins has a conserved Bcl-2 fold, despite the lack of conserved sequence features with the host proteins such as

the BH1-BH4 motifs. Furthermore, based on their structures poxvirus Bcl-2 proteins can be classified into two subgroups those that have a monomeric Bcl-2 fold or those that have a domain swapped dimeric Bcl-2 fold, where $\alpha 1$ helix of one protomer subunit is swapped with the $\alpha 1$ helix of neighbouring subunit (34). The variation of folding of these three poxviruses Bcl-2 proteins shows their structural plasticity and ability to mimic the crucial interactions from endogenous host apoptosis Bcl-2 proteins to empower the successful infection and proliferation in the host cell.

Developing a better knowledge and understanding of the molecular basis of poxvirus mediated host immune evasion is vital as poxviruses are emerging human pathogens that threaten public health, and furthermore pox viruses have also been proposed as oncolytic viruses as well as vaccine vectors (167-169). Also, understanding the molecular basis of the interactions of viral Bcl-2 proteins gives us the potential to design drugs that modulate the apoptotic response as potential new antiviral strategies. However, being the largest group of pathogenic viruses together with their extensive genomes, makes it likely that many more virally encoded cell death inhibitors may be discovered in the future, which may act using novel modes of action.

Bibliography

1.   Strasser A, Vaux DL. Viewing BCL2 and cell death control from an evolutionary perspective. Cell Death Differ. 2018;25(1):13-20.
2.   Banjara S, Suraweera CD, Hinds MG, Kvansakul M. The Bcl-2 Family: Ancient Origins, Conserved Structures, and Divergent Mechanisms. Biomolecules. 2020;10(1).
3.   Youle RJ, Strasser A. The BCL-2 protein family: opposing activities that mediate cell death. Nature Reviews Molecular Cell Biology. 2008;9(1):47-59.
4.   Kvansakul M, Hinds MG. The Bcl-2 family: structures, interactions and targets for drug discovery. Apoptosis. 2015;20(2):136-50.
5.   Ashkenazi A. Targeting death and decoy receptors of the tumour-necrosis factor superfamily. Nature Reviews Cancer. 2002;2(6):420-30.
6.   Degterev A, Yuan J. Expansion and evolution of cell death programmes. Nature Reviews Molecular Cell Biology. 2008;9(5):378-90.
7.   Strasser A, Cory S, Adams JM. Deciphering the rules of programmed cell death to improve therapy of cancer and other diseases. Embo j. 2011;30(18):3667-83.
8.   Bugert JJ, Darai G. Poxvirus Homologues of Cellular Genes. In: Becker Y, Darai G, editors. Molecular Evolution of Viruses — Past and Present: Evolution of Viruses by Acquisition of Cellular RNA and DNA. Boston, MA: Springer US; 2000. p. 111-33.
9.   Nichols DB, De Martini W, Cottrell J. Poxviruses Utilize Multiple Strategies to Inhibit Apoptosis. Viruses. 2017;9(8):215.
10.   Caria S, Hinds MG, Kvansakul M. Structural insight into an evolutionarily ancient programmed cell death regulator - the crystal structure of marine sponge BHP2 bound to LB-Bak-2. Cell Death Dis. 2017;8(1):e2543.
11.   Garcia-Calvo M, Peterson EP, Leiting B, Ruel R, Nicholson DW, Thornberry NA. Inhibition of human caspases by peptide-based and macromolecular inhibitors. J Biol Chem. 1998;273(49):32608-13.
12.   Mariño G, Niso-Santano M, Baehrecke EH, Kroemer G. Self-consumption: the interplay of autophagy and apoptosis. Nature Reviews Molecular Cell Biology. 2014;15(2):81-94.
13.   Czabotar PE, Lessene G, Strasser A, Adams JM. Control of apoptosis by the BCL-2 protein family: implications for physiology and therapy. Nature Reviews Molecular Cell Biology. 2014;15(1):49-63.
14.   Vervliet T, Parys JB, Bultynck G. Bcl-2 proteins and calcium signaling: complexity beneath the surface. Oncogene. 2016;35(39):5079-92.
15.   Kvansakul M, Hinds MG. Structural biology of the Bcl-2 family and its mimicry by viral proteins. Cell Death & Disease. 2013;4(11):e909-e.
16.   Cartron P-F, Gallenne T, Bougras G, Gautier F, Manero F, Vusio P, et al. The First α Helix of Bax Plays a Necessary Role in Its Ligand-Induced Activation by the BH3-Only Proteins Bid and PUMA. Molecular Cell. 2004;16(5):807-18.
17.   Kim H, Rafiuddin-Shah M, Tu H-C, Jeffers JR, Zambetti GP, Hsieh JJD, et al. Hierarchical regulation of mitochondrion-dependent apoptosis by BCL-2 subfamilies. Nature Cell Biology. 2006;8(12):1348-58.
18.   Gallenne T, Gautier F, Oliver L, Hervouet E, Noël B, Hickman JA, et al. Bax activation by the BH3-only protein Puma promotes cell dependence on antiapoptotic Bcl-2 family members. Journal of Cell Biology. 2009;185(2):279-90.

19. Certo M, Moore VDG, Nishino M, Wei G, Korsmeyer S, Armstrong SA, et al. Mitochondria primed by death signals determine cellular addiction to antiapoptotic BCL-2 family members. Cancer Cell. 2006;9(5):351-65.

20. Jabbour AM, Heraud JE, Daunt CP, Kaufmann T, Sandow J, O'Reilly LA, et al. Puma indirectly activates Bax to cause apoptosis in the absence of Bid or Bim. Cell Death & Differentiation. 2009;16(4):555-63.

21. Hockings C, Anwari K, Ninnis RL, Brouwer J, O'Hely M, Evangelista M, et al. Bid chimeras indicate that most BH3-only proteins can directly activate Bak and Bax, and show no preference for Bak versus Bax. Cell death & disease. 2015;6(4):e1735-e.

22. Huang K, O'Neill KL, Li J, Zhou W, Han N, Pang X, et al. BH3-only proteins target BCL-xL/MCL-1, not BAX/BAK, to initiate apoptosis. Cell Res. 2019;29(11):942-52.

23. O'Neill KL, Huang K, Zhang J, Chen Y, Luo X. Inactivation of prosurvival Bcl-2 proteins activates Bax/Bak through the outer mitochondrial membrane. Genes Dev. 2016;30(8):973-88.

24. Adams JM. BAX and BAK become killers without a BH3 trigger. Cell Research. 2019;29(12):967-8.

25. Strasser A. The role of BH3-only proteins in the immune system. Nature Reviews Immunology. 2005;5(3):189-200.

26. Shamas-Din A, Brahmbhatt H, Leber B, Andrews DW. BH3-only proteins: Orchestrators of apoptosis. Biochimica et Biophysica Acta (BBA) - Molecular Cell Research. 2011;1813(4):508-20.

27. Breckenridge DG, Germain M, Mathai JP, Nguyen M, Shore GC. Regulation of apoptosis by endoplasmic reticulum pathways. Oncogene. 2003;22(53):8608-18.

28. Hsu Y-T, Wolter KG, Youle RJ. Cytosol-to-membrane redistribution of Bax and Bcl-X<sub>L</sub> during apoptosis. Proceedings of the National Academy of Sciences. 1997;94(8):3668.

29. Echeverry N, Bachmann D, Ke F, Strasser A, Simon HU, Kaufmann T. Intracellular localization of the BCL-2 family member BOK and functional implications. Cell Death Differ. 2013;20(6):785-99.

30. Taylor JM, Barry M. Near death experiences: Poxvirus regulation of apoptotic death. Virology. 2006;344(1):139-50.

31. Benedict CA, Norris PS, Ware CF. To kill or be killed: viral evasion of apoptosis. Nat Immunol. 2002;3(11):1013-8.

32. Hardwick JM, Bellows DS. Viral versus cellular BCL-2 proteins. Cell Death & Differentiation. 2003;10(1):S68-S76.

33. Kvansakul M, van Delft MF, Lee EF, Gulbis JM, Fairlie WD, Huang David CS, et al. A Structural Viral Mimic of Prosurvival Bcl-2: A Pivotal Role for Sequestering Proapoptotic Bax and Bak. Molecular Cell. 2007;25(6):933-42.

34. Kvansakul M, Yang H, Fairlie WD, Czabotar PE, Fischer SF, Perugini MA, et al. Vaccinia virus anti-apoptotic F1L is a novel Bcl-2-like domain-swapped dimer that binds a highly selective subset of BH3-containing death ligands. Cell Death & Differentiation. 2008;15(10):1564-71.

35. Marshall B, Puthalakath H, Caria S, Chugh S, Doerflinger M, Colman PM, et al. Variola virus F1L is a Bcl-2-like protein that unlike its vaccinia virus counterpart inhibits apoptosis independent of Bim. Cell Death & Disease. 2015;6(3):e1680-e.

36.   Altmann M, Hammerschmidt W. Epstein-Barr Virus Provides a New Paradigm: A Requirement for the Immediate Inhibition of Apoptosis. PLOS Biology. 2005;3(12):e404.

37.   Chiou SK, Tseng CC, Rao L, White E. Functional complementation of the adenovirus E1B 19-kilodalton protein with Bcl-2 in the inhibition of apoptosis in infected cells. J Virol. 1994;68(10):6553-66.

38.   White E, Cipriani R, Sabbatini P, Denton A. Adenovirus E1B 19-kilodalton protein overcomes the cytotoxicity of E1A proteins. J Virol. 1991;65(6):2968-78.

39.   Han J, Sabbatini P, Perez D, Rao L, Modha D, White E. The E1B 19K protein blocks apoptosis by interacting with and inhibiting the p53-inducible and death-promoting Bax protein. Genes Dev. 1996;10(4):461-77.

40.   Kvansakul M, Wei AH, Fletcher JI, Willis SN, Chen L, Roberts AW, et al. Structural Basis for Apoptosis Inhibition by Epstein-Barr Virus BHRF1. PLOS Pathogens. 2010;6(12):e1001236.

41.   Desbien AL, Kappler JW, Marrack P. The Epstein–Barr virus Bcl-2 homolog, BHRF1, blocks apoptosis by binding to a limited amount of Bim. Proceedings of the National Academy of Sciences. 2009;106(14):5663.

42.   Cheng EHY, Nicholas J, Bellows DS, Hayward GS, Guo H-G, Reitz MS, et al. A Bcl-2 homolog encoded by Kaposi sarcoma-associated virus, human herpesvirus 8, inhibits apoptosis but does not heterodimerize with Bax or Bak. Proceedings of the National Academy of Sciences. 1997;94(2):690.

43.   Reddy VRAP, Sadigh Y, Tang N, Yao Y, Nair V. Novel Insights into the Roles of Bcl-2 Homolog Nr-13 (vNr-13) Encoded by Herpesvirus of Turkeys in the Virus Replication Cycle, Mitochondrial Networks, and Apoptosis Inhibition. J Virol. 2020;94(10):e02049-19.

44.   Nava VE, Cheng EH, Veliuona M, Zou S, Clem RJ, Mayer ML, et al. Herpesvirus saimiri encodes a functional homolog of the human bcl-2 oncogene. J Virol. 1997;71(5):4118.

45.   Ku B, Woo J-S, Liang C, Lee K-H, Hong H-S, E X, et al. Structural and Biochemical Bases for the Inhibition of Autophagy and Apoptosis by Viral BCL-2 of Murine γ-Herpesvirus 68. PLOS Pathogens. 2008;4(2):e25.

46.   Galindo I, Hernaez B, Díaz-Gil G, Escribano JM, Alonso C. A179L, a viral Bcl-2 homologue, targets the core Bcl-2 apoptotic machinery and its upstream BH3 activators with selective binding restrictions for Bid and Noxa. Virology. 2008;375(2):561-72.

47.   Banjara S, Caria S, Dixon LK, Hinds MG, Kvansakul M. Structural Insight into African Swine Fever Virus A179L-Mediated Inhibition of Apoptosis. J Virol. 2017;91(6):e02228-16.

48.   Banjara S, Mao J, Ryan TM, Caria S, Kvansakul M. Grouper Iridovirus GIV66 is a Bcl-2 protein that inhibits apoptosis by exclusively sequestering Bim. Journal of Biological Chemistry. 2018.

49.   Campbell S, Thibault J, Mehta N, Colman PM, Barry M, Kvansakul M. Structural Insight into BH3 Domain Binding of Vaccinia Virus Antiapoptotic F1L. J Virol. 2014;88(15):8667.

50.   Kvansakul M, Caria S, Hinds MG. The Bcl-2 Family in Host-Virus Interactions. Viruses. 2017;9(10):290.

51.   Rautureau GJP, Yabal M, Yang H, Huang DCS, Kvansakul M, Hinds MG. The restricted binding repertoire of Bcl-B leaves Bim as the universal BH3-only prosurvival Bcl-2 protein antagonist. Cell Death & Disease. 2012;3(12):e443-e.

52. Loparev VN, Parsons JM, Knight JC, Panus JF, Ray CA, Buller RM, et al. A third distinct tumor necrosis factor receptor of orthopoxviruses. Proceedings of the National Academy of Sciences of the United States of America. 1998;95(7):3786-91.

53. Kettle S, Alcamí A, Khanna A, Ehret R, Jassoy C, Smith GL. Vaccinia virus serpin B13R (SPI-2) inhibits interleukin-1beta-converting enzyme and protects virus-infected cells from TNF- and Fas-mediated apoptosis, but does not prevent IL-1beta-induced fever. J Gen Virol. 1997;78 (Pt 3):677-85.

54. Macen JL, Upton C, Nation N, McFadden G. SERP1, a serine proteinase inhibitor encoded by myxoma virus, is a secreted glycoprotein that interferes with inflammation. Virology. 1993;195(2):348-63.

55. Saraiva N, Prole DL, Carrara G, Maluquer de Motes C, Johnson BF, Byrne B, et al. Human and viral Golgi anti-apoptotic proteins (GAAPs) oligomerize via different mechanisms and monomeric GAAP inhibits apoptosis and modulates calcium. The Journal of biological chemistry. 2013;288(18):13057-67.

56. Czabotar PE, Lee EF, Thompson GV, Wardak AZ, Fairlie WD, Colman PM. Mutation to Bax beyond the BH3 domain disrupts interactions with pro-survival proteins and promotes apoptosis. J Biol Chem. 2011;286(9):7123-31.

57. Burton DR, Caria S, Marshall B, Barry M, Kvansakul M. Structural basis of Deerpox virus-mediated inhibition of apoptosis. Acta Crystallographica Section D. 2015;71(8):1593-603.

58. Kibler KV, Shors T, Perkins KB, Zeman CC, Banaszak MP, Biesterfeldt J, et al. Double-stranded RNA is a trigger for apoptosis in vaccinia virus-infected cells. J Virol. 1997;71(3):1992.

59. González-Santamaría J, Campagna M, García MA, Marcos-Villar L, González D, Gallego P, et al. Regulation of Vaccinia Virus E3 Protein by Small Ubiquitin-Like Modifier Proteins. J Virol. 2011;85(24):12890.

60. Liu S-W, Katsafanas George C, Liu R, Wyatt Linda S, Moss B. Poxvirus Decapping Enzymes Enhance Virulence by Preventing the Accumulation of dsRNA and the Induction of Innate Antiviral Responses. Cell Host & Microbe. 2015;17(3):320-31.

61. Teoh MLT, Walasek PJ, Evans DH. Leporipoxvirus Cu,Zn-Superoxide Dismutase (SOD) Homologs Are Catalytically Inert Decoy Proteins That Bind Copper Chaperone for SOD. Journal of Biological Chemistry. 2003;278(35):33175-84.

62. Weaver JR, Isaacs SN. Monkeypox virus and insights into its immunomodulatory proteins. Immunol Rev. 2008;225:96-113.

63. Moss B. Poxvirus DNA replication. Cold Spring Harb Perspect Biol. 2013;5(9):a010199.

64. Barrett JW, McFadden G. CHAPTER 19 - Origin and Evolution of Poxviruses. In: Domingo E, Parrish CR, Holland JJ, editors. Origin and Evolution of Viruses (Second Edition). London: Academic Press; 2008. p. 431-46.

65. McCollum AM, Damon IK. Human monkeypox. Clin Infect Dis. 2014;58(2):260-7.

66. Haller SL, Peng C, McFadden G, Rothenburg S. Poxviruses and the evolution of host range and virulence. Infection, Genetics and Evolution. 2014;21:15-40.

67. Wehrle PF. A reality in our time--certification of the global eradication of smallpox. J Infect Dis. 1980;142(4):636-8.

68. Barry M, Wasilenko ST, Stewart TL, Taylor JM. Apoptosis regulator genes encoded by poxviruses. Prog Mol Subcell Biol. 2004;36:19-37.

69. Everett H, McFadden G. Poxviruses and apoptosis: a time to die. Curr Opin Microbiol. 2002;5(4):395-402.

70. Seet BT, Johnston JB, Brunetti CR, Barrett JW, Everett H, Cameron C, et al. Poxviruses and immune evasion. Annu Rev Immunol. 2003;21:377-423.

71. Aoyagi M, Zhai D, Jin C, Aleshin AE, Stec B, Reed JC, et al. Vaccinia virus N1L protein resembles a B cell lymphoma-2 (Bcl-2) family protein. Protein Sci. 2007;16(1):118-24.

72. Veyer DL, Carrara G, Maluquer de Motes C, Smith GL. Vaccinia virus evasion of regulated cell death. Immunol Lett. 2017;186:68-80.

73. Smith GL, Benfield CTO, Maluquer de Motes C, Mazzon M, Ember SWJ, Ferguson BJ, et al. Vaccinia virus immune evasion: mechanisms, virulence and immunogenicity. J Gen Virol. 2013;94(Pt 11):2367-92.

74. DiPerna G, Stack J, Bowie AG, Boyd A, Kotwal G, Zhang Z, et al. Poxvirus protein N1L targets the I-kappaB kinase complex, inhibits signaling to NF-kappaB by the tumor necrosis factor superfamily of receptors, and inhibits NF-kappaB and IRF3 signaling by toll-like receptors. J Biol Chem. 2004;279(35):36570-8.

75. González JM, Esteban M. A poxvirus Bcl-2-like gene family involved in regulation of host immune response: sequence similarity and evolutionary history. Virology Journal. 2010;7(1):59.

76. Di Pilato M, Mejías-Pérez E, Sorzano COS, Esteban M. Distinct Roles of Vaccinia Virus NF-κB Inhibitor Proteins A52, B15, and K7 in the Immune Response. J Virol. 2017;91(13):e00575-17.

77. Graham SC, Bahar MW, Cooray S, Chen RAJ, Whalen DM, Abrescia NGA, et al. Vaccinia Virus Proteins A52 and B14 Share a Bcl-2–Like Fold but Have Evolved to Inhibit NF-κB rather than Apoptosis. PLOS Pathogens. 2008;4(8):e1000128.

78. Lawrence T. The nuclear factor NF-kappaB pathway in inflammation. Cold Spring Harb Perspect Biol. 2009;1(6):a001651-a.

79. O'Neill LAJ, Bowie AG. The family of five: TIR-domain-containing adaptors in Toll-like receptor signalling. Nature Reviews Immunology. 2007;7(5):353-64.

80. Fedosyuk S, Grishkovskaya I, de Almeida Ribeiro E, Jr., Skern T. Characterization and structure of the vaccinia virus NF-κB antagonist A46. J Biol Chem. 2014;289(6):3749-62.

81. Toshchakov VY, Fenton MJ, Vogel SN. Cutting Edge: Differential Inhibition of TLR Signaling Pathways by Cell-Permeable Peptides Representing BB Loops of TLRs. The Journal of Immunology. 2007;178(5):2655.

82. Kim Y, Lee H, Heo L, Seok C, Choe J. Structure of vaccinia virus A46, an inhibitor of TLR4 signaling pathway, shows the conformation of VIPER motif. Protein Sci. 2014;23(7):906-14.

83. Bartlett N, Symons JA, Tscharke DC, Smith GL. The vaccinia virus N1L protein is an intracellular homodimer that promotes virulenceAccession numbers for the vaccinia virus N1L genes are: VV strain Western Reserve, AF451287; strain Wyeth, AF455803; strain Lister, AF455804; strain King Institute, AF455805; strain USSR, AF455806. Journal of General Virology. 2002;83(8):1965-76.

84. Harte MT, Haga IR, Maloney G, Gray P, Reading PC, Bartlett NW, et al. The Poxvirus Protein A52R Targets Toll-like Receptor Signaling Complexes to Suppress Host Defense. Journal of Experimental Medicine. 2003;197(3):343-51.

85. Schröder M, Baran M, Bowie AG. Viral targeting of DEAD box protein 3 reveals its role in TBK1/IKKε-mediated IRF activation. The EMBO Journal. 2008;27(15):2147-57.

86. Oda S-i, Schröder M, Khan AR. Structural Basis for Targeting of Human RNA Helicase DDX3 by Poxvirus Protein K7. Structure. 2009;17(11):1528-37.

87. Neidel S, Ren H, Torres AA, Smith GL. NF-κB activation is a turn on for vaccinia virus phosphoprotein A49 to turn off NF-κB activation. Proceedings of the National Academy of Sciences. 2019;116(12):5699.

88. Mansur DS, Maluquer de Motes C, Unterholzner L, Sumner RP, Ferguson BJ, Ren H, et al. Poxvirus targeting of E3 ligase β-TrCP by molecular mimicry: a mechanism to inhibit NF-κB activation and promote immune evasion and virulence. PLoS Pathog. 2013;9(2):e1003183.

89. Neidel S, Maluquer de Motes C, Mansur DS, Strnadova P, Smith GL, Graham SC. Vaccinia Virus Protein A49 Is an Unexpected Member of the B-cell Lymphoma (Bcl)-2 Protein Family. Journal of Biological Chemistry. 2015;290(10):5991-6002.

90. Wasilenko ST, Stewart TL, Meyers AFA, Barry M. Vaccinia virus encodes a previously uncharacterized mitochondrial-associated inhibitor of apoptosis. Proceedings of the National Academy of Sciences. 2003;100(24):14345.

91. Fischer SF, Ludwig H, Holzapfel J, Kvansakul M, Chen L, Huang DC, et al. Modified vaccinia virus Ankara protein F1L is a novel BH3-domain-binding protein and acts together with the early viral protein E3L to block virus-associated apoptosis. Cell Death Differ. 2006;13(1):109-18.

92. Yu E, Zhai D, Jin C, Gerlic M, Reed JC, Liddington R. Structural Determinants of Caspase-9 Inhibition by the Vaccinia Virus Protein, F1L. Journal of Biological Chemistry. 2011;286(35):30748-58.

93. Caria S, Marshall B, Burton RL, Campbell S, Pantaki-Eimany D, Hawkins CJ, et al. The N Terminus of the Vaccinia Virus Protein F1L Is an Intrinsically Unstructured Region That Is Not Involved in Apoptosis Regulation. J Biol Chem. 2016;291(28):14600-8.

94. Martinon F, Mayor A, Tschopp J. The inflammasomes: guardians of the body. Annu Rev Immunol. 2009;27:229-65.

95. Gerlic M, Faustin B, Postigo A, Yu EC-W, Proell M, Gombosuren N, et al. Vaccinia virus F1L protein promotes virulence by inhibiting inflammasome activation. Proceedings of the National Academy of Sciences. 2013;110(19):7808.

96. Cooray S, Bahar MW, Abrescia NGA, McVey CE, Bartlett NW, Chen RAJ, et al. Functional and structural studies of the vaccinia virus virulence factor N1 reveal a Bcl-2-like anti-apoptotic protein. The Journal of general virology. 2007;88(Pt 6):1656-66.

97. Maluquer de Motes C, Cooray S, Ren H, Almeida GMF, McGourty K, Bahar MW, et al. Inhibition of apoptosis and NF-κB activation by vaccinia protein N1 occur via distinct binding surfaces and make different contributions to virulence. PLoS pathogens. 2011;7(12):e1002430-e.

98. Mehta N, Taylor J, Quilty D, Barry M. Ectromelia virus encodes an anti-apoptotic protein that regulates cell death. Virology. 2015;475:74-87.

99. Antignani A, Youle RJ. How do Bax and Bak lead to permeabilization of the outer mitochondrial membrane? Current Opinion in Cell Biology. 2006;18(6):685-9.

100. Su J, Wang G, Barrett JW, Irvine TS, Gao X, McFadden G. Myxoma Virus M11L Blocks Apoptosis through Inhibition of Conformational Activation of Bax at the Mitochondria. J Virol. 2006;80(3):1140.

101. Douglas AE, Corbett KD, Berger JM, McFadden G, Handel TM. Structure of M11L: A myxoma virus structural homolog of the apoptosis inhibitor, Bcl-2. Protein Sci. 2007;16(4):695-703.

102. Wang G, Barrett JW, Nazarian SH, Everett H, Gao X, Bleackley C, et al. Myxoma virus M11L prevents apoptosis through constitutive interaction with Bak. J Virol. 2004;78(13):7097-111.

103. Suraweera CD, Anasir MI, Chugh S, Javorsky A, Impey RE, Hasan Zadeh M, et al. Structural insight into tanapoxvirus-mediated inhibition of apoptosis. The FEBS Journal.n/a(n/a).

104. Haig D, Mercer AA. Parapoxviruses. In: Mahy BWJ, Van Regenmortel MHV, editors. Encyclopedia of Virology (Third Edition). Oxford: Academic Press; 2008. p. 57-63.

105. Westphal D, Ledgerwood EC, Hibma MH, Fleming SB, Whelan EM, Mercer AA. A Novel Bcl-2-Like Inhibitor of Apoptosis Is Encoded by the Parapoxvirus Orf Virus. J Virol. 2007;81(13):7178.

106. Westphal D, Ledgerwood EC, Tyndall JDA, Hibma MH, Ueda N, Fleming SB, et al. The orf virus inhibitor of apoptosis functions in a Bcl-2-like manner, binding and neutralizing a set of BH3-only proteins and active Bax. Apoptosis. 2009;14(11):1317.

107. Tuppurainen ESM, Venter EH, Shisler JL, Gari G, Mekonnen GA, Juleff N, et al. Review: Capripoxvirus Diseases: Current Status and Opportunities for Control. Transbound Emerg Dis. 2017;64(3):729-45.

108. Suraweera CD, Burton DR, Hinds MG, Kvansakul M. Crystal structures of the sheeppox virus encoded inhibitor of apoptosis SPPV14 bound to the proapoptotic BH3 peptides Hrk and Bax. FEBS Letters. 2020;594(12):2016-26.

109. Okamoto T, Campbell S, Mehta N, Thibault J, Colman PM, Barry M, et al. Sheeppox Virus SPPV14 Encodes a Bcl-2-Like Cell Death Inhibitor That Counters a Distinct Set of Mammalian Proapoptotic Proteins. J Virol. 2012;86(21):11501.

110. Banadyga L, Lam S-C, Okamoto T, Kvansakul M, Huang DC, Barry M. Deerpox Virus Encodes an Inhibitor of Apoptosis That Regulates Bak and Bax. J Virol. 2011;85(5):1922.

111. Khan JS, Provencher JF, Forbes MR, Mallory ML, Lebarbenchon C, McCoy KD. Chapter One - Parasites of seabirds: A survey of effects and ecological implications. In: Sheppard C, editor. Advances in Marine Biology. 82: Academic Press; 2019. p. 1-50.

112. Anasir MI, Caria S, Skinner MA, Kvansakul M. Structural basis of apoptosis inhibition by the fowlpox virus protein FPV039. The Journal of biological chemistry. 2017;292(22):9010-21.

113. Anasir MI, Baxter AA, Poon IKH, Hulett MD, Kvansakul M. Structural and Functional Insight into Canarypox Virus CNP058 Mediated Regulation of Apoptosis. Viruses. 2017;9(10).

114. Banadyga L, Veugelers K, Campbell S, Barry M. The Fowlpox Virus BCL-2 Homologue, FPV039, Interacts with Activated Bax and a Discrete Subset of BH3-Only Proteins To Inhibit Apoptosis. J Virol. 2009;83(14):7085.

115. Luo X, Budihardjo I, Zou H, Slaughter C, Wang X. Bid, a Bcl2 Interacting Protein, Mediates Cytochrome c Release from Mitochondria in Response to Activation of Cell Surface Death Receptors. Cell. 1998;94(4):481-90.

116. Pickup DJ, Ink BS, Hu W, Ray CA, Joklik WK. Hemorrhage in lesions caused by cowpox virus is induced by a viral protein that is related to plasma protein inhibitors of serine proteases. Proceedings of the National Academy of Sciences. 1986;83(20):7698.

117. Komiyama T, Ray CA, Pickup DJ, Howard AD, Thornberry NA, Peterson EP, et al. Inhibition of interleukin-1 beta converting enzyme by the cowpox virus serpin

CrmA. An example of cross-class inhibition. Journal of Biological Chemistry. 1994;269(30):19331-7.

118. Ray CA, Black RA, Kronheim SR, Greenstreet TA, Sleath PR, Salvesen GS, et al. Viral inhibition of inflammation: Cowpox virus encodes an inhibitor of the interleukin-1β converting enzyme. Cell. 1992;69(4):597-604.

119. Zhou Q, Snipas S, Orth K, Muzio M, Dixit VM, Salvesen GS. Target Protease Specificity of the Viral Serpin CrmA: ANALYSIS OF FIVE CASPASES. Journal of Biological Chemistry. 1997;272(12):7797-800.

120. Ekert PG, Silke J, Vaux DL. Caspase inhibitors. Cell Death Differ. 1999;6(11):1081-6.

121. Tewari M, Dixit VM. Fas- and Tumor Necrosis Factor-induced Apoptosis Is Inhibited by the Poxvirus crmA Gene Product. Journal of Biological Chemistry. 1995;270(7):3255-60.

122. Datta R, Kojima H, Banach D, Bump NJ, Talanian RV, Alnemri ES, et al. Activation of a CrmA-insensitive, p35-sensitive Pathway in Ionizing Radiation-induced Apoptosis. Journal of Biological Chemistry. 1997;272(3):1965-9.

123. Quan LT, Caputo A, Bleackley RC, Pickup DJ, Salvesen GS. Granzyme B Is Inhibited by the Cowpox Virus Serpin Cytokine Response Modifier A. Journal of Biological Chemistry. 1995;270(18):10377-9.

124. Dobbelstein M, Shenk T. Protection against apoptosis by the vaccinia virus SPI-2 (B13R) gene product. J Virol. 1996;70(9):6479-85.

125. Cameron C, Hota-Mitchell S, Chen L, Barrett J, Cao JX, Macaulay C, et al. The complete DNA sequence of myxoma virus. Virology. 1999;264(2):298-318.

126. Turner PC, Sancho MC, Thoennes SR, Caputo A, Bleackley RC, Moyer RW. Myxoma virus Serp2 is a weak inhibitor of granzyme B and interleukin-1beta-converting enzyme in vitro and unlike CrmA cannot block apoptosis in cowpox virus-infected cells. J Virol. 1999;73(8):6394-404.

127. Messud-Petit F, Gelfi J, Delverdier M, Amardeilh MF, Py R, Sutter G, et al. Serp2, an inhibitor of the interleukin-1beta-converting enzyme, is critical in the pathobiology of myxoma virus. J Virol. 1998;72(10):7830-9.

128. Guerin JL, Gelfi J, Camus C, Delverdier M, Whisstock JC, Amardeihl MF, et al. Characterization and functional analysis of Serp3: a novel myxoma virus-encoded serpin involved in virulence. J Gen Virol. 2001;82(Pt 6):1407-17.

129. Seet BT, McFadden G. Viral chemokine-binding proteins. Journal of Leukocyte Biology. 2002;72(1):24-34.

130. Smith CA, Davis T, Anderson D, Solam L, Beckmann MP, Jerzy R, et al. A receptor for tumor necrosis factor defines an unusual family of cellular and viral proteins. Science. 1990;248(4958):1019.

131. Schreiber M, Rajarathnam K, McFadden G. Myxoma virus T2 protein, a tumor necrosis factor (TNF) receptor homolog, is secreted as a monomer and dimer that each bind rabbit TNFalpha, but the dimer is a more potent TNF inhibitor. J Biol Chem. 1996;271(23):13333-41.

132. Sedger LM, Osvath SR, Xu XM, Li G, Chan FK, Barrett JW, et al. Poxvirus tumor necrosis factor receptor (TNFR)-like T2 proteins contain a conserved preligand assembly domain that inhibits cellular TNFR1-induced cell death. J Virol. 2006;80(18):9300-9.

133. Reading PC, Khanna A, Smith GL. Vaccinia Virus CrmE Encodes a Soluble and Cell Surface Tumor Necrosis Factor Receptor That Contributes to Virus Virulence. Virology. 2002;292(2):285-98.

134. Panus JF, Smith CA, Ray CA, Smith TD, Patel DD, Pickup DJ. Cowpox virus encodes a fifth member of the tumor necrosis factor receptor family: A soluble, secreted CD30 homologue. Proceedings of the National Academy of Sciences. 2002;99(12):8348.

135. Schwab U, Stein H, Gerdes J, Lemke H, Kirchner H, Schaadt M, et al. Production of a monoclonal antibody specific for Hodgkin and Sternberg-Reed cells of Hodgkin's disease and a subset of normal lymphoid cells. Nature. 1982;299(5878):65-7.

136. Saraiva M, Smith P, Fallon PG, Alcami A. Inhibition of Type 1 Cytokine–mediated Inflammation by a Soluble CD30 Homologue Encoded by Ectromelia (Mousepox) Virus. Journal of Experimental Medicine. 2002;196(6):829-39.

137. Yang Z, West AP, Bjorkman PJ. Crystal structure of TNFα complexed with a poxvirus MHC-related TNF binding protein. Nature Structural & Molecular Biology. 2009;16(11):1189-91.

138. Mendez-Rios JD, Yang Z, Erlandson KJ, Cohen JI, Martens CA, Bruno DP, et al. Molluscum Contagiosum Virus Transcriptome in Abortively Infected Cultured Cells and a Human Skin Lesion. J Virol. 2016;90(9):4469.

139. Bertin J, Armstrong RC, Ottilie S, Martin DA, Wang Y, Banks S, et al. Death effector domain-containing herpesvirus and poxvirus proteins inhibit both Fas- and TNFR1-induced apoptosis. Proceedings of the National Academy of Sciences. 1997;94(4):1172.

140. Shisler JL, Moss B. Molluscum Contagiosum Virus Inhibitors of Apoptosis: The MC159 v-FLIP Protein Blocks Fas-Induced Activation of Procaspases and Degradation of the Related MC160 Protein. Virology. 2001;282(1):14-25.

141. Garvey TL, Bertin J, Siegel RM, Wang G-h, Lenardo MJ, Cohen JI. Binding of FADD and Caspase-8 to Molluscum Contagiosum Virus MC159 v-FLIP Is Not Sufficient for Its Antiapoptotic Function. J Virol. 2002;76(2):697.

142. Murao LE, Shisler JL. The MCV MC159 protein inhibits late, but not early, events of TNF-α-induced NF-κB activation. Virology. 2005;340(2):255-64.

143. Gubser C, Bergamaschi D, Hollinshead M, Lu X, van Kuppeveld FJM, Smith GL. A New Inhibitor of Apoptosis from Vaccinia Virus and Eukaryotes. PLOS Pathogens. 2007;3(2):e17.

144. Kotwal GJ, Moss B. Vaccinia virus encodes two proteins that are structurally related to members of the plasma serine protease inhibitor superfamily. J Virol. 1989;63(2):600-6.

145. Turner PC, Moyer RW. Orthopoxvirus fusion inhibitor glycoprotein SPI-3 (open reading frame K2L) contains motifs characteristic of serine proteinase inhibitors that are not required for control of cell fusion. J Virol. 1995;69(10):5978-87.

146. Smith VP, Bryant NA, Alcamí A. Ectromelia, vaccinia and cowpox viruses encode secreted interleukin-18-binding proteins. J Gen Virol. 2000;81(Pt 5):1223-30.

147. Teoh ML, Turner PV, Evans DH. Tumorigenic poxviruses up-regulate intracellular superoxide to inhibit apoptosis and promote cell proliferation. J Virol. 2005;79(9):5799-811.

148. Rahman MM, Liu J, Chan WM, Rothenburg S, McFadden G. Myxoma virus protein M029 is a dual function immunomodulator that inhibits PKR and also conscripts RHA/DHX9 to promote expanded host tropism and viral replication. PLoS Pathog. 2013;9(7):e1003465.

149. Myskiw C, Arsenio J, Hammett C, van Bruggen R, Deschambault Y, Beausoleil N, et al. Comparative Analysis of Poxvirus Orthologues of the Vaccinia Virus E3

Protein: Modulation of Protein Kinase R Activity, Cytokine Responses, and Virus Pathogenicity. J Virol. 2011;85(23):12280.

150. Coutu J, Ryerson MR, Bugert J, Brian Nichols D. The Molluscum Contagiosum Virus protein MC163 localizes to the mitochondria and dampens mitochondrial mediated apoptotic responses. Virology. 2017;505:91-101.

151. Downie AW, Taylor-Robinson CH, Caunt AE, Nelson GS, Manson-Bahr PE, Matthews TC. Tanapox: a new disease caused by a pox virus. Br Med J. 1971;1(5745):363-8.

152. Fuchs Y, Steller H. Live to die another way: modes of programmed cell death and the signals emanating from dying cells. Nat Rev Mol Cell Biol. 2015;16(6):329-44.

153. Galluzzi L, Brenner C, Morselli E, Touat Z, Kroemer G. Viral Control of Mitochondrial Apoptosis. PLOS Pathogens. 2008;4(5):e1000018.

154. Zhai D, Yu E, Jin C, Welsh K, Shiau C-w, Chen L, et al. Vaccinia virus protein F1L is a caspase-9 inhibitor. The Journal of biological chemistry. 2010;285(8):5569-80.

155. van Delft MF, Wei AH, Mason KD, Vandenberg CJ, Chen L, Czabotar PE, et al. The BH3 mimetic ABT-737 targets selective Bcl-2 proteins and efficiently induces apoptosis via Bak/Bax if Mcl-1 is neutralized. Cancer Cell. 2006;10(5):389-99.

156. Long F, Vagin AA, Young P, Murshudov GN. BALBES: a molecular-replacement pipeline. Acta Crystallogr D Biol Crystallogr. 2008;64(Pt 1):125-32.

157. Mahmoud MA, Khafagi MH. Detection, identification, and differentiation of sheep pox virus and goat pox virus from clinical cases in Giza Governorate, Egypt. Vet World. 2016;9(12):1445-9.

158. Cory S, Adams JM. The Bcl2 family: regulators of the cellular life-or-death switch. Nature Reviews Cancer. 2002;2(9):647-56.

159. Sattler M, Liang H, Nettesheim D, Meadows RP, Harlan JE, Eberstadt M, et al. Structure of Bcl-xL-Bak peptide complex: recognition between regulators of apoptosis. Science. 1997;275(5302):983-6.

160. Day CL, Smits C, Fan FC, Lee EF, Fairlie WD, Hinds MG. Structure of the BH3 Domains from the p53-Inducible BH3-Only Proteins Noxa and Puma in Complex with Mcl-1. Journal of Molecular Biology. 2008;380(5):958-71.

161. Kvansakul M, Hinds MG. Chapter Three - The Structural Biology of BH3-Only Proteins. In: Ashkenazi A, Yuan J, Wells JA, editors. Methods in Enzymology. 544: Academic Press; 2014. p. 49-74.

162. Eitz Ferrer P, Potthoff S, Kirschnek S, Gasteiger G, Kastenmüller W, Ludwig H, et al. Induction of Noxa-mediated apoptosis by modified vaccinia virus Ankara depends on viral recognition by cytosolic helicases, leading to IRF-3/IFN-β-dependent induction of pro-apoptotic Noxa. PLoS pathogens. 2011;7(6):e1002083-e.

163. Puthalakath H, O'Reilly LA, Gunn P, Lee L, Kelly PN, Huntington ND, et al. ER stress triggers apoptosis by activating BH3-only protein Bim. Cell. 2007;129(7):1337-49.

164. Fischer SF, Belz GT, Strasser A. BH3-only protein Puma contributes to death of antigen-specific T cells during shutdown of an immune response to acute viral infection. Proceedings of the National Academy of Sciences. 2008;105(8):3035.

165. Sun Y, Leaman DW. Involvement of Noxa in Cellular Apoptotic Responses to Interferon, Double-stranded RNA, and Virus Infection. Journal of Biological Chemistry. 2005;280(16):15561-8.

166. Wei MC, Zong WX, Cheng EH, Lindsten T, Panoutsakopoulou V, Ross AJ, et al. Proapoptotic BAX and BAK: a requisite gateway to mitochondrial dysfunction and death. Science (New York, NY). 2001;292(5517):727-30.

167. Torres-Domínguez LE, McFadden G. Poxvirus oncolytic virotherapy. Expert Opin Biol Ther. 2019;19(6):561-73.

168. Chan WM, McFadden G. Oncolytic Poxviruses. Annu Rev Virol. 2014;1(1):119-41.

169. García-Arriaza J, Esteban M. Enhancing poxvirus vectors vaccine immunogenicity. Hum Vaccin Immunother. 2014;10(8):2235-44.

Appendix 1

Paper V: A structural investigation of NRZ mediated apoptosis regulation in zebrafish

A1   Co-author contribution

Chathura D. Suraweera	Protein Expression and purification
	Determination of NRZ binding partners
	Protein crystallization, X-ray diffraction and data collection
	Structure solution and refinement
	Structural analysis
	Manuscript writing (Introduction, Material and Methods Results and Discussion)
	Preparation of figures and tables in the manuscript
Sofia Caria	Diffraction data processing
	Structure solution and refinement
Michael Java	Diffraction data processing
	Structure solution and refinement
Mark G. Hinds	Overall scientific direction of the project
	Structural analysis and interpretation
	Drafted and revised the manuscript
Marc Kvansakul	Overall scientific direction of the project
	X-ray diffraction and data collection
	Structure solution and refinement
	Structural analysis
	Drafted and revised the manuscript

ARTICLE   **Open Access**

A structural investigation of NRZ mediated apoptosis regulation in zebrafish

Chathura D. Suraweera[1], Sofia Caria[1], Michael Järvå[1], Mark G. Hinds[2] and Marc Kvansakul[1]

Abstract

Bcl-2 family proteins play a crucial role in regulating apoptosis, a process critical for development, eliminating damaged or infected cells, host-pathogen interactions and in disease. Dysregulation of Bcl-2 proteins elicits an expansive cell survival mechanism promoting cell migration, invasion and metastasis. Through a network of intra-family protein–protein interactions Bcl-2 family members regulate the release of cell death factors from mitochondria. NRZ is a novel zebrafish pro-survival Bcl-2 orthologue resident on mitochondria and the endoplasmic reticulum (ER). However, the mechanism of NRZ apoptosis inhibition has not yet been clarified. Here we examined the interactions of NRZ with pro-apoptotic members of the Bcl-2 family using a combination of isothermal calorimetry and mutational analysis of NRZ. We show that NRZ binds almost all zebrafish pro-apoptotic proteins and displays a broad range of affinities. Furthermore, we define the structural basis for apoptosis inhibition of NRZ by solving the crystal structure of both *apo*-NRZ and a *holo* form bound to a peptide spanning the binding motif of the pro-apoptotic zBad, a BH3-only protein orthologous to mammalian Bad. The crystal structure of NRZ revealed that it adopts the conserved Bcl-2 like fold observed for other cellular pro-survival Bcl-2 proteins and employs the canonical ligand binding groove to bind Bad BH3 peptide. NRZ engagement of Bad BH3 involves the canonical ionic interaction between NRZ R86 and Bad D104 and an additional ionic interaction between NRZ D79 and Bad R100, and substitution of either NRZ R86 or D79 to Ala reduces the binding to Bad BH3 tenfold or more. Our findings provide a detailed mechanistic understanding for NRZ mediated anti-apoptotic activity in zebrafish by revealing binding to both Bad and Noxa, suggesting that NRZ is likely to occupy a unique mechanistic role in zebrafish apoptosis regulation by acting as a highly promiscuous pro-apoptotic Bcl-2 binder.

Introduction

Multicellular organisms have evolved a multitude of mechanisms to remove superfluous cells[1]. Pivotal among the mechanisms for cell removal is programmed cell death or apoptosis, a process that maintains tissue homeostasis, removes damaged, infected in response to pathogen invasion[2], or otherwise unwanted cells, such as during embryonic development, where it plays a critical role in shaping body and tissue structures[3,4]. Members of

the B-cell lymphoma-2 (Bcl-2) family of proteins are key players of cellular life and death decisions and regulate the intrinsic or mitochondrial associated cell death[3,4]. Consisting of ~20 proteins the Bcl-2 family is characterized by the presence of conserved sequence motifs referred to as Bcl-2 homology or BH motifs. Structurally, the Bcl-2 proteins are organized into two major subfamilies, those that share the Bcl-2 fold (Bcl-2, Bcl-x_L, Bcl-w, Mcl-1, A1, Bcl-B, Bax, Bak Bok) and a distantly related group, the BH3-only proteins that bear only a BH3-motif (Bim, Bad, Bmf, Bid, Bik, Hrk, Puma and Noxa) that with the exception of Bid are disordered[5]. Those with pro-survival activity in mammals comprise Bcl-2, Bcl-x_L, Bcl-w, Mcl-1, A1 and Bcl-B. Their primary function is to antagonize the activation of caspases by

Correspondence: Mark G. Hinds (mhinds@unimelb.edu.au) or
Marc Kvansakul (m.kvansakul@latrobe.edu.au)
[1]Department of Biochemistry and Genetics, La Trobe Institute for Molecular
Science, La Trobe University, Melbourne, Victoria 3086, Australia
[2]Bio21 Molecular Science and Biotechnology Institute, The University of
Melbourne, Parkville, Australia
Edited by: P. Bouillet

SPRINGER NATURE
CDD*press*

directly interacting and inhibiting pro-apoptotic Bcl-2 proteins[4,6] of the BH3-only group or Bax, Bak and Bok. It is ultimately the balance and specificity[7] of interactions between pro-apoptotic and pro-survival Bcl-2 proteins that regulates apoptosis and determines cellular fate[8].

The pro-apoptotic Bcl-2 proteins promote apoptosis via mitochondrial outer membrane permeabilization (MOMP)[4,5]. Critical to the execution of MOMP are Bax and Bak[9,10] as they trigger formation of oligomeric pores that breach the mitochondrial outer membrane and release pro-apoptogenic molecules such as SMAC/DIA-BLO and cytochrome-c[11] into the cytoplasm to activate the caspase cascade that proteolyses key cellular components and ultimately demolishes the cell[4]. In contrast to Bax and Bak, the BH3-only proteins induce apoptosis by utilizing their BH3 motif via two mechanisms: either indirectly by neutralizing pro-survival Bcl-2 by binding to a conserved ligand binding groove or directly by interacting with Bax and Bak via an alternative interaction site[5,12]. In healthy cells, BH3-only proteins act as sentinels of cellular well-being and are up-regulated in response to cellular insults including growth factor deprivation, exposure to cytotoxic drugs or viral infections, leading to the activation of cell death mechanisms[6]. Other less well described functions have also been attributed to the Bcl-2 family. For example, Bcl-2 family members may regulate or monitor intracellular calcium[13,14] in the unfolded protein response (UPR) and trigger apoptosis through activation of the BH3-only proteins[15] when the unfolded protein levels in the endoplasmic reticulum (ER) become excessive[16]. While elements of the intrinsic apoptotic pathway are highly conserved from sponges[17] to mammals[6] there are also significant differences between organisms[18].

Many Bcl-2 family members are conserved between fish and mammals[19–21], but some notable differences exist between the apoptotic machineries in mammals and fish. For instance, overexpression of the zebrafish (*Danio rerio*) pro-apoptotic Bcl-2 proteins zBmf1, zBik, zPuma and zNoxa triggered dose-dependent caspase activation and subsequent cell death, whereas overexpression of zBad and zBok did not lead to cell death compared to overexpression of human Bad[22]. Also, expression of zebrafish *bad* gene did not result in embryonic lethality[23]. Furthermore, zBad pro-apoptotic activity is regulated through phosphorylation of conserved serine residues[23,24], in a manner similar to mouse Bad[25]. One significant difference from mammals is that zebrafish lack orthologues of the pro-survival Bcl-2 proteins Bcl-w and A1, as well as pro-apoptotic Bak and Hrk[20], but contain a novel pro-survival protein called NRZ, that was initially identified as an orthologue of the avian pro-survival Bcl-2 protein NR-13[26–28]. Also present is a recently described pro-apoptotic Bcl-2 protein Bcl-wav[29] that is without a mammalian orthologue. Thus, there are a number of significant differences between Bcl-2-regulated apoptosis in zebrafish and mammals.

NRZ is a 19 kDa protein expressed in the epiboly of the extra-maternal yolk syncytial layer (YSL) of zebrafish eggs[28]. In vivo, NRZ has been shown to be a potent inhibitor of apoptosis after serum withdrawal, and controls development during somatogenesis and gastrulation[28]. Mechanistically, NRZ was shown to inhibit apoptosis by antagonizing zBax-BH3[28]. *Nrz* knockout triggers intracellular Ca^{2+} increase in YSL, which results in the blockade of development prior to gastrulation[13]. Additionally, NRZ appears to arrest Ca^{2+} release from endoplasmic reticulum (ER) by direct interaction with the inositol triphosphate type 1 receptor, IP3R1, calcium channel[13]. Knockdown of NRZ is lethal in zebrafish embryos, and intriguingly, some of this activity appears to be independent of its role in apoptosis[28]. Loss of NRZ prevents embryonic development via upregulation of the transcription factor Snail-1, a cell adhesion regulator to arrest gastrulation at the shield stage[28,30]. Other activities ascribed to NRZ include inhibition of the apoptosis accelerating function of Bcl-wav, a pro-apoptotic Bcl-2 member found in teleost fish[29].

Although there are significant differences between the apoptosis machinery of zebrafish and mammals there remains a high degree of conservation with many direct orthologues of mammalian apoptotic genes present in the genome of the zebrafish[19,20]. Coupled with the presence of many orthologous mammalian genes are the advantages of zebrafish as a model organism, such as their rapid development, embryo transparency and genetic accessibility[20]. Analysis of zebrafish genetics is providing a better understanding of the fundamental interactions governing apoptosis and is of significant interest in deciphering human disease, including cancer[20] and host-pathogen interactions[31]. Here we report the first systematic biochemical analysis and high-resolution structure determination of a zebrafish pro-survival Bcl-2 protein, NRZ. Our findings suggest that NRZ is a unique pro-survival Bcl-2 protein with an unusual pro-apoptotic Bcl-2 binding profile unlike its counterparts in mammalian systems.

Materials and methods
Protein expression and purification

Synthetic cDNA encoding for codon-optimized NRZ (Uniprot Accession number Q8UWD5) lacking the 28 C-terminal residues (Bioneer, Melbourne, Australia) was cloned into the bacterial expression vector pCoofy4[32] Recombinant NRZ was expressed in BL21-CodonPlus cells using the auto-induction method[33] for 24 h at 25 °C with shaking. Bacterial cells were collected by centrifugation at 4000 rpm (JLA 9.1000 rotor, Avanti J-E Beckman Coulter, Mount Waverly, Australia) for 20 min

and re-suspended in 50 ml lysis buffer A (50 mM Tris, pH 8.5, 300 mM NaCl and 2 mM BME (β-Mercaptoethanol) supplemented with lysozyme and DNaseI. The cells were lysed using sonication (programme 7, Model 705 Sonic Dismembrator, Fisher Scientific, Hampton, New Hampshire, US) and the resultant lysate was transferred into SS34 tubes for further centrifugation at 16,000 rpm (JA-25.50 rotor, Beckman Coulter Avanti J-E) for 30 min. The supernatant was loaded onto a HisTrap HP, 5 ml (GE Healthcare, Little Chalford, UK) equilibrated with buffer A. After sample application, the column was washed with 100 ml of buffer B (50 mM Tris, pH 8.5, 300 mM NaCl, 25 mM imidazole and 2 mM BME (β-Mercaptoethanol) and the target protein was eluted with buffer C (50 mM Tris, pH 8.5, 300 mM NaCl, 300 mM imidazole and 2 mM BME (β-Mercaptoethanol)) followed by HRV 3C protease cleavage while dialyzed overnight into buffer A at 4 °C. The cleaved protein was passed again through the column to remove the cleaved His-MBP tag, with the remaining protein being concentrated using a centrifugal concentrator with 10 kDa molecular weight cutoff (Amicon® Ultra 15) to a final volume of 4 ml. Concentrated NRZ was subjected to size-exclusion chromatography using a Superdex S75 16/600 column mounted on an ÄKTAX-press system (GE Healthcare) equilibrated in 25 mM HEPES, pH 7.5, 150 mM NaCl, 2 mM BME where it eluted as a single peak. The final sample purity was estimated to be higher than 95% based on SDS–PAGE analysis. Appropriate fractions were pooled and concentrated using a centrifugal concentrator with 10 kDa molecular weight cutoff (Amicon ® Ultra 15) to final concentration of 28 mg ml^{-1}.

Expression and purification of NRZ mutants R86A and D79A

NRZ mutants D79A and R86A were codon-optimized and synthesized (Genscript) and subsequently cloned into the pGEX-6P-3 vector (Invitrogen). Expression and purification were performed using the same protocol as for wild-type NRZ.

Measurement of dissociation constants

Binding affinities were measured by isothermal titration calorimetry (ITC) employing a MicroCal iTC200 system (GE Healthcare) at 25 °C using wt-NRZ, and NRZ mutants D79A and R86A in 25 mM HEPES, pH 7.5, 150 mM NaCl, 2 mM BME at a final concentration of 30 μM as previously described[34]. BH3 motif peptide ligands were used at a concentration of 300 μM and titrated using 19 injections of 2.0 μl of ligand. All affinity measurements were performed in triplicate. Protein concentrations were measured using a Nanodrop UV spectrophotometer (Thermo Scientific, Scoresbury, Australia) at a wavelength of 280 nm. Peptide concentrations were calculated based on the dry peptide weight after synthesis. The zebrafish BH3-motif peptides

used were commercially synthesized and were purified to a final purity of 95% (GenScript, Piscataway, New Jersey, US). zBim: ALPPEMVVARELRRIGDEFNRLYCEA (UniProt accession code B2KKY9, residues 117–142), zPuma: EEQAVERVAVQLRTIGDEMNAVFLQR (accession code Q0GKC9, residues 123–148), zBik: NMRVTQTIGRQLAQI GDEMDNKWRQE (accession code Q5RGV6, residues 30–55), zBax: ELCDPSHKRLAQCLQQIGDELDGNAQLQ (accession code Q9I9N4, residues 52–79), zBid: EARAA REMAAELIRIADLLEQSVLSQAA (accession code Q0GK C5, residues 85–112), zBad: ALWAAKKYGQQLRRMSD EFDKGQMKR (accession code A7MCM4, 88–113 residues), zBmf: AQSVETLIGQKLQLIGDQFYQEHIMH (accession code Q0GKC7, residues 89–114), zNoxa: EQT AVVECAQQLRNIGDLLNWKYKLL (accession code Q0GKC8, residues 5–30), zBok: PRGVLVDVSVVL LKLGDELECMRPYV (accession code Q7T381, residues 60–85), zBeclin: DGGTMENLSRRLKVTSNLFDIMSGQT (accession code F1RCP1, residues 102–127), zBcl-wav: LCPAPSRASAALRHAGDELLIRFPIF (accession code D2Y5Q2, residues 42–67).

Crystallization and data collection

Crystals of *apo* NRZ were obtained at a protein concentration of 28 mg/ml in 1.0 M magnesium sulphate hydrate, 0.1 M sodium acetate trihydrate pH 4.6. The crystals were cryo-protected in mother liquor supplemented with 30% glucose and flash cooled in liquid nitrogen. The *apo* NRZ crystals in this condition appeared as thick needles belonging to the P4$_3$ space group of the tetragonal crystal system.

All diffraction data were collected on the MX2 beamline at the Australian Synchrotron using an Eiger detector (Dectris, Baden-Dättwil, Switzerland) with an oscillation range of 0.1° per frame using wavelength 0.9537 Å. The diffraction data were integrated using XDS[35] and scaled using AIMLESS[36]. The crystals of *apo*-NRZ contained one molecule of NRZ in the asymmetric unit with a calculated solvent content of 47.0%. The structure of *apo*-NRZ was solved by molecular replacement using PHASER[37] with previously solved structure of NRZ: Bad BH3 (PDB ID: 6FBX) as a search model. The final TFZ and LLG values were 15.4 and 541.6, respectively. The final *apo*-NRZ structure was built manually over multiple cycles using Coot[38] and refined using PHENIX[39] to a final R_{work}/R_{free} of 0.194/0.222 with 96.3% of residues in Ramachandran favoured region of the plot and no outliers. All data collection and refinement statistics are summarized in Table 2.

Complexes of NRZ with zBad BH3 were prepared as previously described[40]. Briefly, NRZ: zBad BH3 complexes were reconstituted by adding zBad BH3 peptides at a 1:1.25 molar ratio to NRZ. The reconstituted complex was concentrated to 28 mg ml^{-1} using a 3 kDa molecular

weight cutoff centrifugal concentrator (Millipore), flash-cooled and stored under liquid nitrogen. High-throughput sparse matrix screening was carried out using 96-well sitting-drop trays (Swissci, Neuheim, Switzerland) and the vapour-diffusion method at 20 °C. Crystals of NRZ: zBad

BH3 were obtained at 28 mg ml^{-1} using the sitting-drop method at 20 °C in 0.2 M sodium fluoride, 0.1 M Bis-Tris propane, pH 6.5, 20% (W/V) PEG 3350. The crystals were flash-cooled at −173 °C in mother liquor supplemented with 30% (w/v) glucose. The NRZ: zBad BH3 complex
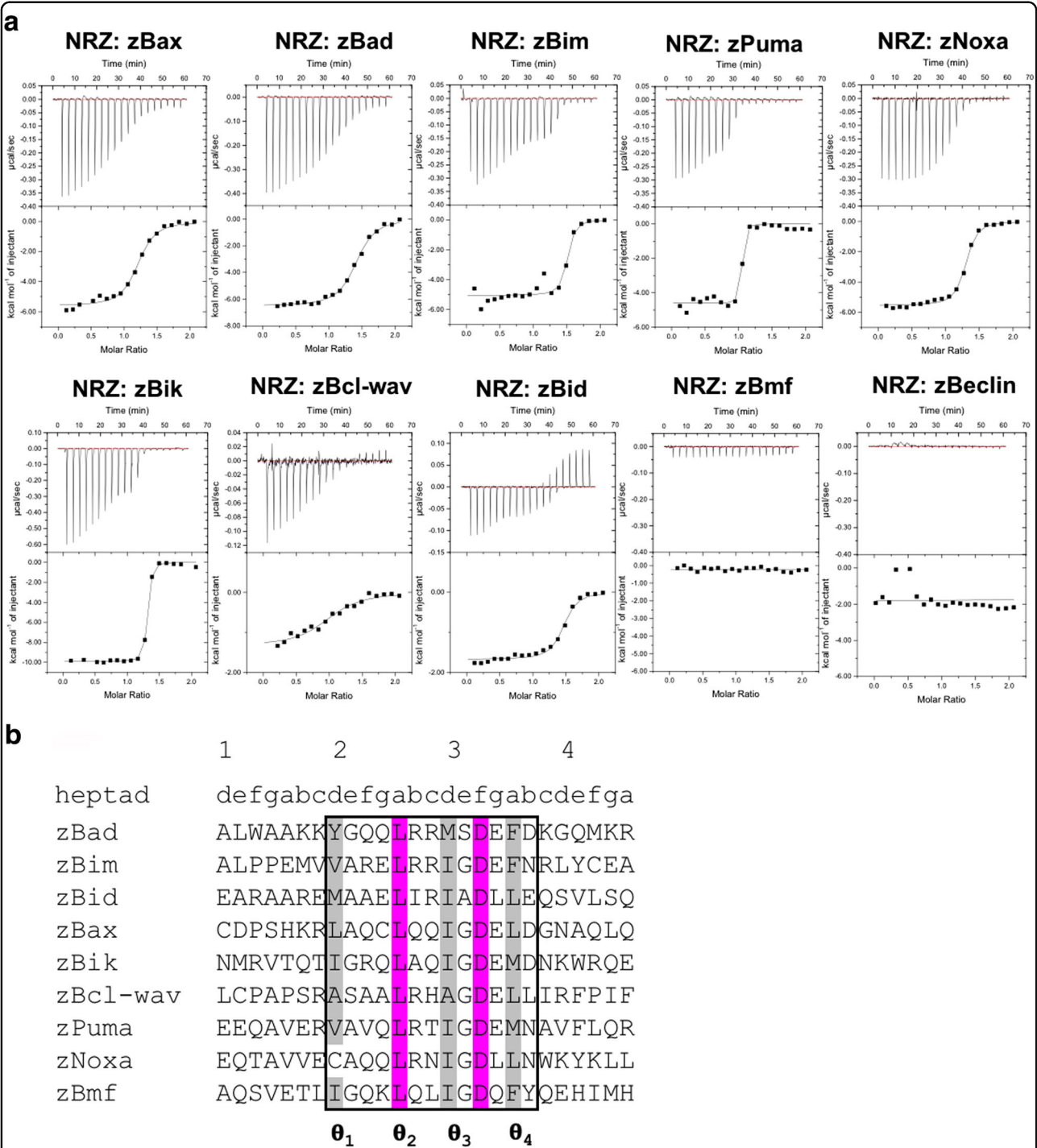

Fig. 1 Titration curves showing the raw heats of titration for ITC measurements of NRZ: BH3 motif interactions. NRZ interacts with Bax as well as all other BH3-only proteins but not Bmf or Beclin-1. Affinities are summarized in Table 1

formed single rod-shaped crystals belonging to space group P6$_3$ in the hexagonal crystal system.

Diffraction data for NRZ: zBad BH3 complex were collected on the MX2 beamline at the Australian Synchrotron using a with an Eiger detector with an oscillation range of 0.1° per frame using wavelength 0.9537. Collected diffraction data were integrated using XDS[35] and scaled using AIMLESS[36]. Molecular replacement was performed using PHASER[37] with the structure of Mcl-1 (PDB ID: 5KU9)[41] as a search model. NRZ: zBad BH3 crystals contain one molecule of NRZ and 1 molecule of zBad BH3 in the asymmetric unit, with a 43.7% solvent content and final TFZ and LLG values of 9.2 and 63.76, respectively. The final model of NRZ: zBad BH3 was built manually over several cycles using Coot[38] and refined using PHENIX[39] with a final R$_{work}$/R$_{free}$ of 0.187/0.206, with 98.7% of residues in Ramachandran favoured region of the plot and no outliers.

All images for NRZ *apo* and NRZ: zBad BH3 complex were generated using PyMOL molecular graphic system, version 1.8.6 (Schrödinger, LLC, New York, USA). All software was accessed through the SBGrid suite[42].

Sequence alignments

Sequence alignments were performed using MUSCLE (https://www.ebi.ac.uk/Tools/msa/muscle/) with the default settings.

Results

In order to determine the molecular basis for apoptosis control mediated by NRZ in zebrafish we systematically examined the ability of NRZ to bind to peptides spanning the BH3 motif of zebrafish encoded pro-apoptotic Bcl-2 proteins. Analysis of the *D. rerio* genome indicated that genes are present for orthologues of the mammalian pro-apoptotic Bcl-2 family members Bid, Bim, Bax, Bad, Bik, Bmf, Puma and Noxa[4,23,24,44], as well as Bcl-wav, a pro-apoptotic paralogue unique to fish[29]. In addition a Beclin 1 orthologue, a protein that harbours a BH3-like motif that is involved in autophagy[45] and was previously shown to interact with pro-survival Bcl-2 proteins[46], is also present. Isothermal titration calorimetry (ITC) was used to determine the affinity of NRZ for peptides that span the BH3 motifs of zBid, zBim, zBax, zBad, zBik, zBmf, zPuma, zNoxa, zBcl-wav and zBeclin (Fig 1, Table 1). The BH3 motifs were chosen through sequence alignment with the known mammalian pro-apoptotic Bcl-2 proteins by identifying the signature sequence LXXXGDE of the BH3 motif[5], where X is any amino acid. Interestingly, our ITC data showed that NRZ binds most BH3 motifs with the exception of those from Bmf and Beclin, which displayed no detectable affinity. Several BH3-only proteins interacted with NRZ with high affinities, including zBik (K_D 12 nM), zPuma (K_D 36 nM) and zBim (K_D 41 nM), while

Table 1 ITC affinity measurements of NRZ: BH3 motif interactions

Peptide	WT NRZ K_D (nM)	NRZ R86A K_D (nM)	NRZ D79A K_D (nM)
Bax	688 ± 111	4600 ± 440	264 ± 42
Bim	41 ± 5	168 ± 8	13 ± 4
Bad	343 ± 48	4800 ± 88	3330 ± 41
Puma	36 ± 4	2770 ± 162	117 ± 5
Bik	12 ± 2	17 ± 3	14 ± 3
Noxa	142 ± 16	510 ± 41	335 ± 31
Bcl-wav	3570 ± 162	NB	NB
Bid	409 ± 55	NB	220 ± 16
Bmf	NB	NB	NB
Beclin	NB	NB	NB

26-mer peptides spanning the BH3-motyif of *D. rerio* pro-apoptotic Bcl-2 family members or Beclin-1 from zebrafish were employed. All K_D values (in nM) are the means of three replicates with standard error

NB no binding

zNoxa (K_D 142 nM), zBad (K_D 343 nM), zBid (K_D 409 nM) and zBax (K_D 688 nM) were bound with more modest affinities. In contrast, Bcl-wav, a recently discovered novel pro-apoptotic Bcl-2 family member of zebrafish[29] engaged NRZ with only micromolar affinity (K_D 3570 nM).

To determine the structural basis of NRZ interaction with BH3 motifs of pro-apoptotic Bcl-2 proteins, we determined the crystal structures of *apo*-NRZ and its complexed *holo* form bound to the BH3-motif of zBad (Fig. 2a, d, Table 2). Similar to other pro-survival Bcl-2 proteins, NRZ adopts a conserved Bcl-2-like fold consisting of eight α-helices that form a globular helical bundle. Helices α2-5 form the canonical hydrophobic ligand binding groove observed in other Bcl-2 family proteins[47] that is utilized to accommodate the zBad BH3 peptide (Fig. 2d). An analysis using DALI[48] showed that complexes of Mcl-1 (PDB ID 2NL9)[49] (Fig. 2b, f) and Bcl-x$_L$ (PDB ID 4QNQ)[50] bound to Bim and Bad BH3 peptides are the closest structural Bcl-2 homologs with R.M.S.D. value 1.7 Å and 1.9 Å over 136 and 132 Cα atoms, respectively, with sequence identities of 15% and 18%, respectively. The closest viral Bcl-2 homolog to NRZ is CNP058[51] (R.M.S.D. of 2.0 Å over 133 Cα atoms, Fig. 2c) with a sequence identity of 16%.

NRZ: BH3 motif interactions

NRZ utilizes the canonical hydrophobic binding groove that is also found in other pro-survival Bcl-2 proteins[4] to accommodate the zBad BH3-motif (Fig. 3a) using a combination of hydrophobic and ionic interactions as well as hydrogen bonds. To accommodate the zBad BH3-peptide NRZ undergoes localized conformational changes
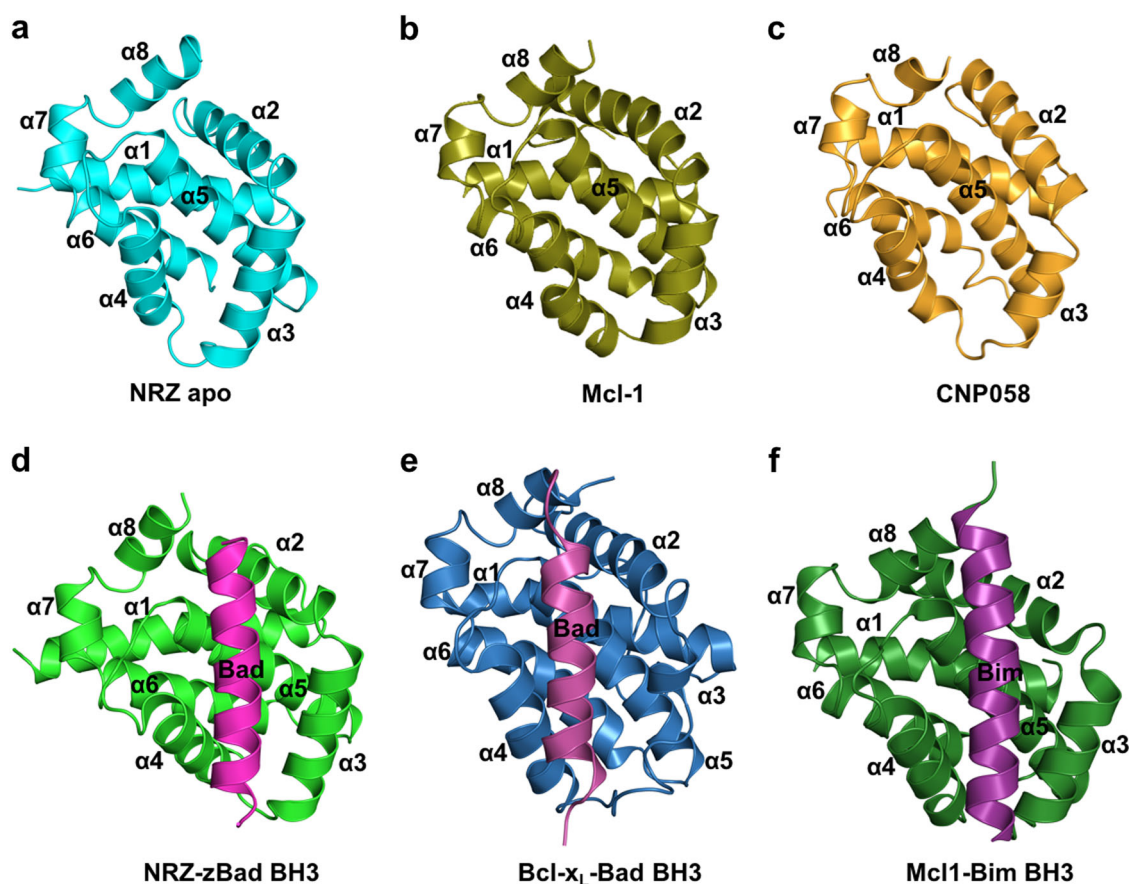
Fig. 2 Crystal structures of NRZ, NRZ: Bad BH3 complex and comparison with closely related complexes. Cartoon representation of (**a**) *apo* NRZ (light blue). Helices are labelled as α1–8, with the view being into the hydrophobic groove formed by α2–5. **b** Cartoon representation of Mcl-1 (olive)[49]. **c** CNP058 (orange)[51], the closest structural homolog from viral pro-survival Bcl-2 proteins for NRZ. **d** NRZ (green) in complex with zBad BH3 motif (hot pink). **e** Bcl-x$_L$ (blue) in complex with Bad BH3 motif (yellow)[50], **f** Mcl-1 (brown) in complex with Bim (magenta) BH3 motif[49]. All views in **b**–**f** are as in **a**

(Fig. 3a, d). Upon binding of the BH3-motif, the C-terminal end of α4-helix moves by 3.0 Å (Fig. 4a, b) relative to *apo*-NRZ, thus enlarging the binding groove to accommodate the Bad BH3 motif. Detailed inspection of the NRZ: zBad BH3 complex interface reveals five salt bridges between Lys93^{Bad} and Glu75^{NRZ}, Lys94^{Bad} and Glu56^{NRZ}, Glu105^{Bad} and His46^{NRZ}, Arg100^{Bad} with Asp79^{NRZ} and Asp104^{Bad} with Arg86^{NRZ}. In addition to ionic interactions, the NRZ: zBad interface also features three hydrogen bonds between Arg100^{Bad}–Leu76^{NRZ}, Arg100^{Bad}–Glu75^{NRZ}, Gln98^{Bad}–Lys49^{NRZ}. Finally, the four highly conserved hydrophobic residues Y95, 99L, M102 and F106 from the zBad BH3 motif protrude into the ligand binding groove of NRZ and are accommodated in four hydrophobic pockets at the floor of the binding groove.

To validate the structure of NRZ: Bad BH3 we mutated two key NRZ residues involved in ionic interactions, Asp79 and Arg86 to Ala, and examined the ability of these mutants to bind BH3-motif peptides (Table 1). Both mutants showed substantially reduced binding to Bad, with D79A displaying a tenfold reduction in Bad binding, whereas NRZ R86A displayed a 14-fold reduction in affinity. However, the contributions to binding BH3-motif peptides from these residues are not uniform across all BH3-motifs, indicating differences in the specific importance of these contacts. For example, Bik is not affected strongly by these two mutations and Bid binding is only impacted by R86A, whereas Bcl-wav binding is ablated for both R86A and D79A.

Discussion

Developing a detailed understanding of Bcl-2 family function in apoptosis regulation is not only important for identifying their biological roles but, is crucial in the design of new therapeutic strategies directed against this family[4,52]. Indeed, as a major arbiter of programmed cell death, there is a significant interest in resolving the

Table 2 X-ray crystallographic data collection and refinement statistics

	Native NRZ Apo	Native NRZ: Bad BH3
Data collection		
Space group	P4$_3$	P6$_3$
Cell dimensions		
a, b, c (Å)	48.18, 48.18, 75.33	87.62, 87.62, 36.77
α, β, γ (°)	90, 90, 90	90, 90, 120
Wavelength (Å)	0.9537	0.9537
Resolution (Å)	48.18–2.0 (2.07–2.0) *	43.81–1.639 (1.68–1.64) *
R_{sym} or R_{merge}	0.051 (1.16)	0.092 (1.92)
I/σI	18.3 (1.7)	15.4 (1.3)
Completeness (%)	99.93 (99.57)	100 (100)
Redundancy	6.9 (6.9)	18.6 (9.9)
Refinement		
Resolution (Å)	48.18–2.0 (2.07–2.0)	43.81–1.639 (1.68–1.64)
No. of reflections	11,653	19,885
R_{work}/R_{free}	0.194/0.222	0.187/0.206
No. of atoms		
Protein	1194	1361
Ligand/ion	0	0
Water	39	105
B-factors		
Protein	54.98	39.6
Ligand/ion	0	0
Water	52.42	44.2
R.m.s. deviations		
Bond lengths (Å)	0.007	0.003
Bond angles (°)	0.84	0.51

* Values in parentheses are for the highest resolution shell.

function of Bcl-2 family proteins at a molecular level with the aim of targeting them for their role in cancer[6,53]. Zebrafish are proving a valuable model system in this context as the mechanisms of apoptosis activation and function appear to be similar to those found in mammals[28]. Although there are many similarities between the Bcl-2 families in mammals and fish there are also significant differences that require clarification[20]. NRZ was initially identified as a *D. rerio* Bcl-2 orthologue of avian NR-13[26] via database searches[26,28]. Sequence alignment revealed that NRZ shares 40 and 39% identity with chicken NR-13 and turkey herpes virus NR-13 with respectively. Significantly lower sequence identity is shared with the mammalian orthologues of NRZ where only 25 and 23% sequence identity are observed for the human pro-survival Bcl-2 protein Bcl-B (also known as Bcl-2 like protein 10 or NrH) and the mouse orthologue Boo (or Diva), respectively[54]. Zebrafish NRZ features significant sequence differences from other Bcl-2 proteins with only three residues identical between NRZ, Bcl-B and Boo in the region spanning helices α3–5 that constitute the canonical ligand binding groove (Fig. 5), thus potentially providing a basis for a unique ligand binding profile for this pro-survival Bcl-2 family member[4,28]. Here we examined the structure and interactions of NRZ by determining the structures of *apo*-NRZ and its complex with zBad BH3, the orthologue of mammalian Bad and measuring the binding affinities for BH3-motifs. The structures revealed the conformational changes in NRZ after binding of BH3 motif ligand and provide a structural basis for NRZ mediated apoptosis inhibition.

Surprisingly, our structural search and comparison using DALI[48] revealed that the closest structural homolog of NRZ is in fact Mcl-1[55] with an R.M.S.D value of 1.7 Å over 136 Cα atoms, and a sequence identity of 15%. Sequence alignment of NRZ (Fig. 5) showed that NRZ shares sequence features of other multi-domain members of Bcl-2 family. However, the BH regions show considerable sequence variation and these sequence variations that are located in the binding groove account in part for the selectivity differences observed for BH3-ligands[47] compared to NRZ's mammalian counterparts. Interestingly, NRZ shares only 18% sequence identity with the two zebrafish encoded Mcl-1 homologs zMcl-1a and zMcl-1b, suggesting that they may not be functionally redundant and differentially interact with pro-apoptotic Bcl-2 proteins in zebrafish.

The overall fold of the NRZ: zBad BH3 complex is very similar to that observed in other Bcl-2 complexes. Despite the overall similarity in fold, several interesting differences are observed in the crystal structures and protein:peptide interfaces of the NRZ: zBad and Mcl-1: Bim complexes. The difference in peptide binding mode of these complexes were calculated[56] as solvent accessible surface and associated thermodynamic properties of Gibb's free energy change (ΔG) of interface formation and dissociation. The binding of zBad to NRZ buries a total of 2366 Å^2 solvent accessible surface and solvation energy of isolated structure −10.1 kcal/mol and ΔG of interface formation and dissociation of −3.9 kcal/mol. In contrast, binding of human Bim to human Mcl-1 buries a total of 2665 Å^2 and solvent accessible surface and solvation energy of isolated structure −10.4 kcal/mol and ΔG of interface formation and dissociation of −4.8 kcal/mol. However, the human Bcl-x$_L$:Bad complex forms a larger (total of 3268 Å^2 and solvent accessible surface and solvation energy of isolated structure

−14.4 kcal/mol and ΔG of interface formation and dissociation of −2.2 kcal/mol) ligand binding interface than that of NRZ: zBad and human Mcl-1:Bim. Structurally, NRZ features a more ordered α3 helix compared to human Bcl-x$_L$, which upon Bim binding unravels the α3 helix[57], and leads to an opening of the canonical ligand binding groove of ~9 Å due to an outward movement of α3 and a pivoting of α4. In contrast, NRZ maintains the ordered α3 helix on binding Bad, which leads to the C-terminal end of α4 helix moving by 3 Å relative to that in *apo*-NRZ (Fig. 4b).

Similar to other multi-domain Bcl-2 family proteins, including pro-apoptotic proteins Bax, Bak and Bok, NRZ also contains the highly conserved sequence motif "NWGR" as part of the BH1 motif at the N-terminal end of α5 (Fig. 2). In addition to forming a helix cap[4] this region plays a vital role for recognition of the BH3-only proteins[58]. A hallmark of BH3 motif interactions with
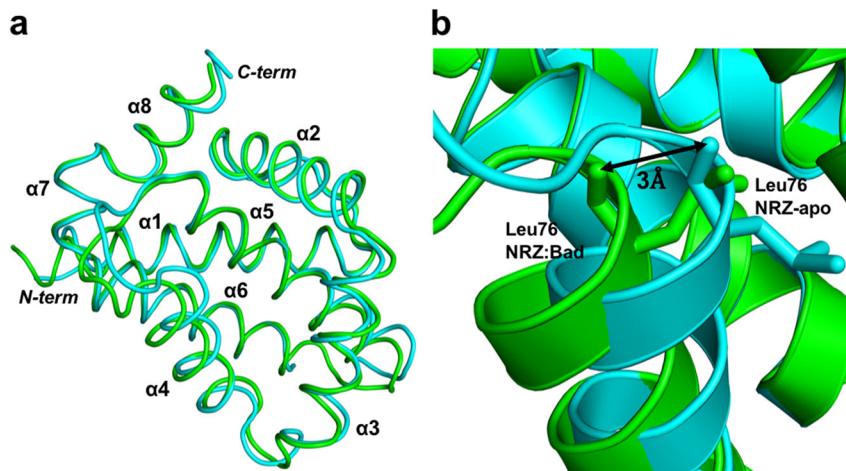

Fig. 3 Superimposition of apo NRZ with NRZ: zBad BH3 complex. Comparison of the backbone structures of NRZ and NRZ: zBad BH3 complex. **a** Cartoon representation of *apo* NRZ (light blue) superimposed onto NRZ: zBad BH3 complex (green). The view is into the canonical hydrophobic binding groove formed by α2–5. **b** Close up view of NRZ helix α4, which is shifted by 3 Å from its original position in the apo NRZ structure upon zBad BH3 motif binding, thus enlarging the binding groove
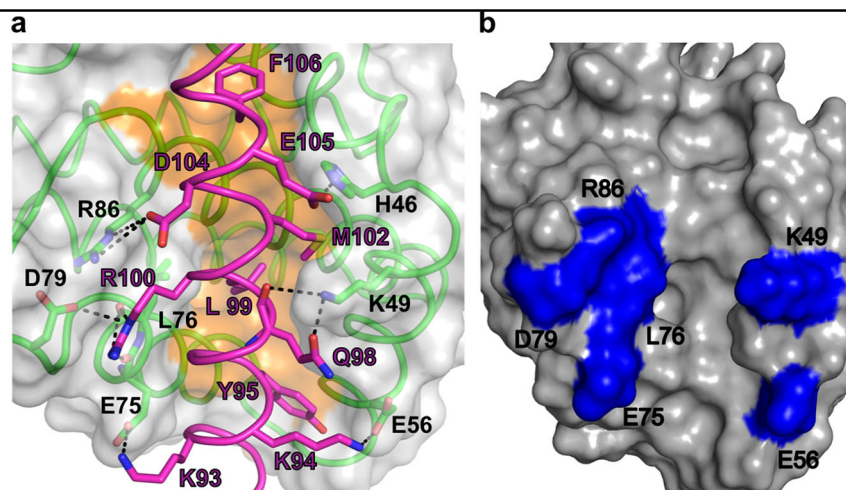

Fig. 4 Binding of BH3 motif peptides to NRZ result in local reorganization of the canonical NRZ binding groove. a Detailed view of the NRZ: zBad BH3 motif interface. The NRZ surface, backbone and floor of the binding groove are shown in grey, green and orange, respectively, while zBad BH3 is shown in hot pink. The four key hydrophobic residues of zBad (Y95, L99, M102, F106) protruding into the binding groove, and the conserved salt-bridge formed by NRZ D79 and zBad BH3 R100 are labelled, as well as all other residues involved in additional ionic interactions and hydrogen bonds. Interactions are denoted as dashed black lines. **b** Surface view of the conserved residues that are involved in NRZ-zBad BH3 interactions. Residues shown in blue are residues within canonical binding groove of NRZ (K49, E56, E75, L76, D79 and R86) that are conserved in NRZ-like proteins amongst different fish species
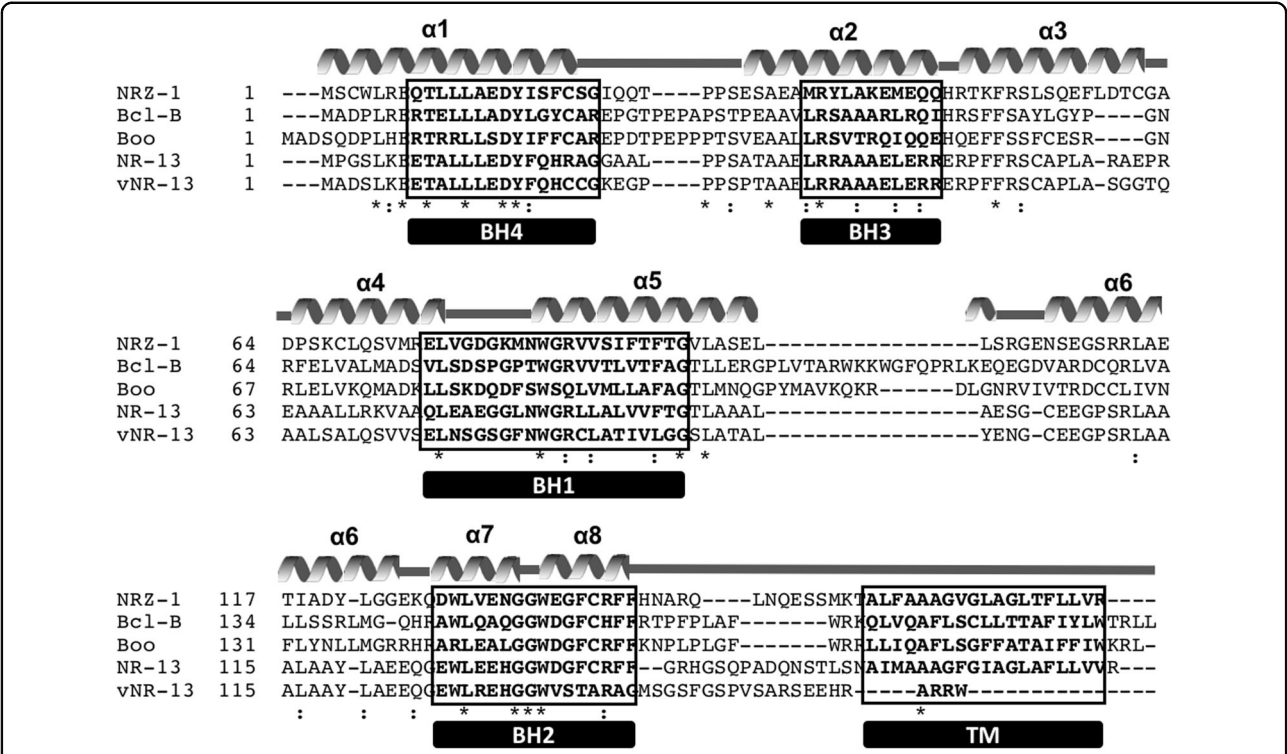
Fig. 5 Sequence alignment of NRZ with Bcl-2 homologs from other organisms. The sequence alignment of Bcl-2 family proteins was generated with MUSCLE[66] using sequences from zebrafish NRZ (Uniprot Accession number Q8UWD5), human Bcl-B (Q9HD36), mouse Boo (Q9Z0F3), chicken NR-13 (Q90ZN1) and herpes virus vNR-13 (Q9DH00). The α-helical secondary structure elements (α1–8) are marked as grey helices and loop regions are indicated as grey lines based on the crystal structure of NRZ. The boxed regions of the sequences are denoting the Bcl-2 homology motifs (BH motifs 1–4) and trans-membrane domains (TM) at the end of the sequences. Conserved identical residues between sequences are denoted as "*", similar residues are denoted as ":" and semi conserved residues denoted as "."

mammalian pro-survival Bcl-2 proteins is the formation of an ionic bond between the conserved Arginine of the "NWGR" sequence motif of pro-survival Bcl-2 proteins with the absolutely conserved Aspartate residue of the BH3 motif[58]. In the human Bcl-x$_L$:Bad complex (1G5J[50]) (Fig. 3e), the corresponding R139 residue in the NWGR motif interacts with D119 of the Bad BH3 peptide[50]. Previous studies revealed that a R139Q mutation in Bcl-x$_L$ results in loss of pro-survival function and ability to interact with Bax[59]. Surprisingly, this highly conserved interaction between the Arginine in the NWGR motif that is present in all other mammalian Bcl-2:BH3 complexes solved to date[4,60] is very weak in the NRZ: zBad BH3 complex, instead an additional ionic interaction between Asp79^{NRZ}-Arg100^{Bad} is observed that may compensate for the weaker and longer range canonical ionic interaction between Arg86^{NRZ}-Asp104^{Bad}. Mutagenesis of both Asp79 and Arg86 in NRZ indicated that indeed both contribute to the binding of Bad, with Arg86 still playing an important role in binding BH3-motif peptides despite being more distant from the partner Asp104 in Bad when compared to other pro-survival Bcl-2: BH3 peptide

complexes (Table 1). Notably, the individual mutations affected binding to several BH3 motif peptides differentially, suggesting that careful mutagenesis may be utilized to probe the role of individual NRZ interactions with pro-apoptotic Bcl-2 proteins[61].

NRZ displays a very distinct ligand interaction profile when compared to its most structurally related proteins, Mcl-1, Bcl-x$_L$ and CNP058. Intriguingly the sole viral Bcl-2 member encoded by a fish virus, grouper iridovirus GIV66, only binds Bim, thus displaying a radically different ligand binding profile compared to NRZ[62]. Among mammalian pro-survival Bcl-2 proteins a distinct Bad/Noxa dyad is observed, with Bcl-2, Bcl-x$_L$ and Bcl-w binding Bad, but not Noxa, whereas Mcl-1 and A1 bind Noxa but not Bad[7]. In contrast, NRZ binds both Bad and Noxa with 340 nM and 140 nM affinity, respectively, a feature not previously seen outside of virus encoded pro-survival Bcl-2, with African swine fever virus encoded A179L and fowlpox virus encoded FPV039 the only known pro-survival Bcl-2 proteins that are Bad and Noxa binders[63,64]. NRZ shows no affinity for Bmf, which is bound by both human Mcl-1 and Bcl-
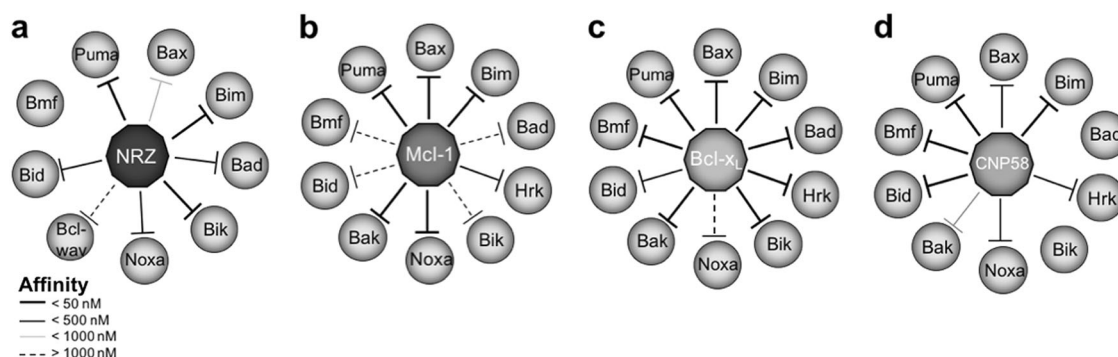
Fig. 6 Comparison of the BH3 motif binding profile of NRZ with Mcl-1, Bcl-x_L and CNP058. a Binding profile of zebrafish NRZ with BH3 motif peptides (**b**) binding profile of human Mcl-1 (**c**) binding profile of human Bcl-x_L and (**d**) binding profile of canarypox virus CNP058. BH3 motif peptides used in (**b**) and (**c**) are of human origin, whereas peptides in (**d**) are from chicken. Bars indicate binding affinity ranges from <50 nM, <500 nM, <1000 nM, and >1000 nM as shown in inset

x_L (Fig. 6)[7], and overall displays a ligand binding profile that most closely resembles A1, albeit with different affinities for individual ligands[65]. Overall, the affinity measurements suggest that NRZ is unlikely to be a functional Mcl-1 homolog, as might be expected as there are two Mcl-1 orthologues in *D. rerio*, Mcl-1a and Mcl-1b[26], and it is also unlikely to be a functional Bcl-B homolog, considering that human Bcl-B is only able to engage Bax and Bim[54]. NRZ also does not bind the BH3 motif of the autophagy regulator Beclin-1, a feature previously observed for both mammalian Bcl-2 and Bcl-x_L[50], suggesting that NRZ does not harbour a dual role in regulating apoptosis and autophagy.

In summary, like other pro-survival Bcl-2 protein structures solved to-date, NRZ adopts a Bcl-2 like fold and its most closely related structural homologs are the cellular apoptosis inhibitor Mcl-1 and the canarypox viral Bcl-2 protein CNP058. Furthermore, we demonstrated that NRZ harbours a unique BH3 motif binding profile. However, while NRZ is a close structural homolog of Mcl-1 it seems unlikely to be a functional orthologue based on its different binding profile, in particular the ability to engage both Bad and Noxa, a feature that has not been previously observed in mammalian pro-survival Bcl-2 proteins. This study suggests that NRZ likely occupies a unique mechanistic role in zebrafish apoptosis regulation. Thus, further functional studies are required in vivo to delineate the role of NRZ in apoptosis signalling. Our findings demonstrate the complexities of delineating Bcl-2 family function and the pitfalls of assumed functional and evolutionary similarity based on sequence and structure alone.

Data availability

The raw X-ray diffraction data were deposited at the SBGrid Data Bank (http://data.sbgrid.org)[43] as dataset entries doi: 10.15785/SBGRID/6H1N and 10.15785/

SBGRID/6FBX. The coordinates have been deposited in the Protein Data Bank (accession code 6H1N and 6FBX).

Competing interests
The authors declare that they have no conflict of interest.

Publisher's note
Springer Nature remains neutral with regard to jurisdictional claims in published maps and institutional affiliations.

References
1. Green, D. R., Llambi, F. Cell death signaling. *Cold Spring Harb. Perspect. Biol.* **7**: a006080, (2015).
2. Kvansakul, M., Caria, S., Hinds, G. M. The Bcl-2 family in host-virus interactions. *Viruses* **9**, (2017).
3. Strasser, A., Cory, S. & Adams, J. M. Deciphering the rules of programmed cell death to improve therapy of cancer and other diseases. *EMBO J.* **30**, 3667–3683 (2011).
4. Kvansakul, M. & Hinds, M. G. The Bcl-2 family: structures, interactions and targets for drug discovery. *Apoptosis* **20**, 136–150 (2015).
5. Kvansakul, M. & Hinds, M. G. The structural biology of BH3-only proteins. *Methods Enzymol.* **544**, 49–74 (2014).
6. Luna-Vargas, M. P. & Chipuk, J. E. The deadly landscape of pro-apoptotic BCL-2 proteins in the outer mitochondrial membrane. *FEBS J.* **283**, 2676–2689 (2016).
7. Chen, L. et al. Differential targeting of prosurvival Bcl-2 proteins by their BH3-only ligands allows complementary apoptotic function. *Mol. Cell* **17**, 393–403 (2005).
8. Kalkavan, H. & Green, D. R. MOMP, cell suicide as a BCL-2 family business. *Cell Death Differ.* **25**, 46–55 (2018).
9. Czabotar, P. E. et al. Bax crystal structures reveal how BH3 domains activate Bax and nucleate its oligomerization to induce apoptosis. *Cell* **152**, 519–531 (2013).
10. Lindsten, T. et al. The combined functions of proapoptotic Bcl-2 family members bak and bax are essential for normal development of multiple tissues. *Mol. Cell* **6**, 1389–1399 (2000).

11. Vaux, D. L. Apoptogenic factors released from mitochondria. *Biochim. Biophys. Acta* **1813**, 546–550 (2011).

12. Shamas-Din, A., Kale, J., Leber, B. & Andrews, D. W. Mechanisms of action of Bcl-2 family proteins. *Cold Spring Harb. Perspect. Biol.* **5**, a008714 (2013).

13. Popgeorgiev, N. et al. The apoptotic regulator Nrz controls cytoskeletal dynamics via the regulation of Ca2+ trafficking in the zebrafish blastula. *Dev. Cell* **20**, 663–676 (2011).

14. Prudent, J., Popgeorgiev, N., Bonneau, B. & Gillet, G. Bcl-2 proteins, cell migration and embryonic development: lessons from zebrafish. *Cell Death Dis.* **6**, e1910 (2015).

15. Bonneau, B., Prudent, J., Popgeorgiev, N. & Gillet, G. Non-apoptotic roles of Bcl-2 family: The calcium connection. *Biochim. Et. Biophys. Acta* **1833**, 1755–1765 (2013).

16. Szegezdi, E., MacDonald, D. C., Ní Chonghaile, T., Gupta, S. & Samali, A. Bcl-2 family on guard at the ER. *Am. J. Physiol.* **296**, C941–C953 (2009).

17. Caria, S., Hinds, M. G. & Kvansakul, M. Structural insight into an evolutionarily ancient programmed cell death regulator – the crystal structure of marine sponge BHP2 bound to LB-Bak-2. *Cell Death Dis.* **8**, e2543 (2017).

18. Vaux, D. L., Haecker, G. & Strasser, A. An evolutionary perspective on apoptosis. *Cell* **76**, 777–779 (1994).

19. Santos, N. M. Sd, Vale, Ad, Reis, M. I. R. & Silva, M. T. Fish and apoptosis: molecules and pathways. *Curr. Pharm. Des.* **14**, 148–169 (2008).

20. Eimon, P. M. & Ashkenazi, A. The zebrafish as a model organism for the study of apoptosis. *Apoptosis* **15**, 331–349 (2010).

21. Yuan, Z. et al. Expression of Bcl-2 genes in channel catfish after bacterial infection and hypoxia stress. *Dev. Comp. Immunol.* **65**, 79–90 (2016).

22. Krumschnabel, G. & Podrabsky, J. E. Fish as model systems for the study of vertebrate apoptosis. *Apoptosis* **14**, 1–21 (2009).

23. Jette, C. A. et al. BIM and other BCL-2 family proteins exhibit cross-species conservation of function between zebrafish and mammals. *Cell Death Differ.* **15**, 1063 (2008).

24. Shamas-Din, A., Brahmbhatt, H., Leber, B. & Andrews, D. W. BH3-only proteins: orchestrators of apoptosis. *Biochim. Et. Biophys. Acta* **1813**, 508–520 (2011).

25. Akhtar, R. S., Ness, J. M. & Roth, K. A. Bcl-2 family regulation of neuronal development and neurodegeneration. *Biochim. Et. Biophys. Acta* **1644**, 189–203 (2004).

26. Inohara, N. & Nunez, G. Genes with homology to mammalian apoptosis regulators identified in zebrafish. *Cell Death Differ.* **7**, 509–510 (2000).

27. Lee, R-m, Gillet, G., Burnside, J., Thomas, S. J. & Neiman, P. Role of Nr13 in regulation of programmed cell death in the bursa of Fabricius. *Genes Dev.* **13**, 718–728 (1999).

28. Arnaud, E. et al. The zebrafish bcl-2 homologue Nrz controls development during somitogenesis and gastrulation via apoptosis-dependent and -independent mechanisms. *Cell Death Differ.* **13**, 1128 (2005).

29. Prudent, J. et al. Bcl-wav and the mitochondrial calcium uniporter drive gastrula morphogenesis in zebrafish. *Nat. Commun.* **4**, 2330 (2013).

30. Vega, S. et al. Snail blocks the cell cycle and confers resistance to cell death. *Genes Dev.* **18**, 1131–1143 (2004).

31. Torraca, V. & Mostowy, S. Zebrafish infection: from pathogenesis to cell biology. *Trends Cell Biol.* **28**, 143–156 (2018).

32. Scholz, J., Besir, H., Strasser, C. & Suppmann, S. A new method to customize protein expression vectors for fast, efficient and background free parallel cloning. *BMC Biotechnol.* **13**, 12 (2013).

33. Studier, F. W. Protein production by auto-induction in high density shaking cultures. *Protein Expr. Purif.* **41**, 207–234 (2005).

34. Burton, D. R., Caria, S., Marshall, B., Barry, M. & Kvansakul, M. Structural basis of Deerpox virus-mediated inhibition of apoptosis. *Acta Crystallogr. D Biol. Crystallogr.* **71**, 1593–1603 (2015).

35. Kabsch, W. XDS. *Acta Crystallogr. D Biol. Crystallogr.* **66**, 125–132 (2010).

36. Evans, P. Scaling and assessment of data quality. *Acta Crystallogr. D Biol. Crystallogr.* **62**, 72–82 (2006).

37. McCoy, A. Solving structures of protein complexes by molecular replacement with Phaser. *Acta Crystallogr. D* **63**, 32–41 (2007).

38. Emsley, P., Lohkamp, B., Scott, W. G. & Cowtan, K. Features and development of Coot. *Acta Crystallogr. D* **66**, 486–501 (2010).

39. Afonine, P. V. et al. Towards automated crystallographic structure refinement with phenix.refine. *Acta Crystallogr. D.* **68**, 352–367 (2012).

40. Kvansakul, M. & Czabotar, P. E. Preparing Samples for Crystallization of Bcl-2 Family Complexes. In: H. Puthalakath, C. J. Hawkins (eds). *Programmed Cell Death: Methods and Protocols*. (pp. 213–229. Springer New York, New York, NY, 2016).

41. Johannes, J. W. et al. Structure based design of non-natural peptidic macro-cyclic Mcl-1 inhibitors. *ACS Med. Chem. Lett.* **8**, 239–244 (2017).

42. Morin, A. et al. Collaboration gets the most out of software. *Elife* **2**, e01456 (2013).

43. Meyer, P. A. et al. Data publication with the structural biology data grid supports live analysis. *Nat. Commun.* **7**, 10882 (2016).

44. Martinou, J.-C. & Youle, R. J. Mitochondria in apoptosis: Bcl-2 family members and mitochondrial dynamics. *Dev. Cell* **21**, 92–101 (2011).

45. Kang, R., Zeh, H. J., Lotze, M. T. & Tang, D. The Beclin 1 network regulates autophagy and apoptosis. *Cell Death Differ.* **18**, 571–580 (2011).

46. Priault, M. et al. Differential dependence on Beclin 1 for the regulation of pro-survival autophagy by Bcl-2 and Bcl-xL in HCT116 colorectal cancer cells. *PLoS ONE* **5**, e8755 (2010).

47. Kvansakul, M. & Hinds, M. G. Structural biology of the Bcl-2 family and its mimicry by viral proteins. *Cell Death Dis.* **4**, e909 (2013).

48. Holm, L. & Rosenström, Pi Dali server: conservation mapping in 3D. *Nucleic Acids Res.* **38**, W545–W549 (2010).

49. Czabotar, P. E. et al. Structural insights into the degradation of Mcl-1 induced by BH3 domains. *Proc. Natl Acad. Sci. USA* **104**, 6217–6222 (2007).

50. Petros, A. M. et al. Rationale for Bcl-XL/Bad peptide complex formation from structure, mutagenesis, and biophysical studies. *Protein Sci.* **9**, 2528–2534 (2000).

51. Anasir, M., Baxter, A., Poon, I., Hulett, M. & Kvansakul, M. Structural and functional insight into canarypox virus CNP058 mediated regulation of apoptosis. *Viruses* **9**, 305 (2017).

52. Cory, S., Roberts, A. W., Colman, P. M. & Adams, J. M. Targeting BCL-2-like proteins to kill cancer cells. *Trends Cancer* **2**, 443–460 (2016).

53. Fuchs, Y. & Steller, H. Live to die another way: modes of programmed cell death and the signals emanating from dying cells. *Nat. Rev. Mol. Cell Biol.* **16**, 329–344 (2015).

54. Rautureau, G. J. P. et al. The restricted binding repertoire of Bcl-B leaves Bim as the universal BH3-only prosurvival Bcl-2 protein antagonist. *Cell Death Dis.* **3**, e443 (2012).

55. Fire, E., Gullá, S. V., Grant, R. A. & Keating, A. E. Mcl-1–Bim complexes accommodate surprising point mutations via minor structural changes. *Protein Sci.* **19**, 507–519 (2010).

56. Krissinel, E. & Henrick, K. Inference of macromolecular assemblies from crystalline state. *J. Mol. Biol.* **372**, 774–797 (2007).

57. Liu, X., Dai, S., Zhu, Y., Marrack, P. & Kappler, J. W. The structure of a Bcl-xL/Bim fragment complex: implications for Bim function. *Immunity* **19**, 341–352 (2003).

58. Day, C. L. et al. Structure of the BH3 domains from the p53-inducible bh3-only proteins noxa and puma in complex with Mcl-1. *J. Mol. Biol.* **380**, 958–971 (2008).

59. Sattler, M., Liang, H., Nettesheim, D., Meadows, R. P., Harlan, J. E. & Eberstadt, M. et al. Structure of Bcl-X\$_L\$-Bak peptide complex: recognition between regulators of apoptosis. *Science* **275**, 983–986 (1997).

60. Petros, A. M., Olejniczak, E. T. & Fesik, S. W. Structural biology of the Bcl-2 family of proteins. *Biochim. Biophys. Acta* **1644**, 83–94 (2004).

61. Campbell, S. et al. Structural insight into BH3 domain binding of vaccinia virus antiapoptotic F1L. *J. Virol.* **88**, 8667–8677 (2014).

62. Banjara, S., Mao, J., Ryan, T. M., Caria, S. & Kvansakul, M. Grouper iridovirus GIV66 is a Bcl-2 protein that inhibits apoptosis by exclusively sequestering Bim. *J. Biol. Chem.* **293**, 5464–5477 (2018).

63. Banjara, S., Caria, S., Dixon, L. K., Hinds, M. G. & Kvansakul, M. Structural Insight into African Swine Fever Virus A179L-mediated inhibition of apoptosis. *J. Virol.* **91**, e02228–16 (2017).

64. Anasir, M. I., Caria, S., Skinner, M. A. & Kvansakul, M. Structural basis of apoptosis inhibition by the fowlpox virus protein FPV039. *J. Biol. Chem.* **292**, 9010–9021 (2017).

65. Smits, C., Czabotar, P. E., Hinds, M. G. & Day, C. L. Structural plasticity underpins promiscuous binding of the prosurvival protein A1. *Structure* **16**, 818–829 (2008).

66. Edgar, R. C. MUSCLE: multiple sequence alignment with high accuracy and high throughput. *Nucleic Acids Res.* **32**, 1792–1797 (2004).

Appendix 2
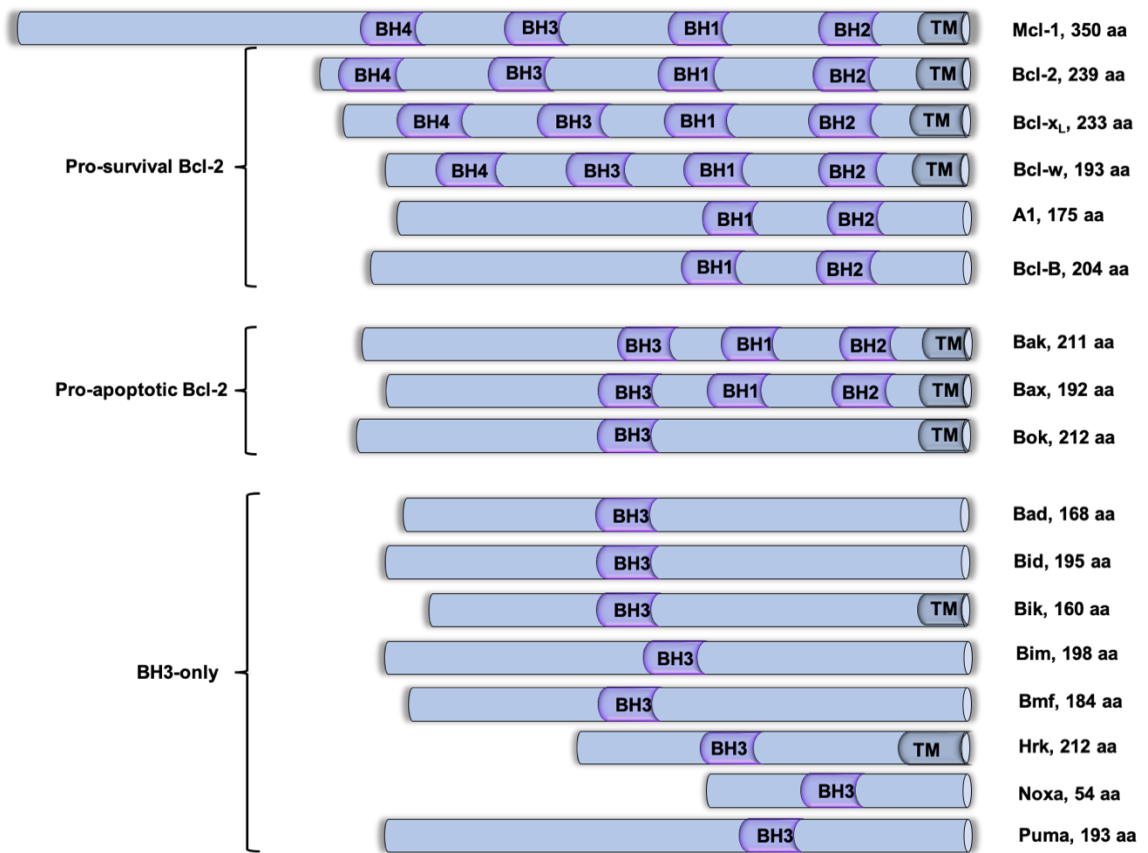
Figure A2: Schematic diagram represents the availability of BH motifs of Bcl-2 family proteins. different BH domains (BH 1-4) are coloured in blue and transmembrane domain (TM) coloured in grey. Names of the individual proteins were shown in the right-hand side panel with corresponding amino acid length. All these proteins were classified into three major sub-groups as pro-survival Bcl-2 proteins (Mcl-1, Bcl-2, Bcl-x_L, Bcl-w, A1 and Bcl-B), pro-apoptotic proteins (Bak, Bax and Bok) and BH3-only proteins (Bad, Bid, Bik, Bim, Bmf, Hrk, Noxa and Puma).

Appendix 3

Chapter 2, table 1 has been updated and added the ΔH values and N values as follows,

Table A3: Affinity measurements of TANV16L, mutant R90A and K52A with BH3 motif peptides from human pro-apoptotic Bcl-2 proteins. TANV16L interacts with BH3 motif peptides of human pro-apoptotic Bcl-2 proteins. All K_D values (in nM), ΔH values (in kcal mol^{-1}) and N denotes the stoichiometry. All values are the means of three replicates with standard error. NB denotes no binding.

Peptide	WT KD (nM)	ΔH$_{association}$ (kcal mol^{-1})	N	R90A KD (nM)	ΔH$_{association}$ (kcal mol^{-1})	N
Bak	38 ± 4.0	-4.27 ±0.07	0.99 ±0.08	2325 ± 261.0	-4.07± 0.26	0.95 ±0.02
Bax	70 ± 5.0	-4.55 ±0.20	1.01 ±0.06	2301 ± 374.0	-7.36± 0.37	1.03 ±0.03
Bok	NB	NB	NB	NB	NB	NB
Bad	219 ± 34.0	-6.3 ±1.3	0.95 ±0.07	10206 ± 1570.0	-4.45 ±0.20	0.87 ±0.06
Bid	719 ± 66.0	-4.13 ±0.5	1.02 ±0.07	nd	nd	nd
Bik	1250 ± 111.0	-2.51 ±0.31	0.85 ±0.03	14356 ± 1370.0	-3.17 ±0.75	1.12 ±0.05
Bim	180 ± 15.0	-4.93 ±0.31	0.90 ±0.03	1766 ± 320.0	-6.16 ±0.63	0.98 ±0.1
Bmf	606±76.0	-5.83 ±0.52	0.98 ±0.06	nd	nd	nd
Hrk	3220 ± 301.0	-5.07 ±0.10	1.02 ±0.09	nd	nd	nd
Noxa	NB	NB	NB	NB	NB	NB
Puma	468 ± 47.0	-5.87 0.15	0.88 ±0.08	911 ± 39.0	-1.17 ±0.1	0.99 ±0.08

Peptide	K52A KD (nM)	ΔH$_{association}$ (kcal mol^{-1})	N
Bak	113 ± 3.00	-8.24± 0.73	1.03 ±0.04
Bax	266± 11.00	-6.23± 0.32	1.05 ±0.04
Bok	NB	NB	NB
Bad	5857± 732.0	-3.63 ±0.40	0.89 ±0.04
Bid	976± 126	-5.8 ±0.26	1.04 ±0.03
Bik	3382± 85.00	-5,67 ±0.11	0.97 ±0.06
Bim	558± 27.0	-4.61 ±0.29	1.01 ±0.006
Bmf	nd	nd	nd
Hrk	nd	nd	nd
Noxa	NB	NB	NB
Puma	1010± 130.0	-2.95 ±0.15	1.04 ±0.02

Comment

The tightest interactors, Bak BH3 and Bax BH3 have similar enthalpies of association with WT_16L where Bik BH3 is showing the lowest heat release when it binds to 16L. In contrast, Hrk BH3 has shown the lowest K_D value of 3.2 uM. However, its energy release during association with TANV16 is more similar to that observed in Bak and Bax BH3 motif peptides. This suggested that enthalpic association of Bak, Bax and Hrk are similar.

Interactions of Bax BH3 with R90A mutant or Bak BH3 interactions with K52A mutant are having more favourable association enthalpy values compared to wt 16L.

All KD values are calculated and averaged from triplicated ITC runs. All ligand to protein ratios are included on the table 03 of the published manuscript. It was somewhat difficult to get more consistent error particularly for K_D value >1000 nM.

- ✓ Crystallization condition of TANV16L: Puma BH3 complex (6TQP)

  1M LiCl, 0.1M Citrate pH 4.0, 20% PEG 6000

Appendix 4

Chapter 3, table 1 has been updated and added the ΔH values and N values as follows,

Table 01: Affinity measurements of C7L and BH3 motif peptides from human pro-apoptotic Bcl-2 proteins. C7L interacts with BH3 motif peptides of human pro-apoptotic Bcl-2 proteins. All K_D values (in nM), ΔH values (in kcal mol^{-1}) and N denotes the stoichiometry. All values are the means of three replicates with standard error. NB denotes no binding.

Peptide	K_D (nM)	$\Delta H_{association}$ (kcal mol-1)	N
Bak	401 ± 31.0	-12.06 ± 0.63	1.06 ± 0.03
Bax	22 ± 5.0	-15.53 ± 1.42	1.02 ± 0.04
Bok	1370 ± 194.0	-4.03 ± 0.49	1.10 ± 0.15
Bad	NB	NB	NB
Bid	560 ± 30.0	-5.71 ± 0.086	0.98 ± 0.06
Bik	930 ± 88.0	-4.87 ± 0.25	1.11 ± 0.12
Bim	131 ± 20.0	-7.73 ± 0.17	1.06 ± 0.04
Bmf	NB	NB	NB
Hrk	1285 ± 221.0	-3.30 ± 0.23	1.12 ± 0.15
Noxa	NB	NB	NB
Puma	2605 ± 308.0	-3.00 ± 0.41	0.95 ± 0.16

Comment:

Comparison of Bax and Bak interactions with MPXV C7L revealed significantly different K_D values. However, their enthalpy of association is only mildly different. A similar pattern of interactions can be seen between Bok and Puma enthalpy of association with C7L.
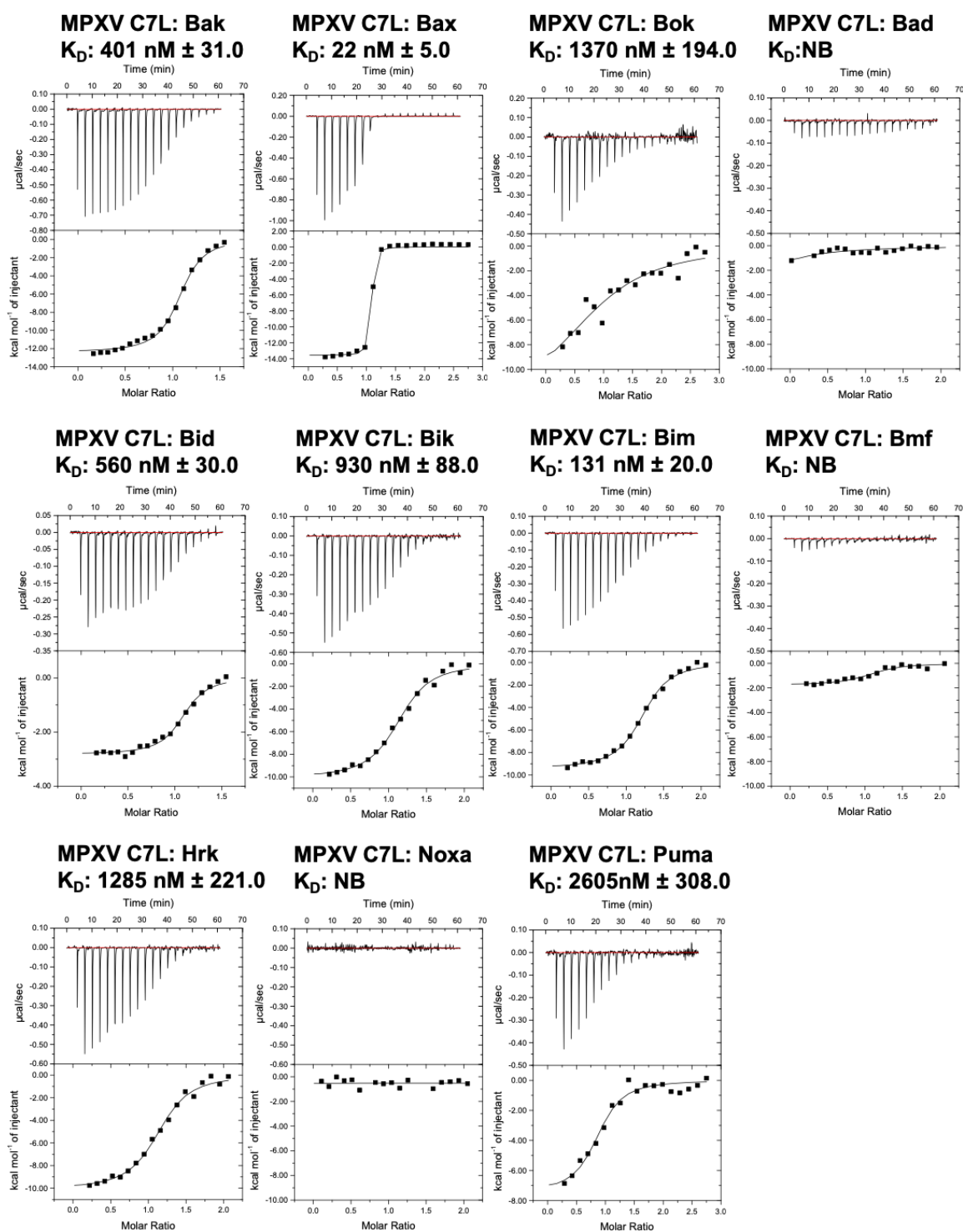
Figure A4: The binding affinities of MPXV C7L with BH3 motif peptides were measured using ITC and the raw thermograms shown with corresponding K_D values in (nM) are the average of triplicate experiments. NB: no binding detected.
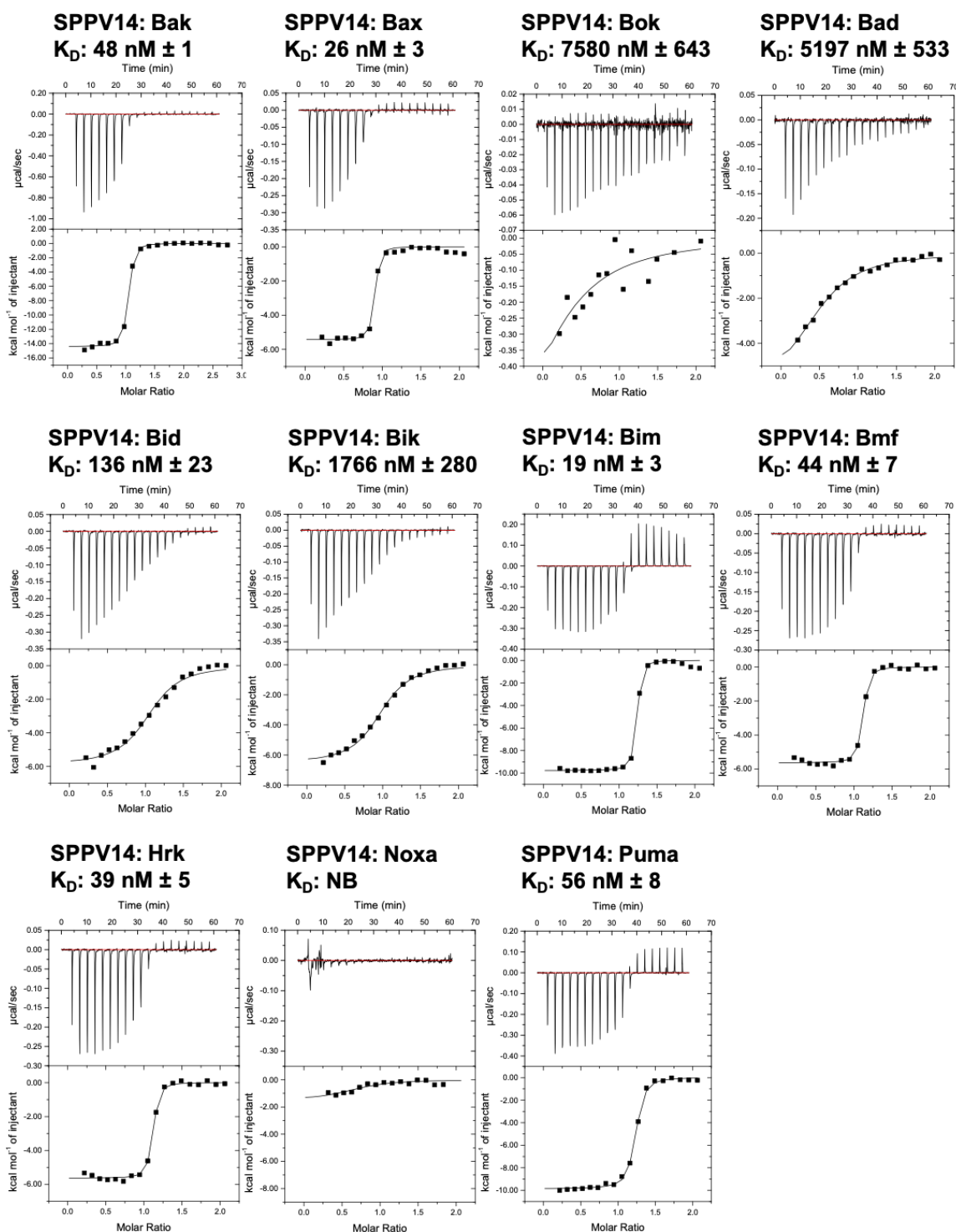
Appendix 5

Chapter 4, table 1 was updated with adding thermodynamic data (K_D, ΔH and N values).

Table 01: Thermodynamic measurements of SPPV14 wild type, mutant R90A and mutant Y46A with human pro-apoptotic BH3 motif peptides. All affinity measurements, $\Delta H_{association}$ and N values were reported as means of triplicates with standard deviation. NB denotes as no binding.

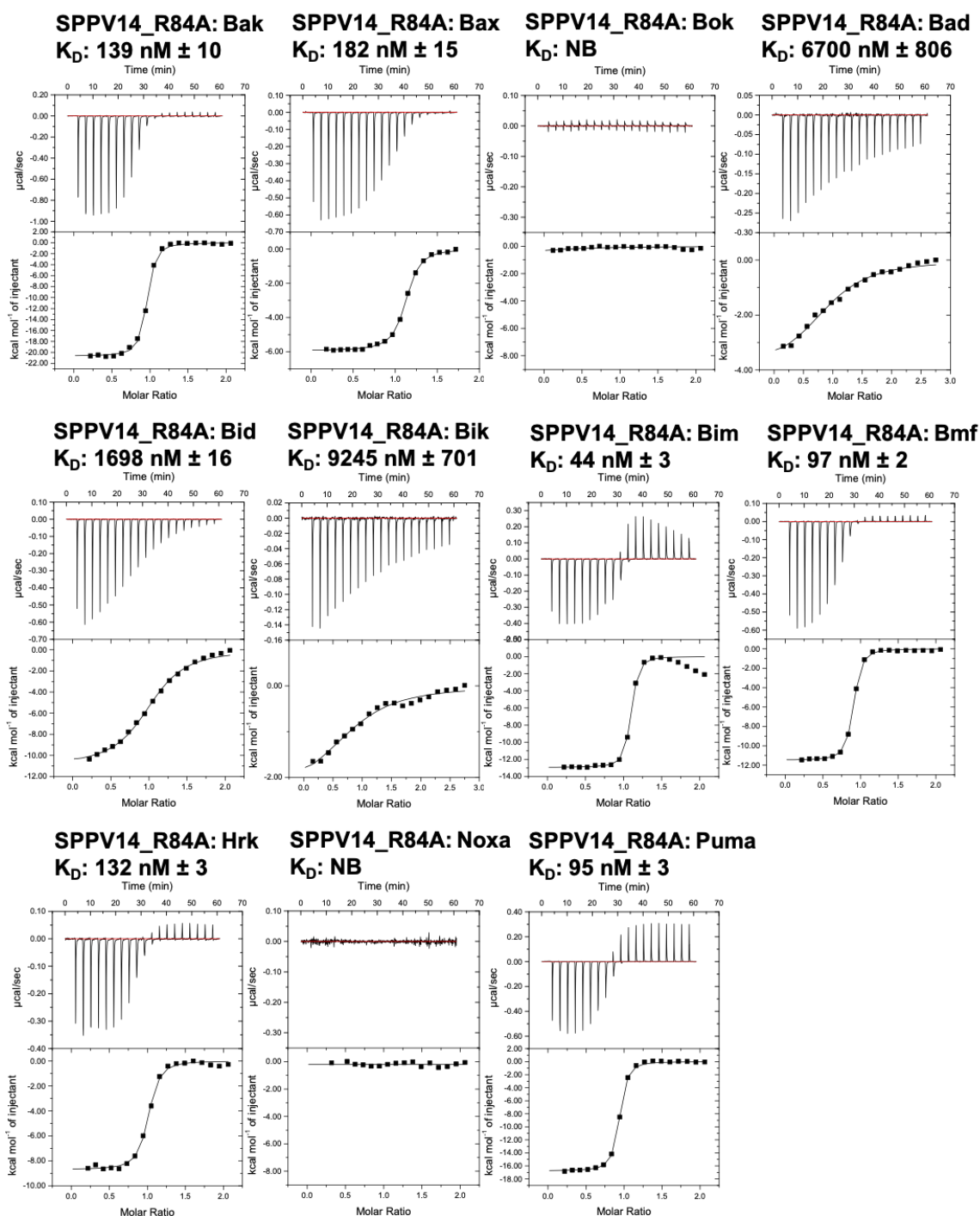| BH3 motif Peptide	WT KD (nM)	$\Delta H_{association}$ (kcal mol^{-1})	N	R84A KD (nM)	$\Delta H_{association}$ (kcal mol^{-1})	N
Bak	48 ± 1.2	-14.4 ± 0.33	1.02 ± 0.03	139 ± 10	-20.1 ± 0.37	1.05 ± 0.06
Bax	26 ± 3.1	-6.90 ± 0.76	0.96 ± 0.08	182 ± 15	-11.1 ± 0.35	1.12 ± 0.04
Bok	7580 ± 643.5	-2.88 ± 0.41	0.90 ± 0.20	NB	NB	NB
Bad	5197 ± 533.0	-5.90 ± 0.07	0.92 ± 0.15	6700 ± 806	-3.31 ± 0.42	1.15 ± 0.21
Bid	136 ± 23.3	-5.37 ± 0.54	1.01 ± 0.06	1698 ± 16	-10.9 ± 0.05	1.10 ± 0.04
Bik	1766 ± 280.2	-5.92 ± 0.36	1.03 ± 0.10	9245 ± 701	-2.40 ± 0.72	1.08 ± 0.10
Bim	19 ± 3.6	-10.3 ± 0.82	1.22 ± 0.12	44 ± 3	-12.6 ± 0.24	1.05 ± 0.12
Bmf	44 ± 7.1	-5.87 ± 0.15	1.12 ± 0.04	97 ± 2	-9.90 ± 0.23	0.98 ± 0.10
Hrk	39 ± 5.0	-3.93 ± 0.47	1.15 ± 0.12	132 ± 3	-8.45 ± 0.19	1.02 ± 0.04
Noxa	NB	NB	NB	NB	NB	NB
Puma	56 ± 8.1	-10.6 ± 0.47	1.22 ± 0.16	95 ± 3	-15.8 ± 0.06	1.05 ± 0 0.12

BH3 motif Peptide	Y46A KD (nM)	$\Delta H_{association}$ (kcal mol^{-1})	N
Bak	2553 ± 353	-3.10 ± 0.16	0.98 ± 0.10
Bax	4645 ± 393	-2.65 ± 0.44	1.04 ± 0.13
Bok	NB	NB	NB
Bad	NB	NB	NB
Bid	NB	NB	NB
Bik	NB	NB	NB
Bim	165 ± 18	-2.33 ± 0.07	1.08 ± 0.06
Bmf	151 ± 18	-4.41 ± 0.28	1.32 ± 0.24
Hrk	2250 ± 318	-2.00 ± 0.15	0.96 ± 0.13
Noxa	NB	NB	NB
Puma	988 ± 142	-0.92 ± 0.01	1.13 ± 0.21

A5a

SPPV14: Bak
K_D: 48 nM ± 1

SPPV14: Bax
K_D: 26 nM ± 3

SPPV14: Bok
K_D: 7580 nM ± 643

SPPV14: Bad
K_D: 5197 nM ± 533

SPPV14: Bid
K_D: 136 nM ± 23

SPPV14: Bik
K_D: 1766 nM ± 280

SPPV14: Bim
K_D: 19 nM ± 3

SPPV14: Bmf
K_D: 44 nM ± 7

SPPV14: Hrk
K_D: 39 nM ± 5

SPPV14: Noxa
K_D: NB

SPPV14: Puma
K_D: 56 nM ± 8

152

A5b

SPPV14_R84A: Bak
K_D: 139 nM ± 10

SPPV14_R84A: Bax
K_D: 182 nM ± 15

SPPV14_R84A: Bok
K_D: NB

SPPV14_R84A: Bad
K_D: 6700 nM ± 806

SPPV14_R84A: Bid
K_D: 1698 nM ± 16

SPPV14_R84A: Bik
K_D: 9245 nM ± 701

SPPV14_R84A: Bim
K_D: 44 nM ± 3

SPPV14_R84A: Bmf
K_D: 97 nM ± 2

SPPV14_R84A: Hrk
K_D: 132 nM ± 3

SPPV14_R84A: Noxa
K_D: NB

SPPV14_R84A: Puma
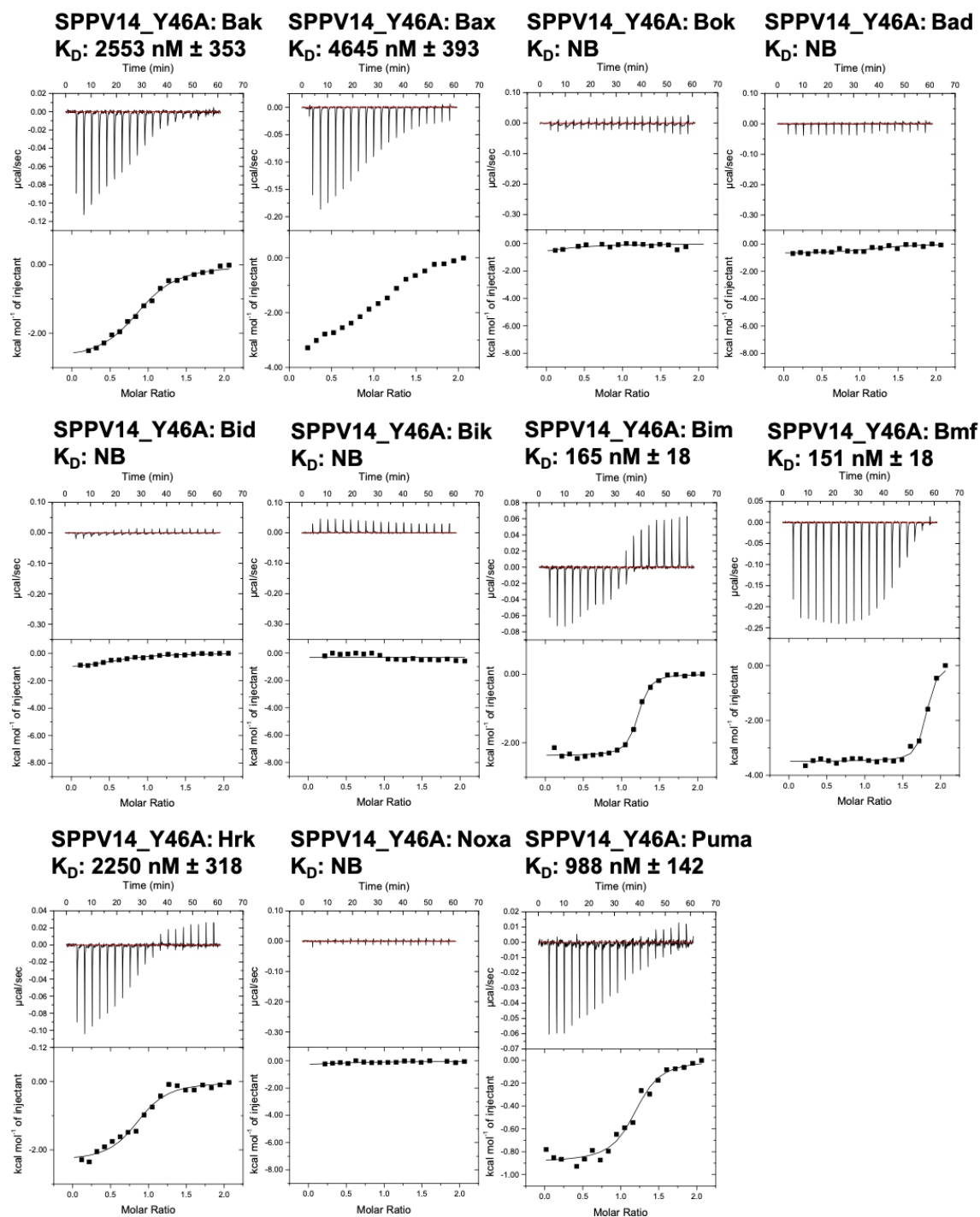K_D: 95 nM ± 3

A5c

Figure A5: ITC thermograms of interactions between SPPV14 with BH3 motif peptides from human pro-apoptotic Bcl-2 proteins, A5a) Wild type SPPV14, A5b) SPPV14 R84A mmutant and A5c) SPPV14 Y46A mutant. All thermogrames are shown with their binding affinities (K_D). The reported values (nM) are mean of the triplicated measurements.

Comment

- SPPV14 wild type and mutants (R84A and Y46A) proteins were expressed as GST fussion proteins and GST-tag was cleaved by using HRV-3C protease during the purification.

- Comparison of Bax and Bak interactions with MPXV C7L revealed significantly different K_D values. However, their enthalpy of association is only mildy different. A similar pattern of interactions can be seen between Bok and Puma enthalpy of association with C7L.

- Quality control data for the commercially synthesized protein expression constructs suggests that no cloning errors were present that would lead to truncation of full-length proteins that could have an effect on ITC interactions. All ITC measurements were performed in optimal range of $1 < c=n*[protein]/K_D < 1000$. Furthermore, all BH3-only proteins were intrinsically disordered except for Bid, and I could not purify them on their own.